Development of Radiolabelled Bombesin Analogues for Imaging Prostate Cancer with SPECT and PET

Yu, Zilin

Development of Radiolabelled Bombesin Analogues for Imaging Prostate Cancer with SPECT and PET

Zilin Yu

The printing of this thesis was financially supported by Graduate School of Medical Sciences, University Medical Center Groningen, University of Groningen, and CTMM (project PCMM, project number 03O-203).

Cover image: Night scene of groningen

Cover design: Z. Yu

Printed by: CPI Koninklijke Wöhrmann , Zutphen

ISBN: 978-90-367-6763-7

university of groningen

Development of Radiolabelled BombesinAnalogues for Imaging Prostate Cancer with SPECT and PET

PhD thesis

to obtain the degree of PhD at the
University of Groningen
on the authority of the
Rector Magnificus, Prof. E. Sterken
and in accordance with
the decision by the College of Deans.

This thesis will be defended in public on

Monday 10 february 2014 at 12.45 hours

by

Zilin Yu

born on 15 march 1984
in Jiangxi, China

Supervisors:
Prof. P.H. Elsinga
Prof. F. Wang
Prof. R.A.J.O. Dierckx

Co-supervisor:
Dr. I.J. de Jong

Assessment committee:
Prof. J.A. Gietema
Prof. S. Liu
Prof. M. H. de Jong

Contents

Chapter 1 General Introduction

1.1 Background

In men prostate cancer is the most common cancer and one of the leading causes of cancer death in western countries. In 2008, the estimated incidence of prostate cancer and resulting deaths in Europe was 3.2 million cases and 1.7 million cases, respectively.

Compared to other solid tumors, prostate cancer is a disease with slow progression. The 5-year survival of patients with localized prostate cancer approximates 100%, but almost half of the patients will be assessed for metastases and five-year survival of these patients drops to 31%. The most common site of prostate cancer metastasis is bone, particularly the axial skeleton. Bone metastases of prostate cancer may be painful and represents a functionally limiting stage of the disease.

Nowadays, the screening of prostate cancer is mainly based on serum prostate-specific antigen (PSA) testing and digital rectal examination (DRE) (*1*). Random transrectal ultrasound (TRUS) guided biopsy is the gold standard method for histological diagnosis of prostate cancer. PSA is a 34 kD androgen-regulated exocrine serine protease. It cleaves the prostate-derived protein “seminogelin” in the seminal fluid for the liquefaction of the semen. Normal cells as well as diseased prostate cells produce PSA. A PSA level of 4.0 ng/mL or higher is used as cut-off to refer for further evaluation or biopsy. However, it has been estimated that 23% - 42% of patients are over-diagnosed using a PSA test (*2*). Also DRE has its drawback with regard to sensitivity and specificity.

Abnormal results from screening using PSA or DRE will be confirmed by random TRUS-guided biopsy. However, sampling of biopsies remains a significant problem, especially when small tumors are present in a large gland. The entire TRUS-guided biopsy procedure has a false negative rate as high as 30 % and is affected by the number of cores obtained. The adverse effects from treatment of prostate cancer due to over-diagnosis are serious. On the other hand, imaging methods allowing accurate localization of tumors in the prostate are still lacking. Hence, new non-invasive imaging techniques of prostate cancer to improve cancer detection and guide proper therapy are warranted.

Positron Emission Tomography (PET) and Single Photon Emission Computed Tomography (SPECT) are non-invasive nuclear imaging technologies that may provide true 3D information of the areas of interest. When applying suitable radiotracers to patients, it is possible to measure and quantify important body functions such as blood flow, oxygen use, and glucose metabolism that are involved in several diseases, including cancer. In prostate cancer diagnosis, PET/SPECT could offer regional information of the primary cancer and metastasis. PET/SPECT could also serve as a tool to measure the effect of therapy.

The quality of PET and SPECT images is mainly depending on the distribution of radiotracers. The critical issue in prostate cancer imaging using PET and SPECT is the development of suitable radiotracers, which selectively accumulate in cancer, but not in other normal organs, and of which uptake correlates with tumor growth. In this regard several promising radiotracers such as ^{18}F-FDG, ^{18}F or ^{11}C-labelled acetate, and ^{18}F of^{11}C-labelled choline are being investigated. The most common PET tracer used for imaging of cancer, 2-deoxy-2-^{18}F-fluoro-D-glucose (^{18}F-FDG), is a glucose analogue taken up by highly-glucose-consuming cells, such as brain, kidney, and cancer cells. The overexpression of cellular membrane glucose transporters and enhanced hexokinase enzymatic activity in tumor cells leads to the malignancy-induced hypermetabolism of ^{18}F-FDG. Unfortunately, accumulation of ^{18}F-FDG in prostate cancer may overlap with normal prostate activity and uptake in benign prostatic hyperplasia. Radioactivity excreted in the urinary bladder may also affect detection of lesions in the prostate gland.

Therefore, ^{18}F-FDG is not suitable for diagnosis or staging of primary prostate cancer and of local recurrence in general (*3-4*). On the other hand, ^{18}F-FDG may be useful in the detection of poorly differentiated primary tumors (Gleason scores 8-10) with high serum PSA values (*5*), and it may be also useful in evaluating treatment response of patients with metastatic disease and in prognostication of castrate-resistance.

Acetate participates in cytoplasmic lipid synthesis, which is increased in tumors. Although ^{11}C-acetate uptake in primary prostate cancer, in benign prostatic hyperplasia and in normal prostate tissue may overlap, uptake in prostate cancer generally is higher. In comparison with ^{18}F-FDG, ^{11}C-acetate is more sensitive in the detection of primary prostate cancer (*6*). The limited urinary excretion of ^{11}C-acetate is another advantage over ^{18}F-FDG for imaging prostate cancer.

The upregulation of choline kinase in malignancy leads to the accumulation of phosphatidylcholine (lecithin) in membranes of tumor cells. ^{11}C-choline and^{11}C-acetate appear to be equally useful in imaging prostate cancer in individual patients. Similar to ^{11}C-acetate and ^{18}F-FDG, ^{11}C-choline cannot differentiate between tumor and benign prostate disease.

Radiolabelled antibodies and peptides were developed as probes for nuclear imaging of cancer because of their specific binding affinity to receptors overexpressing in primary tumor and/or metastasis, but not so in healthy tissues. Gastrin-releasing peptide receptor (GRPR) is a well-studied target for prostate cancer imaging. As imaging probes radiolabelled peptides have several advantages over antibodies: lack of immunogenicity, quick diffusion and well-established conjugation and labeling strategies. On the other hand, the drawback of peptides may be metabolic stability which needs to be improved. Although research focusing on developing radiolabelled bombesins for GRPR imaging was blooming the last two decades, only a few bombesins were translated into clinical trials. Improvement of the binding affinity to the GRPR, *in vivo* stability, and pharmaceutical kinetics of radiolabelled bombesins are still needed for imaging prostate cancer. Therefore we developed a variety of new radiolabelled bombesin peptides for imaging of prostate cancer using PET or SPECT.

1.2 Aim and Outline

The aim of this thesis was to develop radiotracers, based on bombesin peptides, for SPECT or PET imaging of GRPR receptor expressing cancers, especially prostate cancer.

Chapter 2 reviews the trends in the development of new bombesin radiotracers over the last years. This chapter is conceived as an update of a previous review from our group.

In **Chapter 3**, we describe the synthesis and evaluation of a ^{99m}Tc labelled truncated bombesin peptide for imaging GRPR. In this study, we used bombesin(7-14) as the biomolecule as it is the peptide sequence responsible for specific binding to the GRPR. HYNIC was employed as the bifunctional chelator to constitute the ternary ligand system with TPPTS and tricine for the labeling of ^{99m}Tc, which is the most common radionuclide used in clinical SPECT imaging. The optimal labeling efficiency, stability, and *in vivo* kinetics of the ^{99m}Tc-HYNIC core (combined with TPPTS and tricine) have been demonstrated in a previous study on Arginine-Glycine-Aspartic acid (RGD) peptides. An alpha -alanine linker was applied as a spacer to reduce the steric effect of the ^{99m}Tc-HYNIC core. Overexpression of GRPR has been reported in colon cancer. Therefore, a human colon cancer (HT-29 cell line) bearing mouse model was chosen as animal model.

As the GRPR is also overexpressed in prostate cancer cells, an attempt to image

prostate cancer using ^{99m}Tc-HYNIC-Tricine/TPPTS-bombesin was carried out. Compared to alpha-Ala-BN(7-14) (24.0±2.0 nM), alpha-aminocaproic acid (Aca) conjugated BN(7-14) showed lower IC_{50} value (20.8±0.3 nM) in competitive binding assay (*7*). By changing alpha-alanine to alpha-aminocaproic acid (Aca) we sought to improve GRPR targeting properties and pharmacokinetics of ^{99m}Tc-HYNIC-Tricine/TPPTS-Aca-bombesin(7-14) (^{99m}Tc-HABN, both in vitro and in vivo in a human prostate cancer bearing mouse model. The results of the in vivo and in vitro evaluation were reported in **Chapter 4**.

The potential prostate cancer imaging candidate ^{99m}Tc-HABN therefore was tested to meet radiopharmaceutical requirements under GMP conditions. The clinical translation and primary clinical study results of the ^{99m}Tc-HABN were summarized in **Chapter 5**.

The results from a clinical imaging trial on biopsy proven prostate cancer of eight patients (four patients scheduled for laparoscopic radical prostatectomy (RP), four planned for external beam radiotherapy (EBRT)) using ^{99m}Tc-HABN SPECT/CT yielded concerns on the low radioactivity retention in tumor, rapid degradation and affinity of the radiotracer.

Three projects which aim to increase the half-life and retention of radioactivity in tumor, to improve the in vivo stability, and to increase the binding affinity to GRPR are reported in Chapter 6, 7, and 8.

In an attempt to obtain a bombesin tracer with relatively long physical half-life allowing extended retention in tumor cells and SPECT imaging, ^{123}I-cubane-TFP ester was coupled with Aca-bombesin(7-14). The ^{123}I-cubane introduced was proven to be stable *in vivo*. The reaction condition for the conjugation between ^{123}I-cubane-TFP ester and peptide was mild and easy to be translated for the radio-labeling of peptides or proteins. As a candidate for SPECT imaging of prostate cancer, the newly developed ^{123}I-bombesin was systematically evaluated *in vitro* and *in vivo* (**Chapter 6**).

To overcome the stability issues of the bombesin tracers, a lanthionine internal bridge was introduced between two cystine residues which placed in bombesin peptide sequence. A series of lanthionine-stablized bombesins were synthesized with variety locations of lanthionine crosslink. The binding affinity of the stabilized bombesins to GRPR was compared in *in vitro* comparative binding assay. Two of the stabilized bombesins (C5 and C6) with best binding affinity to GRPR were selected and labelled with ^{18}F by coupling with the established labeling agent N-succinimidyl-4-^{18}F-fluorobenzoate (^{18}F-SFB). The potential of using ^{18}F-labelled C5 and C6 for imaging prostate cancer with PET was evaluated *in vitro* and *in vivo* with human prostate cancer bearing athymic mice (**Chapter 7**).

Multimerization strategy has been shown to improve the binding kinetics of small peptides (such as RGD peptides) to their targets. In **Chapter 8**, we reported a new bombesin homo-dimer with two identical Aca-BN(7-14) moieties (chapter 4, 5, 6) linked with Glutamine acid. Comparison of the bombesin dimer and monomer on their potential for imaging prostate cancer was feasible by applying same ^{99m}Tc-labeling strategy (as described in Chapter 4) on the dimeric bombesin. The in vitro stability, cellular uptake kinetic, internalization and efflux kinetics, biodistribution and SPECT/CT imaging prostate of ^{99m}Tc-homo-dimer were demonstrated in Chapter 8. Compared to ^{99m}Tc-HABN, the effect of the additional Aca-bombesin(7-14) moiety in ^{99m}Tc-dimer was discussed as well.

Chapter 9 summarizes the studies performed in this thesis and gives a general future perspective for the further development of bombesin tracers.

References

(1) Draisma, G., Etzioni, R., Tsodikov, A., Mariotto, A., Wever, E., Gulati, R., Feuer, E., and de Koning, H. (2009) Lead time and overdiagnosis in prostate-specific antigen screening: importance of methods and context. *Journal of the National Cancer Institute101*, 374-83.

(2) Jadvar, H. (2013) Imaging evaluation of prostate cancer with (18)F-fluorodeoxyglucose PET/CT: utility and limitations. *European journal of nuclear medicine and molecular imaging*.

(3) Salminen, E., Hogg, A., Binns, D., Frydenberg, M., and Hicks, R. (2002) Investigations with FDG-PET scanning in prostate cancer show limited value for clinical practice. *Acta oncologica41*, 425-9.

(4) Oyama, N., Akino, H., Suzuki, Y., Kanamaru, H., Sadato, N., Yonekura, Y., and Okada, K. (1999) The increased accumulation of [^{18}F]fluorodeoxyglucose in untreated prostate cancer. *Japanese journal of clinical oncology29*, 623-9.

(5) Oyama, N., Akino, H., Kanamaru, H., Suzuki, Y., Muramoto, S., Yonekura, Y., Sadato, N., Yamamoto, K., and Okada, K. (2002) ^{11}C-acetate PET imaging of prostate cancer. *Journal of nuclear medicine : official publication, Society of Nuclear Medicine43*, 181-6.

(6) Zhang, X., Cai, W., Cao, F., Schreibmann, E., Wu, Y., Wu, J. C., Xing, L., and Chen, X. (2006) ^{18}F-labelled bombesin analogs for targeting GRP receptor-expressing prostate cancer. *Journal of nuclear medicine : official publication, Society of Nuclear Medicine47*, 492-501.

Chapter 2

An Update of Radiolabelled Bombesin Analogues for Gastrin-Releasing Peptide Receptor Targeting

Zilin Yu, Hildo J. K. Ananias, Giuseppe Carlucci, Hilde D. Hoving, Wijnand Helfrich, Rudi A. J. O. Dierckx, Fan Wang, Igle J. de Jong, Philip H. Elsinga

Curr Pharm Des 2013;19(18):3329-41.

Abstract

Prostate cancer is a critical public health problem in USA and Europe. New non-invasive imaging methods are urgently needed, due to the low accuracy and specificity of current screen methods and the desire of localizing primary prostate cancer and bone metastasis. Positron Emission Tomography (PET) and Single Photon Emission Computed Tomography (SPECT) are the non-invasive and sensitive imaging methods which have been widely used for diagnosing diseases in the clinic. Lack of suitable radiotracers is the major issue for nuclear imaging of prostate cancer, although radiolabelled bombesin peptides targeting the Gastrin-Releasing Peptide Receptor (GRPR) on tumor cells are widely investigated. In this review we discuss the recent trends in the development of GRPR-targeted radiopharmaceuticals based on BN analogues with regard to their potential for imaging and therapy of GRPR-expressing malignancies. Following a brief introduction of GRPR and bombesin peptides, we summarize the properties of prostate cancer specific radiolabelled bombesins. New bombesin tracers published in the last five years are reviewed and compared according to their novelties in biomolecules, radionuclides, labeling methods, bifunctional chelators and linkers. Hot topics such as multimerization, application of agonists and antagonists are highlighted in the review. Lastly, a few clinical trials of cancer nuclear imaging with radiolabelled bombesin are being discussed.

Keywords: Bombesin, GRPR, Prostate cancer, Bone metastasis, PET, SPECT, Targeting, Imaging

2.1 Introduction

Cancer is a major public health problem worldwide. In the United States, one in four deaths is due to cancer. There were an estimated 3.2 million new cases of cancer and 1.7 million deaths from cancer in Europe in 2008 (*1*).

Molecular imaging techniques such as magnetic resonance spectroscopy, single-photon emission computed tomography (SPECT) and positron emission tomography (PET) have been well developed in the last three decades. Suitable imaging probes have been developed for a broad array of molecular targets, allowing *in vivo* detection and functional characterization of tumors. Current molecular imaging techniques can provide relevant biological information needed for a better understanding of tumor biology, thereby enabling more accurate diagnosis and enhanced therapeutic monitoring (*2-5*).

In many cases the exact cause and development of cancer remains largely unknown. However, a variety of receptors (somatostatin receptors (*6*), integrin $\alpha_v\beta_3$ (*7*), gastrin releasing peptide receptors (GRPRs) (*8*), sigma receptors (*9*), neurokinin receptors (*10*), *etc*.) have been identified as over-expressed in cancer cells and appear to play key roles in cancer development. Importantly, many of these receptors are absent or sparsely expressed in normal cells and tissues. Therefore, these receptors could be potential targets for cancer detection if suitable probes and imaging facilities are available.

Radiolabelled peptides for receptor-targeted molecular imaging and radionuclide therapy have been extensively investigated since 1990s. The most successful sample, [^{111}In-DTPA^0]-octreotide (Octreoscan) was introduced since late 1980s and became the gold standard for diagnosis and staging of somatostatin receptor-positive neuroendocrine tumors (*11*). Octreoscan and Neotect are still the only two radiopeptides on the market approved by the Food and Drug Administration. Compared to monoclonal antibody (MAbs), peptides show superiority in clearance kinetics, immunogenicity, ease of manufacturing and radiolabelling. Due to their low molecular weight, peptides easily diffuse into target tissues and clear rapidly from the blood pool, resulting in high tumor-to-non-tumor ratios. In general, peptides are non-immunogenic and can readily be labelled with a variety of radionuclides to serve in SPECT and PET imaging of cancer. Ligands, such as octreotide, Arginine-Glycine-Aspartic (RGD), bombesin, substance P, all have nano-molar binding affinity to specific receptors and as such are promising candidates for cancer imaging (*12, 13*).

Over the past few years, several reviews have been published regarding the development of GRPRs targeting radiopharmaceuticals for nuclear imaging of prostate cancer (*2, 14-16*). In this review, we discuss the latest trends in this rapidly expanding field.

2.2 Peptide-Based Radiopharmaceuticals

A radiolabelled peptide (Figure 1) for SPECT or PET imaging of receptors should fulfill several requirements including:

1) An isotope with optimal nuclear properties, availability and physical half-life matching the biological half-life of the tracer *in vivo*;
2) A multidentate bifunctional chelator (BFC) which enables efficient labeling, stable radionuclide chelating, and optimal *in vivo* behavior is used to attach the metallic radionuclide to the BN peptide, whereas an organic precursor or synthon is often needed for the ^{18}F and ^{11}C-labeling;
3) A pharmacokinetic modifying (PKM) linker, which could improve the excretion

kinetics or/and stability of the radiotracer.

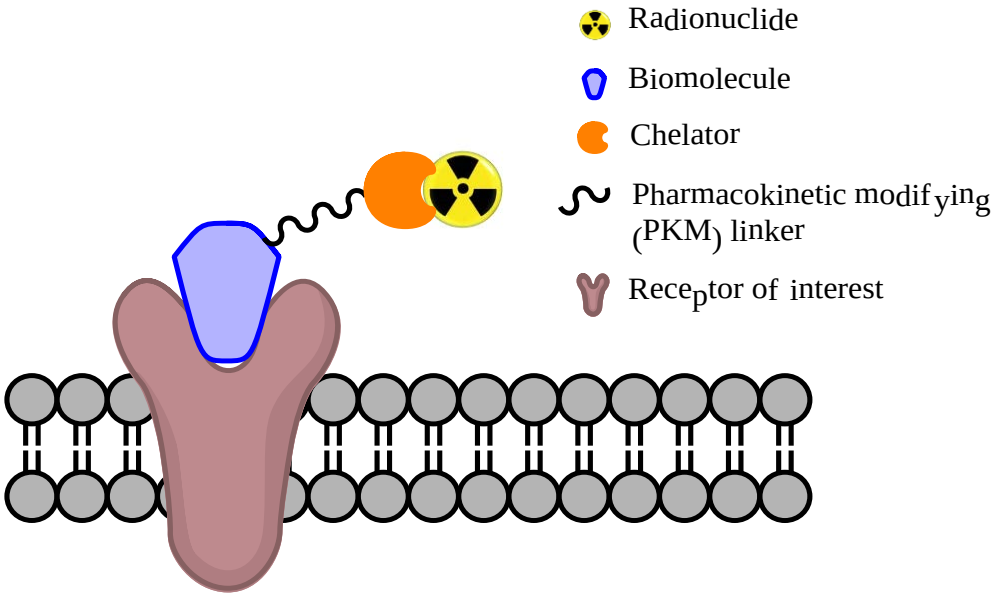

Figure 1. Schematic presentation of the components for membrane receptor-targeting radiotracer design.

The development of novel radiolabelled peptides is aiming to improve the radioactivity accumulation and retention in tumor while reducing the whole body background. However, a simple combination of the elements mentioned above is not a guarantee for a successful receptor-targeting tracer. For predicting the cancer imaging potential of the radiolabelled peptides, chemical, biological and pharmacokinetic characters of the tracer are frequently investigated and discussed, such as the binding affinity to receptors, stability, lipophilicity, internalization and efflux kinetics in tumor cells, tumor uptake and tumor-to-non-tumor (T/NT) ratio, tumor retention time, charge, and *in vivo* clearance. In this article, we addressed the development of bombesin tracers according to the requirements on biomolecule, chelators, linkers and radionuclides mentioned above, and focusing on topics such as the stability issue of peptide, multimerization, bombesin agonist and antagonist.

2.3 Bombesin and GRPRs

BN is a 14 amino-acid peptide (pyroglutamic acid-glutamine-arginine-leucine-glycine-asparagine-glutamine-tryptophan-alanine-valine-glycine-histidine-leucine-methionine -NH_2) first isolated from the skin of frog (*17*). BN and its mammalian counterpart Gastrin-Releasing Peptide (GRP) share an identical C-terminal region of seven amino acid residues. This stretch of 7 residues is essential for binding of GRP and BN to the receptor.

Four subtypes of BN receptors have been reported: neuromedin B receptor, GRPR, and the BB3 and BB4 receptor subtypes (*18-21*). GRPR seems most attractive as it is

over-expressed in many human malignancies, such as prostate, breast, lung, pancreatic, ovarian, renal and gastrointestinal cancer (*8, 22-25*). GRPR expression in breast cancer tissues showed 33 positive cases in 100 carcinomas (*26*).Schally et al. reported the presence of the bombesin receptor subtypes in human ovarian epithelial cancers using RT-PCR (*27*).About 64% of the specimens expressed mRNA for both GRPR and NMBR. In a recently study we found that GRPR is expressed in the vast majority (18 of 21 cases) of lymph node metastases and in 52.9% of bone metastases of prostate cancer (*8, 22-25*). A study investigating the GRPR expression profile in large cohorts of different prostate specimens (benign prostate tissue, primary prostate cancer following radical prostatectomy, castration-resistant prostate cancer (CRPC)) by immunohistochemistry was reported by Beer *et al.*(*28*). They found GRPR expression to be significant ($p<0.001$) higher in prostate carcinomas than in benign prostate tissues, which was significantly inverse correlated to the PSA level ($p=0.026$), tumor size ($p=0.014$) and Gleason scores ($p=0.026$), but not correlated to tumor stage ($p=0.439$) and margin status ($p=0.100$). The expression of GRPR also shows a highly significant correlation with androgen receptor (AR) expression ($p<0.001$), as well as with cyclin D1 expression ($p<0.001$). Cyclin D1 protein over-expression might be related to the evolution of androgen-independent disease in prostate cancer (*29, 30*). These data indicate that GRPR might have influence on the course and therapy of prostate cancer, but also constitute a caveat for the use of GRPR as a target in diagnostic or therapeutic approaches of prostate cancer since high grade prostate cancer can be low in GRPR.

2.4 Targeting Biomolecules

2.4.1 Improving Stability with Non-natural Amino Acids

BN-like peptides have potent biological effects such as stimulating gastric acid and pancreatic enzyme secretion or gall bladder contraction (*31*), so it is common that the peptides could be rapidly and selectively degraded by proteolytic enzymes to regulate expression levels (*32*).

Therefore many attempts to stabilize peptides have been published. Linder *et al.* studied the metabolism of ^{177}Lu-DO3A-CH_2CO-G-(4-aminobenzoyl)-Gln-Trp-Ala-Val-Gly-His-Leu-Met-NH_2 (^{177}Lu-AMBA) *in vitro* and *in vivo* in a mouse and a rat model (*33*). Three major and two minor metabolites (figure 2) of ^{177}Lu-AMBA were reported. Rapid metabolism in blood of mice and rats was observed. Two minutes after *i.v.* administration to normal mice, only ~45% of the radioactivity in the plasma was present as ^{177}Lu-AMBA. None of the metabolites of ^{177}Lu-AMBA showed any significant binding to GRPR. The biodistribution results of animal experiments in human prostate cancer bearing mice indicated that only intact ^{177}Lu-AMBA has GRPR targeting ability.

For prolonging the exposure of GRPR to radiolabelled BN , it's important to improve the stability of radiolabelled BN. Replacement of the original amino acids of BN(7-14) by non-natural amino acids or modified amino acids to increase the metabolic stability of BN peptides have been studied in the last decade (*34-39*).

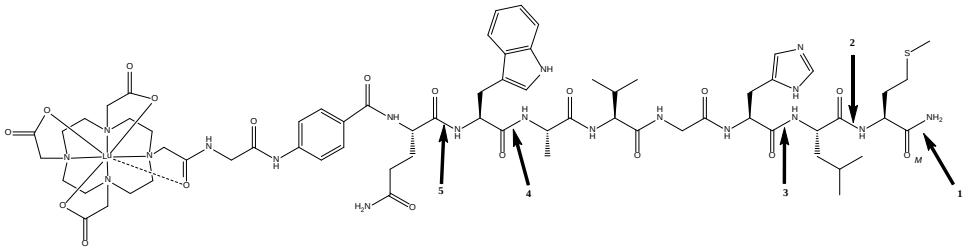

Figure 2. Chemical structure of ^{177}Lu-AMBA and five *in vivo* cleavage sites

Recently, Honel*et al.* reported the synthesis and evaluation of four ^{18}F labelled BN tracers (*34*). Met^{14} was replaced by Leu for stabilization against aminopeptidase 3.4.11.1, and Leu^{13} was replaced by a non-natural amino acid (FA01010 or Sta) to prevent cleavage by neutral endopeptidase 3.4.24.11, while methylated versions of His^{12} and/or Gly^{11} were introduced for the preparation of four truncated BN analogues (Figure 3). Arg-Ava-Gln-Trp-Ala-Val-NMeGly-His-Sta-Leu-NH_2 (4b) was selected according to its higher *in vitro* binding affinity to GRPR than the other three analogues and 2-(4-(di-tert-butyl[^{18}F]fluorosilyl)phenyl)acetyl-Arg-Ava-Gln-Trp-Ala-Val-NMeGly-His-Sta-Leu-NH_2 ([^{18}F]-4b) was further evaluated *in vitro* and *in vivo*. No significant degradation of [^{18}F]-4b was detected in PBS, neither in mouse nor in human plasma within 2 h. This compound also showed high *in vivo* stability against degradation by endogenous enzymes which are present in the blood of mouse. Although the *in vitro* binding affinity of Arg-Ava-Gln-Trp-Ala-Val-NMeGly-His-Sta-Leu-NH_2 was in the low nanomolar range (22.9 nm), the tumor uptake of ^{18}F-4b was low and unspecific in human prostate tumor (PC-3)-bearing nude mice. In contrast, mouse pancreas revealed a high and specific accumulation of [^{18}F]-4b that may be due to the higher GRPR density in pancreas than in PC-3 tumors and the better accessibility of ^{18}F-4b to the pancreatic acinar cells than to PC-3 tumor cells. Due to the lipophilic character of [^{18}F]-4b, it exhibited a mainly hepatobiliary route clearance.

As an improvement of Demobesin 1 (*42*), Wael*et al.* reported an ^{111}In labelled antagonist-BN with the formula DOTA-aminohexanoyl-[D-Phe^{6}, Leu-$NHCH_2CH_2CH_3$^{13}, des Met^{14}]BN(6-14)(Bomproamide) (*36*). Rapid (0.25 h), specific and significant high tumor uptake (6.90 ± 1.06 %ID/g), fast clearance from the other tissues were observed in biodistribution experiments using ^{111}In-Bomproamide. The PC-3 tumor-xenografts were visualized clearly in microSPECT/CT images with low abdominal background. The stability of ^{111}In-Bomproamide was not reported in the article.

Although, non-natural amino acids may enhance the stability of radiolabelled BN, improvement of imaging quality is not guaranteed. The enhanced stability of radiolabelled BN will also lead to the higher accumulation and longer retention of radiolabelled bombesins in normal organs and tissues, which will initially result in increase of background. Therefore the *in vivo* kinetics of the radiolabelled BN should also be considered.

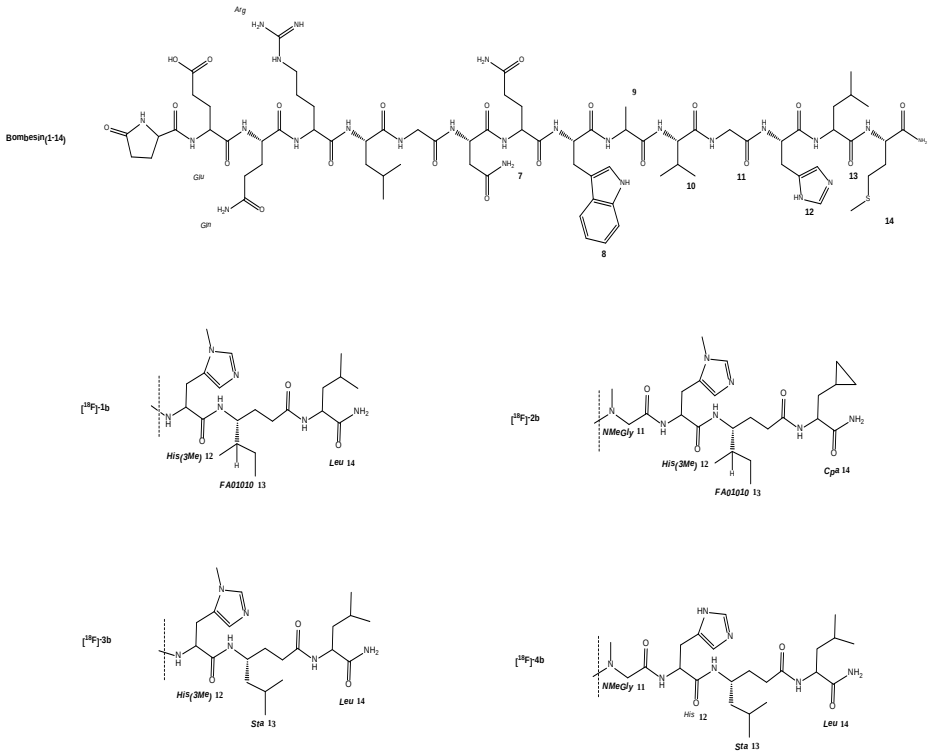

Figure 3. Chemical structure of original BN peptide and non-nature amino acids modified bombesin derivatives.
[^{18}F]-1b=3-(3-(Di-*iso*-propyl[^{18}F]fluorosilyl)phenyl)acetyl-Ava-Gln-Trp-Ala-Val-Gly-His(3Me)-FA01010-Leu-NH_2,
[^{18}F]-2b=2-(4-(Di-*tert*-butyl[^{18}F]fluorosilyl)phenyl)acetyl-Ava-Gln-Trp-Ala-Val-NMeGly-His(3Me)-FA01010-Cpa-NH_2,
[^{18}F]-3b=2-(4-(Di-*tert*-butyl[^{18}F]fluorosilyl)phenyl)acetyl-Arg-Ava-Gln-Trp-Ala-Val-Gly-His(3Me)-Sta-Leu-NH_2,
[^{18}F]-4b=2-(4-(di-tert-butyl[^{18}F]fluorosilyl)phenyl)acetyl-Arg-Ava-Gln-Trp-Ala-Val-NMeGly-His-Sta-Leu-NH_2.

2.4.2 Improving the Binding Affinity with Multimerization

The approach of maximizing binding affinity of radiolabelled peptides for receptors by multimerization started in the 1990s. Usually, a rationally-designed multimer consists of a framework and two or more motifs that target the desired binding site (Figure 4). The multimerization aims at increasing the receptor binding affinity and improving the binding kinetics of the biomolecule (*40*). A prominent example thereof is the use of radiolabelled cyclic RGD multimers(*41*). The monovalent-interactions between one multimer and neighboring receptors are key for a higher integrin $\alpha_v\beta_3$ receptors targeting capability and better tumor uptake with longer tumor retention time.

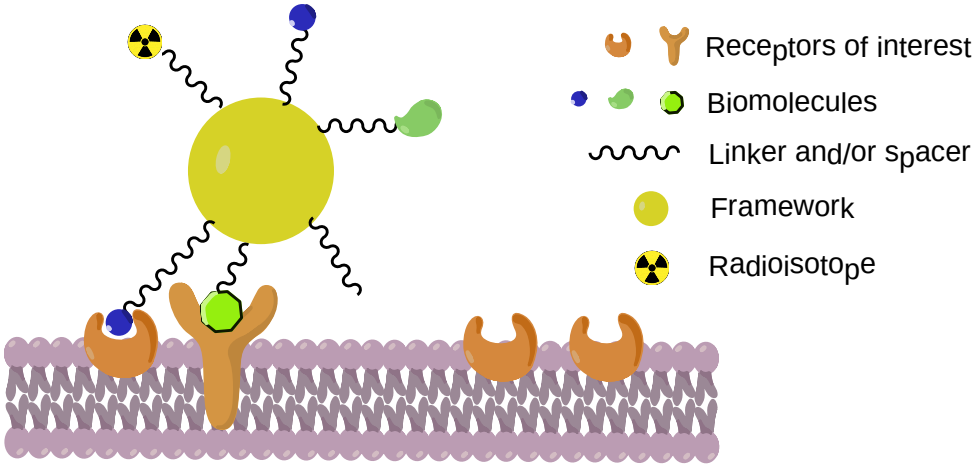

Figure 4. Schematic view of receptor targeted radiolabelled multimer.

Several properties should be taken into account for the design of multimeric tracers, including the choice of frameworks and receptor specific motifs, the distance between motifs (flexibility of the spacer) and receptor density on targeted tumor cells.

The framework of the multimer usually consists of a peptide, protein (antibodies or albumin), liposome, nanoparticle or small chemical compound. The framework mainly functions as a linker for several motifs that target the receptors of interest. Furthermore, the framework supplies active positions for radiolabelling or conjugation of chelators and/or radiolabelling group. For example, polyethylene glycolic acid (PEG) linkers have been successfully used as the framework for a variety of cyclic RGD multimers and are responsible for the enhanced integrin $\alpha_v\beta_3$-mediated avidity and improved *in vivo* kinetics (*42-44*).

Accardo*et al.* (*45*) developed two liposomes obtained by co-assembling two different amphiphilic molecules for selective targeting of BN receptors (Figure 5). Compared to the corresponding aggregate containing the negative control peptide scrBN, only ^{111}In-$(C18)_2$DOTA/$(C18)_2$L5-BN(7-14) has higher specific uptake on PC-3 cells. The presence of the PEG3000 unit on the external liposomal surface may have masked the peptide, thereby preventing receptor binding. Long circulation time (4-5 h half-life) in blood was observed. Only slightly increased on tumor uptake of ^{111}In-$(C18)_2$DOTA/$(C18)_2$ L5-BN(7-14) (2.4%ID/g) was observed when compared to the scrambled peptide as negative control (1.6 %ID/g).

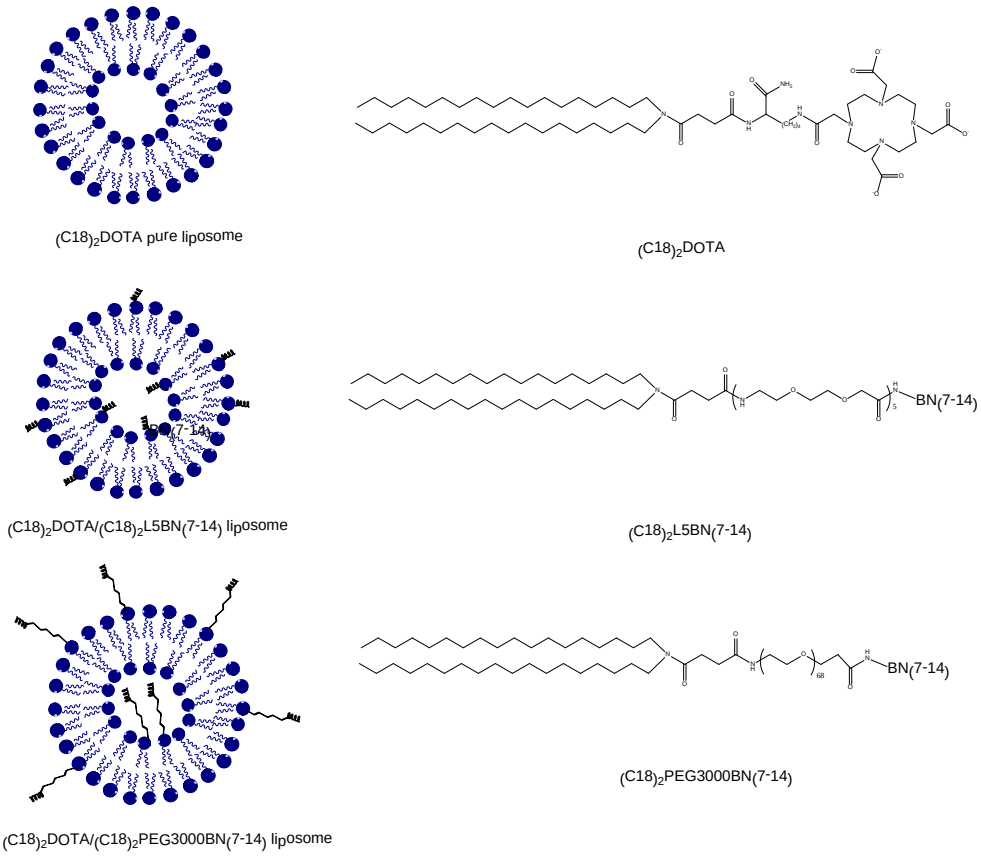

Figure 5. Schematic representation of amphiphilic monomers and liposomal aggregates.

A ^{64}Cu labelled dimeric BN was reported by Ma *et al.* (*46*). The dimeric BN peptide (L^2-BBN_2) was synthesized by conjugation of two Lys^3-BN motifs to a single cage amine ligand (Figure 6). The ^{64}Cu labeling was performed in high radiochemical yield at room temperature. The biological evaluation of the ^{64}Cu-L^2-BBN_2 has not been reported yet.

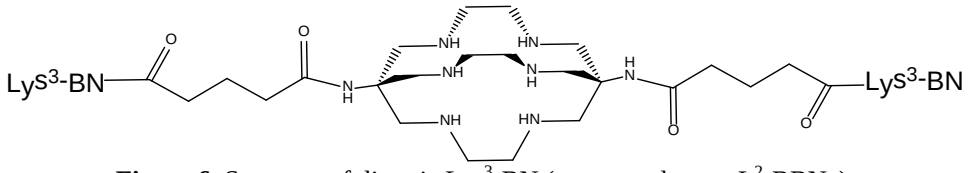

Figure 6. Structure of dimeric Lys^3-BN (compound name L^2-BBN_2).

For BN multimers, as described above, a variety of GRPR specific BN motifs with high binding affinity have been developed.

To further improve the tumor accumulation and imaging contrast of BN tracers, a heterodimer of RGD-BN, which can target two types of receptors (integrin $\alpha_v\beta_3$ and GRPR) simultaneously, was developed (*47-54*). The newly developed RGD-BN heterodimers shared two different bioactive ligands: Aca-BN(7-14) and c(RGDyK). A variety of linkers has been used to improve the *in vivo* pharmacokinetics and tumor accumulation of the

heterodimers. RGD-BN heterodimers have been labelled with ^{64}Cu, ^{68}Ga, ^{18}F, and ^{99m}Tc for PET and SPECT imaging of prostate cancer, breast cancer and lung cancer (Table 1).

The first RGD-BN heterodimer which has comparable binding affinity to the GRPR and integrin $\alpha_v\beta_3$, compared to corresponding BN and RGD monomers, was reported by Li *et al.* (*47*). ^{18}F-RGD-BN had significantly higher tumor uptake and higher T/N ratios compared with ^{18}F-FB-[Lys^3]BN(1-14), resulting in significantly higher imaging quality. The results of blocking experiments in PC-3 tumor bearing mice indicate that both ligands (RGD and BN) are responsible for specific accumulation of the ^{18}F-BN-RGD in tumor. RGD-BN is synthesized with glutamate as the framework. Actually RGD-BN is a mixture of Glu-BN-RGDGlu-RGD-BN (Figure 7). These isomers cannot be separated by HPLC. Also for improving the radiochemical yield, a -Glu-OAll was introduced as orthogonally protecting building block in a follow up study (*48*). A PEG_3 spacer has also been inserted into the glutamate α–amino group to increase the hydrophilicity and to alleviate the steric hindrance without affecting the biological activity of RGD and BN motif (Figure 7). Both ^{18}F RGD-BN heterodimers have comparable tumor uptake and non-specific tissue uptake, while the kidney uptake of ^{18}F- PEG_3-RGD-BN was lower.

The glutamate linker was replaced by a symmetric linker 3, 3'- (2-amino-ethylazanediyl) dipropanoic acid (AEADP) to obtain a mixture of isomers of RGD-BN heterodimer (*52*). The ^{18}F- AEADP-BN-RGD showed comparable tumor imaging ability as ^{18}F- PEG_3-RGD-BN. The ^{64}Cu, ^{68}Ca and ^{99m}Tc labelled bombesin heterodimers have been developed based on the identical RGD-BN (Figure 7, Table 1, table 2) (*49-51, 53-54*). ^{68}Ga-NOTA-RGD-BN showed higher tumor uptake and blood retention as compared to ^{18}F and ^{64}Cu-labelled RGD-BN. The T/NT ratios of ^{18}F-FB-RGD-BN were all significantly higher than those of ^{68}Ga-NOTA-RGD-BN and ^{64}Cu-NOTA-RGD-BN due to the more rapid washout of ^{18}F-FB-RGD-BN in blood and normal organs.

The ^{99m}Tc-labelled HYNIC-RGD-BN dimer was compared with the gold standard tracer ^{18}F-2-fluoro-2-deoxyglucose (^{18}F-FDG) in a lung carcinoma animal model (*54*). Compared to ^{18}F-FDG, the tumor-to-muscle and tumor-to-inflammation ratio were significant higher although the absolute uptake of ^{99m}Tc- HYNIC-RGD-BN was lower. They also found that ^{99m}Tc- HYNIC-RGD-BN was able to detect the pulmonary metastases in mice.

So far, ^{18}F-PEG_3-RGD-BN hetero-dimer is the most promising BN hetero dimer for nuclear imaging of GRPR positive prostate cancer. Compared to the corresponding RGD and BN tracers, ^{18}F-PEG_3-RGD-BN showed superiority in tumor uptake and *in vivo* kinetics.

Table 1 RGD-BN heterodimers mentioned in this article.

Reference	Analogue	IC_{50} (nM)		Uptake values(%ID/g)						T/NT ratios		
		GRPR	Integrin $\alpha_v\beta_3$	Tumor				Liver	Kidney	T/M	T/L	T/K
				GRPR		Integrin $\alpha_v\beta_3$						
Li *et al(47)*	^{18}F-FB-Glu-RGD-BBN/ ^{18}F-FB-Glu-BBN-RGD ^{18}F-FB-RGD ^{18}F-FB-BBN	32.0	282.0	PC-3	5.0^{m}	DU-145	2.2^{m}	4.0 *^{m}	7.0 *^{m}	5.0 * $^{m\ 1h}$	3.0 *$^{m\ 1h}$	1.0 * ^{1h}
Liu *et al(48)*	^{18}F-PEG$_3$-Glu-RGD-BBN FB-RGD FB-BBN	73.3 NA 79.0	13.8 11.2 NA	PC-3	6.4 ^{m} NA NA	NA	NA NA NA	< 2.0 * ^{m} NA NA	7.0 * ^{m} NA NA	10.5 $^{m\ 2h}$ NA NA	6.4 $^{m\ 2h}$ NA NA	1.4 $^{m\ 2h}$ NA NA
Yan *et al(52)*	^{18}F-FB-AEADP-BBN-RGD	167	553	PC-3	5.2 ^{m}	NA	NA	2.6 ^{m}	~5 * ^{m}	6.0 $^{m\ 2h}$	3.3 $^{m\ 2h}$	1.2 $^{m\ 2h}$
Liu *et al(50)*	^{64}Cu-NOTA-RGD-BBN ^{a} ^{64}Cu-DOTA-RGD-BBN ^{a} ^{64}Cu-NOTA-RGD ^{b} ^{64}Cu-NOTA-BBN ^{c}	92.8 85.8 NA 71.6	16.2 21.6 10.8 NA	PC-3	3.1 ^{m} 3.1 ^{m} 1.0 ^{m} 2.3 ^{m}	4T1	1.9 $^{m\ 2h}$ NA 0.7 $^{m\ 2h}$ 0.3 $^{m\ 2h}$	3.5 ^{m} 3.4 ^{m} 2.9 ^{m} 10.5 ^{m}	4.1 ^{m} 6.0 ^{m} 3.3 ^{m} 3.6 ^{m}	NA NA NA NA	1.0 * ^{m} 1.0 * ^{m} 0.5 * ^{m} 0.4 * ^{m}	0.8 * ^{m} 0.5 * ^{m} 0.4 * ^{m} 0.8 * ^{m}
Liu *et al(49)*	^{68}Ga-NOTA-RGD-BBN ^{a} ^{68}Ga-NOTA-RGD ^{b} ^{68}Ga-NOTA-BBN ^{c}	55.9 NA 79.0	22.6 11.2 NA	PC-3	6.6 ^{m} 2.0 * ^{m} 6.4 * ^{m}	MDA-MB-435	3.2 ^{m} 1.6 ^{m} 0.4 ^{m}	2.0 * ^{m} 1.2 * ^{m} 2 ^{m}	10 * ^{m} 9.0 * ^{m} 5.5 * ^{m}	4.5 * $^{m\ 1h}$ 3.0 * $^{m\ 1h}$ 6.0 * $^{m\ 1h}$	5.0 * $^{m\ 1h}$ 2.0 * $^{m\ 1h}$ 3.5 * $^{m\ 1h}$	1.0 * $^{m\ 1h}$ 0.4* $^{m\ 1h}$ 0.8 * $^{m\ 1h}$
Liu *et al(51)*	^{18}F-PEG$_3$-Glu-RGD-BBN ^{68}Ga-NOTA-RGD-BBN ^{a} ^{64}Cu-NOTA-RGD-BBN ^{a}	73.3 92.8 92.8	13.8 16.2 16.2	NA	NA NA NA	T47D& MDA-MB-435	3.0 &2.7 m 3.9 &3.4 m 3.7 &3.4 m	1.1 m 2.7 m 4.8 m	2.8 m 4.4 m 5.3 m	5.5 * $^{m\ 1h\ T}$ 1.5 * $^{m\ 1h\ T}$ 2.2 * $^{m\ 1h\ T}$	3.0 * $^{m\ 1h\ T}$ 1.5 * $^{m\ 1h\ T}$ 0.7 * $^{m\ 1h\ T}$	1.3 * $^{m\ 1h\ T}$ 0.8 * $^{m\ 1h\ T}$ 0.6 * $^{m\ 1h\ T}$
Jackson *et al(53)*	^{64}Cu-NO2A-RGD-BBN^{a} ^{64}Cu-NO2A-BBN ^{c}	8.9 ^{nat} NA	NA NA	PC-3	4.0 ^{1h} 4.7 * ^{1h}	NA	NA NA	1.0 ^{1h} 2.5 * ^{1h}	4.7 ^{1h} 4.6 * ^{1h}	18 ^{1h} NA	3.8 ^{1h} NA	0.9 1h NA
Liu *et al(54)*	^{99m}Tc-HYNIC-RGD-BBN ^{a} RGD BBN ^{18}F-FDG	104.7 NA 71.6 NA	18.8 10.8 NA NA	LLC	2.7 ^{1h} NA NA 6.6 ^{1h}	NA	NA NA NA NA	1.5 * ^{1h} NA NA 5.0 * ^{1h}	16.4 ^{1h} NA NA 36.0 ^{1h}	4.1 ^{1h} NA NA 2.1 ^{1h}	NA NA NA NA	NA NA NA NA

GRPR= gastrin releasing peptide receptor; NA= not available; uptake values (in %ID/g) and T/N ratios are determined in several organs and PC-3 tumor at 0.5 h p.i. unless stated otherwise; a = IC_{50} determined with non-metallated analogue; b = IC_{50} determined with c(RGDyK); c: IC_{50} determined with aca-bombesin(7-14); 1h and 2h = uptake values or T/N ratios determined at 1h or 2h p.i.; T=the T/NT ratios determined in T47D tumor bearing mice; * = *estimated from graph; m = acquired by calculating the average radioactivity accumulation in ROIs drawn in microPET images*.

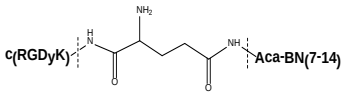

Glu-BN-RGD

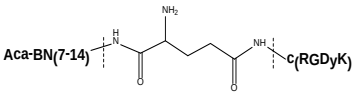

Glu-RGD-BN

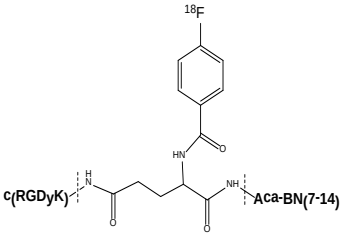

^{18}F-RGD-BN

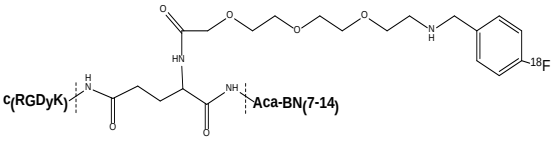

^{18}F-PEG3-RGD-BN

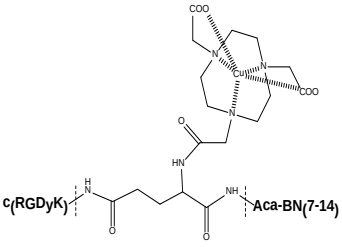

Cu-NO2A-RGD-BN

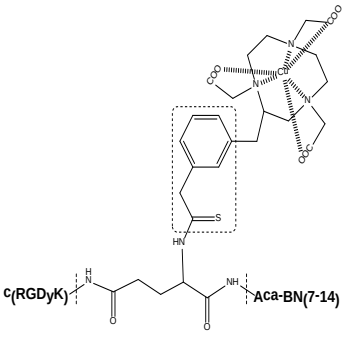

Cu-NOTA-RGD-BN

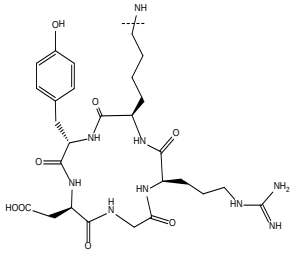

c(RGDyK)

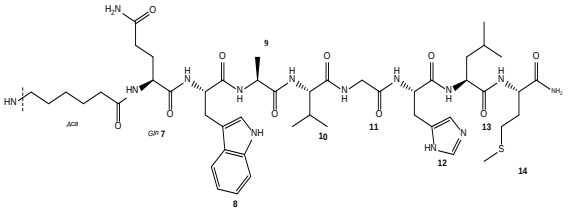

Aca-BN(7-14)

Figure 7. Chemical structures of Glu-BN-RGD, Glu-RGD-BN, ^{18}F-RGD-BN, ^{18}F-PEG$_3$-RGD-BN, Cu-NO2A-RGD-BN, Cu-NOTA-RGD-BN, c(RGDyK), and Aca-BN(7-14).

2.4.3 Agonist versus Antagonist BN Analogues

An agonist is considered to be a ligand that activates receptors to produce second messengerst hat cause a cascade of biochemical transformations. An antagonist produces no effect on its own but blocks the effect of agonist by occupying the same active site of the receptor. Most BN radiotracers developed for cancer imaging are agonists, which can internalize into the tumor cells via membrane receptors. It has been suggested that this could result in higher accumulation than antagonists. The antagonists can be divided in to permissive and non-permissive antagonists according to their binding site on the G-protein coupled receptor (GCPR). 1) Permissive antagonist: if the antagonist binds to its own site on the receptor, it can (changes the shape of the receptor) modify the receptor reactivity toward agonist in different ways from increasing affinity to decreasing it (allostericmodulator), in other words, they impart probe-dependent effects on receptor. 2) Non-permissive antagonist: when antagonists bind to the agonist-binding site, it does not allow any agonist to impart information to the receptor (*55*). The probe could also be radiolabelled antagonist.

Nowadays, newly developed BN antagonists with improved *in vivo* profiles such as high tumor accumulation, rapid clearance from normal organs, etc., may yield qualified candidates for cancer nuclear imaging as well.

A systematic comparison of one BN antagonist and four agonists was reported by Schroeder *et al.* (*56*). The five radiolabelled BN analogues were selected on the basis of their prostate cancer targeting efficacy reported previously and evaluated in PC-3 tumor-bearing mice. The tumor uptake of Demobesin-1(antagonist) (Figure 8) reached peak levels (3.0±0.4 %/ID/g) at 1h p.i., although higher than other four analogues it was not significant different from that of AMBA (Figure 8) (2.7±0.5 %/ID/g) and PESIN (Figure 8) (2.3±0.5 %/ID/g). Comparing the decrease of Demobesin-1 uptake in tumor from 1h to 24h, the tumor uptake of AMBA and PESIN remain fairly stable which indicate better suitability for imaging at later time points or therapeutic applications.

A comparison between an ^{18}F-labelled BN antagonist and agonist was reported by Yang. *et al.* (*57*). The tumor uptake of ^{18}F labelled agonist (MAGBBN (Gly-Gly-Gly-Arg-Asp- Asn-Gln-Trp-Ala-Val-Gly-His-Leu-MetNH_2)) was almost doubled compared to the ^{18}F labelled antagonist (MATBBN(Gly-Gly-Gly-Arg-Asp-Asn-D-Phe-Gln-Trp-Ala-Val-Gly-His-Leu-NHCH_2CH_3)) counterpart at 1h p.i.. They concluded that ^{18}F-labelled BBN peptide agonists may be better tracers for prostate cancer imaging due to their relatively higher tumor uptake and retention as compared with the antagonist counterparts.

Abiraj*et al.* synthesized a ^{99m}Tc labelled BN antagonist N4-X-D-Phe-Gln-Trp-Ala-Val-Gly-His-Sta-Leu-NH_2 (N4-BB-ANT) with high labeling yield (>97%) and specific activity (37 GBq/μmol) using 6-carboxy-1,4,8,11-tetraazaundecane as chelator (*58*). The tumor uptake was 22.5±2.6 %ID/g at 1 h after administration of the tracer and reached the highest uptake of 29.9±4%ID/g at 4 h p.i.. The SPECT images of PC-3 bearing mice showed a clear delineation of the tumor, low abdominal uptake (except the high uptake in pancreas) with the kidneys being the main excretion organ at 12 h p.i.. Due to the excellent accumulation, long retention in tumor, and high tumor-to-non-tumor ratios, ^{99m}Tc-N4-BB-ANT is a potential candidate as imaging probe for GRPR-positive prostate cancer.

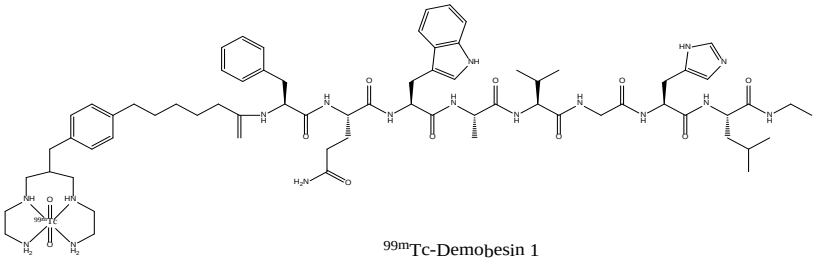

^{99m}Tc-Demobesin 1

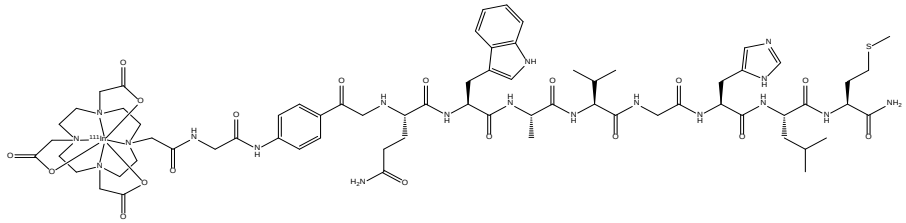

^{111}In-AMBA

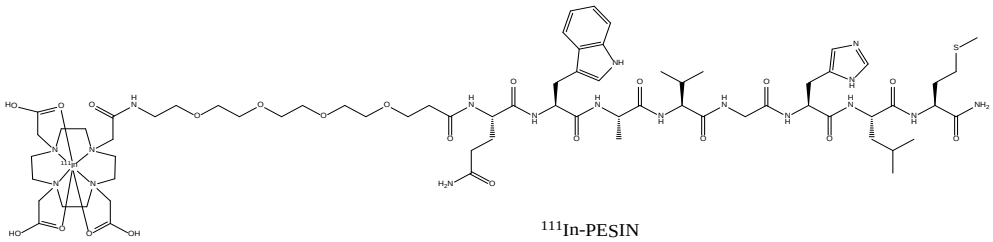

^{111}In-PESIN

Figure 8. Chemical structures of ^{99m}Tc-Demobesin-1, ^{111}In-AMBA and ^{111}In-PESIN.

An ^{18}F-labelled BN antagonist (^{18}F-BAY86-4367) (Figure 9) with favorable pharmacokinetics and rapid tumor targeting and retention has been reported by Honer*et al.*(*59*). The IC_{50} value of BAY86-4367 was 0.94±0.19 nM. The tumor uptake of ^{18}F-BAY86-4367 in prostate cancer-bearing mice was 4.66±0.20%ID/g at 10 min p.i. and steady increased to 6.19±2.49 %ID/g while that of ^{18}F-FDG and ^{18}F-FCH was 1.02 ±0.08 %ID/g and 2.44±0.21 %ID/g at 1h p.i.. GRPR expressing murine pancreas also showed high uptake (>35%ID/g) of the ^{18}F-BAY86-4367 at all examined time points. Consequently, ^{18}F-BAY86-4367 may have higher diagnostic accuracy than the ^{18}F-FDG and ^{18}F-fluorocholine (^{18}F-FCH) for PET imaging of prostate cancer.

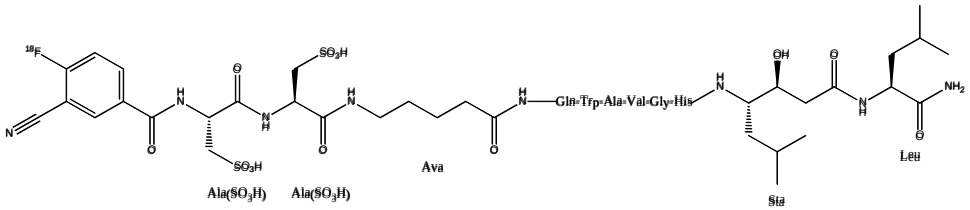

Figure 9. Chemical structure of ^{18}F-BAY86-4367

A few comparative studies suggested that the *in vivo* behavior of receptor antagonists is superior to receptor agonists (*35-36, 56, 60*). However, Yang. *et al. (57)* observed different results from their studies based on a ^{18}F labelled agonist and antagonist. Although radiolabelled BN antagonists with desirable tumor accumulation and *in vivo* behavior have been reported, it's still not clear which would be better candidate for GRPR-positive cancer imaging.

2.5 Chelator and Linker

2.5.1 Bifunctional helator

The choice of the bifunctionalchelator depends on the radionuclide and plays an important role in the performance of radiopharmaceuticals containing radiometals.

The bifunctionalchelators of ^{99m}Tc have quite often been discussed regarding the binding affinity, hydrophilicity, stability of the BN tracers and the retention of these compounds in tumor cells. Ternary ligand systems has been introduced to the synthesis of ^{99m}Tc-HYNIC-Biomecule synthesis since 1990s. 6-hydazinonicotinic acid (HYNIC) is of great interest due to its high ^{99m}Tc-labeling efficiency, the high solution stability of its ^{99m}Tc complexes, and the easy use of different co-ligands (*61*). HYNIC has been employed for ^{99m}Tc labeling of a variety of bioactive peptides, such as RGD, Octreotide, IL-2, BN, and *et al.*(*43, 54, 62-66*). The preparation and preclinical evaluation of ^{99m}Tc-HYNIC (Tricine/TPPTS)-ε-aminocaproic acid-BN(7-14) (^{99m}Tc-HABN) in prostate cancer bearing mice was reported by Ananias *et al.*(*65*). ε-aminocaproic acid-BN(7-14) has also been labelled with ^{18}F (^{18}F-Aca-BN)and compared with 4-^{18}F-Fluorobenzoyl-Lys^3-bombesin (^{18}F-Lys^3-BN) (*67*) . Compared to ^{18}F-Aca-BN (0.71 %ID/g at 30 min p.i.), ^{99m}Tc-HABN exhibited improved GRPR-mediate specific tumor uptake (2.24±0.64 %ID/g at 30 min p.i.) and retention. In contrast with ^{18}F-Lys^3-BN, although the absolute tumor uptake was lower, the T/NT ratios of ^{99m}Tc-HABN were comparable due to the rapid clearance. Due to the hydrophilicity of ^{99m}Tc-HYNIC/Tricine/TPPTS complex, the radioactivity accumulation in liver was 3-fold lower than that of ^{18}F-Aca-BN and ^{18}F-Lys^3-BN at 1h p.i.. Santos-Cuevas *et al.* have reported a clinical study of ^{99m}Tc-EDDA/HYNIC-Lys^3-BN of four breast cancer patients and seven healthy volunteers (*68*). The images of the GRPR expression in breast cancer patients show a distinct accumulation of radioactivity in malignant tissue. Although the uptake of ^{99m}Tc-EDDA/HYNIC-Lys^3-BN in breast of cancer patients was higher than healthy volunteers, no statically significant difference was revealed. DTPA, DOTA, NOTA and their derivatives are the most commonly available chelators for the labeling of ^{177}Lu, ^{111}In, ^{68}Ga, and ^{64}Cu (*11, 49-52, 69-72*). Giacchetti *et al.* reported on the superior microPET imaging quality of ^{64}Cu labelled NOTA-BN over that of DOTA-BN in a GRPR

expressing prostate cancer animal model (*73*). NO2A is a derivative of NOTA, which lacks a p-NCS-Bz arm and forms an amide linkage via the third carboxylic acid unit, resulting in a neutral conjugate upon binding to copper. The neutral conjugation may reduce the retention of ^{64}Cu-BN in renal tissues. Compare to data of corresponding DOTA conjugated BNs, the NO2A conjugated BNs exhibited better *in vivo* profile (*53, 73*).

Two Aoc linker modified BN analogues labelled with ^{64}Cu using (1-*N*-(4-aminobenzyl)-3,6,10,13,16,19-hexaazabicyclo[6.6.6]- eicosane-1,8-diamine)(SarAr) as chelator was reported by Lears*et al.*(*74*). Efficient radiolabelling of SarAr-BNs with ^{64}Cu were achieved at room temperature. The PC-3 tumor uptake of 8.5%ID/g and 13.0%ID/g for ^{64}Cu-SarAr-SA-Aoc-GSG-BN(7-14) and ^{64}Cu-SarAr-SA-Aoc-BN(7-14) respectively at 1h p.i were much higher than other ^{64}Cu labelled BN analogues using DOTA or NOTA as chelators. The liver uptake of ^{64}Cu-SarAr-SA-Aoc-GSG-BN(7-14) and ^{64}Cu-SarAr -SA-Aoc-BN(7-14) were 5.1 and 9.5%ID/g at 1h p.i. which are at same level of most DOTA-BN analogues.

Several new chelators such as Oxo-DO3A, PCAT, TRAP and bis(thiosemicarbanzone) chelators have been applied on BN radiopharmaceuticals (*75-76*), but the *in vivo* behavior of those novel BN tracers has not been evaluated yet.

2.5.2.1 Full Length BN (Instead of Linker)

The amino acids 7 to14 of BN are responsible for binding to the GRPR receptor. For full length BN analogues, first 6 amino acids in N terminal of BN could be considered as a linker. The Arg^3, Leu^4 are often replaced by Lys^3 and Tyr^4 for the attachment of chelators or labeling prosthetic groups for full length BN. Lys^3-BN, one of the most well studied BN analogues, has been labelled with ^{99m}Tc, ^{64}Cu, and ^{18}F (*67, 71, 77-78*). Recently, Ho *et al.* synthesized a full length BN: [DTPA^1, Lys^3, Tyr^4]BN and labelled with ^{111}In (*72*). The Tyr^4 may allow further studies with radioiodine. Lower IC_{50} (1.05±0.46 nM) of [DTPA^1, Lys^3, Tyr^4]BN was observed compared to the IC_{50} (2.2±0.5 nM)value of DOTA-Lys^3-BN reported previously (*71*). The tumor uptake of ^{111}In-[DTPA^1, Lys^3, Tyr^4]BN was 2.48±0.48% %ID/g at 8h p.i. High accumulation (32.0±9.78 %ID/g) of radioactivity was also observed in pancreas at 8h p.i.. Compared to the ^{99m}Tc-Lys^3-BN (*78*), ^{111}In-[DTPA^1, Lys^3, Tyr^4]BN exhibited much higher accumulation in tumor and murine pancreas. The uptake values of ^{111}In-[DTPA^1, Lys^3, Tyr^4]BN in non-targeted organs such as blood, kidney, liver were also much higher than that of ^{99m}Tc-Lys^3-BN.

^{111}In-[DTPA^1, Lys^3, Tyr^4]BN was mainly excreted via urine, and high uptake was observed in kidney(>14%ID/g) until 48 hours post injection. When compared to ^{64}Cu and ^{18}F labelled Lys^3-BN analogues, the ^{111}In-[DTPA^1, Lys^3, Tyr^4]BN exhibited lower PC-3 tumor uptake but much higher pancreas uptake with much slower clearance from normal organs.

2.5.2 Linkers

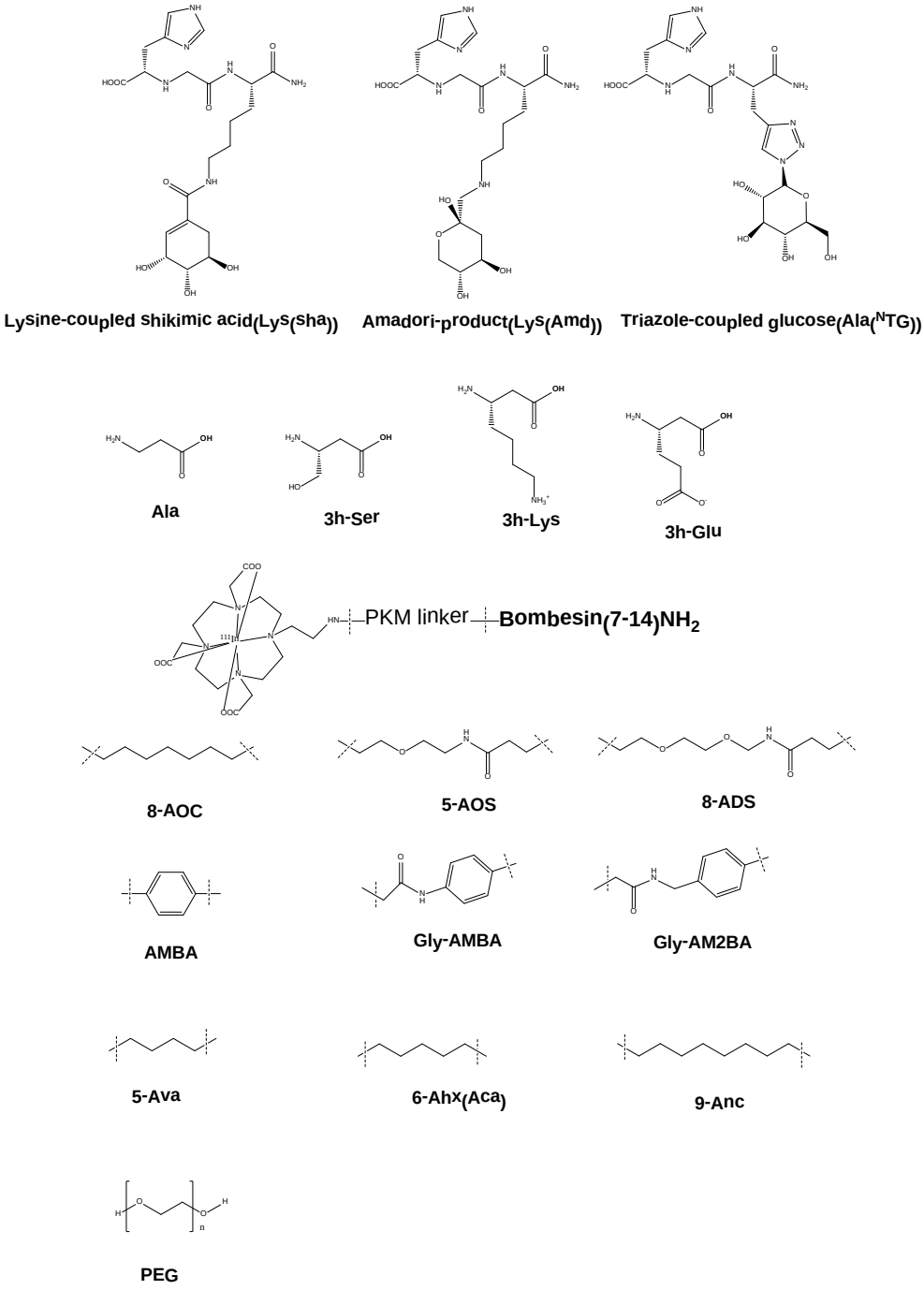

Figure 10. Chemical structures of PKM linkers

2.5.2.2 Other Linkers

In general, linkers have been employed to improve the *in vivo* kinetics of the radiolabelled biomolecules. Garrison *et al.* concluded that the linker not only effects the *in vivo* clearance but also the *in vivo* uptake and retention of the radiopharmaceutical in targeted tissues (*79*). When comparing different linkers in similar bombesin peptides, the ^{nat}In-labelled conjugates had IC_{50} values of 0.51 ± 0.05, 0.7 ± 0.1, 1.13 ± 0.07, 1.88 ± 0.06, 3.2 ± 0.3 and 6.2 ± 0.3 nM for the 8-AOC, Gly-AM2BA, AMBA, Gly-AMBA, 8-ADS and 5-AOS (Figure 10), respectively. In general, the ^{nat}In-conjugates containing aromatic linking groups possessed higher binding affinities for the GRPR than ^{nat}In-conjugates with ether linking groups. The *in vivo* pancreatic uptake of the radiotracers did not correlate strongly with the tumor uptake. The differences of the radioactivity accumulation between pancreas and PC-3 tumor could be due to differences in the tumor vascular system and/or difference between murine and human GRPR homology.

Since the high lipophilicity of the tracer leads to hepatobiliary excretion, and positive charge cause long retention in kidney, negatively charged or neutral and/or hydrophilic linkers such as amino acids and PEG were introduced to reduce the abdominal background of the radiolabelled BN analogues (*48, 79-83*).

To optimize the GRPR-expressing tumor uptake and retention of the ^{64}Cu labelled BN while retaining good pharmacokinetic properties, Lane *et al.* synthesized a series of ^{64}Cu-NO2A-(X)-BN(7-14)NH_2 (X=β-Ala, 5-Ava, 6-Ahx, 8-Aoc, 9-Anc or AMBA)(Figure 10). The spacer modification by substituting an aliphatic or aromatic linking substituent with varied length for X did not change the binding affinity of BN to GRPR. But the effect of hydrophilicity/hydrophobicity caused by linkers did change the *in vivo* kinetics of the radiotracer. The shorter, more hydrophilic pharmacokinetic modifier, AMBA was found to be the best candidate with highest tumor accumulation and most efficient clearance via renal excretion pathway, of the linkers which have been evaluated in their study (*82*).

Series of hydrophilic carbohydrated groups (βAla-βAla, Lys(Sha)- βAla-βAla, Lys(Amd)- βAla-βAla, Ala(^{N}TG)-βAlaβAla)(Figure 10) have been reported as linkers for the ^{99m}Tc-labelled truncated BN (*80*). Although the introduction of βAla-βAla led to improved*in vivo* tumor uptake, poor tumor-to-liver and tumor-to-kidney ratios were reported due to the high radioactivity accumulation in liver and kidney. The introduction of shikimic acid and glucose results in increased polarity of the new ^{99m}Tc-labelled analogues. The results of *in vivo* studies indicate that the introduced polar carbohydrates had no effect on internalization, efflux, or metabolic stability *in vitro* but led to a significant positive impact of the *in vivo* kinetics which include higher tumor uptake, reduction of abdominal accumulation and improved tumor-to-background ratios. The inference of molecular charge of polar linkers on the biodistribution of the ^{99m}Tc-labelled BN analogues was also evaluated (*83*). The introduction of a positive charge (β3hLys) resulted in unfavorable increased kidney uptake. The introduction of an uncharged hydroxyl group (β3hSer), one or two negative charges compounds (β3hGlu, β3hGlu-β3hGlu) significant improved the tumor-to-tissue ratios. Better SPECT imaging with an enhanced delineation of the xenografts and decreased radioactivity in the abdominal area was provided by single charge linker (β3hGlu-βAla-βAla) containing BN tracer than by other analogues with uncharged (βAla-βAla) or two negative charges (β3hGlu-βAla-βAla) linker. The superior biodistribution characteristics of the negative charge linker than of the positive charge linker for the ^{18}F-labelled non-natural amino acids modified BN has also been reported by

Mu *et al.*(*81*). ^{18}F-7b with negative charged linker Ala(SO_3H)-Ava exhibited more than doubled tumor accumulation (4.67±0.04 %ID/g at 1h p.i.) than the ^{18}F-6b (2.36±0.47 %ID/g at 1h p.i.) with the positive charged linker Arg-Ava. Although bearing the same BN peptide sequence and having the same lipophilicity, the charge of the linker plays a major role in *in vivo* pharmacokinetics. Liu *et al.* also found that the introduction of the PEG linker can improve the tumor uptake and excretion kinetics of RGD-BN hetero dimer (*48*).

Linkers/spacers which can improve the *in vivo* kinetics and clearance are very useful for the development of radiopharmaceuticals. The hydrophilic linkers/spacers with an aromatic group, or/and negative charge may be the best option of the linkers that reviewed in this article.

2.6 Clinical Imaging Studies with GRPR Targeted Radiotracers

The safety, radiopharmaceutical biokinetics, dosimetry of ^{99m}Tc-HYNIC-BN and the feasibility of imaging GRPR in breast cancer were determined in seven healthy women and in four women with breast cancer (*68*). No adverse reaction was found after administration of ^{99m}Tc-HYNIC-BN (555-740 MBq). No significant differences of blood clearance and absorbed doses for the main organs were observed between health women and patients with breast cancer. Tumor-to-normal-breast tissue ratio was 1.58±0.19 at 90 min. Although a significant difference ($p<0.05$) was found in the accumulation of ^{99m}Tc-HYNIC-BN between normal mammary gland and mammary gland of patients, the relationship between radioactivity accumulation and GRPR expression has not been confirmed.

Two clinical studies of ^{68}Ga-labelled BN analogues (^{68}Ga-BZH_3) were reported by Dimitrakopoulou-Strauss *et al.*. and Strauss *et al.*(*84-85*). Fifteen patients with histologically confirmed recurrent gliomas were studied to investigate the relation between the pharmacokinetics of^{68}Ga-BZH_3 data and the (WHO) grading of recurrent gliomas (*85*). Furthermore, the pharmacokinetic ^{68}Ga-BZH_3 was compared with the ^{18}F-FDG kinetics. Of fifteen patients, ten patients revealed an increased uptake of as ^{68}Ga-BZH_3 compared with surrounding brain parenchyma while three patients also demonstrated an increase uptake of^{18}F-FDG as well. Another three patients revealed an enhanced FDG metabolism without increased ^{68}Ga-BZH_3 uptake. They found that, the identification of high-grade gliomas was better with ^{68}Ga-BZH_3 than with^{18}F-FDG, since ^{68}Ga-BZH_3 revealed an enhanced uptake in more patients with high WHO grade than ^{18}F-FDG (4 vs 3 of 6 with WHOII, and 3 vs 0 of 3 patients with WHO IV). From the results with ^{68}Ga-BZH_3, they found high fractional blood volume VB (>0.07) and k1 (>0.2) values gave evidence of a high-grade glioma.

The kinetics of ^{68}Ga-BZH_3 was compared to molecular data obtained from gene arrays in seven recurrent glioma patients in their second clinical article on ^{68}Ga-BZH_3 (*84*). Their results demonstrated a preferential enhancement of the BB_2 and BB_3 receptor. The compartment parameter k1 was correlated with the expression of BB_2 (r=0.89), while k3, reflecting the internalization, revealed no significant correlation. They concluded that the expression of BB_2 may be predicted by kinetics of ^{68}Ga-BZH_3.

2.7 Conclusion

In the last decade, the development of BN tracers for receptor targeting nuclear imaging has increasingly gained attention. New biomolecules (multimers) and concepts

(agonist, antagonist) have been successfully introduced for improving the targeting ability and nuclear imaging quality of GRPR expressing cancer.

Novel tracers which were based on BN such as [^{111}In] DOTA-PESIN, [^{111}In]AMBA, ^{99m}Tc-Demobesin 1 (*56*) , [^{111}In/^{68}Ga]-RM1 (*60*), ^{99m}Tc-N4-BB-ANT (*58*), ^{18}F-BAY86-4367 (*59*) have better imaging characteristics than previously reported BN analogues. These tracers are promising probes for GRPR nuclear imaging.

Table 2 Radionuclides reviewed in this article.

Radionuclide	**$T_{1/2}$**	**E_{max} (kev)**
^{99m}Tc	6.0 h	141
^{111}In	67.2 h	245
^{18}F	109.7 min	635
^{64}Cu	12.7 h	655
^{68}Ga	68.1 min	1900
^{177}Lu	6.7 d	497
^{90}Y	2.7 d	2270

Acknowledgements

This work was made possible by a financial contribution from CTMM, project PCMM, project number 03O-203.

References

(1) Ferlay, J., Parkin, D. M., and Steliarova-Foucher, E. (2010) Estimates of cancer incidence and mortality in Europe in 2008. *Eur J Cancer 46*, 765-81.

(2) Hong, H., Zhang, Y., Sun, J., and Cai, W. (2010) Positron emission tomography imaging of prostate cancer. *Amino Acids 39*, 11-27.

(3) Connors, J. M. (2011) Positron emission tomography in the management of Hodgkin lymphoma. *Hematology Am Soc Hematol Educ Program 2011*, 317-22.

(4) Czernin, J., Allen-Auerbach, M., and Schelbert, H. R. (2007) Improvements in cancer staging with PET/CT: literature-based evidence as of September 2006. *J Nucl Med 48 Suppl 1*, 78S-88S.

(5) Tumeh, P. C., Radu, C. G., and Ribas, A. (2008) PET imaging of cancer immunotherapy. *J Nucl Med 49*, 865-8.

(6) Gatto, F., and Hofland, L. J. (2011) The role of somatostatin and dopamine D2 receptors in endocrine tumors. *Endocr Relat Cancer 18*, R233-51.

(7) Varner, J. A., and Cheresh, D. A. (1996) Integrins and cancer. *Curr Opin Cell Biol 8*, 724-30.

(8) Ananias, H. J., van den Heuvel, M. C., Helfrich, W., and de Jong, I. J. (2009) Expression of the gastrin-releasing peptide receptor, the prostate stem cell antigen and the

prostate-specific membrane antigen in lymph node and bone metastases of prostate cancer. *Prostate 69*, 1101-8.

(9) van Waarde, A., Rybczynska, A. A., Ramakrishnan, N., Ishiwata, K., Elsinga, P. H., and Dierckx, R. A. (2010) Sigma receptors in oncology: therapeutic and diagnostic applications of sigma ligands. *Curr Pharm Des 16*, 3519-37.

(10) Palma, C., and Maggi, C. A. (2000) The role of tachykinins via NK1 receptors in progression of human gliomas. *Life Sci 67*, 985-1001.

(11) Kwekkeboom, D., Krenning, E. P., and de Jong, M. (2000) Peptide receptor imaging and therapy. *J Nucl Med 41*, 1704-13.

(12) Graham, M. M., and Menda, Y. (2011) Radiopeptide imaging and therapy in the United States. *J Nucl Med 52 Suppl 2*, 56S-63S.

(13) Ambrosini, V., Fani, M., Fanti, S., Forrer, F., and Maecke, H. R. (2011) Radiopeptide imaging and therapy in Europe. *J Nucl Med 52 Suppl 2*, 42S-55S.

(14) Ananias, H. J., de Jong, I. J., Dierckx, R. A., van de Wiele, C., Helfrich, W., and Elsinga, P. H. (2008) Nuclear imaging of prostate cancer with gastrin-releasing-peptide-receptor targeted radiopharmaceuticals. *Curr Pharm Des 14*, 3033-47.

(15) Schroeder, R. P., van Weerden, W. M., Bangma, C., Krenning, E. P., and de Jong, M. (2009) Peptide receptor imaging of prostate cancer with radiolabelled bombesin analogues. *Methods 48*, 200-4.

(16) Smith, C. J., Volkert, W. A., and Hoffman, T. J. (2005) Radiolabelled peptide conjugates for targeting of the bombesin receptor superfamily subtypes. *Nucl Med Biol 32*, 733-40.

(17) McDonald, T. J., Jornvall, H., Nilsson, G., Vagne, M., Ghatei, M., Bloom, S. R., and Mutt, V. (1979) Characterization of a gastrin releasing peptide from porcine non-antral gastric tissue. *Biochem Biophys Res Commun 90*, 227-33.

(18) Fathi, Z., Corjay, M. H., Shapira, H., Wada, E., Benya, R., Jensen, R., Viallet, J., Sausville, E. A., and Battey, J. F. (1993) BRS-3: a novel bombesin receptor subtype selectively expressed in testis and lung carcinoma cells. *J Biol Chem 268*, 5979-84.

(19) Wada, E., Way, J., Shapira, H., Kusano, K., Lebacq-Verheyden, A. M., Coy, D., Jensen, R., and Battery, J. (1991) cDNA cloning, characterization, and brain region-specific expression of a neuromedin-B-preferring bombesin receptor. *Neuron 6*, 421-30.

(20) Spindel, E. R., Giladi, E., Brehm, P., Goodman, R. H., and Segerson, T. P. (1990) Cloning and functional characterization of a complementary DNA encoding the murine fibroblast bombesin/gastrin-releasing peptide receptor. *Mol Endocrinol 4*, 1956-63.

(21) Nagalla, S. R., Barry, B. J., Creswick, K. C., Eden, P., Taylor, J. T., and Spindel, E. R. (1995) Cloning of a receptor for amphibian [Phe^{13}]bombesin distinct from the receptor for gastrin-releasing peptide: identification of a fourth bombesin receptor subtype (BB4). *Proc Natl Acad Sci U S A 92*, 6205-9.

(22) Markwalder, R., and Reubi, J. C. (1999) Gastrin-releasing peptide receptors in the human prostate: relation to neoplastic transformation. *Cancer Res 59*, 1152-9.

(23) Bartholdi, M. F., Wu, J. M., Pu, H., Troncoso, P., Eden, P. A., and Feldman, R. I. (1998) In situ hybridization for gastrin-releasing peptide receptor (GRP receptor) expression in prostatic carcinoma. *Int J Cancer 79*, 82-90.

(24) Carroll, R. E., Matkowskyj, K. A., Chakrabarti, S., McDonald, T. J., and Benya, R. V. (1999) Aberrant expression of gastrin-releasing peptide and its receptor by well-differentiated colon cancers in humans. *Am J Physiol 276*, G655-65.

(25) Gugger, M., and Reubi, J. C. (1999) Gastrin-releasing peptide receptors in non-neoplastic and neoplastic human breast. *Am J Pathol 155*, 2067-76.

(26) Halmos, G., Wittliff, J. L., and Schally, A. V. (1995) Characterization of bombesin/gastrin-releasing peptide receptors in human breast cancer and their relationship to steroid receptor expression. *Cancer Res 55*, 280-7.

(27) Sun, B., Schally, A. V., and Halmos, G. (2000) The presence of receptors for bombesin/GRP and mRNA for three receptor subtypes in human ovarian epithelial cancers. *Regulatory peptides 90*, 77-84.

(28) Beer, M., Montani, M., Gerhardt, J., Wild, P. J., Hany, T. F., Hermanns, T., Muntener, M.,

and Kristiansen, G. (2012) Profiling gastrin-releasing peptide receptor in prostate tissues: clinical implications and molecular correlates. *Prostate 72*, 318-25.

(29) Drobnjak, M., Osman, I., Scher, H. I., Fazzari, M., and Cordon-Cardo, C. (2000) Overexpression of cyclin D1 is associated with metastatic prostate cancer to bone. *Clin Cancer Res 6*, 1891-5.

(30) Kallakury, B. V., Sheehan, C. E., Ambros, R. A., Fisher, H. A., Kaufman, R. P., Jr., and Ross, J. S. (1997) The prognostic significance of p34cdc2 and cyclin D1 protein expression in prostate adenocarcinoma. *Cancer 80*, 753-63.

(31) Erspamer, V. (1988) Discovery, isolation, and characterization of bombesin-like peptides. *Ann N Y Acad Sci 547*, 3-9.

(32) Barrett, A. J., Rawlings, N. D., and Woessner, J. F. (2004) Introduction: metallopeptidases and their clan., in *Handbook of Proteolytic Enzymes* pp 231-268, Elsevier Ltd., London.

(33) Linder, K. E., Metcalfe, E., Arunachalam, T., Chen, J., Eaton, S. M., Feng, W., Fan, H., Raju, N., Cagnolini, A., Lantry, L. E., Nunn, A. D., and Swenson, R. E. (2009) In vitro and in vivo metabolism of Lu-AMBA, a GRP-receptor binding compound, and the synthesis and characterization of its metabolites. *Bioconjug Chem 20*, 1171-8.

(34) Hohne, A., Mu, L., Honer, M., Schubiger, P. A., Ametamey, S. M., Graham, K., Stellfeld, T., Borkowski, S., Berndorff, D., Klar, U., Voigtmann, U., Cyr, J. E., Friebe, M., Dinkelborg, L., and Srinivasan, A. (2008) Synthesis, ^{18}F-labeling, and in vitro and in vivo studies of bombesin peptides modified with silicon-based building blocks. *Bioconjug Chem 19*, 1871-9.

(35) Nock, B., Nikolopoulou, A., Chiotellis, E., Loudos, G., Maintas, D., Reubi, J. C., and Maina, T. (2003) ^{99m}Tc-Demobesin 1, a novel potent bombesin analogue for GRP receptor-targeted tumour imaging. *Eur J Nucl Med Mol Imaging 30*, 247-58.

(36) Abd-Elgaliel, W. R., Gallazzi, F., Garrison, J. C., Rold, T. L., Sieckman, G. L., Figueroa, S. D., Hoffman, T. J., and Lever, S. Z. (2008) Design, synthesis, and biological evaluation of an antagonist-bombesin analogue as targeting vector. *Bioconjug Chem 19*, 2040-8.

(37) Garcia Garayoa, E., Schweinsberg, C., Maes, V., Ruegg, D., Blanc, A., Blauenstein, P., Tourwe, D. A., Beck-Sickinger, A. G., and Schubiger, P. A. (2007) New ^{99m}Tc-bombesin analogues with improved biodistribution for targeting gastrin releasing-peptide receptor-positive tumors. *Q J Nucl Med Mol Imaging 51*, 42-50.

(38) Garcia Garayoa, E., Ruegg, D., Blauenstein, P., Zwimpfer, M., Khan, I. U., Maes, V., Blanc, A., Beck-Sickinger, A. G., Tourwe, D. A., and Schubiger, P. A. (2007) Chemical and biological characterization of new $Re(CO)_3$/^{99m}Tc-$(CO)_3$ bombesin analogues. *Nucl Med Biol 34*, 17-28.

(39) La Bella, R., Garcia-Garayoa, E., Bahler, M., Blauenstein, P., Schibli, R., Conrath, P., Tourwe, D., and Schubiger, P. A. (2002) A ^{99m}Tc(I)-postlabelled high affinity bombesin analogue as a potential tumor imaging agent. *Bioconjug Chem 13*, 599-604.

(40) Carlucci, G., Ananias, H. J., Yu, Z., Van de Wiele, C., Dierckx, R. A., de Jong, I. J., and Elsinga, P. H. (2012) Multimerization improves targeting of Peptide radio-pharmaceuticals. *Curr Pharm Des 18*, 2501-16.

(41) Liu, S. (2009) Radiolabelled cyclic RGD peptides as integrin $alpha_v beta_3$-targeted radiotracers: maximizing binding affinity via bivalency. *Bioconjug Chem 20*, 2199-213.

(42) Wang, L., Shi, J., Kim, Y. S., Zhai, S., Jia, B., Zhao, H., Liu, Z., Wang, F., Chen, X., and Liu, S. (2009) Improving tumor-targeting capability and pharmacokinetics of ^{99m}Tc-labelled cyclic RGD dimers with PEG_4 linkers. *Mol Pharm 6*, 231-45.

(43) Shi, J., Wang, L., Kim, Y. S., Zhai, S., Liu, Z., Chen, X., and Liu, S. (2008) Improving tumor uptake and excretion kinetics of ^{99m}Tc-labelled cyclic arginine-glycine-aspartic (RGD) dimers with triglycine linkers. *J Med Chem 51*, 7980-90.

(44) Shi, J., Kim, Y. S., Zhai, S., Liu, Z., Chen, X., and Liu, S. (2009) Improving tumor uptake and pharmacokinetics of ^{64}Cu-labelled cyclic RGD peptide dimers with Gly^3 and PEG_4 linkers. *Bioconjug Chem 20*, 750-9.

(45) Accardo, A., Mansi, R., Morisco, A., Mangiapia, G., Paduano, L., Tesauro, D., Radulescu, A., Aurilio, M., Aloj, L., Arra, C., and Morelli, G. (2010) Peptide modified nanocarriers for

selective targeting of bombesin receptors. *Mol Biosyst 6*, 878-87.

(46) Ma, M. T., Cooper, M. S., Paul, R. L., Shaw, K. P., Karas, J. A., Scanlon, D., White, J. M., Blower, P. J., and Donnelly, P. S. (2011) Macrobicyclic cage amine ligands for copper radiopharmaceuticals: a single bivalent cage amine containing two Lys^3-bombesin targeting peptides. *Inorg Chem 50*, 6701-10.

(47) Li, Z. B., Wu, Z., Chen, K., Ryu, E. K., and Chen, X. (2008) ^{18}F-labelled BBN-RGD heterodimer for prostate cancer imaging. *J Nucl Med 49*, 453-61.

(48) Liu, Z., Yan, Y., Chin, F. T., Wang, F., and Chen, X. (2009) Dual integrin and gastrin-releasing peptide receptor targeted tumor imaging using 18F-labelled PEGylated RGD-bombesin heterodimer ^{18}F-FB-PEG_3-Glu-RGD-BBN. *J Med Chem 52*, 425-32.

(49) Liu, Z., Niu, G., Wang, F., and Chen, X. (2009) ^{68}Ga-labelled NOTA-RGD-BBN peptide for dual integrin and GRPR-targeted tumor imaging. *Eur J Nucl Med Mol Imaging 36*, 1483-94.

(50) Liu, Z., Li, Z. B., Cao, Q., Liu, S., Wang, F., and Chen, X. (2009) Small-animal PET of tumors with ^{64}Cu-labelled RGD-bombesin heterodimer. *J Nucl Med 50*, 1168-77.

(51) Liu, Z., Yan, Y., Liu, S., Wang, F., and Chen, X. (2009) ^{18}F, ^{64}Cu, and ^{68}Ga labelled RGD-bombesin heterodimeric peptides for PET imaging of breast cancer. *Bioconjug Chem 20*, 1016-25.

(52) Yan, Y., Chen, K., Yang, M., Sun, X., Liu, S., and Chen, X. (2011) A new ^{18}F-labelled BBN-RGD peptide heterodimer with a symmetric linker for prostate cancer imaging. *Amino Acids 41*, 439-47.

(53) Jackson, A. B., Nanda, P. K., Rold, T. L., Sieckman, G. L., Szczodroski, A. F., Hoffman, T. J., Chen, X., and Smith, C. J. (2012) ^{64}Cu-NO2A-RGD-Glu-6-Ahx-BBN(7-14)NH_2: a heterodimeric targeting vector for positron emission tomography imaging of prostate cancer. *Nucl Med Biol 39*, 377-87.

(54) Liu, Z., Huang, J., Dong, C., Cui, L., Jin, X., Jia, B., Zhu, Z., Li, F., and Wang, F. (2012) ^{99m}Tc-labelled RGD-BBN peptide for small-animal SPECT/CT of lung carcinoma. *Mol Pharm*.

(55) Kenakin, T. (2005) New concepts in drug discovery: collateral efficacy and permissive antagonism. *Nat Rev Drug Discov 4*, 919-27.

(56) Schroeder, R. P., Muller, C., Reneman, S., Melis, M. L., Breeman, W. A., de Blois, E., Bangma, C. H., Krenning, E. P., van Weerden, W. M., and de Jong, M. (2010) A standardised study to compare prostate cancer targeting efficacy of five radiolabelled bombesin analogues. *Eur J Nucl Med Mol Imaging 37*, 1386-96.

(57) Yang, M., Gao, H., Zhou, Y., Ma, Y., Quan, Q., Lang, L., Chen, K., Niu, G., Yan, Y., and Chen, X. (2011) F-Labelled GRPR Agonists and Antagonists: A Comparative Study in Prostate Cancer Imaging. *Theranostics 1*, 220-9.

(58) Abiraj, K., Mansi, R., Tamma, M. L., Forrer, F., Cescato, R., Reubi, J. C., Akyel, K. G., and Maecke, H. R. (2010) Tetraamine-derived bifunctional chelators for technetium-99m labelling: synthesis, bioconjugation and evaluation as targeted SPECT imaging probes for GRP-receptor-positive tumours. *Chemistry 16*, 2115-24.

(59) Honer, M., Mu, L., Stellfeld, T., Graham, K., Martic, M., Fischer, C. R., Lehmann, L., Schubiger, P. A., Ametamey, S. M., Dinkelborg, L., Srinivasan, A., and Borkowski, S. (2011) ^{18}F-labelled bombesin analog for specific and effective targeting of prostate tumors expressing gastrin-releasing peptide receptors. *J Nucl Med 52*, 270-8.

(60) Mansi, R., Wang, X., Forrer, F., Kneifel, S., Tamma, M. L., Waser, B., Cescato, R., Reubi, J. C., and Maecke, H. R. (2009) Evaluation of a 1,4,7,10-tetraazacyclododecane-1,4,7,10-tetraacetic acid-conjugated bombesin-based radioantagonist for the labeling with single-photon emission computed tomography, positron emission tomography, and therapeutic radionuclides. *Clin Cancer Res 15*, 5240-9.

(61) Liu, S., Hsieh, W. Y., Kim, Y. S., and Mohammed, S. I. (2005) Effect of coligands on biodistribution characteristics of ternary ligand ^{99m}Tc complexes of a HYNIC-conjugated cyclic RGDfK dimer. *Bioconjug Chem 16*, 1580-8.

(62) Jia, B., Liu, Z., Zhu, Z., Shi, J., Jin, X., Zhao, H., Li, F., Liu, S., and Wang, F. (2011) Blood

clearance kinetics, biodistribution, and radiation dosimetry of a kit-formulated integrin alpha$_v$beta$_3$-selective radiotracer ^{99m}Tc-3PRGD$_2$ in non-human primates. *Mol Imaging Biol 13*, 730-6.

(63) Shi, J., Jia, B., Liu, Z., Yang, Z., Yu, Z., Chen, K., Chen, X., Liu, S., and Wang, F. (2008) ^{99m}Tc-labelled bombesin(7-14)NH$_2$ with favorable properties for SPECT imaging of colon cancer. *Bioconjug Chem 19*, 1170-8.

(64) D'Alessandria, C., di Gialleonardo, V., Chianelli, M., Mather, S. J., de Vries, E. F., Scopinaro, F., Dierck, R. A., and Signore, A. (2010) Synthesis and optimization of the labeling procedure of ^{99m}Tc-HYNIC-interleukin-2 for in vivo imaging of activated T lymphocytes. *Mol Imaging Biol 12*, 539-46.

(65) Ananias, H. J., Yu, Z., Dierckx, R. A., van der Wiele, C., Helfrich, W., Wang, F., Yan, Y., Chen, X., de Jong, I. J., and Elsinga, P. H. (2011) ^{99m}technetium-HYNIC(tricine/TPPTS)-Aca-bombesin(7-14) as a targeted imaging agent with microSPECT in a PC-3 prostate cancer xenograft model. *Mol Pharm 8*, 1165-73.

(66) Li, Y., Si, J. M., Zhang, J., Du, J., Wang, F., and Jia, B. (2005) Somatostatin receptor subtype 2-mediated scintigraphy and localization using ^{99m}Tc-HYNIC-Tyr^3-octreotide in human hepatocellular carcinoma-bearing nude mice. *World J Gastroenterol 11*, 3953-7.

(67) Zhang, X., Cai, W., Cao, F., Schreibmann, E., Wu, Y., Wu, J. C., Xing, L., and Chen, X. (2006) ^{18}F-labelled bombesin analogs for targeting GRP receptor-expressing prostate cancer. *J Nucl Med 47*, 492-501.

(68) Santos-Cuevas, C. L., Ferro-Flores, G., Arteaga de Murphy, C., and Pichardo-Romero, P. A. (2008) Targeted imaging of gastrin-releasing peptide receptors with ^{99m}Tc-EDDA/HYNIC-[Lys^3]-bombesin: biokinetics and dosimetry in women. *Nucl Med Commun 29*, 741-7.

(69) Wild, D., Frischknecht, M., Zhang, H., Morgenstern, A., Bruchertseifer, F., Boisclair, J., Provencher-Bolliger, A., Reubi, J. C., and Maecke, H. R. (2011) Alpha- versus beta-particle radiopeptide therapy in a human prostate cancer model (^{213}Bi-DOTA-PESIN and ^{213}Bi-AMBA versus ^{177}Lu-DOTA-PESIN). *Cancer Res 71*, 1009-18.

(70) Smith, S. V. (2004) Molecular imaging with copper-64. *J Inorg Biochem 98*, 1874-901.

(71) Chen, X., Park, R., Hou, Y., Tohme, M., Shahinian, A. H., Bading, J. R., and Conti, P. S. (2004) microPET and autoradiographic imaging of GRP receptor expression with ^{64}Cu-DOTA-[Lys^3]bombesin in human prostate adenocarcinoma xenografts. *J Nucl Med 45*, 1390-7.

(72) Ho, C. L., Chen, L. C., Lee, W. C., Chiu, S. P., Hsu, W. C., Wu, Y. H., Yeh, C. H., Stabin, M. G., Jan, M. L., Lin, W. J., Lee, T. W., and Chang, C. H. (2009) Receptor-binding, biodistribution, dosimetry, and micro-SPECT/CT imaging of ^{111}In-[DTPA^1, Lys^3, Tyr^4]-bombesin analog in human prostate tumor-bearing mice. *Cancer Biother Radiopharm 24*, 435-43.

(73) Prasanphanich, A. F., Nanda, P. K., Rold, T. L., Ma, L., Lewis, M. R., Garrison, J. C., Hoffman, T. J., Sieckman, G. L., Figueroa, S. D., and Smith, C. J. (2007) [^{64}Cu-NOTA-8-Aoc-BBN(7-14)NH$_2$] targeting vector for positron-emission tomography imaging of gastrin-releasing peptide receptor-expressing tissues. *Proc Natl Acad Sci U S A 104*, 12462-7.

(74) Lears, K. A., Ferdani, R., Liang, K., Zheleznyak, A., Andrews, R., Sherman, C. D., Achilefu, S., Anderson, C. J., and Rogers, B. E. (2011) In vitro and in vivo evaluation of ^{64}Cu-labelled SarAr-bombesin analogs in gastrin-releasing peptide receptor-expressing prostate cancer. *J Nucl Med 52*, 470-7.

(75) Ait-Mohand, S., Fournier, P., Dumulon-Perreault, V., Kiefer, G. E., Jurek, P., Ferreira, C. L., Benard, F., and Guerin, B. (2011) Evaluation of ^{64}Cu-labelled bifunctional chelate-bombesin conjugates. *Bioconjug Chem 22*, 1729-35.

(76) Paterson, B. M., Karas, J. A., Scanlon, D. B., White, J. M., and Donnelly, P. S. (2010) Versatile new bis(thiosemicarbazone) bifunctional chelators: synthesis, conjugation to bombesin(7-14)-NH$_2$, and copper-64 radiolabelling. *Inorg Chem 49*, 1884-93.

(77) Lin, K. S., Luu, A., Baidoo, K. E., Hashemzadeh-Gargari, H., Chen, M. K., Brenneman, K.,

Pili, R., Pomper, M., Carducci, M. A., and Wagner, H. N., Jr. (2005) A new high affinity technetium-99m-bombesin analogue with low abdominal accumulation. *Bioconjug Chem 16*, 43-50.

(78) Ferro-Flores, G., Arteaga de Murphy, C., Rodriguez-Cortes, J., Pedraza-Lopez, M., and Ramirez-Iglesias, M. T. (2006) Preparation and evaluation of ^{99m}Tc-EDDA/HYNIC-[Lys^3]-bombesin for imaging gastrin-releasing peptide receptor-positive tumours. *Nucl Med Commun 27*, 371-6.

(79) Garrison, J. C., Rold, T. L., Sieckman, G. L., Naz, F., Sublett, S. V., Figueroa, S. D., Volkert, W. A., and Hoffman, T. J. (2008) Evaluation of the pharmacokinetic effects of various linking group using the ^{111}In-DOTA-X-BBN(7-14)NH_2 structural paradigm in a prostate cancer model. *Bioconjug Chem 19*, 1803-12.

(80) Schweinsberg, C., Maes, V., Brans, L., Blauenstein, P., Tourwe, D. A., Schubiger, P. A., Schibli, R., and Garcia Garayoa, E. (2008) Novel glycated ^{99m}Tc$(CO)_3$-labelled bombesin analogues for improved targeting of gastrin-releasing peptide receptor-positive tumors. *Bioconjug Chem 19*, 2432-9.

(81) Mu, L., Honer, M., Becaud, J., Martic, M., Schubiger, P. A., Ametamey, S. M., Stellfeld, T., Graham, K., Borkowski, S., Lehmann, L., Dinkelborg, L., and Srinivasan, A. (2010) In vitro and in vivo characterization of novel ^{18}F-labelled bombesin analogues for targeting GRPR-positive tumors. *Bioconjug Chem 21*, 1864-71.

(82) Lane, S. R., Nanda, P., Rold, T. L., Sieckman, G. L., Figueroa, S. D., Hoffman, T. J., Jurisson, S. S., and Smith, C. J. (2010) Optimization, biological evaluation and microPET imaging of copper-64-labelled bombesin agonists, [^{64}Cu-NO2A-(X)-BBN(7-14)NH_2], in a prostate tumor xenografted mouse model. *Nucl Med Biol 37*, 751-61.

(83) Garcia Garayoa, E., Schweinsberg, C., Maes, V., Brans, L., Blauenstein, P., Tourwe, D. A., Schibli, R., and Schubiger, P. A. (2008) Influence of the molecular charge on the biodistribution of bombesin analogues labelled with the [^{99m}Tc$(CO)_3$]-core. *Bioconjug Chem 19*, 2409-16.

(84) Strauss, L. G., Koczan, D., Seiz, M., Tuettenberg, J., Schmieder, K., Pan, L., Cheng, C., and Dimitrakopoulou-Strauss, A. (2012) Correlation of the ^{68}Ga-Bombesin Analog ^{68}Ga-BZH_3 with Receptors Expression in Gliomas as Measured by Quantitative Dynamic Positron Emission Tomography (dPET) and Gene Arrays. *Mol Imaging Biol 14*, 376-83.

(85) Dimitrakopoulou-Strauss, A., Seiz, M., Tuettenberg, J., Schmieder, K., Eisenhut, M., Haberkorn, U., and Strauss, L. G. (2011) Pharmacokinetic studies of ^{68}Ga-labelled Bombesin (^{68}Ga-BZH_3) and ^{18}F-FDG PET in patients with recurrent gliomas and comparison to grading: preliminary results. *Clin Nucl Med 36*, 101-8.

Chapter 3

^{99m}Tc-Labelled Bombesin(7-14)NH_2 with Favorable Properties for SPECT Imaging of Colon Cancer

Jiyun Shi, Bing Jia, Zhaofei Liu, Zhi Yang, **Zilin Yu**, Kai Chen,

Xiaoyuan Chen, Shuang Liu, and Fan Wang

Bioconjug Chem, 2008; 19(6):1170-8

Abstract

In this report, we present the synthesis and evaluation of the ^{99m}Tc-labelled β-Ala-BN(7-14)NH_2 (ABN = β-Ala-Gln-Trp-Ala-Val-Gly-His-Leu-Met-NH_2) as a new radiotracer for tumor imaging in the BALB/c nude mice bearing HT-29 human colon cancer xenografts. The gastrin releasing peptide receptor binding affinity of ABN and HYNIC-ABN (6-hydrazinonicotinamide) were assessed via a competitive displacement of ^{125}I-[Tyr4]BBN bound to the PC-3 human prostate carcinoma cells. The IC_{50} values were calculated to be 24 ± 2 nM and 38 ± 1 nM for ABN and HYNIC-ABN, respectively. HYNIC is the bifunctional coupling agent for ^{99m}Tc-labeling while tricine and TPPTS (trisodium triphenylphosphine-3,3',3"-trisulfonate) are used as coligands to prepare the ternary ligand complex [^{99m}Tc(HYNIC-ABN)(tricine)(TPPTS)] in very high yield and high specific activity. Because of its high hydrophilicity (log P = -2.39 ± 0.06), [^{99m}Tc(HYNIC-ABN)(tricine)(TPPS)] was excreted mainly through the renal route with little radioactivity accumulation in the liver, lungs, stomach, and gastrointestinal tract. The tumor uptake at 30 min postinjection (p.i.) was 1.59 ± 0.23 %ID/g with a steady tumor washout over the 4 h study period. As a result, it had the best T/B ratios in the blood (2.37 ± 0.68), liver (1.69 ± 0.41) and muscle (11.17 ± 3.32) at 1 h p.i. Most of the injected radioactivity was found in the urine sample at 1 h p.i., and there was no intact [^{99m}Tc(HYNIC-ABN](tricine)(TPPTS)] detectable in the urine, kidney and liver samples. Its metabolic instability may contribute to its rapid clearance from the liver, lungs and stomach. Despite the steady radioactivity washout, the tumors could be clearly visualized in planar images of the BALB/c nude mice bearing the HT-29 human colon xenografts at 1 and 4 h p.i. The favorable excretion kinetics from the liver, lungs, stomach, and gastrointestinal tract makes [^{99m}Tc(HYNIC-ABN)(tricine)(TPPTS)] a promising SPECT radiotracer for imaging colon cancer.

Key words: Bombesin (7-14)NH_2 , HYNIC, ^{99m}Tc Labeling, colon cancer

3.1 Introduction

Colon cancer is the second leading cause of cancer-related death. It is estimated that about 130,000 men and women will develop colon cancer and more than 50,000 will die from it each year in the United States (American Cancer Society: http://www.cancer.org). The life-time risk for individuals to develop colon cancer is ~6%, but it may increase to 18% among the individuals who have a relative (parent, sibling or child) with colon cancer. Therefore, accurate early detection is highly desirable so that various therapeutic regimens can be given before the primary tumors become widely spread.

Bombesin (BN) is a small peptide containing 14 amino acids(Glu-Gln-Arg-Leu-Gly-Asn-Gln-Trp-Ala-Val-Gly-His-Leu-Met-NH_2). It was originally isolated from the skin of amphibian Bombina Orientalis (*1*, *2*). The BN-like peptides have very high binding affinity for the gastrin releasing peptide (GRP) receptor (*3-5*), and produce a wide range of biological responses in peripheral tissues as well as in the central nervous system, including stimulation of gastrointestinal hormone release, exocrine secretion and maintenance of circadian rhythms. In addition, it has been established that the GRP/BN peptides promotes proliferation in cancer cells. The overexpression of GRP receptor (GRPR) has been demonstrated in a large number of tumors, including prostate, breast, colon and small cell lung cancer (*6-13*). The distribution of BN-like peptides and the expression of their receptors have been reviewed (*3, 4*). Because of its highly restricted overexpression on tumor cells, the GRPR is emerging as an attractive target for both cancer therapy and early detection (*3, 4, 14-17*).

BN(7-14)NH_2 is the peptide sequence responsible for specific binding of the GRPRs overexpressed on tumor cells. Most of the radiolabelled BN-like peptides are based on or contain the BN(7-14)NH_2 peptide sequence. These radiolabelled BN-like peptides were designed as tumor-specific radiotracers for early diagnosis or systemic radiotherapy of the GRPR-positive tumors, and have been reviewed extensively (*14-17*). The radionuclides include ^{111}In (*18-20*), ^{177}Lu (*21-23*), ^{68}Ga (*24*), ^{64}Cu (*25-32*), ^{188}Re (*33*), and ^{99m}Tc (*34-47*). While ^{68}Ga and ^{64}Cu are particularly useful for imaging tumors by positron emission tomography (PET), ^{99m}Tc is the radionuclide of choice for tumor imaging by single photon computed tomography (SPECT) due to its excellent nuclear properties ($t_{1/2}$ = 6 h and single photon emission at 140 keV), rich and diverse coordination chemistry, easy availability at low cost, and high specific activity (*48-50*).

In this study, we used β-Ala-BN(7-14)NH_2 (Figure 1: ABN in short) as the biomolecule for tumor targeting and 6-hydrazinonicotinic acid (HYNIC) as the bifunctional coupling agent (BFC) for the ^{99m}Tc-labeling. Since HYNIC is monodentate in the ^{99m}Tc-HYNIC core, tricine and TPPTS (trisodium triphenylphosphine-3,3',3"-trisulfonate) are used as coligands to prepare the complex [^{99m}Tc(HYNIC-ABN)(tricine)(TPPTS)] (Figure 1). This ternary ligand system (HYNIC, tricine and TPPTS) has been successfully used for the ^{99m}Tc-labeling of small biomolecules, including chemotactic peptides (*51*) and LTB_4 receptor antagonists (*52, 53*) for imaging infection and inflammation, integrin $\alpha_v\beta_3$ antagonists for imaging tumor angiogenesis (*54-58*), and GPIIb/IIIa receptor antagonists for imaging deep vein thrombosis (*59*). The BALB/c nude mice bearing HT-29 human colon cancer xenografts were used for both biodistribution and imaging studies. Normal BALB/c nude mice were used for metabolism study. The main objective is to evaluate [^{99m}Tc(HYNIC-ABN)(tricine)(TPPTS)] as a potential new radiotracer for SPECT imaging

of colon cancer.

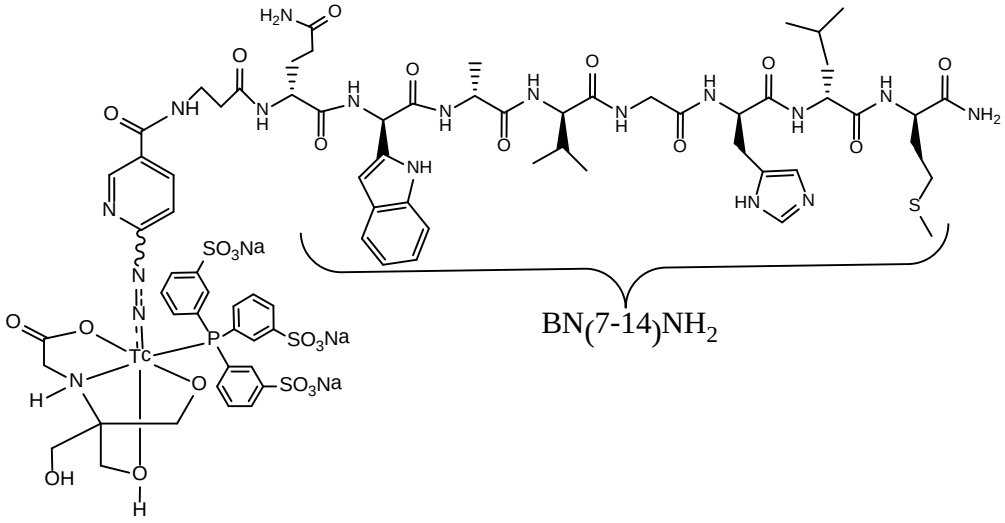

Figure 1. Structure of the ternary ligand complex [^{99m}Tc(HYNIC-ABN)(tricine)(TPPTS)].

3.2 Experimental

3.2.1 Materials

Tricine and TPPTS were purchased from *Sigma/Aldrich* (St. Louis, MO), and were used without further purification. The peptide conjugate, HYNIC-β-Ala-BN(7-14)NH_2 (HYNIC-ABN), was obtained from CS Bio Co. (Menlo Park, CA). $Na^{99m}TcO_4$ was obtained from a commercial $^{99}Mo/^{99m}Tc$ generator **(**Beijing Atom High Tech Co. Ltd., Beijing, China). ^{125}I-[Tyr4]BBN was obtained from Perkin-Elmer Life and Analytical Sciences (North Billarica, MA).

3.2.2 Methods

The radio-HPLC method used a HP Hewlett® Packard Series 1100 HPLC system equipped with a Radioflow Detector LB509 and a reversed-phase Zorbax SB-C18 column (4.6 mm x 250 mm, 5 μm). The flow rate was 1.0 mL/min. The mobile phase was isocratic with 90% solvent A (0.01 M phosphate buffer, pH = 6.0) and 10% solvent B (acetonitrile) at 0-5 min, followed by a gradient mobile phase going from 10% solvent B at 5 min to 50% solvent B at 20 min, then to 80% solvent B at 22 min, and back to baseline 10% solvent B at 25 min. The ITLC method used Gelman Sciences silica-gel paper strips and a 1:1 mixture of acetone and saline as eluant. The ^{99m}Tc complexes migrated to solvent front while $^{99m}TcO_4^-$ and [^{99m}Tc]colloid remained at origin.

3.2.3 Synthesis of [^{99m}Tc(HYNIC-ABN](tricine)(TPPTS)]

To a clean 5 cc vial were added 100 μL of the HYNIC-ABN solution (100 μg/mL in H_2O), 100 μL of tricine solution (100 mg/mL in 25 mM succinate buffer, pH 5.0), 20 μL of $SnCl_2$ solution (3.0 mg/mL in 0.1 N HCl) and 100 μL of $Na^{99m}TcO_4$ (370 MBq) in saline. The reaction mixture was kept at room temperature for 10 min. To the reaction mixture above was added 120 μL of the TPPTS solution (50 mg/mL in 25 mM succinate buffer, pH 5.0). The vial containing the reaction mixture was sealed, cramped, and heated at 100 ^oC for 30 min. After cooling to room temperature, a sample of the resulting solution was analyzed by ITLC and radio-HPLC.

3.2.4 Dose Preparation for Animal Studies

[^{99m}Tc(HYNIC-ABN](tricine)(TPPTS)] was purified using a Sep-Pak C-18 cartridge (Waters, MA) before being used for animal studies. The Sep-Pak C-18 cartridge was activated with ethanol (10 mL) and was washed with water (10 mL). After the radiotracer was loaded, the Sep-Pak C-18 cartridge was washed with saline (10 mL) to remove the unlabelled ^{99m}Tc and excess coligands. The radiotracer was eluted with 80% ethanol (0.4 mL). Doses for animal studies were prepared by dissolving the Sep-Pak purified radiotracer in saline to give a concentration of 150 μCi/mL for biodistribution study, 4.0 mCi/mL for the metabolism study, and 2.0 mCi/mL for the planar imaging study.

3.2.5 Partition Coefficient

The partition coefficient was determined using the following procedure: [^{99m}Tc(HYNIC-ABN](tricine)(TPPTS)] was prepared and purified using the Sep-Pak C-18 cartridge. Volatiles in the mobile phase were completely removed under vacuum. The residue was dissolved in a mixture of equal volume (0.5 mL:0.5 mL) n-octanol and 25 mM phosphate buffer (pH = 7.4). After vortexing for 2 min, samples in triplicate were obtained from n-octanol and aqueous layers, and were counted in a γ-counter (Wallac 1470-002, Perkin Elmer, Finland). The log P value is reported as an average of three different measurements.

3.2.6 *In Vitro* Cell-Binding Assay

In vitro GRPR binding affinity and specificity of ABN and HYNIC-ABN were assessed via a competitive displacement assay with ^{125}I-[Tyr4]BBN as the radioligand. Experiments were performed using the GRPR-positive PC-3 prostate carcinoma cells according to the literature method (*32*). The 50% inhibitory concentration (IC_{50}) values were calculated by fitting the data with nonlinear regression using Graph-Pad Prism 4.0 (GraphPad Software, San Diego, CA). Experiments were performed twice with triplicate samples. IC_{50} values are reported as an average of these samples plus the standard

deviation.

3.2.7 Internalization Kinetics

The internalization assay was performed according to the literature method (*37, 47*) with slight modification. Briefly, the HT-29 cells were incubated in the 24-well plates in quadruplicate with [^{99m}Tc(HYNIC-ABN](tricine)(TPPTS)] (~0.1 μCi/well) for 2 h at 4 ºC, and then were washed with ice-cold PBS to remove the unbound radioactivity. After washing, the cells were incubated in the pre-warmed culture medium at 37 ºC for 0, 5, 15, 30, 60 and 120 min for internalization. The cell-surface bound radiotracer was removed by acid wash (50 mM glycine-HCl/100 mM NaCl, pH 2.8). Subsequently, the cells were solubilized by incubation with 2 M NaOH at 37 °C, and the resulting solution in each well was harvested to determine the internalized radioactivity in a γ-counter (Wallac 1470-002, Perkin Elmer, Finland). The results were expressed as a percentage of the total radioactivity (surface-bound plus internalized). The same experiment was performed twice with quadruplicate samples.

3.2.8 Efflux Kinetics

The HT-29 cells cultured in 24-well plates were incubated at 37 ºC with [^{99m}Tc(HYNIC-ABN](tricine)(TPPTS)] (~0.1 μCi/well) for 1 h to allow maximal internalization. The cells were washed three times with ice-cold PBS to remove the unbound radioactivity, then were incubated in the pre-warmed culture medium at 37 ºC for a specific period of time (0, 15, 30, 60, 120 and 240 min). At the specified time point, the cell-surface bound radioactivity was removed by acid wash (50 mM glycine-HCl/100 mM NaCl, pH 2.8). Subsequently, the cells were solubilized by incubation with 2 M NaOH at 37 °C, and the resulting solution in each well was harvested to determine the internalized radioactivity in a γ-counter (Wallac 1470-002, Perkin Elmer, Finland). Data is expressed as percentage of maximal intracellular radioactivity. The same experiment was performed twice with quadruplicate samples.

3.2.9 Animal Model

All animal experiments were performed in accordance with guidelines of Peking University Health Science Center Animal Care and Use Committee. The HT-29 human colon cancer cells were obtained from Professor Xiaoyan Qiu, Peking University Health Science Center, and were maintained at 37 ^{o}C and 5% CO_2 in Dulbecco's modified Eagle's medium (DMEM) containing 10% fetal bovine serum (FBS). Female BALB/c nude mice (4 – 5 weeks of age) were purchased from the Department of Experimental Animal, Peking University Health Science Center. The HT-29 cells (5×10^6) were implanted subcutaneously into the right upper flanks of nude mice. When tumors reached ~0.8 cm in mean diameter, the tumor-bearing mice were used for biodistribution and imaging studies. Sixteen tumor-bearing mice were randomly divided into four groups, each of which had four animals. Each tumor-bearing mouse was administered intravenously with

[^{99m}Tc(HYNIC-ABN](tricine)(TPPTS)] (~15 μCi) dissolved in 0.1 mL of saline via the tail vein. Animals were anesthetized with intraperitoneal injection of sodium pentobarbital at a dose of 45.0 mg/kg, and were sacrificed by cervical dislocation at 0.5, 1, 2 and 4 h postinjection (p.i.). Blood was withdrawn from the eye through a capillary tube. Organs of interest (tumor, heart, liver, spleen, kidney, lung, stomach, intestine, and muscle) were harvested, washed with saline, dried with absorbent tissues, weighed, and measured for radioactivity in a γ-counter (Wallac 1470-002, Perkin Elmer, Finland). The organ uptake was calculated as a percentage of the injected dose per gram of tissue mass (%ID/g). The biodistribution data and T/B ratios were reported as an average plus the standard deviation based on the results from four animals at each time point.

3.2.10 Metabolism

The metabolic stability of [^{99m}Tc(HYNIC-ABN](tricine)(TPPTS)] was evaluated using two normal BALB/c nude mice. Each mouse was administered via tail vein with the radiotracer (~800 μCi) dissolved in 0.2 mL saline. The urine samples were collected at 1 h p.i. by manual void, and were mixed with an equal volume of saline. The mixture was centrifuged at 8000 rpm for 5 min. The supernatant was collected and filtered through a 0.22 μm Millex-LG syringe driven filter unit to remove the precipitate and large proteins. The filtrate was analyzed by radio-HPLC. Both the liver and kidney simples were also harvested at 1 h p.i., and were pulped. The homogenates were mixed with an equal volume of saline, separately. The resulting mixture was vortexed for 5 – 10 min. After centrifuging at 8000 rpm for 5 min, the supernatant was collected and passed through a 0.22 μm Millex-LG syringe driven filter unit to remove any precipitate and particles. The filtrate was then analyzed by radio-HPLC.

3.2.11 Scintigraphic Imaging

The imaging study was performed using the female BALB/c nude mice bearing the HT-29 human colon cancer xenografts. Animals were anesthetized with intraperitoneal injection of sodium pentobarbital at a dose of 45.0 mg/kg. Each tumor-bearing mouse was administered intravenously with [^{99m}Tc(HYNIC-ABN](tricine)(TPPTS)] (~400 μCi) in 0.2 mL saline via tail vein. Animals were placed prone on a two-head γ-camera (SIEMENS, E. CAM) equipped with a parallel-hole, low-energy, and high-resolution collimator. Posterior images were acquired 1 h and 4 h p.i. The imaging data were stored digitally in a 128 x 128 matrix. The acquisition count limits were set at 200 K. In the blocking experiment, each tumor-bearing mouse was administered intravenously with excess HYNIC-ABN (300 μg dissolved in 0.1 mL of saline) 30 min prior to administration of [^{99m}Tc(HYNIC-ABN](tricine)(TPPTS)]. The posterior images were acquired 1 h p.i. using the same procedure above. After completion of imaging, animals were sacrificed by cervical dislocation.

3.3 Results

3.3.1 GRP Receptor Binding Affinity of ABN and HYNIC-ABN

The *in vitro* GRPR binding affinities and specificities of ABN and HYNIC-ABN were assessed via a competitive displacement assay using ^{125}I-[Tyr4]BBN as the radioligand. It was found that ABN and HYNIC-ABN were able to compete with ^{125}I-[Tyr4]BBN bound to PC-3 prostate carcinoma cells (Figure 2). The IC_{50} values were 24 ± 2 nM and 38 ± 1 nM for ABN and HYNIC-ABN, respectively. The attachment of HYNIC group seems to slightly reduce the GRPR binding affinity of ABN; but this difference may not be significant within the error of this assay.

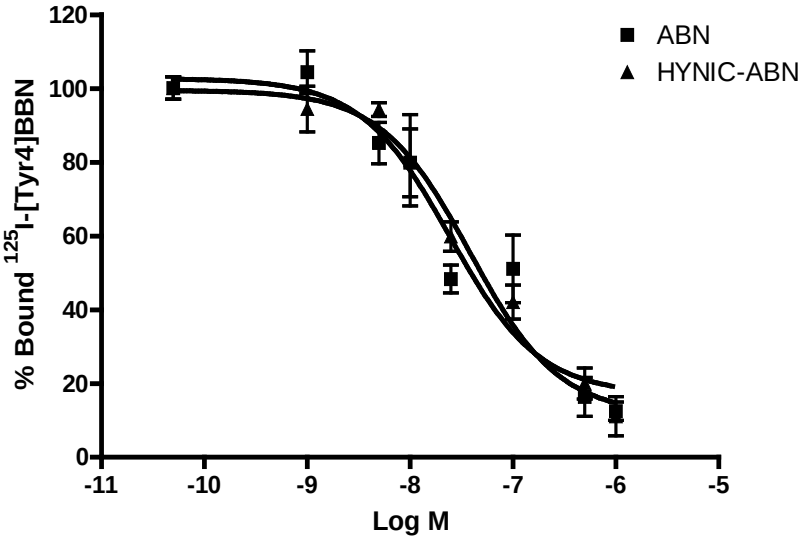

Figure 2. Displacement curves of ^{125}I-[Tyr^4]BBN bound to the GRPR-positive PC-3 human prostate carcinoma cells by ABN and HYNIC-ABN. The IC_{50} values were calculated to be 24 ± 2 nM and 38 ± 1 nM for ABN and HYNIC-ABN, respectively.

3.3.2 Radiochemistry

[^{99m}Tc(HYNIC-ABN](tricine)(TPPTS)] was prepared in two steps. First, HYNIC-ABN reacted with $Na^{99m}TcO_4$ in the presence of excess tricine and $SnCl_2$ to form the intermediate [^{99m}Tc(HYNIC-ABN)(tricine)$_2$], which was then allowed to react with TPPTS to form the ternary ligand complex [^{99m}Tc(HYNIC-ABN](tricine)(TPPTS)]. The specific activity was ~120 mCi/μmol. The radiochemical purity was >95% after Sep-Pak purification. [^{99m}Tc(HYNIC-ABN](tricine)(TPPTS)] was analyzed using a reversed-phase HPLC method. A radio-HPLC chromatogram is shown in the top panel of Figure 3. The HPLC retention time was 12.2 min for [^{99m}Tc(HYNIC-ABN](tricine)(TPPTS)]. The

partition coefficient was determined in an equal volume mixture of n-octanol and 25 mM phosphate buffer (pH = 7.4). The log P value was -2.39 ± 0.06. The solution stability of [^{99m}Tc(HYNIC-ABN](tricine)(TPPTS)] was monitored by radio-HPLC in saline and in the presence of excess cysteine (1.0 mg/mL, pH = 7.4). The solution stability data of [^{99m}Tc(HYNIC-ABN](tricine)(TPPTS)] is shown in the bottom panel of Figure 3. It is quite clear that [^{99m}Tc(HYNIC-ABN](tricine)(TPPTS)] is able to maintain its stability over 12 h in saline and in the presence of excess cysteine.

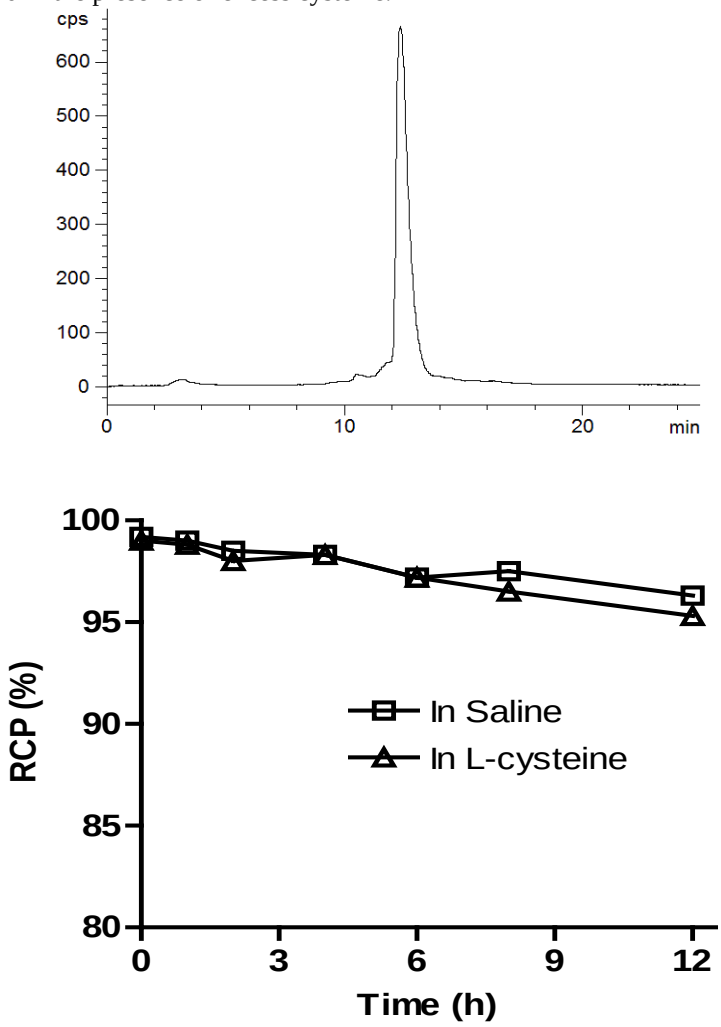

Figure 3.A typical radio-HPLC chromatogram (*92*) and solution stability data (bottom) for [^{99m}Tc(HYNIC-ABN)(tricine)(TPPTS)] in saline and in the presence of excess cysteine (1 mg/mL, pH = 7.4).

3.3.3 Internalization and Efflux Kinetics

The internalization and efflux kinetics of [^{99m}Tc(HYNIC-ABN](tricine)(TPPTS)] is shown in Figure 4. The rate of internalization was time and temperature dependent. At 4°C, the receptor binding took place; but there was no internalization (< 1%). At 37°C, there was a rapid internalization with 35 ± 2% of the cell-associated radioactivity being internalized at 5 min post-incubation (Figure 4, Left). The maximum was reached with 68 ± 5% of the internalized radioactivity at 30 min post-incubation. In spite of the fast internalization, there was no significant retention of radioactivity inside tumor cells since the internalized radioactivity was quickly released. After 15 min incubation at 37 °C, 49 ± 3% of the internalized radioactivity remained. Only ~20% of the internalized radioactivity remained after 1 h (Figure 4, Right).

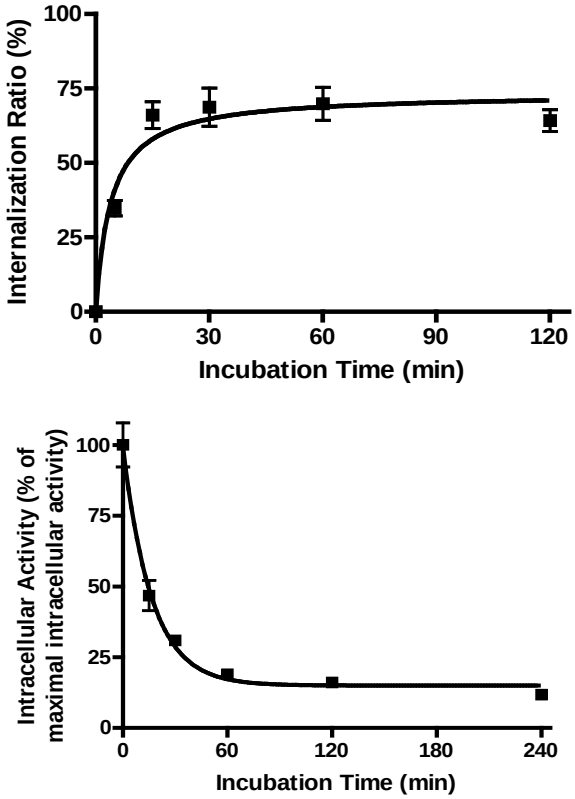

Figure 4. Internalization (left) and efflux (right) kinetics of [^{99m}Tc(HYNIC-ABN)(tricine) (TPPTS)].

3.3.4 Biodistribution Characteristics

The biodistribution study was performed using the BALB/c nude mice bearing HT-29 human colon cancer xenografts. The selected biodistribution data and T/B ratios for

[^{99m}Tc(HYNIC-ABN)(tricine)(TPPTS)] are summarized in Figure 5. In general, [^{99m}Tc(HYNIC-ABN)(tricine)(TPPTS)] had a rapid clearance, predominantly through the renal route. Most of the injected dose was in the urinary system by 1 h p.i. with little radioactivity accumulation in the blood (0.50 ± 0.15 %ID/g), liver (0.68 ± 0.16 %ID/g), muscle (0.14±0.04 %ID/g), and gastrointestinal tract (0.63 ± 0.21 %ID/g) at 1 h p.i. The tumor uptake was the highest (1.59 ± 0.23 %ID/g) at 30 min p.i., with a steady decrease over the 4 h study period. [^{99m}Tc(HYNIC-ABN](tricine)(TPPTS)] had the best T/B ratios for blood (2.37 ± 0.68), liver (1.69 ± 0.41), and muscle (11.17 ± 3.32) at 1 h p.i.

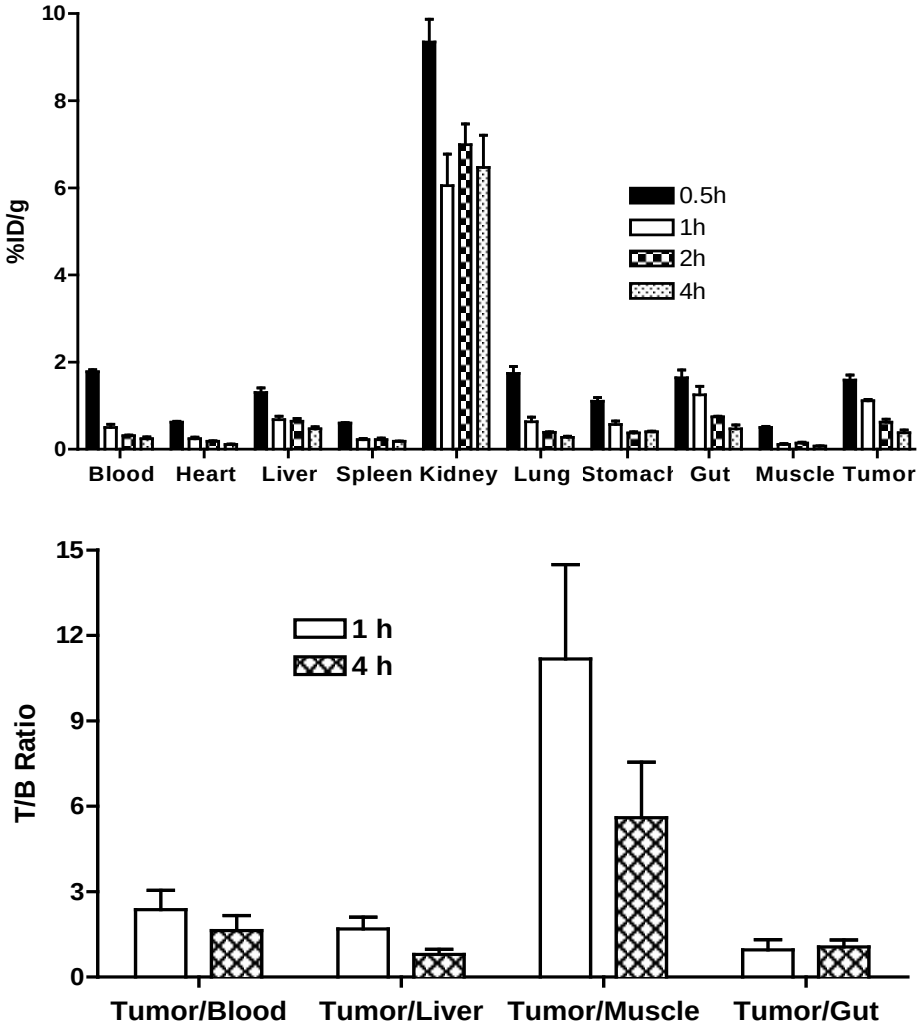

Figure 5. Organ uptake (*92*) and T/B ratios (bottom) for [^{99m}Tc(HYNIC-ABN)(tricine)(TPPTS)] in BALB/c nude mice bearing the HT-29 human colon cancer xenografts. Each data point represents an average of biodistribution data in four animals.

3.3.5 Imaging Studies

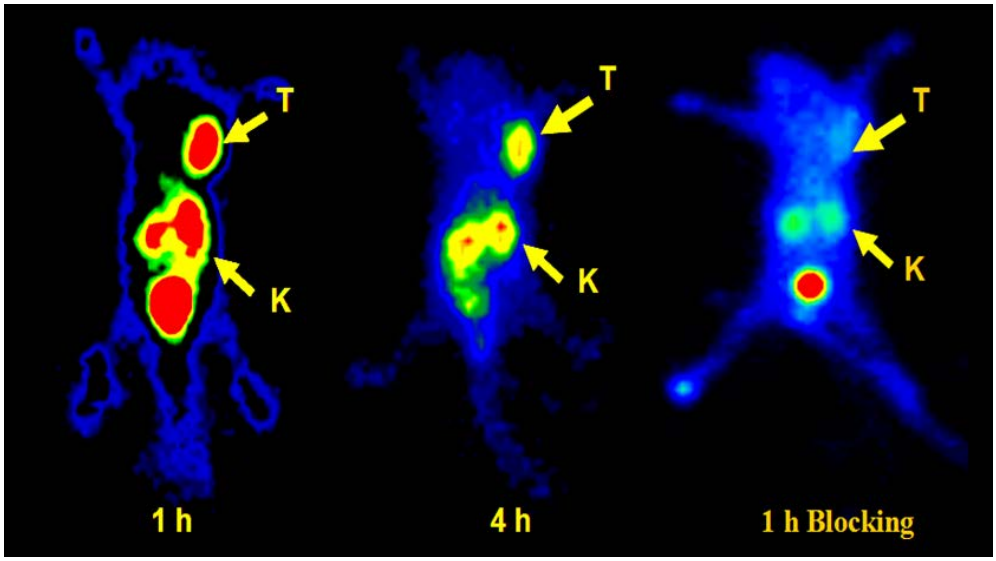

Figure 6. Static planar images of the tumor-bearing mice administered with ~400 μCi of [^{99m}Tc(HYNIC-ABN)(tricine)(TPPTS)] at 1 h (left) and 4 h p.i. (middle), as well as in the presence of excess HYNIC-ABN (right). Arrows indicate the presence of the tumor (T) and kidneys (K).

Figure 6 illustrates representative planar images of the tumor-bearing mice administered with ~400 μCi of [^{99m}Tc(HYNIC-ABN)(tricine)(TPPTS)] at 1 h (left) and 4 h p.i. (middle), as well as in the presence of excess HYNIC-ABN (right) at 1 h p.i. Arrows indicate the presence of the tumor (T) and kidneys (K). The HT-29 tumor is clearly visualized at 1 h p.i. with excellent tumor-to-background contrast. At 1 h p.i., the "hottest" spots are tumor, kidneys and bladder. By 4 h p.i., the radioactivity in the chest region almost completely disappears while the tumor is still clearly seen. These data are consistent with those obtained from the *ex vivo* biodistribution study (Figure 5).

The blocking experiment by pre-injecting or co-injecting a known receptor ligand is often used to demonstrate the tumor-specificity of the target-specific radiotracers. In this study, we used HYNIC-ABN as the blocking agent. Pre-injection of excess HYNIC-ABN result in a significant reduction in the tumor uptake of [^{99m}Tc(HYNIC-ABN)(tricine)(TPPTS)] (Figure 6: right), indicating that its tumor localization is at least partially GRPR-mediated. There is also a significant reduction in radiotracer accumulation in several non-cancerous organs, such as liver, stomach, intestine and kidneys, due to the blockage of GRPRs in these organs (*1*, *3*, *4*).

3.3.6 Metabolic Properties

Metabolism study was performed using normal BALB/c mice by analyzing the samples from urine, kidney and liver. Figure 7 shows typical radio-HPLC chromatograms

of [^{99m}Tc(HYNIC-ABN](tricine)(TPPTS)] in the kit matrix before injection (A), in the urine (B), in the kidney (C), and in the liver (D). [^{99m}Tc(HYNIC-ABN](tricine)(TPPTS)] was completely metabolized in urine, kidney and liver samples at 1 h p.i. The majority of the injected radioactivity was found in the urine sample at 1 h p.i. The radioactivity level was almost undetectable in the liver and kidney samples.

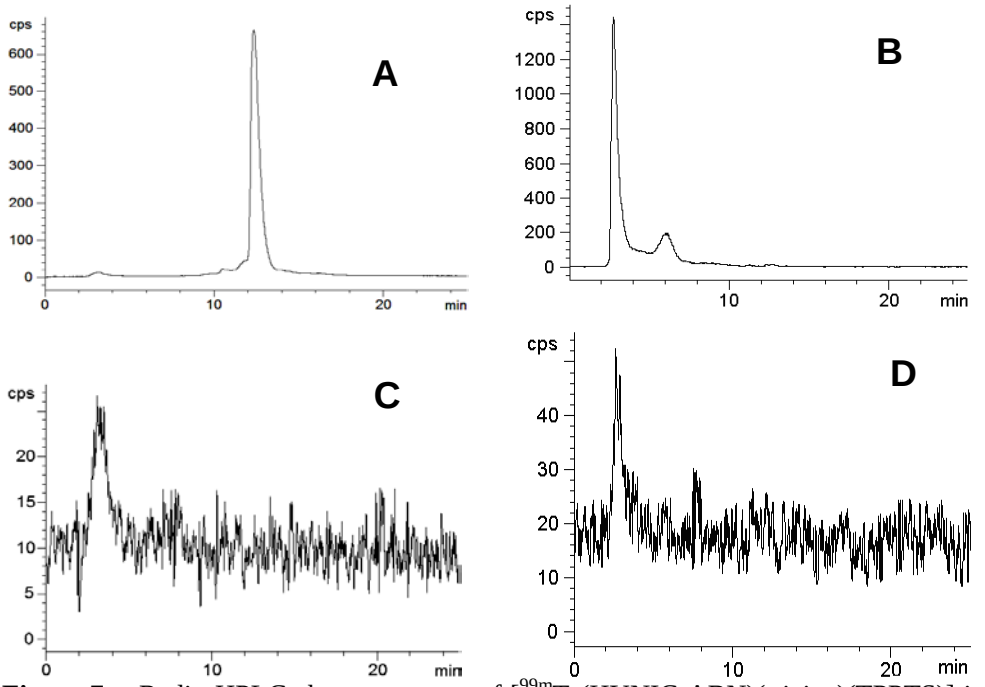

Figure 7. Radio-HPLC chromatograms of [^{99m}Tc(HYNIC-ABN)(tricine)(TPPTS)] in the kit matrix before injection (A), in the urine (B), in the liver (C), and in the kidney (D) at 1 h p.i.

3.4 Discussion

Since colon cancer occurs in the torso area, it is necessary for the radiotracer to have a minimal radioactivity accumulation in the liver, lungs, stomach and gastrointestinal tract. There are several factors influencing the radiotracer excretion kinetics. These include the molecular charge, solution stability, lipophilicity and metabolic stability of the radiotracer. For the last several years, intensive efforts have been made to optimize the radiotracer pharmacokinetics by using different ^{99m}Tc cores (*34*, *36*, *37*, *41*, *44*, *46*), BFCs (*34*, *39*, *44*) and linker groups (*36*, *39*). It was reported that the linker groups, such as β-Ala–β-Ala or 3,6-dioxa-8-aminooctanoic acid, had a significant impact on tumor uptake, excretion kinetics and metabolic stability of the ^{99m}Tc-labelled BN(7-14)NH_2 (*36*). A major disadvantage of using the ^{99m}Tc$(CO)_3^+$ core for the ^{99m}Tc-labeling of BN(7-14)NH_2 derivatives is that the radiotracer often has high uptake in the liver and intestine (*36*). Recently, NOTA and DOTA were used as BFCs for preparation of the ^{64}Cu-labelled BN-like peptides (*25-29*). Results from biodistribution and microPET imaging studies show that the ^{64}Cu-labelled NOTA-BN conjugates have very little accumulation in the liver,

lungs, stomach and intestine (*29*). The BFCs and radiometal chelates can be used to improve the radiotracer clearance from the non-cancerous organs.

In this study, we used HYNIC as the BFC and tricine/TPPTS as coligands to prepare [^{99m}Tc(HYNIC-ABN](tricine)(TPPTS)]. We found that [^{99m}Tc(HYNIC-ABN](tricine)(TPPTS)] was excreted rapidly via the renal route with very little radioactivity accumulation in the blood, liver, muscle and gastrointestinal tract at >1 h p.i. (Figure 5). The tumor uptake was the highest (1.59 ± 0.23 %ID/g) at 30 min p.i. with a steady decrease over the 4 h study period. This radiotracer had the best T/B ratios in the blood (2.37 ± 0.68), liver (1.69 ± 0.41) and muscle (11.17 ± 3.32) at 1 h p.i. The rapid tumor washout is also seen in images of the tumor-bearing mice (Figure 6), which is consistent with the rapid efflux kinetics of [^{99m}Tc(HYNIC-ABN](tricine)(TPPTS)] (Figure 4). Similar tumor washout was also reported for the $^{99m}Tc(CO)_3$-labelled BN(7-14)NH_2 derivatives (*36*, *37*). Results from the blocking experiment show that the tumor uptake of [^{99m}Tc(HYNIC-ABN](tricine)(TPPTS)] is at least partially GRPR-mediated. The radiotracer uptake decreased in the liver, stomach and intestine in the presence of excess HYNIC-ABN, which strongly suggests that the GRPRs are also expressed in these organs. Compared with the $^{99m}Tc(CO)_3$-labelled His-linker-BN(7-14)NH_2 (linker = β-Ala–β-Ala or 3,6-dioxa-8-aminooctanoic acid) (*36*), [^{99m}Tc(HYNIC-ABN](tricine)(TPPTS)] has the advantage with respect to its rapid clearance from blood, liver, muscle and gastrointestinal tract.

The solution stability data shows that [^{99m}Tc(HYNIC-ABN](tricine)(TPPTS)] is stable for > 12 h in the presence of excess cysteine (Figure 3). However, results from the metabolism study indicate that [^{99m}Tc(HYNIC-ABN](tricine)(TPPTS)] is completely metabolized at 1 h p.i. in the urine, kidney and liver samples, probably due to rapid enzymatic degradation. Earlier studies showed that BN-like peptides could be easily metabolized by the neutral endopeptidase E.C.3.4.24.11 and the angiotensin-converting enzyme (*60*-*62*). This metabolic instability may contribute, in part, to the rapid washout of [^{99m}Tc(HYNIC-ABN](tricine)(TPPTS)] from tumor and non-cancerous organs, such as the liver, lungs, muscle, stomach and gastrointestinal tract.

The GRPR binding affinities of ABN and HYNIC-ABN are very similar to those reported for DOTA-Linker-Bombesin(7-14) (Linker = triglycine, glycine-serine-glycine or glycine-serine-serine) (*27*) and those reported for the $Re(CO)_3$ complexes of His-linker-BN(7-14)NH_2 (linker = β-Ala–β-Ala or 3,6-dioxa-8-aminooctanoic acid) (*36*). However, the tumor uptake of [^{99m}Tc(HYNIC-ABN](tricine)(TPPTS)] in HT-29 colon cancer is not as high as those reported for the ^{64}Cu-labelled DOTA-Linker-Bombesin(7-14) conjugates (Linker = triglycine, glycine-serine-glycine or glycine-serine-serine) in the PC-3 prostate cancer (*27*). There are two main reasons for the low tumor uptake of [^{99m}Tc(HYNIC-ABN](tricine)(TPPTS)] reported in this study. The expression level of GRPRs on HT-29 cells may not be as high as that PC-3 prostate cancer cells. The attachment of the ^{99m}Tc chelate (^{99m}Tc, HYNIC, tricine and TPPTS) may significantly reduce the GRPR binding affinity of [^{99m}Tc(HYNIC-ABN](tricine)(TPPTS)], which seems to be supported by the fact that the IC_{50} value of ABN (24 ± 2 nM) is slightly lower than that of HYNIC-ABN (38 ± 1 nM). It must be emphasized that the difference in the tumor-bearing mice (BALB/c versus SCID) may also contribute to the variation of the tumor uptake and excretion kinetics of the radiotracer. Therefore, caution must be taken when comparing the biodistribution data obtained by two different research laboratories using two different tumor-bearing animal models.

3.5 Conclusion

The ternary ligand system (HYNIC, tricine and TPPTS) has been successfully used for ^{99m}Tc-labeling of β-Ala-BN(7-14)NH_2. [^{99m}Tc(HYNIC-ABN)(tricine)(TPPTS)] can be prepared in high yield and high specific activity. Because of its hydrophilicity (log P = -2.39 ± 0.06), [^{99m}Tc(HYNIC-ABN)(tricine)(TPPS)] is excreted mainly via the renal route with little radioactivity accumulation in the liver, lungs, stomach, and gastrointestinal tract. Its metabolic instability may contribute, in part, to its rapid clearance from the tumor and non-tumor organs, such as the blood, liver, lungs and stomach. As a result, it has the best T/B ratios in the blood, liver and muscle at 1 h p.i. The tumor can be clearly visualized as early as 30 – 60 min p.i. by planar imaging of the BALB/c nude mice bearing the HT-29 human colon xenografts. The combination of relatively high tumor uptake with its extremely favorable pharmacokinetics makes [^{99m}Tc(HYNIC-ABN)(tricine)(TPPTS)] a promising SPECT radiotracer for imaging colon cancer.

Acknowledgements

Authors would like to thank Professor Xiaoyan Qiu, Peking University Health Science Center, for providing the HT-29 human colon cancer cells, and Huiyun Zhao, Peking University Medical Isotopes Research Center, for technical support. This work is supported, in part, by research grants: Z00004105040311 and D0206001041991 (F.W.) from the Beijing Science and Technology Program, 30640067(F.W.) from the NSF, 1R01 CA115883-01A2 (S.L.) from the National Cancer Institute (NCI), and BCTR0503947 (S.L.) from the Susan G. Komen Breast Cancer Foundation.

References

(1) Erspamer, V., Erpamer, G. F., and Inselvini, M. (1970) Some pharmacological actions of alytesin and bombesin. *J. Pharm. Pharmacol. 22*, 875-876.

(2) Prasad, S., Mathur, A., Gupta, N., Jaggi, M., and Singh, A. T. (2007) Bombesin analogs containing α-amino-isobutyric acid with potent anticancer activity. *J. Pept. Sci. 13*, 54-62.

(3) Ohki-Hamazaki, H., Iwabuchi, M., and Maekawa, F. (2005) Development and function of bombesin-like peptides and their receptors. *Int. J. Dev. Biol. 49*, 293-300.

(4) Patel, O. Shulkes, A., and Baldwin, G. S. (2006) Gastrin-releasing peptide and cancer. *Biochim. Biophys. Acta 1766*, 23-41.

(5) Nakagawa, T., Hocart, S. J., Schumann, M., Tapia, J. A., Mantey, S. A., Coy, D. H., Tokita, K., Katsuno, T., and Jensen, R. T. (2005) Identification of key amino acids in the gastrin-releasing peptide receptor (GRPR) responsible for high affinity binding of gastrin-releasing peptide (GRP). *Biochem. Pharmacol. 69*, 579-593.

(6) Moody, T. W., Carney, D. N., Cuttitta, F., Quattrocchi, K., and Minna, J. D. (1985) High affinity receptors for bombesin/GRP-like peptides on human small cell lung cancer. *Life Sci. 37*, 105-113.

(7) Radulovic, S. S., Milovanovic, S. R., Cai, R. Z., and Schally, A. V. (1992) The binding of bombesin and somatostatin and their analogs to human colon cancers. *Proc. Soc. Exp. Biol. Med. 200*, 394-401.

(8) Carroll, R. E., Matkowskyj, K. A., Chakrabarti, S., McDonald, T. J., and Benya, R. V. (1999) Aberrant expression of gastrin-releasing peptide and its receptor by well-differentiated colon cancers in humans. *Am. J. Physiol. 276,* G655-G665.

(9) Saurin, J. C., Nemoz-Gaillard, E., Sordat, B., Cuber, J. C., Coy, D. H., Abello, J., and Chayvialle, J. A. (1999) Bombesin stimulates adhesion, spreading, lamellipodia formation, and proliferation in the human colon carcinoma Isreco1 cell line[1]. *Cancer Res. 59,* 962-967.

(10) Carroll, R. E., Ostrovskiy, D., Lee, S., Danilkovich, A., and Benya, R. V. (2000) Characterization of gastrin-releasing peptide and its receptor aberrantly expressed by human colon cancer cell lines. *Mol. Pharmacol 58,* 601-607.

(11) Saurin, J. C., Fallavier, M., Sordat, B., Gevrey, J. C., Chayvialle, J. A., and Abello, J. (2002) Bombesin stimulates invasion and migration of isreco1 colon carcinoma cells in a Rho-dependent manner. *Cancer Res. 62,* 4829-4835.

(12) Cassano, G., Resta, N., Gasparre, G., Lippe, C., and Guanti, G. (2001) The proliferative response of HT-29 human colon adenocarcinoma cells to bombesin-like peptides. *Cancer Lett. 172,* 151-157.

(13) Varvarigou, A., Bouziotis, P., Zikos, C., Scopinaro, F., and De Vincentis G. (2004) Gastrin-releasing peptide (GRP) analogues for cancer imaging. *Cancer Biother. Radiopharm. 19,* 219-229.

(14) Reubi, J. C. (2003) Peptide receptors as molecular targets for cancer diagnosis and therapy. *Endocr. Rev. 24,* 389-427.

(15) Jong, M., Kwekkeboom, D., Valkema, R., and Krenning, E. P. (2003) Radiolabelled peptides for tumour therapy: Current status and future directions. *Eur. J. Nucl. Med. 30,* 463-469.

(16) Van de Wiele, C., Dumont, F., van Belle, S., Slegers, G., Peers, S. H., and Dierckx, R. A. (2001) Is there a role for agonist gastrin-releasing peptide receptor radioligands in tumour imaging? *Nucl. Med. Commun. 22,* 5-15.

(17) Hoffman, T. J., Quinn, T. P., and Volkert, W. A. (2001) Radiometallated receptor-avid peptide conjugates for specific in vivo targeting of cancer cells. *Nucl. Med. Biol. 28,* 527-539.

(18) Breeman, W. A., De Jong, M., Bernard, B. F., Kwekkeboom, D. J., Srinivasan, A., van der Pluijm, M. E., Hofland, L. J., Visser, T. J., and Krenning, E. P. (1999) Pre-clinical evaluation of [^{111}In-DTPA-Pro^{1}, Tyr^{4}] bombesin, a new radioligand for bombesin-receptor scintigraphy. *Int. J. Cancer. 83,* 657-663.

(19) Zhang, H. W., Chen, J. H., Waldherr, C., Hinni, K., Waser, B., Reubi, J. C., and Maecke, H. R. (2004) Synthesis and evaluation of bombesin derivatives on the basis of pan-bombesin peptides labelled with indium-111, lutetium-177, and yttrium-90 for targeting bombesin receptor-expressing tumors. *Cancer Res. 64,* 6707-6715.

(20) Hoffman, T. J., Gali, H., Smith, C. J., Sieckman, G. L., Hayes, D. L., Owen, N. K., and Volkert, W. A. (2003) Novel series of ^{111}In labelled bombesin analogs as potential radiopharmaceuticals for specific targeting of gastrin-releasing peptide receptors expressed on human prostate cancer cells. *J. Nucl. Med. 44,* 823-831.

(21) Smith, C. J., Gali, H., Sieckman, G. L., Hayes, D. L., Owen, N. K., Mazuru, D. G., Volkert, W. A., and Hoffman, T. J. (2003) Radiochemical investigations of ^{177}Lu-DOTA-8-Aoc-BBN[7-14]NH_2: an in vitro/in vivo assessment of the targeting ability of this new radiopharmaceutical for PC-3 human prostate cancer cells. *Nucl. Med. Biol. 30,* 101-109.

(22) Hu, F., Cutler, C. S., Hoffman, T., Sieckman, G., Volkert, W. A., and Jurisson, S. S. (2002) Pm-149 DOTA bombesin analogs for potential radiotherapy in vivo comparison

with Sm-153 and Lu-177 labelled DO3A-amide-βAla-BBN(7-14)NH_2. *Nucl. Med. Biol. 29*, 423-430.

(23) Waser, B., Eltschinger, V., Linder, K., Nunn, A., and Reubi, J. C. (2007) Selective in vitro targeting of GRP and NMB receptors in human tumours with the new bombesin tracer ^{177}Lu-AMBA. *Eur. J. Nucl. Med. Mol. Imaging 34*, 95-100.

(24) Schuhmacher, J., Zhang, H., Doll, J., Mäcke, H. R., Matys, R., Hauser, H., Henze, M., Haberkorn, U., and Eisenhut, M. (2005) GRP receptor-targeted PET of a rat pancreas carcinoma xenograft in nude mice with a ^{68}Ga-labelled bombesin(6-14) analog. *J. Nucl. Med. 46*, 691-699.

(25) Biddlecombe, G. B., Rogers, B. E., de Visser, M., Parry, J. J., de Jong, M., Erion, J. L., and Lewis, J. S. (2007) Molecular imaging of gastrin-releasing peptide receptor-positive tumors in mice using ^{64}Cu- and ^{86}Y-DOTA-(Pro^1, Tyr^4)-Bombesin(1-14). *Bioconj. Chem. 18*, 724-730.

(26) Parry, J. J., Andrews, R., and Rogers, B. E. (2007) MicroPET imaging of breast cancer using radiolabelled bombesin analogs targeting the gastrin-releasing peptide receptor. *Breast Cancer Res. Treat. 101*, 175-183.

(27) Parry, J. J., Kelly, T. S., Andrews, J., and Rogers, B. E. (2007) in vitro and in vivo evaluation of ^{64}Cu-labelled DOTA-Linker-Bombesin(7-14) analogues containing different amino acid linker moiety. *Bioconj. Chem. 18*, 1110-1117.

(28) Garrison, J. C., Rold, T. L., Sieckman, G. L., Figueroa, S. D., Volkert, W. A., Jurisson, S. S., and Hoffman, T. J. (2007) In vivo evaluation and small-animal PET/CT of a prostate cancer mouse model using ^{64}Cu Bombesin analogs: side-by-side comparison of the CB-TE2A and DOTA chelation systems. *J. Nucl. Med. 48*, 1327-1337.

(29) Prasanphanich, A. F., Nanda, P. K., Rold, T. L., Ma, L., Lewis, M. J., Garrison, J. C., Hoffman, T. J., Sieckman, G. L., Figueroa, S. D., and Smith, C. J. (2007) [^{64}Cu-NOTA-8-Aoc-BBN(7-14)NH_2] targeting vector for positron-emission tomography imaging of gastrin-releasing peptide receptor-expressing tissues. *PNAS 104*, 12462-12467.

(30) Yang, Y., Zhang, X., Xiong, Z., and Chen, X. (2006) Comparative in vitro and in vivo evaluation of two ^{64}Cu-labelled bombesin analogs in a mouse model of human prostate adenocarcinoma. *Nucl. Med. Biol. 33*, 371-380.

(31) Rogers, B. E., Bigott, H. M., McCarthy, D. W., Manna, D. D., Kim, J., Sharp, T. L., and Welch, M. J. (2003) MicroPET Imaging of a gastrin-releasing peptide receptor-positive tumor in a mouse model of human prostate cancer using a ^{64}Cu-labelled bombesin analogue. *Bioconj. Chem. 14*, 756-763.

(32) Chen, X., Park, R., Hou, Y., Tohme, M., Shahinian, A. H., Bading, J. R., Conti, P. S. (2004) MicroPET and autoradiographic imaging of GRP receptor expression with ^{64}Cu-DOTA-[Lys^3]bombesin in human prostate adenocarcinoma xenografts. *J. Nucl. Med. 45*, 1390-1397.

(33) Smith, C. J., Sieckman, G. L., Owen, N. K., Hayes, D. L., Mazuru, D. G., Volkert, W. A., and Hoffman, T. J. (2003) Radiochemical investigation of [^{188}Re(H_2O)$(CO)_3$-diaminopropionic acid-SSS-bombesin(7-14)NH_2]: syntheses, radiolabelling and in Vitro/in Vivo GRP receptor targeting studies. *Anticancer Res. 23*, 63-70.

(34) Karra, S. R., Schibli, R., Gali, H., Katti, K. V., Hoffman, T. J., Higginbotham, C., Sieckman, G. L., and Volkert, W. A. (1999) ^{99m}Tc-labeling and in vivo studies of a bombesin analogue with a novel water-soluble dithiadiphosphine-based bifunctional chelating agent. *Bioconj. Chem. 10*, 254-260.

(35) Van de Wiele, C., Dumont, F., Broecke, V. R., Oosterlinck, W., Cocquyt, V., Serreyn, R., Peers, S., Thornback, J., Slegers, G., Dierckx, R. A. (2000) Technetium-99m RP527, a GRP analogue for visualisation of GRP receptor-expressing malignancies: a feasibility study. *Eur. J. Nucl. Med. 27,* 1694-1699.

(36) Garayoa, E. G., Rüegg, D., Bläuenstein, P., Zwimpfer, M., Khan, I. U., Maes, V., Blanc, A., Beck-Sickinger, A. G., Tourwé, D. A., and Schubiger, P. A. (2007) Chemical and biological characterization of new $Re(CO)_3$/[^{99m}Tc]$(CO)_3$ bombesin analogues. *Nucl. Med. Biol. 34,* 17-28.

(37) La Bella, R., Garayoa, E. G., Bähler, M., Bläuenstein, P., Schibli, R., Conrath, P., Tourwé, D., and Schubiger, P. A. (2002) A ^{99m}Tc(I)-postlabelled high affinity bombesin analogue as a potential tumor imaging agent. *Bioconj. Chem. 13,* 599-604.

(38) Scopinaro, F., Varvarigou, A., Ussof, W., De Vincentis, G., Sourlingas, T. G., Evangelatos, G. P., Datsteris, J., Archimandritis, S. C. (2002) Technetium labelled bombesin like peptide: preliminary report on breast cancer uptake in patients. *Cancer Biother. Radiopharm. 17,* 327-335.

(39) Smith, C. J., Gali, H., Sieckman, G. L., Higginbotham, C., Volkert, W. A., and Hoffman, T. J. (2003) Radiochemical investigations of ^{99m}Tc-N_3S-X-BBN[7-14]NH_2: an in vitro/in vivo structure-activity relationship study where X = 0-, 3-, 5-, 8-, and 11-carbon tethering moieties. *Bioconj. Chem. 14,* 93-102.

(40) Scopinaro, F., De Vincentis, G., Varvarigou, A. D., Laurenti, C., Iori, F., Remediani, S., Chiarini, S., and Stella, S. (2003) ^{99m}Tc-bombesin detects prostate cancer and invasion of pelvic lymph nodes. *Eur. J. Nucl. Med. Mol. Imaging. 30,* 1378-1382.

(41) Nock, B., Nikolopoulou, A., Chiotellis, E., Loudos, G., Maintas, D., Reubi, J. C., and Maina, T. (2003) [^{99m}Tc]Demobesin 1, a novel potent bombesin analogue for GRP receptor-targeted tumour imaging. *Eur. J. Nucl. Med. Mol. Imaging. 30,* 247-258.

(42) Scopinaro, F., De Vincentis, G.e, and Corazziari, E., (2004) Detection of colon cancer with ^{99m}Tc-labelled bombesin derivative (^{99m}Tc-leu13-BN1). *Cancer Bioth. Radiopharm. 19,* 245-252.

(43) Nock, B. A., Nikolopoulou, A., Galanis, A., Cordopatis, P., Waser, B., Reubi, J. C. and Maina, T. (2005) Potent Bombesin-like Peptides for GRP-Receptor Targeting of Tumors with ^{99m}Tc: A Preclinical Study. *J. Med. Chem. 48,* 100-110.

(44) Faintuch, B. L., Santos, S. R., Souza, A. L. F. M., Hoffman, T. J., Greeley, M., and Smith, C. J. (2005) ^{99m}Tc-HYNIC-bombesin(7-14)NH_2: radiochemical evaluation with co-ligands EDDA (EDDA = Ethylenediamine-N,N′-diacetic Acid), tricine, and nicotinic acid. *Synth. React. Inorg. Met.-Org. Chem. 35,* 43-51.

(45) Lin, K. S., Luu, A., Baidoo, K. E., Hossein, H. G. Chen, M-K., Brenneman, K., Pili, R., Pomper, M., Carducci, M. A., and Wagner, H. N., Jr. (2005) A new high affinity technetium-99m-bombesin analogue with low abdominal accumulation. *Bioconj. Chem. 16,* 43-50.

(46) Kunstler, J-U., Veerendra, B., Figueroa, S. D., Sieckman, G. L., Rold, T. L., Hoffman, T. J., Smith, C. J., and Pietzsch, H. J. (2007) Organometallic ^{99m}Tc(III) '4 + 1' bombesin(7-14) conjugates: synthesis, radiolabelling, and *in vitro/in vivo* studies. *Bioconj. Chem. 18,* 1651-1661.

(47) Guillermina, F-F., Consuelo, A. de M., Jeanette, R-C., Martha, P-L., and María T. R-I. (2006) Preparation and evaluation of ^{99m}Tc-EDDA/HYNIC-[Lys^3]-bombesin for imaging gastrin-releasing peptide receptor-positive tumours. *Nucl.r Med. Commun.* 27, 371-376.

(48) Liu, S., Edwards, D.S., and Barrett, J. A. (1997) ^{99m}Tc-labeling of highly potent small peptides. *Bioconj. Chem. 8,* 621-636.

(49) Liu, S., and Edwards, D.S. (1999) ^{99m}Tc-labelled small peptides as diagnostic radiopharmaceuticals. *Chem. Rev. 99.* 2235-2268.

(50) Liu, S. (2004) The role of coordination chemistry in development of target-specific radiopharmaceuticals. *Chem. Soc. Rev. 33*, 1-18.

(51) Edwards, D. S., Liu, S., Ziegler, M. C., Harris, A. R., Crocker, A. C., Heminway, S. J., and Barrett, J. A. (1999) RP463: A stabilized technetium-99m complex of a hydrazino nicotinamide conjugated chemotactic peptide for infection imaging. *Bioconj. Chem. 10*, 884-891.

(52) Brouwers, A. H., Laverman, P., Boerman, O. C., Oyen, W. J. G., Barrett, J. A., Harris, T. D., Edwards, D. S., and Corstens, F. H. M. (2000) A ^{99}Tc^{m}-labelled leukotriene B4 receptor antagonist for scintigraphic detection of infection in rabbits. *Nucl. Med. Commun. 21*. 1043-1051.

(53) Liu, S., Harris, A. R., Ziegler, M. C., Edwards, D. S., and Williams, N. E. (2002) ^{99m}Tc-labeling of a hydrazinonictotinamide-conjugated LTB_4 receptor antagonist useful for imaging infection and inflammation. *Bioconj. Chem. 13*, 881-886.

(54) Liu, S., Edwards, D. S., Ziegler, M. C., Harris, A. R., Hemingway, S. J., and Barrett, J. A. (2001) ^{99m}Tc-Labeling of a hydrazinonictotinamide-conjugated vitronectin receptor antagonist useful for imaging tumors. *Bioconj. Chem. 12*, 624-629.

(55) Liu, S., Hsieh, W., Kim, Y. S., and Mohammed, S. I. (2005) Effect of coligands on biodistribution characteristics of ternary ligand ^{99m}Tc complexes of a HYNIC-conjugated cyclic RGDfK dimer. *Bioconj. Chem. 16*, 1580-1588.

(56) Liu, S., He, Z., Hsieh, W. Y., Kim, Y. S., and Jiang, Y. (2006) Impact of PKM Linkers on Biodistribution Characteristics of the ^{99m}Tc-Labelled Cyclic RGDfK Dimer. *Bioconj. Chem. 17*, 1499-1507.

(57) Jia, B., Shi, J., Yang, Z., Xu, B., Liu, Z., Zhao, H., Liu, S., and Wang, F. (2006) ^{99m}Tc-labelled cyclic RGDfK dimer: initial evaluation for SPECT imaging of glioma integrin $\alpha_v\beta_3$ expression. *Bioconj. Chem. 17*, 1069-1076.

(58) Liu, S., Hsieh, W., Jiang, Y., Kim, Y. S., Sreerama, S. G., Chen, X., Jia, B., and Wang, F. (2007) Evaluation of a ^{99m}Tc-labelled cyclic RGD tetramer for non-invasive imaging integrin $\alpha_v\beta_3$-positive breast cancer. *Bioconj. Chem. 18*, 438-446.

(59) Edwards, D. S., Liu, S., Barrett, J. A., Harris, A. R., Looby, R. J., Ziegler, M. C., Heminway, S. J., and Carroll, T. R. (1997) New and versatile ternary ligand system for technetium radiopharmaceuticals: water soluble phosphines and tricine as coligands in labeling a hydrazinonicotinamide-modified cyclic glycoprotein IIb/IIIa receptor antagonist with ^{99m}Tc. *Bioconj. Chem. 8*, 146-154.

(60) Grady, E. F., Slice, L. W., Brant, W. O., Walsh, J. H., Payan, D. G., and Bunnett, N. W. (1995) Direct observation of endocytosis of gastrin releasing peptide and its receptor. *J. Biol. Chem. 270*, 4603-4611.

(61) Slice, L. W., Yee, H. F., Jr., and Walsh, J. H. (1998) Visualization of internalization and recycling of the gastrin releasing peptide receptor-green fluorescent protein chimera expressed in epithelial cells. *Receptors Channels 6*, 201-212.

(62) Coy, D. H., Mungan, Z., Rossowski, W. J., Cheng, B. L., Lin, J. T., Mrozinski, J. E., Jr., and Jensen, R. T. (1992) Development of a potent bombesin receptor antagonist with prolonged in vivo inhibitory activity on bombesin-stimulated amylase and protein release in the rat. *Peptides 13*, 775-781.

Chapter 4

^{99m}Technetium-HYNIC(tricine/TPPTS)-Aca-Bombesin(7-14) as a Targeted Imaging Agent with MicroSPECT in a PC-3 Prostate Cancer Xenograft Model

Hildo J.K. Ananias, **Zilin Yu**, Rudi A. Dierckx, Christophe van der Wiele, Wijnand Helfrich, Fan Wang, Yongjun Yan, Xiaoyuan Chen, Igle J. de Jong, Philip H. Elsinga

Mol Pharm, 2011; 8(4):1165-73.

Abstract

Introduction: The peptide bombesin (BN) and derivates thereof show high binding affinity for the gastrin-releasing peptide receptor (GRPR), which is highly expressed in primary and metastasized prostate cancer. We have synthesized a new BN-based radiopharmaceutical ^{99m}Technetium-HYNIC(tricine/TPPTS)-Aca-BN(7-14) (^{99m}Tc-HABN) and evaluated its GRPR targeting properties *in vitro* and in a xenograft tumor model for human prostate cancer in athymic mice.

Methods: ^{99m}Tc-HABN was synthesized and its lipophilicity and stability were investigated. The IC_{50}, internalization and efflux properties were determined *in vitro* using the GRPR expressing human prostate cancer cell line PC-3. ^{99m}Tc-HABN biodistribution and microSPECT imaging were performed in PC-3 tumor-bearing athymic mice.

Results: ^{99m}Tc-HABN was prepared with high labeling yield (>90%), high radiochemical purity (>95%) and a specific activity of ~19.8 MBq/nmol. The partition coefficient *log D* value was -1.60±0.06.^{99m}Tc-HABN proved to be stable in human serum for 6 hours. The IC_{50} of HYNIC-Aca-BN(7-14) was 12.81±0.14 nM. Incubation of PC-3 cells with ^{99m}Tc-HABN demonstrated rapid cellular internalization and a long intracellular retention time. When mice were injected with ^{99m}Tc-HABN the activity was predominantly cleared via the kidneys. Uptake in the tumor was 2.24±0.64 %ID/g after 30 minutes, with a steady decrease during the 4 hours study period. *In vivo* experiments with a blocking agent showed GRPR mediated uptake. ^{99m}Tc-HABN microSPECT imaging resulted in clear delineation of the tumor.

Conclusion: ^{99m}Tc-HABN is a novel BN-based radiopharmaceutical that proved to be suitable for targeted imaging of prostate cancer with microSPECTusing the human prostate cancer cell line PC-3 in a xenograft mouse model.

Key words: Bombesin; prostate; cancer; imaging; SPECT; microSPECT; GRPR; GRP

4.1 Introduction

Worldwide, prostate cancer is one of the most common causes of cancer in men and a common cause of morbidity and death (*1-2*). As current conventional diagnostic techniques are not sensitive enough to accurately detect early, advanced or recurrent prostate cancer, new diagnostic modalities have to be developed (*3-5*). Radionuclide imaging with SPECT or PET (single photon emission computed tomography and positron emission tomography, respectively) may provide a sensitive technique for reliable diagnosis and/or staging of prostate cancer. However, current radiopharmaceuticals appear to have drawbacks with regard to sensitivity or specificity in prostate cancer assessment (*6-8*). Crucial for accurate new radionuclide imaging techniques is the development of radiopharmaceuticals that can be targeted to tumor-associated specific antigens, which are overexpressed in prostate cancer and sparse in normal tissue.

In this respect the gastrin-releasing peptide receptor (GRPR) appears to be particularly appealing since it is overexpressed in a variety of human malignancies including primary and metastatic prostate cancer (*9-12*). Importantly, GRPR expression in normal tissue is relatively low (*13-16*). The natural ligand for GRPR in mammals is the gastrin-releasing peptide (GRP). GRP is not suitable for modification into a radiopharmaceutical since it has poor *in vivo* stability. The amphibian counterpart of GRP, the 14 amino acid peptide bombesin (BN), appeared to be more suitable. GRP and BN share an identical 7-amino acid long C-terminal region that is needed for binding to GRPR. A series of BN analogues have been constructed that were labelled with a variety of radionuclides (i.e. ^{99m}Tc, ^{111}In, ^{64}Cu, ^{18}F) (*17*). Several groups have used either the full length BN molecule, BN(1-14), or the truncated peptide BN(7-14), with or without amino acid substitutions, spacer insertion and different radionuclide-chelator complexes in order to achieve increased affinity for GRPR, higher metabolic stability, improved biodistribution properties or manipulation of the mode of excretion.

Although radiolabelled BN derivatives have been extensively investigated for diagnosis and treatment of GRPR positive prostate tumors in preclinical studies (*17-19*), clinical research in prostate cancer patients is limited to only a few compounds (*20-24*). For that reason, in this study we investigated the efficacy of a novel BN-based radiopharmaceutical in a human prostate cancer xenograft mouse model as a prelude to clinical evaluation.

Therefore, we synthesized a novel radiopharmaceutical composed of the truncated BN peptide BN(7-14) which was conjugated to the bifunctional coupling agent 6-hydrazinonicotinic acid (HYNIC) linked by ε-Aminocaproic acid (Aca) that was used as a spacer. With the co-ligands tricine and trisodium triphenylphosphine-3,3',3''-trisulfonate (TPPTS), the HYNIC/tricine/TPPTS complex was used for ^{99m}Tc labeling and to form ^{99m}Tc-HYNIC(tricine/TPPTS)-Aca-BN(7-14) (^{99m}Tc-HABN, figure 1). The ternary ligand system was chosen because of its high labeling efficiency (rapid and high yield radiolabelling), high stability, relatively easy use and hydrophilicity(*25*). The HYNIC(tricine/TPPTS) complex has been successfully used for radiolabelling peptides and receptor antagonists(*26-31*).

The main objective of the current study is to preclinically evaluate the suitability of the novel radiopharmaceutical ^{99m}Tc-HABN as a targeted imaging agent of prostate cancer using the human prostate cancer cell line PC-3 in a xenograft mouse model.

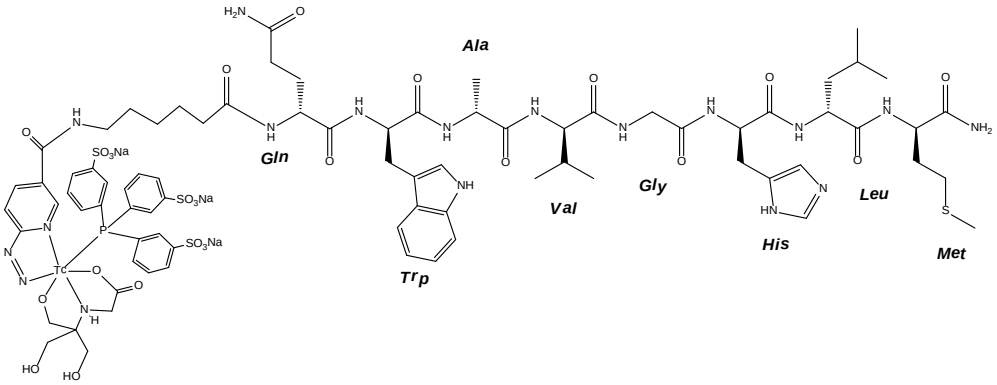

Figure 1: ^{99m}Tc-HYNIC(tricine/TPPTS)-Aca-BN(7-14)
Note: coordination of the ternary ligand complex to ^{99m}Tc according to Surfraz *et al.*[53]

4.2 Experimental Section

4.2.1 Chemicals

Tricine (N-(Tri(hydroxymethyl)methyl)glycine) and Aca-BN(1-14) were purchased from Sigma/Aldrich (St. Louis, Missouri, USA), TPPTS was purchased from Alfa Aesar (Karlsruhe,Germany). Both were used without further purification. The peptide conjugate Aca-BN(7-14) was acquired as described previously(*32*). HYNIC-Aca-BN(7-14) was synthesized as described below. $Na^{99m}TcO_4$ was produced according to standard procedures using the $^{99}Mo/^{99m}Tc$ generator in our department. ^{125}I-Tyr^4-BN was obtained from Perkin-Elmer Life and Analytical Sciences (Waltham, Massachusetts, USA).

4.2.2 Equipment

Analytical as well as semi-preparative reversed-phase high-performance liquid chromatography (RP-HPLC) was performed on a *HITACHI L-2130 HPLC* system (Hitachi High Technologies America Inc., Pleasanton, California, USA) equipped with a Bicron Frisk-Tech area monitor. Isolation of radiolabelled peptides was performed using a Phenomenex reversed-phase Luna C18 column (10 mm × 250 mm, 5µm) (Torrance, California, USA). The flow was set at 2.5 ml/min using a gradient system starting from 90% solvent A (0.01 M phosphate buffer, pH=6.0) and 10% solvent B (acetonitrile) (5 minutes)and ramped to 45% solvent A and 55% solvent B at 35 minutes. The analytic HPLC was performed using the same gradient system but with a reversed-phase Grace Smart RP-C18 column (Lokeren, Belgium) (4.6 mm × 250 mm, 5 µm) and a flow of 1 ml/min.

4.2.3 Synthesis of HYNIC-Aca-Bombesin(7-14)

HYNIC-Boc 16.7 mg (47.5 μmol) (Boc = tert-butyloxycarbonyl) and BN(7-14) 50 mg (47.5 μmol) were dissolved in 0.3 ml of N,N-dimethylformamide. 30 μL of N,N-diisopropylethylamine was then added and the mixture was vortexed for 1 minute. The reaction was complete after 2 hours and no degradation products of HYNIC-Aca-BN(7-14) were found in the final product. 40 μL of acetic acid was added to quench the reaction. The crude product was subjected to HPLC purification. The desired fraction was collected and lyophilized. Anhydrous trifluoroacetic acid (2 ml) was then added to remove the protecting Boc group. After 20 minutes, the trifluoroacetic acid solution was blown dry. The crude HYNIC-Aca-BN(7-14) was purified by HPLC and lyophilized. Product identity was confirmed by MALDI-TOF MS (matrix-assisted laser desorption/ionization time-of-flight mass spectrometry): m/z 1188.29 for [MH]+ ($C_{55}H_{81}N_{17}O_{11}S$) calculated molecular weight: 1187.60. Pure product was stored in a -20 °C freezer.

4.2.4 Radiochemistry

Twenty μL of the HYNIC-Aca-BN(7-14) solution (1mg/ml in H_2O), 100 μL of tricine solution (100 mg/ml in 25 mM succinate buffer, pH 5.0), 10 μL of $SnCl_2$ solution (3.0 mg/ml in 0.1 N HCl) and 100 μL of $Na^{99m}TcO_4$ (370 MBq) in saline were added to a 1.5 ml Eppendorf vial. The reaction mixture was kept at 95 °C for 5 minutes. 100 μL of the TPPTS solution (50 mg/ml in 25 mM succinate buffer, pH 5.0) was added to the reaction mixture. The Eppendorf vial containing the reaction mixture was sealed and heated at 95 °C for 20 minutes. After cooling to room temperature, the mixture was purified by semi-preparative HPLC. The product was then passed through a Sep-Pak C-18cartridge. The Sep-Pak C-18 cartridge was activated with ethanol (10 ml) and was washed with water (10 ml) before use. After the product was loaded, the Sep-Pak C-18 cartridge was washed with saline (10 ml). The radiotracer was eluted with 70% ethanol (0.4 ml) for *in vitro* and *in vivo* experiments. A sample of the resulting solution was analyzed by radio-HPLC.

4.2.5 Partition Coefficient

The partition coefficient was determined using the method described previously[29]. The tracer was dissolved in a mixture of 0.5 ml n-octanol and 0.5 ml 25 mM phosphate buffer (pH7.4) and well mixed. Then the mixture was centrifuged at 3000 rpm for 5 minutes. 100 μL samples were obtained from *n*-octanol and aqueous layers and were counted in a γ-counter (Compugamma CS1282, LKB-Wallac, Turku, Finland). The *logD* value is reported as an average of three different measurements.

4.2.6 *In Vitro* Stability

^{99m}Tc-HABN was dissolved in 1 ml saline or cysteine solution (1 mg/ml), incubated at room temperature and analyzed by RP-HPLC at 1, 2, 4, 6, and 24 hours post incubation.

The study of metabolic stability was performed in human serum. Human serum from

healthy donors was incubated at 37 °C with ^{99m}Tc-HABN for different time periods (1, 2, 4, 6, 24 hours). After incubation, a sample of 250 µL was precipitated with 750 µL acetonitrile/ethanol ($V_{acetonitrile}/V_{ethanol}$ =1:1) and then centrifuged (3 minutes at 3000 rpm), the supernatants were passed through a filter and afterwards analyzed by RP-HPLC. Results were plotted as the radiochemical purity (RCP) at different time-points.

4.2.7 Dose Preparation for Animal Studies

Doses for animal studies were prepared by dissolving the Sep-Pak C18 cartridge purified radiotracer in saline to give a concentration of 5.6MBq/ml (~0.56 MBq/mouse, ethanol concentration ~0.1%) for the biodistribution study and 300 MBq/ml (~60MBq/mouse, ethanol concentration ~10%) for the imaging study.

4.2.8 Cell Culture

The GRPR positive PC-3 human prostate cancer cell line (ATCC, Manassas, Virginia, USA) was cultured in RPMI 1640 (Lonza, Verviers, France) supplemented with 10% fetal calf serum (Thermo Fisher Scientific Inc., Logan, Utah, USA) at 37 °C in a humidified 5% CO_2 atmosphere.

4.2.9 In Vitro Competitive Receptor Binding Assay

The in vitro GRPR binding affinities of Aca-BN(7-14) and HYNIC-Aca-BN(7-14) were compared to BN(1-14) and assessed via a competitive displacement assay with ^{125}I-Tyr^4-BN(1-14) as the GRPR specific radioligand. Experiments were performed at 37 °C with PC-3 human prostate cancer cells according to a method previously described(*33*). The 50% inhibitory concentration (IC_{50}) values were calculated by fitting the data with nonlinear regression using GraphPad Prism 5.0 (GraphPad Software, San Diego, California, USA). Experiments were performed with triplicate samples. IC_{50} values are reported as an average of these samples plus the standard deviation (SD).

4.2.10 Internalization Studies

One day prior to the assay, PC-3 cells were seeded in 6-well plates. The 6-well plates were then incubated with ^{99m}Tc-HABN (0.0037 MBq/well) for 2 hours at 4 °C. To remove unbound radioactivity, the cells were washed twice afterwards with ice-cold PBS and were then incubated in the pre-warmed culture medium at 37 °C for 0, 5, 15, 30, 45, 60, 90 and 120 minutes in triplicate to allow for internalization.

To remove cell-surface bound ^{99m}Tc-HABN, the cells were washed twice for 3 minutes with acid (50 mM glycine−HCl/100 mMNaCl, pH 2.8). Next, the cells were lysed by incubation with 1 M NaOH at 37 °C and the resulting lysate in each well was aspirated to determine the internalized radioactivity in a γ-counter (Compugamma CS1282, LKB-Wallac, Turku, Finland). Results are expressed as the percentage of total radioactivity

(internalized activity / (surface-bound activity + internalized activity)), (mean±SD).

4.2.11 Efflux Studies

One day prior to the assay, PC-3 cells were seeded in 6-well plates. The 6-well plates were then incubated with ^{99m}Tc-HABN (0.0037 MBq/well) for 1 hour at 37 °C to allow for internalization. To remove unbound radioactivity, the cells were washed twice afterwards with cold (0 °C) PBS and were then incubated using pre-warmed culture medium (37 °C) for 0, 15, 30, 45, 60, 90, 120, and 240 minutes in triplicate to allow for externalization. To remove cell-surface bound ^{99m}Tc-HABN, the cells were washed twice for 3 minutes with acid (50 mM glycine−HCl/100 mMNaCl, pH 2.8). Next, the cells were lysed by incubation with 1 M NaOH at 37 °C, and the resulting lysate in each well was aspirated to determine the remaining radioactivity in a γ-counter (Compugamma CS1282, LKB-Wallac, Turku, Finland). Results are expressed as the percentage of maximum intracellular radioactivity (remaining activity at specific time-point / activity at time-point 0), (mean±SD).

4.2.12 Animal Model

The xenograft tumor model for human prostate cancer in athymic mice was generated by subcutaneous injection of 2×10^6 PC-3 cells (suspended in 0.1 ml sterile saline) in the right front flank of male athymic mice (Harlan, Zeist, The Netherlands). During the injection, animals were anesthetized with a gas composed of ~3.5% isoflurane in an air/oxygen mixture. The mice were used for biodistribution experiments and microSPECT imaging when the tumor volume reached a mean diameter of ~0.8-1.0 cm (3-4 weeks after inoculation).

All animal experiments were performed in accordance with the regulations of Dutch law on animal welfare and the institutional ethics committee for animal procedures approved the protocol.

4.2.13 Biodistribution Experiments

Twelve PC-3 tumor-bearing mice were randomly divided into three groups of four animals. Isoflurane inhalation was used as method of anesthesia. ^{99m}Tc-HABN (~0.56 MBq/mouse) dissolved in 0.1 ml saline was injected intravenously via the penis vein. At time points 0.5, 1, and 4 hours post-injection (p.i.), the mice were anesthetized again and sacrificed by cervical dislocation. Immediately after sacrifice, blood samples were withdrawn from the retro orbital sinus using capillary tubes and organs of interest (heart, liver, spleen, lung, kidney, pancreas, small intestine, large intestine, stomach, bone, muscle and tumor) were collected and wet weighed. Radioactivity was determined in a γ-counter (Compugamma CS1282, LKB-Wallac, Turku, Finland).

To determine specificity of the *in vivo* uptake of ^{99m}Tc-HABN, a fourth group of 4 mice received an intravenous injection of 300 μg of unlabelled HYNIC-Aca-BN(7-14) (in 0.2 ml saline) as blocking agent 30 minutes prior to injection of ^{99m}Tc-HABN (~0.56

MBq/mouse in 0.1 ml). The mice were sacrificed 1 hour after injection of the radiotracer. Blood and organs were collected, weighed and counted as described above.

Organ and tissue uptake was calculated as a percentage of the injected dose per gram of tissue mass (%ID/g). Biodistribution data is reported as an average plus the SD based on the results from four animals at each time point. Significant blocking was calculated with the student's t-test. P-values are considered significant when $p \leq 0.05$.Tumor-to-normal-tissue (T/NT) ratios are reported as an average at each time point (without the blocking group).

4.2.14 MicroSPECT Imaging

The imaging study was performed in seven PC-3 tumor-bearing mice, of which four were used for ^{99m}Tc-HABN imaging and three were used for the blocking experiment. Each PC-3 tumor-bearing mouse was penis vein injected with ^{99m}Tc-HABN (~60 MBq/mouse) in 0.2 ml saline using isoflurane anesthesia. Animals were placed prone on a three-head γ-camera (MILabs, U-SPECT-II, Utrecht, the Netherlands) equipped with a multi-pinhole high-resolution collimator (diameter 0.6 mm, resolution about 0.4 mm). Immediately after injection of the radiotracer, dynamic data was acquired for 1 hour (6 frames, 10 minutes per frame). The mice were sacrificed 4 hours after injection of the radiotracer, placed prone in the U-SPECT-II and a static scan was performed for 1 hour. The imaging data was stored digitally in list mode.

For the blocking experiment, excess cold HYNIC-Aca-BN(7-14) (300 µg dissolved in 0.2 ml saline) was administered intravenously via the penis vein in three mice 30 minutes prior to administration of ^{99m}Tc-HABN(~60 MBq/mouse). Data was acquired using the same procedure as described above.

Images were reconstructed by using U-SPECT-Rec v 1.34i3 (MILabs, Utrecht, the Netherlands) with a pixel-based ordered-subsets expectation maximum (POSEM) algorithm. Final images were 1 mm slices, made with Amide 0.9.1 (open source software).

Radioactivity accumulation in tumor was quantified with the use of Amide 0.9.1 by drawing regions of interest (ROI) around the tumor on U-SPECT images of PC-3 tumor bearing mice at 10, 20, 30, 40, 50, 60, and 240 minutes post injection of ^{99m}Tc-HABN, pre-injected with or without excess blocking agent. ROI values were corrected for the injected dose (final ROI = ROI calculated with Amide software divided by the injected dose) and expressed as mean±SD. Significant blocking was calculated with the student's t-test.

4.3 Results

4.3.1 Synthesis, Radiolabelling, Partition Coefficient and *In Vitro* Stability

Within 30 minutes ^{99m}Tc-HABN (figure 1) was prepared at 95 °C with high labeling yield (>90%) and radiochemical purity after purification (>95%). The specific activity was ~19.8 MBq/nmol. ^{99m}Tc-HABNwas analyzed using a reversed phase HPLC method. The HPLC retention time was 21.5 minutes for ^{99m}Tc-HABN and 19.5 minutes for

HYNIC-Aca-BN(7-14).

The partition coefficient was determined in a mixture of n-octanol and phosphate buffer (pH=7.4). The *log D* value was -1.60±0.06. The *in vitro* stability of ^{99m}Tc-HABNwas tested both in saline, human serum and in the presence of excess cysteine (1.0 mg/ml, pH=7.4) (figure 2). ^{99m}Tc-HABN was stable in the presence of excess cysteine and human serum for at least 6 hours. The RCP of ^{99m}Tc-HABN in serum slowly decreased to 77% after 24 hours.

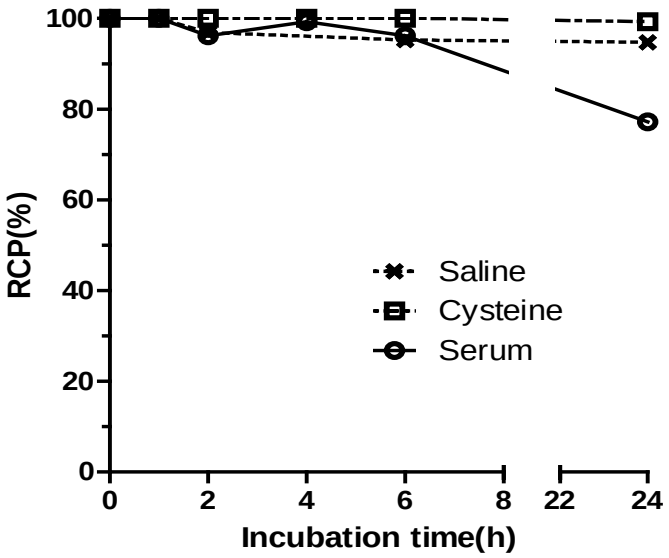

Figure 2: *In vitro* stability of ^{99m}Tc-HYNIC(tricine/TPPTS)-Aca-BN(7-14). Results are plotted as the RCP at different time points.

4.3.2 *In vitro* Competitive Receptor Binding Assay

Using ^{125}I-Tyr^4-BN(1-14) as the GRPR specific radioligand, the binding affinities of Aca-BN(7-14) and HYNIC-Aca-BN(7-14) for GRPR were compared to BN(1-14), set as the standard, via a competitive displacement assay. Results are plotted in sigmoid curves for the displacement of ^{125}I-Tyr^4-BN(1-14) as a function of increasing concentrations of Aca-BN(7-14), BN(1-14) and HYNIC-Aca-BN(7-14) (figure 3). The IC_{50} values were found to be 3.27±0.28, 3.48±0.17 and 12.81±1.34 nM for Aca-BN(7-14), BN(1-14) and HYNIC-Aca-BN(7-14), respectively.

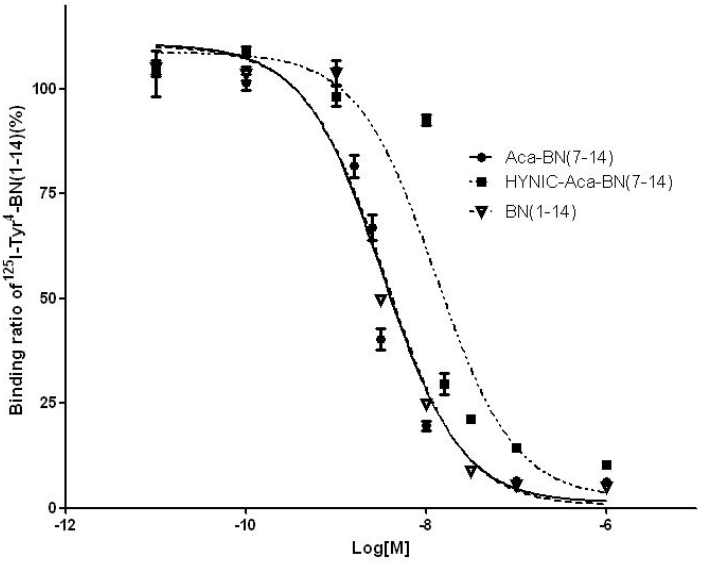

Figure 3: Displacement curve of ^{125}I-Tyr^{4}-BN(1-14) binding to GRPR on PC-3 cells. Log[M] = Log of increasing concentration (Mol/l) of Aca-BN(7-14), BN(1-14) and HYNIC-Aca-BN(7-14).

4.3.3 Internalization and Efflux Studies

The internalization study depicted in figure 4A showed rapid internalization of ^{99m}Tc-HABN into PC-3 cells within 5-15 minutes. Internalization reached a plateau of ~84% after 30 minutes, which remained steady for the duration of the experiment (120 minutes).

Figure 4B shows the efflux kinetics of ^{99m}Tc-HABN. Moderate efflux in the first 60 minutes was demonstrated with only one third of the activity externalized by the PC-3 cells. After 90 minutes a relatively stable situation was created with just over 50% of the internalized radioactivity remaining in the cells for the remainder of the experiment. The $t_{1/2}$-efflux of ^{99m}Tc-HABN PC-3 cells was 38±5 minutes.

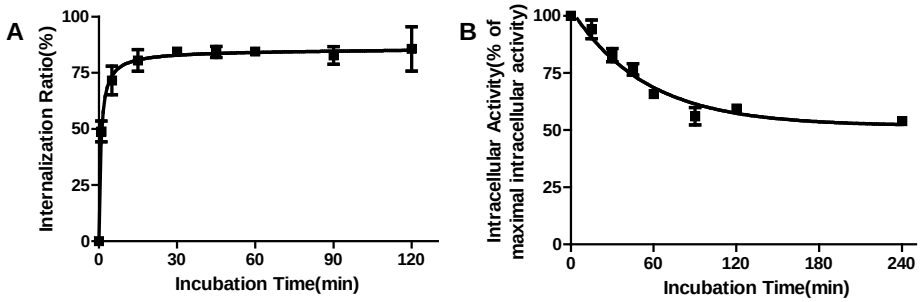

Figure 4: (A) ^{99m}Tc-HYNIC(tricine/TPPTS)-Aca-BN(7-14) internalization experiment.

Results are expressed as the percentage of total radioactivity (internalized activity/(surface-bound activity plus internalized activity)) (mean±SD). **(B)** ^{99m}Tc-HYNIC(tricine/TPPTS)-Aca-BN(7-14) efflux experiment. Results are expressed as the percentage of maximum intracellular radioactivity (remaining activity at specific time-point divided by activity at time-point 0) (mean±SD).

4.3.4 Biodistribution Experiments

Biodistribution of ^{99m}Tc-HABN was evaluated in athymic mice bearing PC-3 tumors. Results of the biodistribution, the blocking experiment and T/NT ratios are shown in table 1.

Uptake in PC-3 tumor and the GRPR rich mouse pancreas(*34*) was highest (2.24±0.64 and 17.3±1.69 %ID/g, respectively) at 30 minutes p.i., with a steady decrease over the 4 hours study period. Uptake in the tumor and pancreas was reduced significantly after injection of the blocking agent, indicating specific GRPR targeting of ^{99m}Tc-HABN. Uptake in other GRPR expressing organs (stomach and intestine) was also significantly reduced in the study of GRPR blockade.

While hepatic uptake was modest, uptake in the kidneys was high and radioactivity was rapidly cleared from the blood via the preferred renal-urinary route. When an excess of cold HYNIC-Aca-BN(7-14) was injected prior to ^{99m}Tc-HABN injection non-specific uptake in the kidneys was increased further, probably as a result of an increased level of circulating unbound ^{99m}Tc-HABN.

Low uptake of radioactivity in bone and muscle, combined with the rapid clearance from the blood pool, resulted in high T/NT ratios, increasing over time.

4.3.5 MicroSPECT Imaging

Figure 5 shows the coronal microSPECT images (sections) acquired with the high resolution U-SPECT-II after injection of ~60 MBq^{99m}Tc-HABN with and without the blocking agent in PC-3 tumor bearing mice. The tumor could already be seen 10 minutes after injection of ^{99m}Tc-HABN and tumor-to-background contrast increased over the first hour (figure 5A) resulting in excellent tumor delineation after 4 hours (figure 5B). Noteworthy, the outer rim of the tumor displayed high uptake of activity while the central part of the tumor shows reduced binding.

Prominent uptake was also seen in the pancreas (not shown) and both kidneys in all time frames. In addition, clearance via the urinary bladder was evident. Pre-injection of an excess of the blocking agent reduced uptake in the tumor and other GRPR positive organs considerably, while the kidneys remained visible (figure 5C and D).

Table 1: Biodistribution of and tumor-to-normal-tissue ratios of ^{99m}Tc-HABN after intravenous injection in PC-3 prostate tumor bearing athymic mice

Organ	*30 minutes*		*1 hour*		*4 hours*		*1 hour + blocking*
	%ID/g	*T/NT*	*%ID/g*	*T/NT*	*%ID/g*	*T/NT*	*%ID/g*
Blood	1.06 ± 0.17	2.12	0.45 ± 0.19	3.66	0.06 ± 0.01	12.69	0.50 ± 0.12
Heart	0.35 ± 0.08	6.44	0.17 ± 0.07	9.56	0.04 ± 0.01	18.71	0.18 ± 0.04
Liver	1.33 ± 0.20	1.76	0.60 ± 0.11	2.52	0.13 ± 0.03	5.19	0.55 ± 0.16
Spleen	0.48 ± 0.08	4.64	0.57 ± 0.54	4.11	0.16 ± 0.08	5.10	0.19 ± 0.04
Lung	1.30 ± 0.16	1.77	0.52 ± 0.18	3.11	0.08 ± 0.02	8.27	0.60 ± 0.19
Kidney	7.09 ± 4.40	0.71	6.39 ± 0.83	0.24	4.00 ± 0.68	0.16	9.57 ± 5.97
Small intestine	6.78 ± 2.24	0.36	4.10 ± 1.60	0.43	1.30 ± 0.79	0.65	1.84 ± 0.94*
Large intestine	3.54 ± 1.00	0.67	2.80 ± 0.71	0.55	2.43 ± 0.73	0.31	0.42 ± 0.12*
Stomach	2.22 ± 0.31	1.05	1.39 ± 0.38	1.11	0.44 ± 0.15	1.65	0.38 ± 0.12*
Bone	0.55 ± 0.46	5.54	0.25 ± 0.11	7.62	0.06 ± 0.02	10.67	0.14 ± 0.05
Muscle	0.48 ± 0.35	5.86	0.12 ± 0.04	13.92	0.02 ± 0.01	40.19	0.13 ± 0.04
Pancreas	17.3 ± 1.69	0.13	8.92 ± 1.74	0.17	5.02 ± 0.94	0.13	0.34 ± 0.11*
PC-3 Tumor	2.24 ± 0.64	1.00	1.51 ± 0.38	1.00	0.67 ± 0.26	1.00	0.47 ± 0.14*

Values are expressed as %ID/g, mean±standard error of the mean/standard deviation (n=4 at each time point) or as T/NT ratios. Blocking was achieved by pre-injection of 300 μg of unlabelled HYNIC-Aca-BN(7-14), * = statistical significant difference ($p<0.05$).

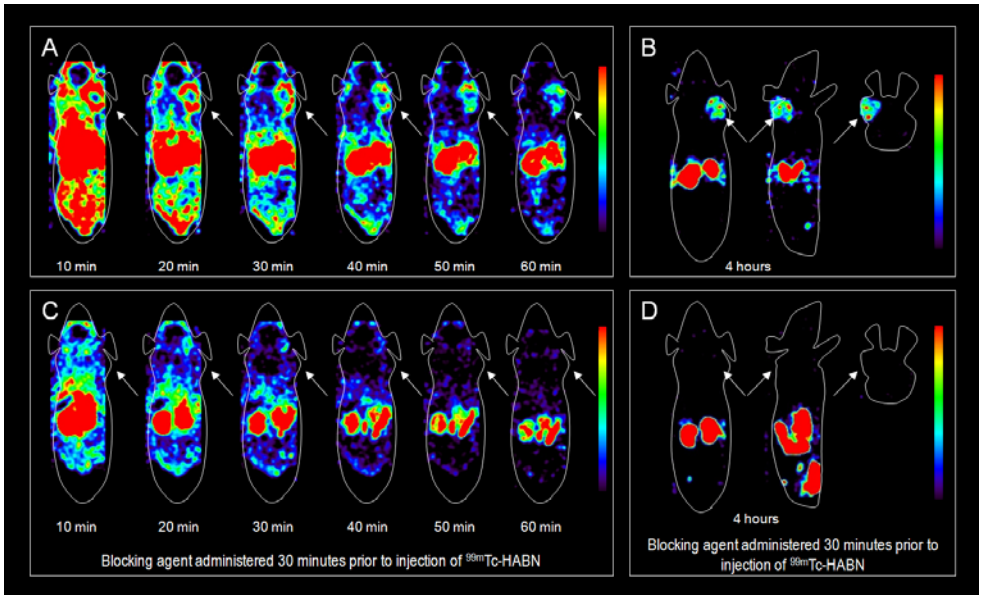

Figure 5: Coronal microSPECT images (sections) at a ten minute interval during the first hour after injection of ^{99m}Tc-HABN without blocking agent (figure 5A) and with blocking agent (figure 5C). Static coronal, sagittal and axial images (sections) 4 hours after injection of ^{99m}Tc-HABN without blocking agent (figure 5B) and with blocking agent (figure 5D). Arrows indicate the tumor.

Figure 6 shows the radioactivity accumulation quantification in thetumor from the ^{99m}Tc-HABN U-SPECT images with and without blocking agent. Tumor uptake diminished over time as was determined before in the biodistribution study. Uptake was significantly higher without the pre-administration of the blocking agent at all time-points, except at 20 and 40 minutes p.i.

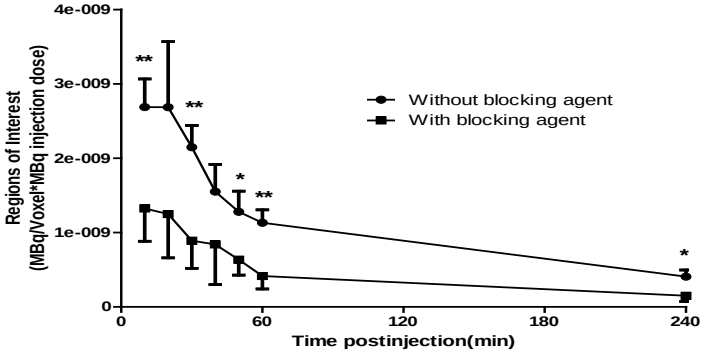

Figure 6: The radioactivity accumulation quantification in tumor from the microSPECT images of PC-3 tumor bearing mice at 10, 20, 30, 40, 50, 60, and 240 min post injection of ^{99m}Tc-HABN, pre-injected with or without excess blocking agent. The ROI values were corrected for the injected dose and expressed as mean±SD. * = statistical significant difference ($p<0.05$), ** = statistical significant difference ($p<0.01$).

4.4 Discussion

Current conventional diagnostic techniques are not sensitive enough to accurately detect early advanced or recurrent prostate cancer. Therefore, better diagnostic modalities are urgently needed. We developed a novel BN-based radiopharmaceutical, designated ^{99m}Tc-HABN, and investigated its potency for the *in vitro* and *in vivo* binding to prostate cancer expressed GRPR.

For widespread use of a tracer in clinical practice, a radio-isotope with a relatively long half-life, high labeling efficiency and good availability is mandatory. We therefore utilized the popular γ-emitting isotope ^{99m}Tc(*17*). The HYNIC/tricine/TPPTS complex was used because of its high labeling efficiency (rapid and high yield radiolabelling), high solution stability and relatively easy use(*25*). It was also chosen because of its hydrophilic character leading to the preferred excretion route via the renal-urinary system(26, 29, 35, 36). Shi *et al.* demonstrated excellent results with HYNIC coupled β-Alanine-BN(7-14) (29)*in vitro* in PC-3 prostate cancer cells and *in vivo* in a colon cancer mouse model. By changing β-Alanine to Aca we sought to improve GRPR targeting properties and pharmacokinetics both *in vitro* and *in vivo* in a prostate cancer model.

^{99m}Tc-HABN was synthesized with high radiochemical yield and purity. In addition, ^{99m}Tc-HABN proved highly stable in saline, cysteine solution and human serum. *In vitro* experiments revealed that although the addition of HYNIC to Aca-BN(7-14) reduces the binding affinity for GRPR, the IC_{50}-value of HYNIC-Aca-BN(7-14) is still in the nanomolar range (12.8±0.14 nM) and therefore very similar to IC_{50}-values reported for other BN derivatives with HYNIC, DOTA or (N^aHis)Ac as chelator(29, 37-43). Internalization into PC-3 cells occurred rapidly, while long retention was seen in the efflux experiments with more than 50% of the internalized radioactivity remaining after 4 hours.

Because primary prostate cancer is located in the pelvis and lymph node metastases are situated mainly in the pelvis and abdomen, rapid renal-urinary clearance is generally preferred over hepato-enteric clearance in order to limit pelvico-abdominal background activity as much as possible and thus to achieve good imaging contrast.

In clinical practice, urinary activity in the bladder can be evacuated by micturition prior to the scan or if needed, by bladder drainage. Determination of the partition coefficient of ^{99m}Tc-HABN demonstrated a hydrophilic compound, which should govern excretion through the kidneys rather than via the liver. This was confirmed by the *in vivo* determination of the biodistribution of ^{99m}Tc-HABN in athymic mice bearing human prostate cancer tumors as uptake in liver was only 1.33±0.20 %ID/g after 30 minutes, while uptake in the kidneys was high after 30 minutes (7.09±4.40 %ID/g) and remained high for 4 hours p.i. Pre-injection with the blocking agent did not reduce kidney uptake or excretion of ^{99m}Tc-HABN.

Furthermore, *in vivo*biodistribution experiments also showed rapid tumor uptake, being the highest at 30 minutes p.i. (2.24±0.64 %ID/g) and decreasing slowly over the evaluated period of 4 hour. Uptake in tumor is even higher before 30 minutes p.i. as could be seen in the experimental part where radioactivity accumulation in thetumor was quantified from the U-SPECT images of ^{99m}Tc-HABN. High tumor-to-background ratios were obtained due to low uptake of radioactivity in bone and muscle on one hand and the rapid clearance from the blood pool on the other hand. Generally, T/NT ratios increased over time because of the long retention time of the radiotracer in tumor, confirming the *in vitro* results of the efflux experiment. As was expected, high uptake was detected in the GRPR rich mouse pancreas (34), but was reduced significantly ($p<0.0001$) when the

blocking agent HYNIC-Aca-BN(7-14) was injected prior to injection of ^{99m}Tc-HABN. Uptake in tumor, stomach, and intestine was also significantly reduced in the study of GRPR blockade, indicating that uptake was also GRPR mediated.

At first glance the tumor uptake appears rather low when compared to the best performing BN analogues reported in literature. However, when the best performing BN analogues Demobesin-1 (reported %ID/g ranging from 13.45 to 24.61)(40, 44, 45), DOTA-PESIN (14.8%ID/g)(41) and AMBA (6.35%ID/g)(39) were compared under the same circumstances in a study by Schroeder *et al.*, uptake by PC-3 xenografts 1 hour p.i. was considerably lower and not statistically significant different from each other (3.0, 2.3 and 2.7%ID/g, respectively)(46). Furthermore, the results of Schroeder *et al*. are not so different from the results reported by other authors or our results (17). Schroeder stated that the variation in radionuclides, amounts of peptide, mouse strain (species, sex, weight), PC-3 cells used (passage number, culture conditions), tumor size and vascularisation of the tumor may all be factors that determine uptake of radioactivity in tumor resulting in variable outcomes (46).

As can be appreciated from our microSPECT images there is high uptake of activity in the outer tumor regions resulting in a “hot rim” around a central area with lower uptake. As several authors have shown before, the central part of a xenografttumor is often necrotic or pre-necrotic with reduced viable cell density, especially in larger tumors, which can result in lower central uptake of a radiotracer (46-48). When measuring total tumor uptake of a radiotracer, the central necrosis, reduced central cell viability and reduced vascularisation or diffusion will result in an underestimation of the actual tumor cell uptake. Even with standardization of the different variables mentioned by Schroeder *et al.*, because of these many variables influencing the outcome of the experiments, a comparison between individual radiopharmaceuticals tested in separate studies is in fact rather difficult.

Absolute tumor uptake is an important factor, but for good image contrast high T/NT ratios are also imperative. Rapid internalization observed *in vitro* (70-80% within 5-15 minutes) is reflected in rapid tumor uptake in mice, which can be appreciated from the microSPECT images as activity is already appearing in the first timeframe after 10 minutes. However, because uptake in other organs is also rapid in combination with high circulating levels of activity in the blood, the tumor-to-background contrast after 10 minutes is rather low. Still, the tumor is clearly visualized after 10 minutes and even better after 20 minutes or more. While internalization was quick, PC-3 cell efflux was slow both *in vitro* and *in vivo*, with persistent retention of activity in the tumor resulting in increasing T/NT ratios and clear delineation of the tumor over time up to 4 hours p.i.

Multiple BN-like radiopharmaceuticals with many different designs have shown to be highly specific for GRPR and sensitive for prostate cancer. So far, studies on antagonists that have been recently published have mostly shown higher or at least similar tumor uptake and T/NT ratios when compared to agonist compounds (42, 49-52). However, in the previously mentioned study by Schroeder *et al*. multiple BN-agonists were compared to an antagonist and although the latter showed the highest uptake in tumor, this was not significant (46). Despite these contrasting results, it will be interesting to see how these preclinical studies will translate into clinical studies as there may be large interspecies differences between mice and men with respect to GRPR imaging. For example, in humans, differences in metabolism, excretion, non-target GRPR expression, prostate tumor characteristics, vascularization or anatomy may account for uptake differences. Also, background interference from bladder or intestinal tissues may or may not hinder detection of (extra)prostatic cancer foci or lymph node metastases.

For clinical imaging purposes, small tumors pose a diagnostic dilemma as they

cannot be detected by conventional imaging techniques like CT or MRI, because these techniques have a limited resolution and depend on morphology (size and shape criteria) for making a diagnosis. SPECT and PET can be superior techniques as they may be able to differentiate between benign or malignant tissue based on differences in metabolism and contrast (e.g. T/NT ratios), rather than on morphology.

In conclusion ^{99m}Tc-HABN is a novel BN-based radiopharmaceutical that proved to be suitable for targeted imaging of prostate cancer using microSPECT in a human derived PC-3 xenograft model.

Acknowledgements

We thank JurgenSijbesma for his assistance with the animal experiments and Chao Wu for his assistance with the microSPECT imaging and image reconstruction. This work was supported by grants of the Dutch Cancer Society (KWF 2008-4243), the Dutch Urology Foundation 1973 (StichtingUrologie 1973) and the Jan Kornelis de Cock Stichting (J.K. de Cock Stichting 08-02).

References

(1) Jemal, A.; Siegel, R.; Ward, E.; Hao, Y.; Xu, J.; Thun, M. J. (2009) Cancer statistics, 2009. *CA Cancer J. Clin. 59*, 225-249.

(2) Ferlay, J.; Parkin, D. M.; Steliarova-Foucher, E. (2010) Estimates of cancer incidence and mortality in Europe in 2008. *Eur. J. Cancer 46*, 765-781.

(3) Albertsen, P. C.; Hanley, J. A.; Harlan, L. C.; Gilliland, F. D.; Hamilton, A.; Liff, J. M.; Stanford, J. L.; Stephenson, R. A. (2000) The positive yield of imaging studies in the evaluation of men with newly diagnosed prostate cancer: a population based analysis. *J. Urol. 163*, 1138-1143.

(4) Hovels, A. M.; Heesakkers, R. A.; Adang, E. M.; Jager, G. J.; Strum, S.; Hoogeveen, Y. L.; Severens, J. L.; Barentsz, J. O. (2008) The diagnostic accuracy of CT and MRI in the staging of pelvic lymph nodes in patients with prostate cancer: a meta-analysis. *Clin. Radiol 63*, 387-395.

(5) Zaheer, A.; Cho, S. Y.; Pomper, M. G. (2009) New agents and techniques for imaging prostate cancer. *J. Nucl. Med 50*, 1387-1390.

(6) Picchio, M.; Giovannini, E.; Messa, C. (2011) The role of PET/computed tomography scan in the management of prostate cancer. *Curr. Opin. Urol 21*, 230-236.

(7) Hong, H.; Zhang, Y.; Sun, J.; Cai, W. (2010) Positron emission tomography imaging of prostate cancer. *Amino. Acids 39*, 11-27.

(8) Beheshti, M.; Langsteger, W.; Fogelman, I. (2009) Prostate cancer: role of SPECT and PET in imaging bone metastases. *Semin. Nucl. Med 39*, 396-407.

(9) Ananias, H. J.; van den Heuvel, M. C.; Helfrich, W.; de Jong, I. J. (2009) Expression of the gastrin-releasing peptide receptor, the prostate stem cell antigen and the prostate-specific membrane antigen in lymph node and bone metastases of prostate cancer. *Prostate 69*, 1101-1108.

(10) Markwalder, R.; Reubi, J. C. (1999) Gastrin-releasing peptide receptors in the human prostate: relation to neoplastic transformation. *Cancer Res 59*, 1152-1159.

(11) Reubi, J. C.; Wenger, S.; Schmuckli-Maurer, J.; Schaer, J. C.; Gugger, M. (2002) Bombesin receptor subtypes in human cancers: detection with the universal

radioligand ^{125}I-[D-Tyr^{6}, beta-Ala^{11}, Phe^{13}, Nle^{14}] bombesin(6-14). *Clin. Cancer Res 8*, 1139-1146.

(12) Waser, B.; Eltschinger, V.; Linder, K.; Nunn, A.; Reubi, J. C. (2007) Selective in vitro targeting of GRP and NMB receptors in human tumours with the new bombesin tracer ^{177}Lu-AMBA. *Eur. J. Nucl. Med. Mol. Imaging 34*, 95-100.

(13) Aprikian, A. G.; Cordon-Cardo, C.; Fair, W. R.; Reuter, V. E. (1993) Characterization of neuroendocrine differentiation in human benign prostate and prostatic adenocarcinoma. *Cancer 71*, 3952-3965.

(14) Cutz, E.; Chan, W.; Track, N. S. (1981) Bombesin, calcitonin and leu-enkephalin immunoreactivity in endocrine cells of human lung. *Experientia 37*, 765-767.

(15) Price, J.; Penman, E.; Wass, J. A.; Rees, L. H. (1984) Bombesin-like immunoreactivity in human gastrointestinal tract. *Regul. Pept 9*, 1-10.

(16) Spindel, E. R.; Chin, W. W.; Price, J.; Rees, L. H.; Besser, G. M.; Habener, J. F. (1984) Cloning and characterization of cDNAs encoding human gastrin-releasing peptide. *Proc. Natl. Acad. Sci. U. S. A 81*, 5699-5703.

(17) Ananias, H. J.; de Jong, I. J.; Dierckx, R. A.; Van de Wiele, C.; Helfrich, W.; Elsinga, P. H. (2008) Nuclear imaging of prostate cancer with gastrin-releasing-peptide-receptor targeted radiopharmaceuticals. *Curr. Pharm. Des 14*, 3033-3047.

(18) Hohla, F.; Schally, A. V. (2010) Targeting gastrin releasing peptide receptors: New options for the therapy and diagnosis of cancer. *Cell Cycle 9*, 1738-1741.

(19) Schroeder, R. P.; van Weerden, W. M.; Bangma, C.; Krenning, E. P.; de, J. M. (2009) Peptide receptor imaging of prostate cancer with radiolabelled bombesin analogues. *Methods 48*, 200-204.

(20) De Vincentis, G.; Scopinaro, F.; Varvarigou, A.; Ussof, W.; Schillaci, O.; Archimandritis, S.; Corleto, V.; Longo, F.; Delle, F. G. (2002) Phase I trial of technetium [Leu^{13}] bombesin as cancer seeking agent: possible scintigraphic guide for surgery? *Tumori 88*, S28-S30.

(21) De Vincentis, G.; Remediani, S.; Varvarigou, A. D.; Di Santo. G.; Iori, F.; Laurenti, C.; Scopinaro, F. (2004) Role of ^{99m}Tc-bombesin scan in diagnosis and staging of prostate cancer. *Cancer Biother. Radiopharm. 19*, 81-84.

(22) Scopinaro, F.; De Vincentis, G.; Varvarigou, A. D.; Laurenti, C.; Iori, F.; Remediani, S.; Chiarini, S.; Stella, S. (2003) ^{99m}Tc-bombesin detects prostate cancer and invasion of pelvic lymph nodes. *Eur. J. Nucl. Med. Mol. Imaging 30*, 1378-1382.

(23) Van de Wiele, C.; Dumont, F.; Vanden Broecke, R.; Oosterlinck, W.; Cocquyt, V.; Serreyn, R.; Peers, S.; Thornback, J.; Slegers, G.; Dierckx, R. A. (2000) Technetium-99m RP527, a GRP analogue for visualisation of GRP receptor-expressing malignancies: a feasibility study. *Eur. J. Nucl. Med 27*, 1694-1699.

(24) Van de Wiele, C.; Dumont, F.; Dierckx, R. A.; Peers, S. H.; Thornback, J. R.; Slegers, G.; Thierens, H. (2001) Biodistribution and dosimetry of ^{99m}Tc-RP527, a gastrin-releasing peptide (GRP) agonist for the visualization of GRP receptor-expressing malignancies. *J. Nucl. Med 42*, 1722-1727.

(25) Liu, S.; Edwards, D. S.(1999) ^{99m}Tc-Labelled Small Peptides as Diagnostic Radiopharmaceuticals. *Chem. Rev 99*, 2235-2268.

(26) Wang, L.; Shi, J.; Kim, Y. S.; Zhai, S.; Jia, B.; Zhao, H.; Liu, Z.; Wang, F.; Chen, X.; Liu, S. (2009) Improving tumor-targeting capability and pharmacokinetics of ^{99m}Tc-labelled cyclic RGD dimers with PEG_4 linkers. *Mol. Pharm 6*, 231-245.

(27) Liu, S.; Harris, A. R.; Williams, N. E.; Edwards, D. S. (2002) ^{99m}Tc-Labeling of a hydrazinonicotinamide-conjugated LTB(4) receptor antagonist useful for imaging infection and inflammation. *Bioconjug. Chem 13*, 881-886.

(28) Edwards, D. S.; Liu, S.; Barrett, J. A.; Harris, A. R.; Looby, R. J.; Ziegler, M. C.; Heminway, S. J.; Carroll, T. R. (1997) New and versatile ternary ligand system for technetium radiopharmaceuticals: water soluble phosphines and tricine as coligands in labeling a hydrazinonicotinamide-modified cyclic glycoprotein IIb/IIIa receptor antagonist with ^{99m}Tc. *Bioconjug. Chem 8*, 146-154.

(29) Shi, J.; Jia, B.; Liu, Z.; Yang, Z.; Yu, Z.; Chen, K.; Chen, X.; Liu, S.; Wang, F. (2008) ^{99m}Tc-Labelled Bombesin(7-14)NH_2 with Favorable Properties for SPECT Imaging of Colon Cancer. *Bioconjug. Chem 19*, 1170-1178.

(30) Guo, H.; Xie, F.; Zhu, M.; Li, Y.; Yang, Z.; Wang, X.; Lu, J. (2011) The synthesis of pteroyl-lys conjugates and its application as Technetium-99m labelled radiotracer for folate receptor-positive tumor targeting. *Bioorg. Med. Chem. Lett. 21*, 2025-2029.

(31) Lu, J.; Pang, Y.; Xie, F.; Guo, H.; Li, Y.; Yang, Z.; Wang, X. (2011) Synthesis and in vitro/in vivo evaluation of ^{99m}Tc-labelled folate conjugates for folate receptor imaging. *Nucl. Med. Biol. 38*, 557-565.

(32) Zhang, X.; Cai, W.; Cao, F.; Schreibmann, E.; Wu, Y.; Wu, J. C.; Xing, L.; Chen, X. (2006) ^{18}F-labelled bombesin analogs for targeting GRP receptor-expressing prostate cancer. *J. Nucl. Med 47*, 492-501.

(33) Chen, X.; Park, R.; Hou, Y.; Tohme, M.; Shahinian, A. H.; Bading, J. R.; Conti, P. S. (2004) microPET and autoradiographic imaging of GRP receptor expression with ^{64}Cu-DOTA-[Lys^3]bombesin in human prostate adenocarcinoma xenografts. *J. Nucl. Med 45*, 1390-1397.

(34) Fanger, B. O.; Wade, A. C.; Cardin, A. D. (1991) Characterization of the murine pancreatic receptor for gastrin releasing peptide and bombesin. *Regul. Pept. 32*, 241-251.

(35) Faintuch, B. L.; Teodoro, R.; Duatti, A.; Muramoto, E.; Faintuch, S.; Smith, C. J. (2008) Radiolabelled bombesin analogs for prostate cancer diagnosis: preclinical studies. *Nucl. Med. Biol 35*, 401-411.

(36) Santos-Cuevas, C. L.; Ferro-Flores, G.; Arteaga de, M. C.; Pichardo-Romero, P. A. (2008) Targeted imaging of gastrin-releasing peptide receptors with ^{99m}Tc-EDDA/HYNIC-[Lys^3]-bombesin: biokinetics and dosimetry in women. *Nucl. Med. Commun 29*, 741-747.

(37) Garcia-Garayoa, E.; Schweinsberg, C.; Maes, V.; Ruegg, D.; Blanc, A.; Blauenstein, P.; Tourwe, D. A.; Beck-Sickinger, A. G.; Schubiger, P. A. (2007) New ^{99m}Tc-bombesin analogues with improved biodistribution for targeting gastrin releasing-peptide receptor-positive tumors. *Q. J. Nucl. Med. Mol. Imaging 51*, 42-50.

(38) Garcia-Garayoa, E.; Ruegg, D.; Blauenstein, P.; Zwimpfer, M.; Khan, I. U.; Maes, V.; Blanc, A.; Beck-Sickinger, A. G.; Tourwe, D. A.; Schubiger, P. A. (2007) Chemical and biological characterization of new $Re(CO)_3$/^{99m}$Tc(CO)_3$ bombesin analogues. *Nucl. Med. Biol.34*, 17-28.

(39) Lantry, L. E.; Cappelletti, E.; Maddalena, M. E.; Fox, J. S.; Feng, W.; Chen, J.; Thomas, R.; Eaton, S. M.; Bogdan, N. J.; Arunachalam, T.; Reubi, J. C.; Raju, N.; Metcalfe, E. C.; Lattuada, L.; Linder, K. E.; Swenson, R. E.; Tweedle, M. F.; Nunn, A. D. (2006) ^{177}Lu-AMBA: Synthesis and characterization of a selective ^{177}Lu-labelled GRP-R agonist for systemic radiotherapy of prostate cancer. *J. Nucl. Med 47*, 1144-1152.

(40) Maina, T.; Nock, B. A.; Zhang, H.; Nikolopoulou, A.; Waser, B.; Reubi, J. C.; Maecke, H. R. (2005) Species differences of bombesin analog interactions with GRP-R define the choice of animal models in the development of GRP-R-targeting drugs. *J. Nucl. Med 46*, 823-830.

(41) Zhang, H.; Schuhmacher, J.; Waser, B.; Wild, D.; Eisenhut, M.; Reubi, J. C.; Maecke, H. R. (2007) DOTA-PESIN, a DOTA-conjugated bombesin derivative designed for the imaging and targeted radionuclide treatment of bombesin receptor-positive tumours. *Eur. J. Nucl. Med. Mol. Imaging 34*, 1198-1208.

(42) Mansi, R.; Wang, X.; Forrer, F.; Waser, B.; Cescato, R.; Graham, K.; Borkowski, S.; Reubi, J. C.; Maecke, H. R. (2011) Development of a potent DOTA-conjugated bombesin antagonist for targeting GRPr-positive tumours. *Eur. J. Nucl. Med. Mol. Imaging 38*, 97-107.

(43) Koumarianou, E.; Mikolajczak, R.; Pawlak, D.; Zikos, X.; Bouziotis, P.; Garnuszek, P.; Karczmarczyk, U.; Maurin, M.; Archimandritis, S. C. (2009) Comparative study on DOTA-derivatized bombesin analog labelled with ^{90}Y and ^{177}Lu: in vitro and in vivo evaluation. *Nucl. Med. Biol. 36*, 591-603.

(44) Nock, B.; Nikolopoulou, A.; Chiotellis, E.; Loudos, G.; Maintas, D.; Reubi, J. C.; Maina, T. (2003) ^{99m}Tc-Demobesin 1, a novel potent bombesin analogue for GRP receptor-targeted tumour imaging. *Eur. J. Nucl. Med. Mol. Imaging 30*, 247-258.

(45) Cescato, R.; Maina, T.; Nock, B.; Nikolopoulou, A.; Charalambidis, D.; Piccand, V.; Reubi, J. C. (2008) Bombesin receptor antagonists may be preferable to agonists for tumor targeting. *J. Nucl. Med. 49*, 318-326.

(46) Schroeder, R. P.; Muller, C.; Reneman, S.; Melis, M. L.; Breeman, W. A.; de, B. E.; Bangma, C. H.; Krenning, E. P.; van Weerden, W. M.; de, J. M. (2010) A standardised study to compare prostate cancer targeting efficacy of five radiolabelled bombesin analogues. *Eur. J. Nucl. Med. Mol. Imaging 37*, 1386-1396.

(47) Dearling, J. L.; Flynn, A. A.; Sutcliffe-Goulden, J.; Petrie, I. A.; Boden, R.; Green, A. J.; Boxer, G. M.; Begent, R. H.; Pedley, R. B. (2004) Analysis of the regional uptake of radiolabelled deoxyglucose analogs in human tumor xenografts. *J. Nucl. Med 45*, 101-107.

(48) Bao, A.; Phillips, W. T.; Goins, B.; McGuff, H. S.; Zheng, X.; Woolley, F. R.; Natarajan, M.; Santoyo, C.; Miller, F. R.; Otto, R. A. (2006) Setup and characterization of a human head and neck squamous cell carcinoma xenograft model in nude rats. *Otolaryngol. Head Neck Surg135*, 853-857.

(49) Honer, M.; Mu, L.; Stellfeld, T.; Graham, K.; Martic, M.; Fischer, C. R.; Lehmann, L.; Schubiger, P. A.; Ametamey, S. M.; Dinkelborg, L.; Srinivasan, A.; Borkowski, S. (2011) ^{18}F-labelled bombesin analog for specific and effective targeting of prostate tumors expressing gastrin-releasing peptide receptors. *J. Nucl. Med 52*, 270-278.

(50) Lane, S. R.; Nanda, P.; Rold, T. L.; Sieckman, G. L.; Figueroa, S. D.; Hoffman, T. J.; Jurisson, S. S.; Smith, C. J. (2010) Optimization, biological evaluation and microPET imaging of copper-64-labelled bombesin agonists, [^{64}Cu-NO2A-(X)-BBN(7-14)NH_2], in a prostate tumor xenografted mouse model. *Nucl. Med. Biol 37*, 751-761.

(51) Mansi, R.; Wang, X.; Forrer, F.; Kneifel, S.; Tamma, M. L.; Waser, B.; Cescato, R.; Reubi, J. C.; Maecke, H. R. (2009) Evaluation of a 1,4,7,10-tetraazacyclododecane-1,4,7,10-tetraacetic acid-conjugated bombesin-based radioantagonist for the labeling with single-photon emission computed tomography, positron emission tomography, and therapeutic radionuclides. *Clin. Cancer Res 15*, 5240-5249.

(52) Lears, K. A.; Ferdani, R.; Liang, K.; Zheleznyak, A.; Andrews, R.; Sherman, C. D.; Achilefu, S.; Anderson, C. J.; Rogers, B. E. (2011) In vitro and in vivo evaluation of ^{64}Cu-labelled SarAr-bombesin analogs in gastrin-releasing peptide receptor-expressing prostate cancer. *J. Nucl. Med. 52*, 470-477.

(53) Surfraz, M. B.; King, R.; Mather, S. J.; Biagini, S.; Blower, P. J. (2009) Technetium-binding in labelled HYNIC-peptide conjugates: role of coordinating amino acids. *J. Inorg. Biochem 103*, 971-977.

Chapter 5

Application of ^{99m}Technetium-HYNIC(tricine/TPPTS)-Aca-Bombesin(7-14) SPECT/CT in Prostate Cancer Patients

A First-in-man Study

Hildo J.K. Ananias, **Zilin Yu**, Hilde D. Hoving, Stefano Rosati, Rudi A. Dierckx, Fan Wang, Yongjun Yan, Xiaoyuan Chen, Jan Pruim, Marjolijn N. Lub-de Hooge, Wijnand Helfrich, Philip H. Elsinga, Igle J. de Jong

Nucl Med Biol. 2013 Oct; 40(7):933-8.

Abstract

Rationale: The peptide bombesin (*8*) and derivates thereof show high binding affinity for the gastrin-releasing peptide receptor (GRPR), which is highly expressed in prostate cancer (PCa). We used the BN-based radiopharmaceutical ^{99m}Technetium-HYNIC(tricine/TPPTS)-Aca-Bombesin(7-14) (^{99m}Tc-HABN) to perform a first-in-man clinical pilot study in order to evaluate the feasibility of ^{99m}Tc-HABN SPECT/CT for detection and localization of PCa in patients.

Methods: Eight patients with biopsy proven PCa and scheduled for either a radical prostatectomy or external beam radiotherapy underwent ^{99m}Tc-HABN scintigraphy and SPECT/CT prior to treatment. Serial blood samples were taken to assess blood radioactivity and to determine *in vivo* metabolic stability. Clinical parameters were measured and reported side-effects were recorded. PCa specimens of all patients were immunohistochemically stained for GRPR.

Results: ^{99m}Tc-HABN was synthesized with high yield, specific activity and purity. There were no significant changes in clinical parameters and there were no adverse or subjective side-effects. Low metabolic stability was observed, with less than 20% of ^{99m}Tc-HABN intact after 30 min. Immunohistochemical staining for GRPR was observed in the PCa specimens in all patients. ^{99m}Tc-HABN scintigraphy and SPECT/CT did not detect or localize PCa in patients with proven disease.

Conclusions: ^{99m}Technetium-HYNIC(tricine/TPPTS)-Aca-Bombesin(7-14) SPECT/CT for visualization of PCa is safe but hampered by unexpected low *in vivo* metabolic stability in men. The difference between the excellent *in vitro* stability in human serum determined in our previous study on ^{99m}Tc-HABN and the low *in vivo* metabolic stability determined in this study, is striking. This issue warrants further study of peptide-based radiopharmaceuticals.

Key words: Prostate cancer, SPECT/CT, Bombesin, GRPR, First-in-man

5.1 Introduction

Prostate cancer is one of the most common causes of cancer in males and a common cause of morbidity and death worldwide (1). Early detection of prostate cancer may lead to an improved cure rate. An increased level of prostate-specific antigen (PSA) in serum or a palpable prostatic nodule found with digital rectal examination raises the suspicion of prostate cancer and necessitates transrectal ultrasound-guided biopsies of the prostate for histological diagnosis. Although performing transrectal ultrasound-guided biopsies is the gold standard procedure, it has certain drawbacks, such as the chance of under- or over-staging due to sampling error in multifocal diseases (2). Furthermore, transrectal ultrasound-guided biopsies have a suboptimal sensitivity with missing up to 35% of cancers (3-5). A negative (repeat) biopsy, despite a persistently elevated PSA, poses a diagnostic dilemma (6,7).

An imaging technique that is sufficiently sensitive to detect prostate cancer and/or sufficiently specific to exclude cancer is necessary. In addition to detection and local staging of prostate cancer, other possible uses of such an imaging technique could be guidance of prostate biopsies, application of intensity-modulated radiotherapy on hot-spots, detection of distant metastases or local recurrence and therapy response monitoring.

Nuclear imaging techniques such as single photon emission computed tomography (SPECT) and positron emission tomography (PET) have emerged as promising diagnostic tools in oncology(8-10). Of the available radiopharmaceuticals for prostate cancer detection, ^{18}F PET/CT and 11C-choline PET/CT are mostly used in centers all worldwide, as they are currently the best–performing nuclear imaging techniques. However, the limited sensitivity for small-size metastases, relatively low uptake of choline at low PSA levels and uptake of choline in normal or inflamed prostate limit the accuracy of choline PET/CT in staging prostate cancer(10,11). Therefore, crucial for accurate new nuclear imaging techniques is the development of radiopharmaceuticals that can be targeted to specific tumor-associated antigens, which are over-expressed in prostate cancer but are sparse in normal tissues.

A tumor-associated antigen that is of particular interest is the gastrin-releasing peptide receptor (GRPR). GRPR is over-expressed in various human malignancies, including primary and metastatic prostate cancer (12,13). Importantly, GRPR expression in normal tissue ranges from absent to low(14-17), making GRPR an excellent target for high-contrast imaging. The mammalian ligand for GRPR and its amphibian counterpart bombesin (BN) share an identical seven-amino-acid carboxyl-terminal region, and both possess the same affinity for GRPR. However, BBN has been shown to be significantly more stable, and a series of BBN analogs has been constructed and labelled with various radionuclides (i.e., ^{99m}Tc, ^{111}In, ^{64}Cu, ^{18}F)(18,19).

Recently we reported on the synthesis of ^{99m}Tc-HYNIC(tricine/TPPTS)-Aca-BN(7-14) (from here on: ^{99m}Tc-HABN; HYNIC = 6-hydrazinonicotinic acid; TPPTS = trisodium triphenylphosphine-3,3',3''- trisulfonate; Aca = ε-Amino-caproic acid) and its promising results as an imaging agent in a xenografted tumor model for human prostate cancer in athymic mice(20).

The aim of the study presented here was to perform a first-in-man clinical pilot study to evaluate the feasibility of ^{99m}Tc-HABN SPECT/CT for detection of prostatic cancer in patients.

5.2 Material and Methods

5.2.1 Chemicals, Materials and Equipment

$Na^{99m}TcO_4$ was eluted from the $^{99}Mo/^{99m}Tc$ generator (Ultra-Technekow, Covidien, Petten, the Netherlands). Succinic acid and tricine (N-(Tri(hydroxymethyl)methyl)glycine) were purchased from Sigma/Aldrich (St. Louis, MO, USA). TPPTS was purchased from Alfa Aesar (Karlsruhe, Germany). The peptide Aca-BN(7-14) was provided by Peptides International (Louisville, KY, USA). HYNIC-Aca-BN(7-14) was synthesized as reported previously(20). For sterilization, a 0.22-µm Millex GV-filter (Merck Millipore, Billerica, MA, USA) was used. High-performance liquid chromatography (HPLC) was performed using a HITACHI L-2130 HPLC system (Hitachi High Technologies America Inc., Pleasanton, CA, USA). Isolation of radiolabelled peptides was performed using a Phenomenex reversed phase Luna C18 column (Phenomenex, Torrance, CA, USA). The Sep-Pak C18 light cartridge was from Waters Corporation (Milford, MA, USA). Radioactivity of samples was measured in a γ-counter (Compugamma CS1282; LKB-Wallac, Turku, Finland). For immunohistochemistry experiments, PC-3 human prostate cancer xenograft tumors (ATCC, Manassas, VA, USA), normal goat serum, 0.05% 3,3'-diaminobenzidine, Eukitt mounting medium, 1% AB serum (Sigma-Aldrich, St. Louis, MO, USA), hematoxylin (Merck,Whitehouse Station, NJ, USA), anti-human-GRPR rabbit polyclonal antibody ab39963 (Abcam, Cambridge, UK) and goat anti-rabbit antibody P0448 (Dako, Glostrup, Denmark) were used.

5.2.2 Preparation of ^{99m}Tc-HABN

Synthesis of ^{99m}Tc-HABN was performed as described previously (20), under GMP conditions with modifications. All solutions (except the HYNIC-Aca-BN(7-14) and the $SnCl_2$ solution) were sterilized before use by passing through a 0.22 µm Millex GV-filter under aseptic conditions (class A) in the cleanroom. Briefly, ^{99m}Tc-pertechnetate solution (~2.8 GBq, ~2 ml saline) was collected in a sterile vial (5 ml). 50 µl of HYNIC-Aca-BN(7-14) (1 mg/ml in sterile water), 100 µl of tricine solution (100 mg/ml in 25 mM succinate buffer, pH 5.0), 100 µl of TPPTS solution (50 mg/ml in 25 mM succinate buffer, pH 5.0) and 15 µl of $SnCl_2$ (1.0 mg/ml in water) were added to the vial and well mixed. The pH value (pH 5.0) of the mixture was checked with pH paper, and then the mixture was incubated at 95° C for 20 min. A needle connected to a 0.22 µm Millex GV-filter was placed in the cap of the vial to avoid overpressure and contamination.

After cooling to room temperature, the reaction mixture was purified with semi-preparative reversed-phase HPLC equipped with a UV detector (wave length =218 nm) and a radioactivity detector. Isolation of radiolabelled peptides was performed using a Phenomenex reversed-phase Luna C18 column (10 mm × 250 mm, 5 µm) with a flow rate at 2.5 mL/min. A gradient system was applied for isolation of ^{99m}Tc-HABN, starting from 90% solvent A (0.01 M phosphate buffer with 0.1 mg/ml ascorbic acid (AA), pH=6.0) and 10% solvent B (acetonitrile (ACN) with 0.1 mg/ml AA) (5 min) and ramped to 45% solvent A and 55% solvent B at 35 min.

The ^{99m}Tc-HABN eluate from the HPLC system was diluted with saline with 1 % AA

(10 mL) before loading on a Sep-Pak C18 light cartridge. The C18 cartridge was washed with saline with 1 % AA (50 mL) and eluted with absolute ethanol (400 μL) afterwards. The ethanol solution was diluted with saline solution (with 1 % AA; limit: ~10 ml) and was sterilized by passing through a 0.22 μm GV-filter. A quantity of 550-700 MBq was dispensed in a syringe under aseptic conditions (class A).

5.2.3 Quality Control of ^{99m}Tc-HABN

Before release of the final product, the integrity of the 0.22 μm Millex GV filter (used for sterilization of the final product) was determined using the bubble point test, and the radiochemical purity of the final product was determined by analyzing a 5-MBq portion using HPLC. After release, the sterility test was performed by keeping two samples (100 μL) of the final product in two bottles of Clausen medium at 25 °C and 37 °C for 1 week. The remaining product was used for the pyrogenicity test, the residual solvents test and the EtOH concentration test performed at the Pharmacy Department of the University Medical Center Groningen after decay.

5.2.4 Patient Recruitment

The present study was approved by the Medical Ethics Committee of the University Medical Center Groningen and was performed according to Good Clinical Practice guidelines.

Eight patients with biopsy proven prostate cancer (four patients scheduled for laparoscopic radical prostatectomy (RP), and four planned for external beam radiotherapy (EBRT)) were recruited on the outpatient clinic of the department of Urology at the University Medical Center Groningen, after providng written informed consent. The pre-therapy PSA level, prostate volume as determined by transrectal ultrasound, tumor stage (according to 1997 TNM staging criteria), results of prostate histology (either via whole prostatectomy specimens or prostate biopsies; Gleason sum score, % tumor volume) and results of the pelvic lymph node dissection (1/4 in the RP group, 4/4 in the EBRT group) were recorded.

5.2.5 Scintigraphy, SPECT/CT and image analysis

SPECT/CT scanning was performed before the EBRT or 1 day before surgery. Subjects were positioned supine with their arms outstretched in holders, and a venous canula was placed in both forearms-left for injection of the radiopharmaceutical and right for blood sampling. For low-dose computed tomography, the arms were positioned above the head. Images of the pelvis were performed using a Siemens Symbia T2 double headed gamma camera, equipped with low-energy, high-resolution collimators, combined with an integrated 2-slice computed tomography. To acquire quantitative results, a sample of ^{99m}Tc of known activity (20-28 MBq) was scanned along with the patient.

Different data acquisition protocols were used in order to acquire an optimal time-point for scanning. Patients 1-4 were subjected to a dynamic scanning protocol with the gamma camera heads in the anterior-posterior (AP) position, 1 min per frame during 20

min, starting immediately after ^{99m}Tc-HABN injection (549-688 MBq). Thereafter, a 2x180° SPECT of the pelvic region was performed with a matrix size of 128*x*128 in 64 positions and an acquisition time of 40 s per position. Next, a low-dose CT of the pelvis was performed (110 kV, 30 mAs). At 2, 4, 6 and 20 hours post-injection(p.i.), SPECT was performed again at the 20 h-time-point combined with a low-dose CT. Patient 5 was subjected to a dynamic scan for 120 min with the gamma camera in the AP position, at 1 min per frame during the first hour and 2 min per frame during the second hour. At 4, 6 and 20 h p.i., a static scan in the AP position was made for 10, 30 and 30 min, respectively. In patients 6-8 a dynamic scan was made for 60 min, 1 min per frame, followed by SPECT/CT and single-frame, 30-min static images at 2, 4 and 6 hours p.i. Additionally, in patients 3, 4, 6, 7 and 8, a transurethral catheter was inserted in order to drain the bladder and reduce local radioactivity.

Images were reconstructed using iterative reconstruction (Flash 3D, 8 iterations, 16 subsets, Gaussian 9.0 filter). In addition to anatomical localization, CT was also used to obtain an attenuation map. Dynamic and static images were displayed in coronal planes, and SPECT images were displayed in transaxial, coronal and sagittal planes. The tumor to normal tissue ratios were determined by placing a region of interest (ROI) over the area showing the most activity in tumor and an identically sized ROI over the gluteal muscles. Image analysis and subjective assessment were performed by a nuclear physician (JP) blinded to patient data and 1 non-blinded researcher (HA) .

5.2.6 Monitoring of Vital Parameters and Side-effects

Because this was a first-in-man study, the heart rate, oxygen saturation and blood pressure were monitored in all patients during the first hour p.i. at regular intervals (0, 5, 10, 15, 20, 25, 30, 45 and 60 min) and were compared with baseline measurements before injection of ^{99m}Tc-HABN. Side-effects, if reported by the patient within 24 h p.i., were documented.

5.2.7 Analysis of radioactivity in blood

Blood samples (2 ml/time point) were collected from six patients via a venous canula in the right forearm at 0, 2, 5, 10, 30, 60, 120, 240, 360 and 1200 min (the last time point was not analyszed for patients 7 and 8) p.i. of ^{99m}Tc-HABN. No blood sampling of patients 2 and 6 was performed due to technical failure.

Blood serum samples were acquired by centrifuging the blood sample at 3000 rpm for 5 min. For each sample, the radioactivity of both full blood and blood serum (250 µl), as well as the original ^{99m}Tc-HABN saline solution (10 µl in triplicate) was determined in a γ-counter. The radioactivity accumulation of ^{99m}Tc-HABN in full blood and serum was calculated as follows: counts of the 250-µl sample *4 / total injected counts (percentage of the injected dose/ml, mean ± SD, n=6).

5.2.8 Metabolic Stability of ^{99m}Tc-HABN

The *in vivo* metabolic stability of ^{99m}Tc-HABN was determined by analyzing blood serum samples collected at 0 (baseline) 2, 5, 10, 30, 60 and 120 min p.i. of ^{99m}Tc-HABN from patients 1, 3, 4 and 5. Blood serum samples were acquired as described above. The protein of blood serum samples was removed by centrifuging at 3000 rpm for 5 min after mixing with a 10-fold volume of ACN. The supernatant was passed through a Sep-Pak C18 Light cartridge and washed with water (5 ml) and EtOH (2 mL). The radioactivity of the eluents was determined in a γ-counter. The percentage of metabolites was calculated as follows: (aqueous eluent radioactivity / (aqueous eluent radioactivity + ethanol eluent radioactivity)) * 100% (mean ± SD, n=4).

5.2.9 Immunohistochemical staining of GRPR

In patients scheduled for RP, prostatectomy specimens were used for immunohistochemical staining of GRPR. In patients who did not undergo RP, prostate biopsy specimens were used. Formalin-fixed, paraffin-embedded blocks of prostate cancer tissue were cut into 3-µm thick sections and mounted on APES (3-aminopropyltriethoxysilane)-coated slides. A human prostate cancer PC-3 xenograft tumor was used as the positive control. As the negative control, the primary antibody was omitted during immunohistochemical analysis on the positive control tissue. Tris buffered saline (TBS) was used for washing and dilution of antibodies. After deparaffinization, antigen retrieval was performed by microwave heating (400 W) for 20 min in a 0.1 M

Tris/HCl buffer at pH 9.0. Endogenous peroxidase was blocked by incubation with 0.3% hydrogen peroxide in TBS for 20 min. To decrease non-specific background staining, slides were incubated with normal goat serum diluted at 1:10 in TBS for 30 min at room temperature. Tissue section slides were incubated with primary anti-human-GRPR rabbit polyclonal antibody ab39963 iluted at 1:250 in 1% bovine serum albumin (BSA)/TBS overnight at 4 °C. A secondary step with goat anti-rabbit antibody P0448 diluted at 1:100 in 1% BSA/TBS with 1% AB serum was applied for 60 min at room temperature. Slides were immersed for 10 min in a solution of 0.05% 3,3′-diaminobenzidine and 0.03% hydrogen peroxide in TBS for visualization of the signal as brown staining. After washing with demineralized water, slides were counterstained with hematoxylin and dehydrated. Finally, a coverslip was applied using Eukitt mounting medium.

5.2.10 Assessment of GRPR Staining

An experienced pathologist (SR) blinded to the clinical data scored the staining intensity (0 = no staining, 1+ = weak staining, 2+ = moderate staining, 3+ = strong staining) of tumor areas for all specimens. Specimens, in which one or more tumor areas with different staining intensities were present, were scored for the most prevalent intensity.

5.3 Results

5.3.1 Synthesis and Quality Control of ^{99m}Tc-HABN

^{99m}Tc-HABN was prepared (n=8) with a radiochemical yield of 43 ± 4%, a specific activity of 87.2 ± 9.4 TBq/mmol and a radiochemical purity of 97.3 ± 0.9%. The bubble point test of the sterilization filter was performed before the injection of ^{99m}Tc-HABN. The sterility, endotoxins and residual solvents tests were performed after the release of the tracer. The final productswas sterile and apyrogenic (<0.25 EU/ml), and resideual solvents were found to be < 50 mg/L and 100 g/L for ACN and EtOH, respectively. Release and post-release specifications are summarized in table 1.

Table 1: release and post-release specifications ^{99m}Tc-HABN.

^{99m}Tc-HABN	**Specification**	**Required before release**	**Frequency**
Appearance	Clear, colorless	Yes	Every synthesis
pH	5-8	Yes	Every synthesis
Radiochemical purity (%)	>95%	Yes	Every synthesis
Specific activity (MBq/mg)	>5000	Yes	Every synthesis
Bubble point test sterilization filter	<20%	Yes	Every synthesis
Sterility	Sterile	No	Every synthesis
Endotoxins (EU/ml)	<0.25	No	Every synthesis
EtOH concentration (g/l)	<100	No	Every synthesis
ACN concentration (mg/l)	<50	No	Every synthesis

5.3.2 Patient characteristics

Details of included patients and results of histology can be found in table 2. Although initially selected for EBRT, patients 7 and 8 proved to have lymph node metastases and were subsequently selected for hormonal therapy.

Table 2: patient characteristics.

Pt.nr	**Age**	**PSA**	**PrV**	**Therapy**	**T-stage**	**TumorV**	**Gl**	**PLND**
1	59	5,9	35	RP	pT2c[a]	5%[a]	7[a]	np
2	55	16	21	RP	pT2c[a]	>50%[a]	6[a]	np
3	69	12	47	RP	pT2c[a]	<50%[a]	7[a]	pN0
4	73	7,8	56	EBRT	cT1c[b]	Left/5/5/75%, Right/5/1/5%[c]	7[c]	pN0
5	55	15,5	23	RP	pT3a[a]	>50%, capsular penetration left[a]	8[a]	np
6	73	69.8	38	EBRT	cT2c[b]	Left/5/2/15%, Right/5/4/45%[c]	9[c]	pN0
7	71	221.5	55	HT	cT3[b]	Left/4/4/65%, Right/4/4/10%[c]	7[c]	pN1
8	70	23.8	39	HT	cT2c[b]	Left/4/4/35%, Right/4/4/20%[c]	7[c]	pN1

Biopsy results are not displayed when histology of a radical prostatectomy is available. In EBRT or hormonal therapy patients, only prostate biopsy histology is available. PSA in ng/ml, PrV = prostate volume in ml, RP = radical prostatectomy, EBRT = external beam radiotherapy, HT = hormonal therapy, T-stage = tumor stage, [a] = based on histology of radical prostatectomy specimens, [b] = based on digital rectal examination and histology of prostate biopsies, [c] = based on histology of prostate biopsies, TumorV = % tumor volume (tumorvolume based on prostate biopsies are presented as: side/biopsy cores taken on that side/number of positive cores on that side/%tumorvolume), Gl = Gleason sum score, PLND = pelvic lymph node dissection, np = not performed, pN0 = no pelvic lymph node metastases, pN1 = pelvic lymph node metastases.

5.3.3 Image Analysis

Thorough analysis of the dynamic, static and SPECT images with or without CT by one dedicated nuclear medicine physician (JP) blinded to patient data and non-blinded one researcher (HA), revealed no uptake of radioactivity in the prostate or pelvic lymph nodes (histologically proven lymph node metastases in patients 7 and 8). Rapid distribution via blood was observed, and excration via urine was observed within 5-7 min. T transurethral catheter reduced radioactivity in the pelvis, improving visualization of tissue in the immediate vicinity of the bladder. The procedure did not lead to detection of a hot-spot in the prostate. Furthermore, no other hot-spots outside the bladder or prostate were observed in the pelvis. No ROIs were drawn because the tumor was not visualized.

5.3.4 Monitoring of Vital Parameters and Side-effects

In the first hour after ^{99m}Tc-HABN injection, vital parameters (heart-rate, oxygen saturation and blood-pressure) were measured at regular intervals and were compared with baseline measurements. No clinically significant changes in heart rate (>15% change), oxygen saturation (>5% change) and blood pressure (>15% change) were recorded. None of the patients suffered from adverse or subjective side effects.

5.3.5 Analysis of Radioactivity in Blood

Figure 1 shows the full blood and serum radioactivity curves after ^{99m}Tc-HABN injections in patients during the 1200-min study period (n=6, except at the 1200-min time point were n=4). A steady decline of the radioactivity was observed in blood and serum during the experimental period. The radioactivity level became almost undetectable at 20 h p.i..

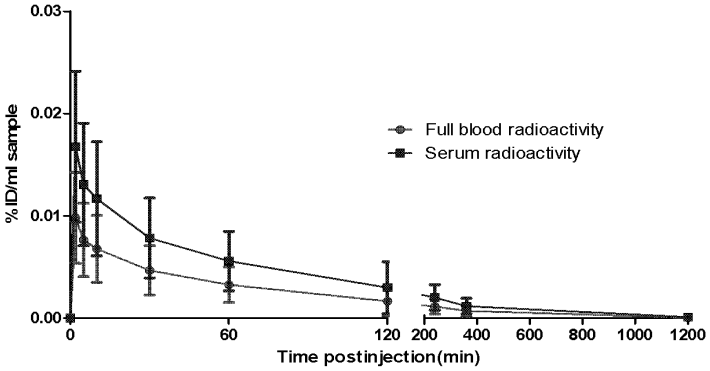

Figure 1: full blood and serum activity curves during the 1200 min study. Values are expressed as percentage of the injected dose per ml (%ID/m, mean ± SD, n=6, 1200 min time-point n=4).

5.3.6 Metabolic Stability of ^{99m}Tc-HABN

Figure 2 shows the *in vivo* degradation of ^{99m}Tc-HABN. There are low metabolic stability and rapid degradation of ^{99m}Tc-HABN, with 22%, 44% and 53% of the radioactivity degraded within 2, 5 and 10 min p.i., respectively. After 30 minutes less than 20% of ^{99m}Tc-HABN was still intact.

5.3.7 Assessment of immunohistochemical GRPR staining

Immunohistochemistry on paraffin slides of prostate cancer specimens (four whole prostate sections, four prostate needle biopsy specimens) demonstrated low-to-moderate staining of prostate cancer for GRPR in 8/8 cases (table 3).

5.4 Discussion

Targeted imaging could improve the lack of accuracy observed in current imaging techniques used in different stages of prostate cancer. Recently, we have developed the novel BN-based radiopharmaceutical, designated ^{99m}Tc-HABN, and evaluated its imaging potential in a xenograft mouse model of human prostate cancer(20). The aim of thestudy presented here was to perform a first-in-man clinical pilot study to evaluate the feasibility of ^{99m}Tc-HABN SPECT/CT for detection of prostate cancer in patients. We were able to synthesize a radiopharmaceutical with high yield, specific activity and purity, in the absence of any signs of adverse or subjective side effects after patientadministration. However, ^{99m}Tc-HABN scintigraphy and SPECT/CT did not detect prostate cancer in patients with proven disease.

Although immediate distribution via the vascular system and rapid excretion via the renal route were deduced from the dynamic images, no uptake in the prostate was observed at any time point in any patient. Although bladder drainage using a transurethral catheter

proved to be helpful in reducing activity in the bladder with an improved ability to assess pelvic organs, it did not aid in detecting hot-spots.

Because small tumors could be missed with SPECT, patients with larger tumor volumes and higher PSA values were selected in the second half of the patient inclusion (patients 5–8). The different patient selection sorted no effect. Additionally, there has been some discussion concerning the level of GRPR expression according to various Gleason sum scores. Although this could not be proven in lymph node and bone metastases of prostate cancer(12), Beer et al. demonstrated that a higher Gleason sum score tends to express lower levels of GRPR(13). Therefore, a range of Gleason sum scores was selected (Gleason 6–9; lower scores are seldom observed, and Gleason 10 is only rarely eligible for local therapy), but did not give other results with ^{99m}Tc-HABN scintigraphy and SPECT/CT. One reason for the failure to visualize the prostate tumors is that, by chance, GRPR expression in 8 prostate cancer patients could be absent. However, with immunohistochemistry on paraffin slides of the prostate cancerspecimens of these patients, we proved the presence of GRPR in all our patients (Table 3). Although immunohistochemistry shows the presence and tissue distribution of an antigen, the technique cannot demonstrate absolute antigen density and is therefore not a strong predictor for uptake of a GRPR-targeting radiopharmaceutical.

Table 3: Staining intensities of the antibodies in prostate cancer specimens

Patient number	Pathology	Staining intensity
1	Radical prostatectomy	+
2	Radical prostatectomy	+
3	Radical prostatectomy	+
4	Prostate needle biopsy	+
5	Radical prostatectomy	+
6	Prostate needle biopsy	+
7	Prostate needle biopsy	++
8	Prostate needle biopsy	+

The difference between the in vitro stability in human serum samples determined in our previous study on ^{99m}Tc-HABN (20) and the in vivo metabolic stability determined in the present study, is striking. In our previous study, we have demonstrated that 77% of ^{99m}Tc-HABN is intact after 24 h in human serum *in vitro* (20). However, the results of the current study indicate that metabolites are formed as early as 10 min p.i. and that less than 20% of ^{99m}Tc-HABN is intact after 30 min. Thus, we must conclude that one of themain reasons for the failure to visualize the prostate tumors is the rapid in vivo degradation of ^{99m}Tc-HABN (Figure 2). Similar results were observed in a study by *Linder et al.*, where the metabolism of ^{177}Lu-AMBA in mice and rats in vivo was much more rapid than that *in vitro* (21).

Rapid and highly selective proteolytic cleavage of bioactive peptides is not unexpected because this is the key in the autonomic regulation of the biologic effects of peptides. It is unknown which enzymes are responsible for the degradation of BN in vivo. In this respect, ecto-enzymes located on the cell surface that shed in blood and are highly expressed in the liver and kidneys could be major players in this process (22). Therefore, to more accurately determine radiochemical stability, it was suggested by Ocak et al. to use liver and kidney homogenates (23). By contrast, in another study by the same author, it was shown that rat liver and kidney homogenates were not good predictors for in vivo stability (24).

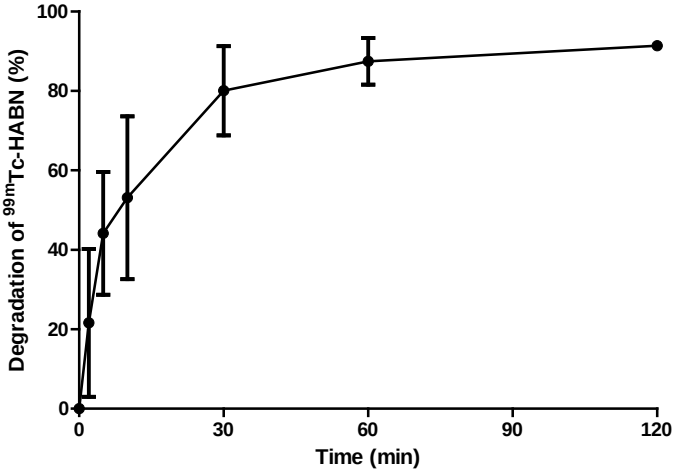

Figure 2: the *in vivo* metabolic stability of ^{99m}Tc-HABN. Results are plotted as the percentage of formed metabolites at different time points (mean ± SD, n=4).

In a pre-clinical study in a xenograft tumor model for human prostate cancer in athymic mice, we have demonstrated moderate uptake of ^{99m}Tc-HABN in tumors (20). Moderate uptake in tumors does not pose a real problem provided that the background uptake is low to create high tumor-to-background ratios and excellent contrast. Performance of a BN-like radiopharmaceutical in a pre-clinical mouse model is not a strong predictor for clinical performance in humans because there is a different body biodistribution of GRPR in mice compared with humans. Nevertheless, the moderate uptake of ^{99m}Tc-HABN in tumor cells as previously demonstrated in the preclinical study could be another contributing factor leading to failure to visualize the prostate tumors in prostate cancer patients in this study.

Other clinical studies in prostate cancer patients with BN-like radiopharmaceuticals have shown fairly good results (19). A study by Scopinaro et al. is particularly interesting because high uptake in the prostate was found in all eight prostate cancer patients, and pathology confirmed invasion in obturator nodes was found in three of these patients (26). Despite the clinical results of other groups and the findings of our pre-clinical studywhere the prostate tumorwas clearly visualized in mice with ^{99m}Tc-HABN microSPECT, we could not detect prostate cancer with^{99m}Tc-HABN scintigraphy and SPECT/CT in patients of the current clinical study. Two main reasons for the inability to detect prostate cancer with scintigraphy and SPECT/CT are most likely the low in vivo stability of ^{99m}Tc-HABN resulting in low-circulating intact radiopeptide and the absolute tumor uptake of ^{99m}Tc-HABN being too low because of the relatively low to moderate expression of GRPR in primary prostate cancer. When considering the IC_{50}, the in vivo tumor uptake and tumor-to-normal-tissue ratios in the pre-clinical study, the affinity and performance of ^{99m}Tc-HABN are essentially similar compared with other BN analogs reported in the literature (19, 25). The pre-clinical data of the BBN-like radiopharmaceuticals that have been used for imaging of prostate cancer patients are not available in the international literature and, therefore, cannot be compared with our pre-clinical data.

The findings that the in vitro stability of a BBN-like radiopharmaceutical in human serum does not correlate with *in vivo* stability and that the in *vivo* performance of a BN-like

radiopharmaceutical in a mouse tumor model does not correlate with *in vivo* performance in man are interesting. As demonstrated previously, determination of the stability of a radiolabelled peptide in vitro in serum has no predictive value for its *in vivo* stability in rodents (21, 23, 24). The development of new or improved in vitro stability tests or better preclinical in vivo tumor models may prove to be a better approach for selecting radiolabelled peptides of appropriate stability and affinity for clinical testing. Future studies should focus on developing high affinity BN-like radiopharmaceuticals that have been proven to be highly stable in a pre-clinical setting. Additionally, instead of using the relatively low-resolution SPECT for imaging, the use of radiopeptides suitable for PET imaging will aid in improvement of imaging.

5.5 Conclusions

^{99m}Technetium-HYNIC(tricine/TPPTS)-Aca-Bombesin(7–14) SPECT/CT for the detection of prostate cancer is safe but is hampered by an unexpectedly low in *vivo* metabolic stability in man. The difference between the excellent *in vitro* stability in human serum determined in our previous study on ^{99m}Tc-HABN and the low *in vivo* metabolic stability determined in the present study is striking. Furthermore, the current study showed that the *in vivo* performance in a mouse tumor model does not correlate with *in vivo* performance in prostate cancer patients. This issue warrants further study of peptide-based radiopharmaceuticals.

Acknowledgements

We thank Karin Groeneveld, Remko Koning, Jose Douma, Hans ter Veen, Johan Wiegers and Johan de Jong for assistance with SPECT/CT imaging and protocol development. This work was supported by grants of the Dutch Cancer Society (KWF 2008- 4243), the Dutch Urology Foundation 1973 Stichting Urologie 1973), the Jan Kornelis de Cock Stichting (J.K. de Cock Stichting 08-02) and the Center for Translational Molecular Medicine (project Prostate Cancer Molecular Medicine 03O-203).

References

(1) Center MM, Jemal A, Lortet-Tieulent J, Ward E, Ferlay J, Brawley O, et al. (2012) International variation in prostate cancer incidence and mortality rates. *Eur Urol* 61(6):1079–92.

(2) Arora R, Koch MO, Eble JN, Ulbright TM, Li L, Cheng L. (2004) Heterogeneity of Gleason grade in multifocal adenocarcinoma of the prostate. *Cancer* 100(11):2362–6.

(3) Eichler K, Hempel S, Wilby J, Myers L, Bachmann LM, Kleijnen J. (2006) Diagnostic value of systematic biopsy methods in the investigation of prostate cancer: a systematic review. *J Urol* 175(5):1605–12.

(4) Chang JJ, Shinohara K, Bhargava V, Presti Jr JC. (1998) Prospective evaluation of lateral biopsies of the peripheral zone for prostate cancer detection. *J Urol* 160(6 Pt 1):2111–4.

(5) Presti Jr JC, Chang JJ, Bhargava V, Shinohara K. (2000) The optimal systematic prostate biopsy scheme should include 8 rather than 6 biopsies: results of a

prospective clinical trial.*J Urol* 163(1):163–6 [discussion 166–7].
(6) Levy DA, Jones JS. (2011) Management of rising prostate-specific antigen after a negative biopsy. *Curr Urol Rep* 2011.
(7) Resnick MJ, Lee DJ, Magerfleisch L, Vanarsdalen KN, Tomaszewski JE, Wein AJ, et al. (2011) Repeat prostate biopsy and the incremental risk of clinically insignificant prostate cancer. *Urology* 77(3):548–52.
(8) Mariani G, Bruselli L, Kuwert T, Kim EE, Flotats A, Israel O, et al. (2010) A review on the clinical uses of SPECT/CT. *Eur J Nucl Med Mol Imaging* 37(10):1959–85.
(9) Ambrosini V, Fani M, Fanti S, Forrer F, Maecke HR. (2011) Radiopeptide imaging and therapy in Europe. *J Nucl Med* 52(Suppl. 2):42S–55S.
(10) De Jong IJ, De Haan TD, Wiegman EM, Van Den Bergh AC, Pruim J, Breeuwsma AJ. (2010) PET/CT and radiotherapy in prostate cancer. *Q J Nucl Med Mol Imaging* 2010;54(5):543–52.
(11) Jadvar H. (2011) Prostate cancer: PET with ^{18}F-FDG, ^{18}F- or ^{11}C-acetate, and ^{18}F- or ^{11}C-choline. *J Nucl Med* 52(1):81–9.
(12) Ananias HJ, van den Heuvel MC, Helfrich W, de Jong IJ.(2009) Expression of the gastrinreleasing peptide receptor, the prostate stem cell antigen and the prostate-specific membrane antigen in lymph node and bone metastases of prostate cancer. *Prostate* 69(10):1101–8.
(13) Beer M, Montani M, Gerhardt J, Wild PJ, Hany TF, Hermanns T, et al. (2012) Profiling gastrin-releasing peptide receptor in prostate tissues: clinical implications and molecular correlates. *Prostate* 72(3):318–25.
(14) Aprikian AG, Cordon-Cardo C, Fair WR, Reuter VE. (1993) Characterization of neuroendocrine differentiation in human benign prostate and prostatic adenocarcinoma. *Cancer* 71(12):3952–65.
(15) Cutz E, Chan W, Track NS. (1981) Bombesin, calcitonin and leu-enkephalin immunoreactivity in endocrine cells of human lung. *Experientia* 37(7):765–7.
(16) Price J, Penman E, Wass JA, Rees LH. (1984) Bombesin-like immunoreactivity in human gastrointestinal tract. *Regul Pept* 9(1–2):1–10.
(17) Spindel ER, Chin WW, Price J, Rees LH, Besser GM, Habener JF. (1984) Cloning and characterization of cDNAs encoding human gastrin-releasing peptide. *Proc Natl Acad Sci U S A* 81(18):5699–703.
(18) Schroeder RP, van Weerden WM, Bangma C, Krenning EP, de Jong M. (2009) Peptide receptor imaging of prostate cancer with radiolabelled bombesin analogues. *Methods* 48(2):200–4.
(19) Ananias HJ, de Jong IJ, Dierckx RA, van de Wiele C, Helfrich W, Elsinga PH. (2008) Nuclear imaging of prostate cancer with gastrin-releasing-peptide-receptor targeted radiopharmaceuticals. *Curr Pharm Des* 14(28):3033–47.
(20) Ananias HJ, Yu Z, Dierckx RA, van der Wiele C, Helfrich W, Wang F, et al. (2011) ^{99m}technetium-HYNIC(tricine/TPPTS)-Aca-bombesin(7-14) as a targeted imaging agent with microSPECT in a PC-3 prostate cancer xenograft model. *Mol Pharm* 8(4):1165–73.
(21) Linder KE, Metcalfe E, Arunachalam T, Chen J, Eaton SM, Feng W, et al. (2009) In vitro and in vivo metabolism of Lu-AMBA, a GRP-receptor binding compound, and the synthesis and characterization of its metabolites. *Bioconjug Chem* 20(6): 1171–8.
(22) Konkoy CS, Davis TP. (1996) Ectoenzymes as sites of peptide regulation. *Trends Pharmacol Sci* 17(8):288–94.
(23) Ocak M, Helbok A, von Guggenberg E, Ozsoy Y, Kabasakal L, Kremser L, et al. (2011) Influence of biological assay conditions on stability assessment of

radiometallabelled peptides exemplified using a ^{177}Lu-DOTA-minigastrin derivative. *Nucl Med Biol* 38(2):171–9.

(24) Ocak M, Helbok A, Rangger C, Peitl PK, Nock BA, Morelli G, et al. (2011) Comparison of biological stability and metabolism of CCK2 receptor targeting peptides, a collaborative project under COST BM0607. *Eur J Nucl Med Mol Imaging* 38(8):1426–35.

(25) Schroeder RP, Muller C, Reneman S, Melis ML, Breeman WA, de Blois E, et al. (2010) A standardised study to compare prostate cancer targeting efficacy of five radiolabelled bombesin analogues. *Eur J Nucl Med Mol Imaging* 37(7):1386–96.

(26) Scopinaro F, De Vincentis G, Varvarigou AD, Laurenti C, Iori F, Remediani S, et al. (2003) ^{99m}Tc-bombesin detects prostate cancer and invasion of pelvic lymph nodes. *Eur J Nucl Med Mol* Imaging 30(10):1378–82.

Chapter 6

Synthesis and Preclinical Evaluation of [^{123}I]-cubyl-carboxyl-ε-aminocaproic acid-bombesin(7-14) for Prostate Cancer Imaging with SPECT

Zilin Yu, Joost Verbeek, Jie Yin, Hildo J. K. Ananias, Chao Wu, Giuseppe Carlucci, Wijnand Helfrich, Rudi A. J. O. Dierckx, Fan Wang, J. D. M. Herscheid, Igle Jan. de Jong, Philip H. Elsinga

Abstract

Radiolabelled bombesin analogues are promising tracers for the Gastrin-Releasing-Peptide-Receptor (GRPR), a receptor highly expressed in human prostate cancer. For achieving high accumulation in tumor and high tumor-to-normal tissue contrast, we designed a [^{123}I]-labelled bombesin tracer. The [^{123}I]-cubyl-carboxyl-ε-aminocaproic acid-bombesin(7-14) ([^{123}I]-CABN) was developed as a potential metabolically stable tracer against deiodination with a relatively long radioactive half-life. In this study, we evaluated the targeting ability of the tracer *in vitro* and in tumor bearing athymic mice *in vivo*.

Methods: [^{123}I]-CABN was synthesized by coupling the synthon [^{123}I]-cubyl-carboxyl-tetrafluorophenyl ([^{123}I]-cubyl-TFP) ester with ε-aminocaproic acid–bombesin (7-14)(Aca-BN). The internalization and efflux properties of [^{123}I]-CABN were determined in a PC-3 human prostate cancer cell line. The biodistribution profiles and the imaging characteristics were determined in athymic mice bearing human PC-3 tumor xenografts.

Results and Conclusion: The novel universal labeling [^{123}I]-cubyl moiety was successfully conjugated to the Aca-BN peptide. The radiochemical yield of [^{123}I]-CABN starting from [^{123}I]-cubyl-TFP ester was 49±18% and the radiochemical purity was higher than 95% after purification. [^{123}I]-CABN showed good cell uptake (11.0 ± 0.7% of incubation dose at 1 h post incubation) and efflux kinetics (efflux half-life was 88 min), but the unfavourable *in vivo* stability proved to be the limiting factor for tumor targeting as the radiotracer was sensitive to peptidase activity. Although [^{123}I]-CABN may not be a proper tracer for prostate cancer imaging, the [^{123}I]-cubyl moiety is a promising motif for labeling of biomolecules.

Keywords: bombesin; GRPR; prostate cancer; SPECT imaging; [^{123}I]-cubyl

6.1 Introduction

Bombesin (Pyr-Gln-Arg-Leu-Gly-Asn-Gln-Trp-Ala-Val-Gly-His-Leu-Met-NH_2) is a 14 amino acid peptide first isolated from frog skin and reported in 1970 (*1*). Neuromedin B receptor (BB1), GRPR (BB2) and Bombesin receptor subtype 3 (BRS-3 or BB3) are known as mammalian bombesin receptors (*2*). GRPR not only functions as a glycosylated, 7-transmembrane G-protein coupled receptor, which, upon binding, rises a complex cascade of intracellular reactions (*3-5*), but is over expressed in several primary human tumours and metastases such as breast and prostate cancer (*6-9*).

Prostate cancer is the most common cancer in males in western countries (*10*). Because of the poor positive predictive value and low resolution of current prostate cancer detection methods, a high sensitive, non-invasive, *in vivo* method is urgently required.

Bombesin derivatives have been labelled for SPECT imaging with ^{99m}Tc, ^{177}Lu, ^{67}Ga and ^{111}In (*11-15*) and for PET imaging with ^{64}Cu, ^{68}Ga and ^{18}F (*16-20*), thus bombesin analogues with a large range of radioactive half-lives are available (*21*). In our previous study it was shown that ^{99m}Tc-HYNIC(Tricine/TPPTS) labeling is a suitable approach for bombesin tracer synthesis (*12*). For ^{99m}Tc-HYNIC(tricine/TPPTS)-Aca-Bombesin(7-14), the optimal tumor-to-background contrast was reached at 4 hours post tracer injection. As an alternative to ^{99m}Tc we explored ^{123}I. The half life of ^{123}I is 13.3 hours which is suitable for peptide labeling for application in SPECT imaging. If the new radioiodinated bombesin would show to be a suitable tracer, other iodine radioisotopes could be applied as well. ^{124}I and ^{131}I could supply alternatives for PET imaging and radioimmunotherapy. Therefore, [^{123}I] was selected for SPECT imaging in this study.

To avoid deiodination and subsequent high accumulation in the thyroid gland, we introduced the [^{123}I]-cubyl-moiety (figure 2, A), as a stable labeling synthon, to develop a stable radiotracer and evaluated the possibility for targeting GRPR in human prostate cancer xenograft.

6.2 Materials and Methods

All chemicals obtained commercially were used without further purification. Aca-BN was obtained from Peptide International (Louisville, KY, USA). ^{125}I-Tyr^4-BN(1-14) was purchased from Perkin-Elmer Life and Analytical Sciences (Waltham, MA, USA).

6.2.1 Methods:

For radio-HPLC, a *HITACHI L-2130 HPLC* system (Hitachi High Technologies America Inc., Pleasanton, CA, USA) equipped with a Bicron Frisk-tech area monitor was used. Analysis and isolation of radiolabelled peptides was performed using a reversed-phase Grace Smart RP-C18 column (Lokeren, Belgium) (4.6 mm × 250 mm, 10 μm). The flow rate was 1 ml/min. The mobile phase was isocratic with 90% solvent A (0.01 M phosphate buffer, pH 6.0) and 10% solvent B (acetonitrile) at 0-5 min, followed by a gradient mobile phase going from 10% solvent B at 5 min to 60% solvent B at 15 min, and from 90% solvent B at 22.5 min, back to baseline 10% solvent B at 25 min afterwards.

6.2.2 Chemistry

6.2.2.1 Hydrolysis of 1,4-iodocubylcarboxylicacid-methylester

1,4-iodocubylcarboxylicacid-methylester**(1)** (65 mg, 0.225 mmol) (Boron molecular, Durham, North Carolina , USA) was suspended in 3 mL THF and 7 mL H_2O. The pH of the solution was adjusted to 13 and maintained at this value for 5 hours at room temperature by the continuous addition of an aqueous KOH solution (2 mol/L). The reaction mixture was then acidified to around pH 4 with 2 M HCl, forming a suspension. The acid containing suspension was extracted by diethyl ether until there was no suspension formed when a new charge of acid was added. The resultant diethyl ether solution was dried over anhydrous $MgSO_4$. After removal of $MgSO_4$, the solvent was evaporated and the crystals were collected. This solid was further dried at 40^oC for 24 hours in the vacuum oven, giving around 50 mg (80%) free acid 1,4-iodocubylcarboxylicacid **(2)**. ^1H NMR (400 MHz, $CDCl_3$, δ): 4.42(3H, m, C<u>H</u>CO), 4.30(3H, m, C<u>H</u>I).

6.2.2.2 Synthesis of 1,4-iodocubylcarboxylicacid-N-hydroxysuccinimide (active ester (3))

1,4-iodocubylcarboxylicacid **(2)** (50 mg, 0.182 mmol) was dissolved in 5 mL methylene chloride. To this solution dry and finely powdered N-hydroxysuccinimide (NHS, 21 mg, 0.183 mmol was added. The flask was cooled in an ice-water bath, after which dicyclohexyl carbodiimide (DCC, 37.7 mg, 0.183 mmol) was added in a molar ratio of 1.001 times of free acid. The reaction mixture was stirred vigorously at 0 ^oC for 1 h and at room temperature for 12 hours. After the removal of precipitated dicyclohexyl urea by filtration, the crude product was extracted with distilled water. The resultant was dried over anhydrous $MgSO_4$. Afterwards, $MgSO_4$ was removed by filtration. The product was collected to give 60.8 mg (90%) 1,4-iodocubylcarboxylicacid-N-hydroxysuccinimide active ester **(3)**. ^1H NMR (400 MHz, $CDCl_3$, δ): 4.58(3H, m, C<u>H</u>CO), 4.36(3H, m, C<u>H</u>I), 2.84(4H, s, CH_2N).

6.2.2.3 Synthesis of Non-Radiolabelled I-CABN:

1,4-iodocubylcarboxylicacid-N-hydroxysuccinimide active ester **(3)** (6 mg) was dissolved in 0.5 mL acetonitrile. 0.5 mL (2 mg/mL in 0.1 M borate buffer) of Aca-BN was added to the active ester and the reaction mixture was well mixed and kept in room temperature for 2 h (figure 1). The reaction mixture was purified with HPLC. The collection was formulated by using Waters Sep-Pak Light C18 cartridge. The I-CABN was eluted with ethanol and dried under nitrogen flow (0.6 mg). The final product was characterized by mass spectrometry, $C_{58}H_{81}IN_{14}O_{11}S$ calculated molecular weight 1305.32, observed 1306.1 ($[M+H]^+$).

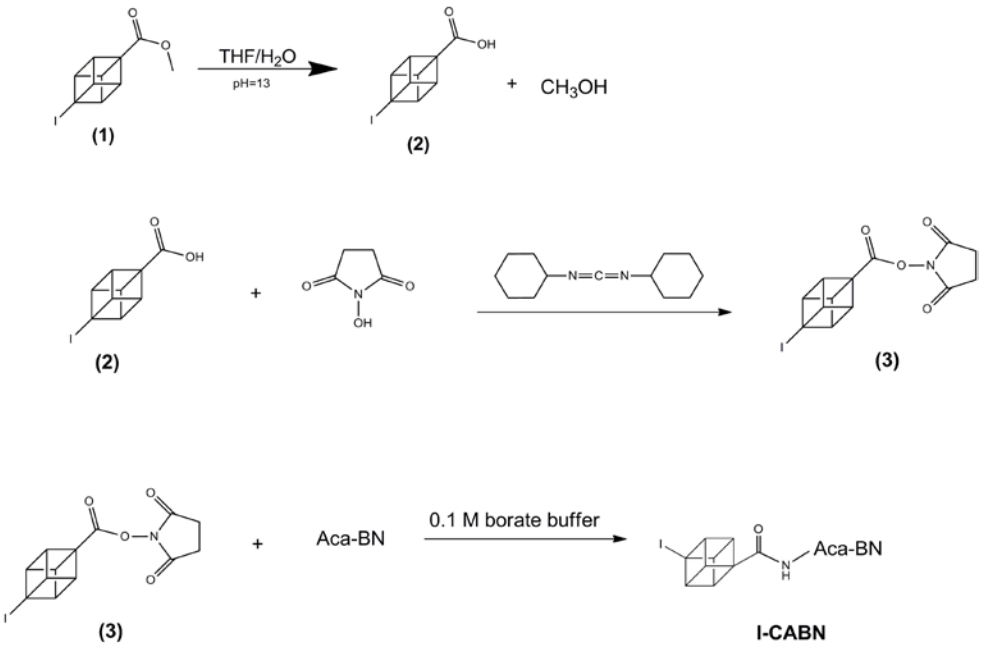

Figure 1. Synthesis of I-CABN. (1)= 1,4-iodocubylcarboxylicacid-methylester, (2)= 1,4-iodocubylcarboxylicacid, (3)= 1,4-iodocubylcarboxylicacid-N-hydroxysuccinimide active ester

6.2.3 Cell Culture

The GRPR positive PC-3 human prostate cancer cell line (ATCC, Manassas, Virginia, USA) was cultured in RPMI 1640 (Lonza, Verviers, France) supplemented with 10% fetal calf serum (Thermo Fisher Scientific Inc., Logan, Utah, USA) at 37 °C in a humidified 5% CO_2 atmosphere.

6.2.4 *In Vitro* Competitive Binding Assay:

The *in vitro* GRPR binding affinities of Aca-BN and non-radiolabelled I-CABN were compared via a competitive displacement assay by using ^{125}I-Tyr^4-BN(1-14) as the GRPR specific radioligand. Experiments were performed with PC-3 human prostate cancer cells according to a method previously described (*12*). The 50% inhibitory concentration (IC_{50}) values were calculated by fitting the data with nonlinear regression using GraphPad Prism 5.0 (GraphPad Software, San Diego, California, USA). Experiments were performed with triplicate samples. IC_{50} values are reported as an average of these samples plus the standard deviation (SD).

6.2.5 Synthesis of [^{123}I]-cubyl-TFP Ester

[^{123}I]-cubyl-TFP ester was prepared by the Department of Nuclear Medicine and PET Research, VU University Medical Center, Amsterdam, The Netherlands. Preparation of [^{123}I]-cubyl-TFP ester was performed as reported [patent WO2006083983(A2)]. In brief, the synthesis was started with Methyl-4-Bromocubylcarboxylate (1.5 mg), Cu(II)triflate (0.01 mg) and N,N-dimethylpiperazine. The mixture was added to non-carrier added [^{123}I] in 150 µL of acetonitrile (*22*). This mixture was heated in a closed vial for 40 min at 140 °C [^{123}I]methyl-4-iodocubylcaboxylate (83% radiochemical yield) was isolated from the precursor by HPLC (Kromasil 100 C18, MeCN/H_2O/DIPA 50/50/0.2, 1 ml/min, with a retention time of 20 -23 min). To the collected fraction 10 µL of 1 M NaOH was added. This mixture was heated for 30 min at 120 °C. Next the mixture was acidified to pH 6 with 1 M HCl, and 80 mg of EDAC and 60 mg of 2,3,5,6-tetrafluorophenol was added to the solution, and was left at room temperature for 45 min. To this solution water was added until the solution became a 10% acetonitrile solution, and was passed over a Sep-Pak C18 plus cartridge and washed with 20 mL water. The final product was eluted with acetonitrile in an overall yield of 40-60%.

6.2.6 Synthesis of [^{123}I]-CABN

The synthesis of [^{123}I]-CABN was performed by coupling Aca-BN with [^{123}I]-cubyl-TFP ester. 400 µl of Aca-BN (1 mg/ml, in 0.1 M sodium bicarbonate buffer, pH 9.5), 100 µl of [^{123}I]-cubyl-TFP ester (~200 MBq, in acetonitrile) were added to a glass vial and gently mixed. The mixture was sealed and kept at room temperature for 30 min. The tracer was analyzed and purified using radio-HPLC system. Retention time of Aca-BN and [^{123}I]-CABN were 16 and 23 min, respectively. The organic solvents in the product were removed by trapping the HPLC-collected product (after dilution with water) on a preactivated Waters Sep-Pak C18 light cartridge. [^{123}I]-CABN was eluted with 0.4 ml ethanol and diluted with saline solution.

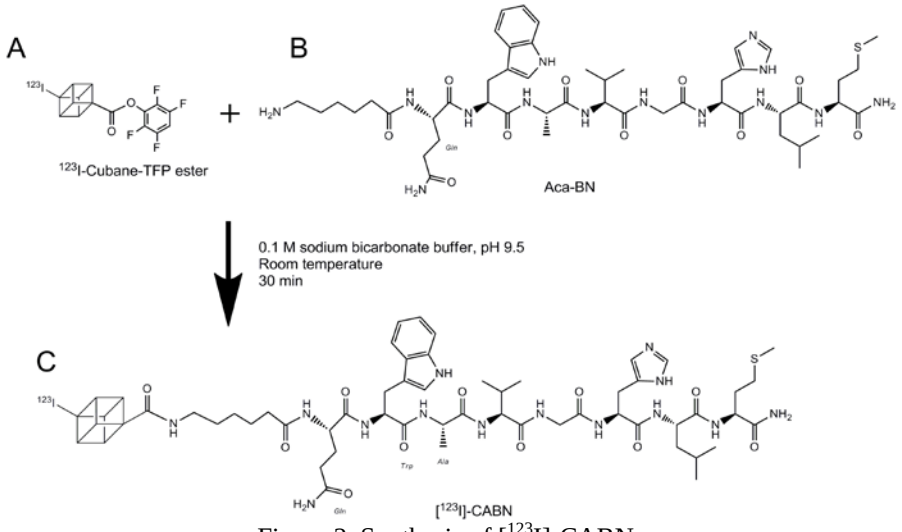

Figure 2. Synthesis of [^{123}I]-CABN.

6.2.7 Partition Coefficient

To measure the partition coefficient, 0.1 MBq of [^{123}I]-CABN was dissolved in 1 ml equivalent volume mixture of PBS (25 mM, pH 7.4) and *n*-octanol. The mixture was vortexed for 5 min at room temperature. After centrifugation (5 min 3000 rpm), 100 µl of both layers were counted with a γ-counter (Compugamma CS1282, LKB-Wallac, Turku, Finland). The experiment was performed in triplicate. The *log D* value was calculated as log(counts of organic phase/counts of water phase) (mean ± SD).

6.2.8 *In vitro* Stability

100 µl of [^{123}I]-CABN was diluted with 2 ml saline and kept at room temperature. Samples were taken and analyzed using radio-HPLC at 1, 2, 4, 24 h after incubation.

Another 100 µl of [^{123}I]-CABN was diluted with 2 ml human serum and incubated at 37 ^{o}C for same time period as mentioned earlier. Serum samples were precipitated with acetonitrile/ethanol solution ($V_{acetonitrile}$: $V_{ethanol}$=1: 1) and centrifuged at 3000 rpm for 3 min. The supernatants were passed through a 0.22 µm filter and analyzed by radio-HPLC.

6.2.9 *In vitro* Cell Uptake Assay

The PC-3 cells were harvested and placed in 6-wells plates (0.5 million cells/well) one day before the experiments. The cells were rinsed three times with PBS before use. PC-3 cells were incubated with 3.7 kBq of [^{123}I]-CABN at 37 °C for 1 hour. For determining the binding specificity of [^{123}I]-CABN, 20 µg of unlabelled Aca-BN was co-incubated with cells in the blocking group. To remove unbound radioactivity, the cells were washed twice with ice-cold PBS and afterwards the cells were lysed by incubation with 1 M NaOH at 37 °C. The cell associated radioactivity was determined by the γ-counter. Experiments were performed in triplicate. The cellular uptake was calibrated against a known aliquot of radiotracer and expressed as percentage of total incubated radioactivity (mean ± SD).

6.2.10 Internalization and Efflux Kinetics

Internalization and efflux kinetics of [^{123}I]-CABN in a PC-3 cell line were evaluated following a protocol reported previously (*12*). The experiments were performed in triplicate.

6.2.11 Animal Models

The animal model for the biodistribution studies, microSPECT/microCT imaging and *in vivo* stability studies was generated by subcutaneous injection of 1×10^{6} PC-3 cells (suspended in 0.1 ml of sterile saline) in the shoulder of male athymic nude mice (Harlan,

Zeist, The Netherlands). During the injection, animals were anesthetized with a gas composed of 3.5% isoflurane in an air and oxygen mixture. The mice were used for animal experiments when the tumor volume reached a mean diameter of 0.8 - 1.0 cm (3 - 4 weeks after inoculation). All animal experiments were performed in accordance with the regulations of Dutch law on animal welfare and the institutional ethics committee for animal procedures approved the protocol.

6.2.12 MicroSPECT Imaging and Biodistribution

The subcutaneous tumor bearing mice were used for microSPECT imaging and biodistribution when the tumor volume reached 250-300 mm^3 (4-5 weeks after inoculation).

MicroSPECT scans were performed using a three-head γ-camera (MILabs, U-SPECT-II, Utrecht, The Netherlands) equipped with a multi-pinhole high-resolution collimator. The MicroSPECT scans were performed with mice under isoflurane anesthesia after penile vein injection of ~33 MBq [^{123}I]-CABN. A dynamic microSPECT scan of 60 min (10 min per frame) was performed immediately after injection. For the receptor-blocking experiment, 300 μg of unlabelled Aca-BN was pre-injected 30 min before the tracer injection through the same catheter. The mice for dynamic scans were sacrificed after the scan. Blood, tumor, major organs and tissue samples were collected, weighted and counted by a γ-counter. The percentage of injected dose per gram (%ID/g) was determined for each sample. For each mouse, radioactivity of the tissue samples was calibrated against a known aliquot of radiotracer.

6.2.13 *In Vivo* Stability

The *in vivo* stability of [^{123}I]-CABN was evaluated in PC-3 prostate cancer bearing athymic nude mice. [^{123}I]-CABN (in 0.2 ml saline, ~ 22 MBq) was administered via penile vein. The animals were sacrificed at 10 min after tracer injection. Blood samples were collected and centrifuged at 3000 rpm for 5 min of Serum samples (250 μl) were extracted and well mixed with 750 μl acetonitrile. The mixture was centrifuged at 3000 rpm for 5 min. The supernatant of the mixture was filtered through a 0.22 μm Millex-LG filter and analyzed by radio-HPLC. The elution of the radio-HPLC was collected with plastic tubes (0.5 ml/tube) and measured by a γ-counter. The results were analyzed using GraphPad Prism 5.0 (GraphPad Software, San Diego, California, USA).

6.2.14 Statistical Analysis

Quantitative data are expressed as mean ± SD. Means were compared using Student's t test. P values<0.05 were considered significant.

6.3 Results

6.3.1 Radiochemistry, Partition Coefficient and *In Vitro* Stability

The preparation of [^{123}I]-CABN was accomplished by coupling the [^{123}I]-cubyl-TFP ester with Aca-BN peptide in moderate condition (pH=9.3, 30 min at room temperature). The labeling yield of [^{123}I]-CABN starting from [^{123}I]-cubyl-TFP ester was 49±18% (n=11). After HPLC purification, the radiochemical purity was > 95% according to radio-HPLC. The specific activity was 326±62 MBq/μmol (n=11) calculated from native Aca-BN. [^{123}I]-CABN was completed separated from Aca-BN by using HPLC. The partition coefficient was determined with a mixture of *n*-octanol and phosphate buffer (pH 7.4). The *log D* value of [^{123}I]-CABN was 1.20 ± 0.02. The *in vitro* stability of [^{123}I]-CABN was tested in saline and human serum. Figure 3 shows the *in vitro* stability of [^{123}I]-CABN. After 4 hours of incubation in saline solution, more than 95 % of the radioactivity corresponds to the parent compound of [^{123}I]-CABN. When incubated with human serum at 37 ^{o}C for 2 h, 50% of radioactivity maintained the form of parent compound. Only ~10 % of [^{123}I] was still in its original form after 4 hours incubation in human serum.

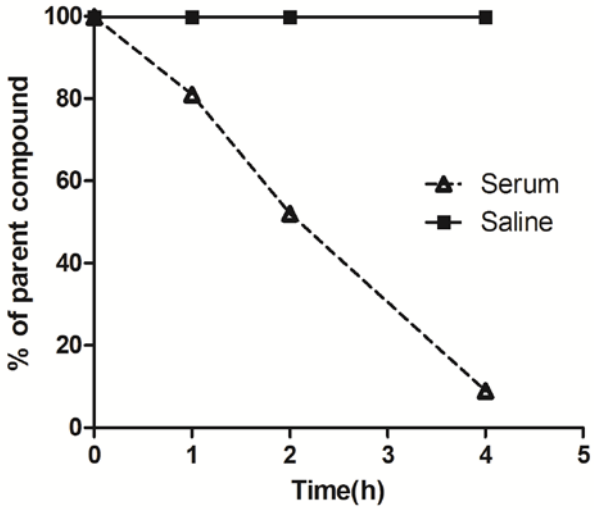

Figure 3. *In vitro* stability of [^{123}I]-CABN in saline (at room temperature), and human serum (at 37 ^{o}C). Results are plotted as % of the parent compound at different time points.

6.3.2 In Vitro Competitive Binding Assay

The GRPR binding affinity of Aca-BN and non-radiolabelled I-CABN was investigated by replacing the GRPR-bound of ^{125}I-Tyr^{4}-BN(1-14) in PC-3 cells. Figure 4 shows the results of the competitive binding assay. The IC_{50} value of Aca-BN and non-radiolabelled I-CABN were 2.5±0.4 and 72.9±1.7 nM, respectively.

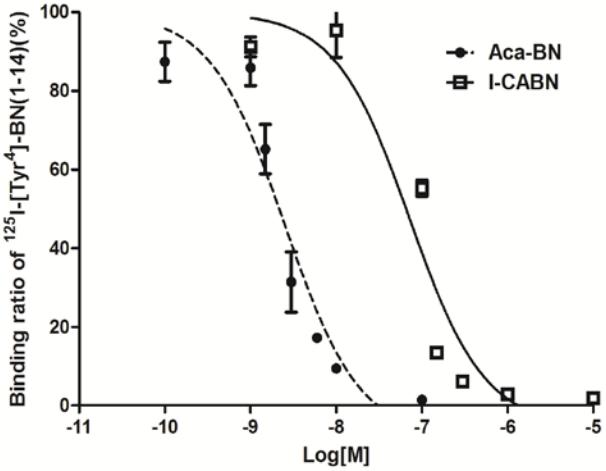

Figure 4. Displacement curve of ^{125}I-Tyr^4-BN(1-14) binding to GRPR in PC-3 cells. Log[M]: log of increasing concentration of Aca-BN and non-radiolabelled I-CABN.

6.3.3 *In vitro* Cell Uptake Assay

The cellular uptake of [^{123}I]-CABN was evaluated in the PC-3 prostate cancer cell line, and the receptor-mediated uptake was determined by co-incubation with excess blocking agent at 37 ^{o}C. The cellular uptake of [^{123}I]-CABN at 1 hour in the presence and absence of excess unlabelled bombesin(1-14) was 11.0 ± 0.7% and 5.6 ± 0.3%, respectively.

6.3.4 Internalization and Efflux Kinetics

Figure 5 shows the internalization and efflux kinetics of [^{123}I]-CABN. The internalization of [^{123}I]-CABN increased rapidly in 15 min after start of the incubation with PC-3 cells and reached plateau after 30 min incubation with maximum internalization ratio 66 ± 4%. After 4 h incubation in medium, 38 ± 2% of the internalized radioactivity remained in the PC-3 cells. $T_{1/2}$ of efflux of [^{123}I]-CABN was 88 min.

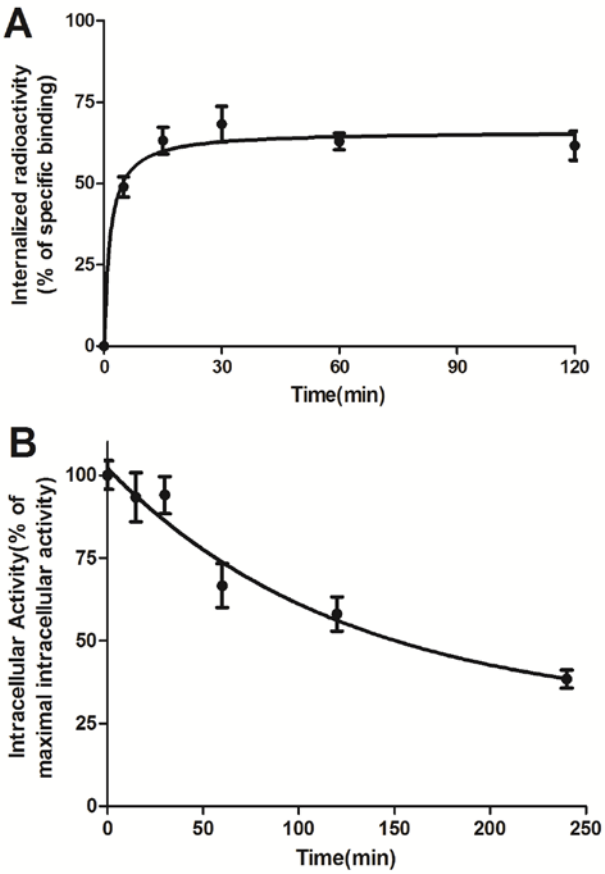

Figure 5. Internalization (A) and efflux (B) kinetics of [^{123}I]-CABN in PC-3 cells (n=3, mean ± SD).

.

6.3.5 MicroSPECT Imaging and Biodistribution

Biodistribution and microSPECT imaging of [^{123}I]-CABN were performed in athymic mice bearing PC-3M human prostate cancer xenograft. The uptake of [^{123}I]-CABN and the tumor-to-normal-tissue ratio (T/NT) in organs of interest are shown in table 1.

The organs with high uptake were liver, kidney and small intestine; the uptake was 30.9±7.3, 23.6±16.5, and 7.3±2.4%ID/g, respectively. The tumor uptake of [^{123}I]-CABN at 1 hour post injection was 0.26±0.08 %ID/g and was reduced to 0.18±0.08 %ID/g with excess of blocking agent. In pancreas, which is a GRPR rich organ, radioactivity uptake was 1.11 ± 0.21%ID/g. Only 32% of the radioactivity accumulation in pancreas was reduced in the blocking group. The tumor-to-non-tumor-tissue ratios were lower than 4.

Table 1 Biodistribution and tumor-to-non-tumor-tissue ratio (T/NT) of [^{123}I]-cubyl-Aca-BN after intravenous injection in PC-3 prostate cancer bearing athymic nude mice.

Organ	**1 h**		**1 h with blocking agent**
	%ID/g	T/NT	%ID/g
Blood	0.27 ± 0.07	0.97	0.25 ± 0.12
Heart	0.19 ± 0.08	1.52	0.20 ± 0.13
Liver	30.99 ± 7.31	0.01	38.74 ± 14.95
Spleen	0.47 ± 0.36	1.38	0.59 ± 0.49
Kidney	7.34 ± 2.43	0.04	9.53 ± 2.37
Small intestine	23.61 ± 16.54	0.03	22.02 ± 11.48
Large intestine	1.65 ± 1.47	0.31	0.97 ±0.36
Stomach	1.00 ± 0.45 *	0.30	0.38 ± 0.21 *
Bone	0.15 ± 0.18	3.63	0.11 ± 0.09
Muscle	0.14 ± 0.09	2.48	0.07 ± 0.03
Pancreas	1.11 ± 0.21	0.23	0.76 ± 0.42
PC-3 tumor	0.26 ± 0.08	1.00	0.18 ± 0.08

Uptake values are expressed as %ID/g, mean ± SD (n=3) and as T/NT ratios. 300 µg of unlabelled Aca-BN was administered as blocking agent; * = statistically significant different (P<0.05).

Figure 6 shows the microSPECT imaging of [^{123}I]-CABN with and without blocking agent in athymic mice bearing PC-3 human prostate cancer xenograft. A strong radioactivity signal was observed in liver and intestines in all SPECT images. The PC-3 tumor xenografts, which are present on the shoulder of the nude mice in the CT images, were not visible on the SPECT images. There was no radioactivity accumulation in thyroid either.

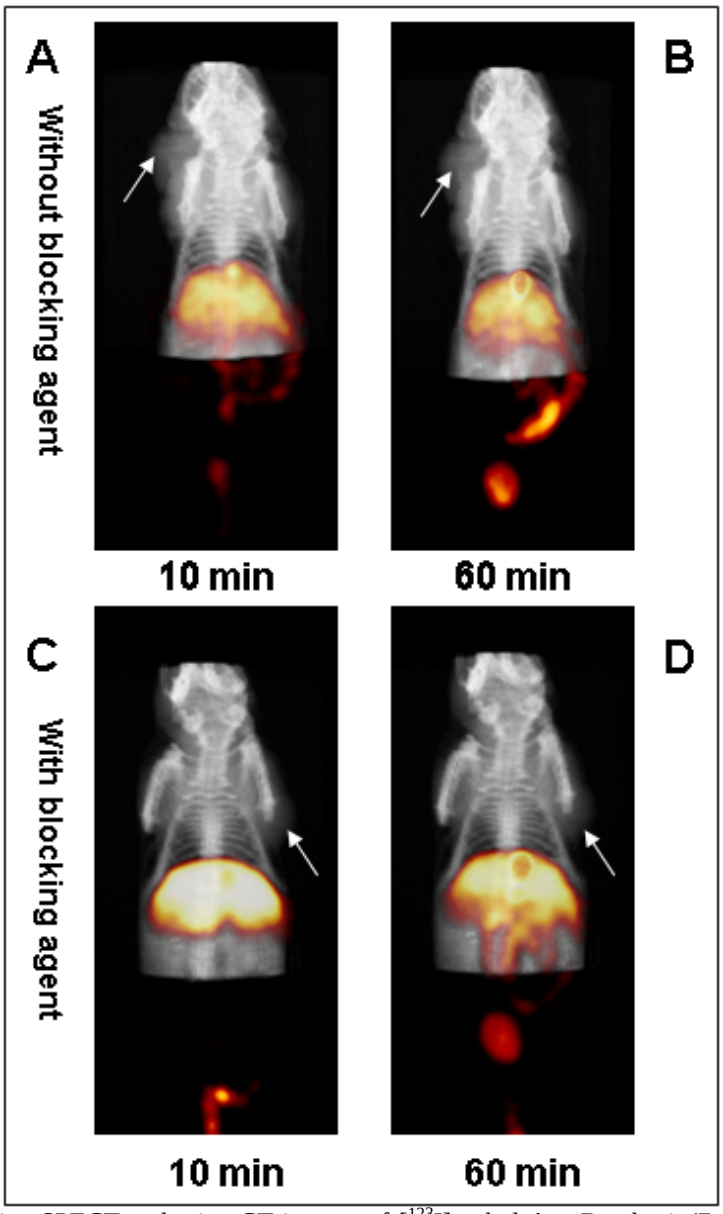

Figure 6. MicroSPECT and microCT images of [^{123}I]-cubyl-Aca-Bombesin(7-14) in PC-3 tumor bearing athymic mice without (A, acquired at 10 min p.i.; B, acquired at 60 min p.i.) and with blocking agent (C, acquired at 10 min p.i.; D, acquired at 60 min p.i.;). Arrows are pointed at the tumor.

6.3.6 *In Vivo* Stability

Since the tumor uptake of [^{123}I]-CABN at 1 h p.i. was low and non-specific, a

metabolite study was performed in PC-3 tumor bearing athymic nude mice to investigate the in vivo stability of the [^{123}I]-CABN at early time point (10min). Figure 7 shows a typical HPLC chromatogram of the blood sample collected at 10 min post injection. The retention time of original [^{123}I]-CABN was around 23 min. Two major metabolites were found in the blood samples with a retention time of 16 min (25.2 % of sample radioactivity) and 19 min (27.3 % of sample radioactivity). Unbound radioiodine which has a retention time around 5 min (< 2% of sample radioactivity), was not found in the blood samples.

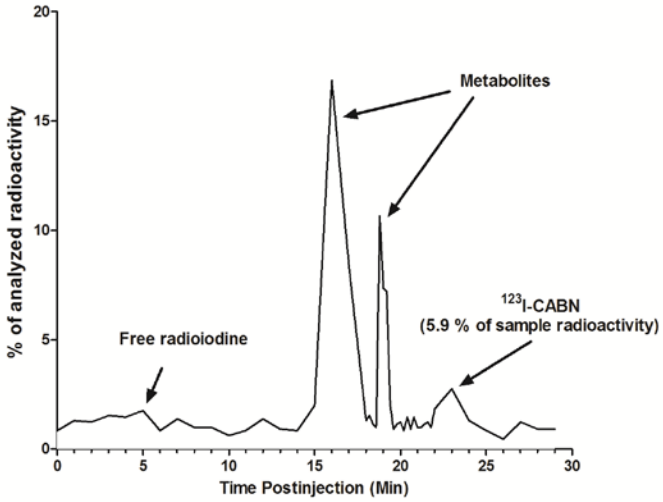

Figure 7. Radio-HPLC chromatogram of blood samples collected at 10 min post tracer injection in PC-3 tumor bearing athymic mice.

6.4 Discussion

Compared to radiolabelled antibodies, tumor targeting radiopharmaceuticals based on peptides show superb *in vivo* behaviour on immunogenicity, clearance, rapid penetration and accumulation in tumor, but underperform on metabolic stability, tumor retention (*23*). In this study, we introduced a [^{123}I]-cubyl-TFP ester for peptide based SPECT tracer preparation. The carbon-iodine bond of the [^{123}I]-cubyl-TFP ester has been proven metabolically stable in preclinical studies (*24*). Therefore we chose this labeling moiety to apply in radiolabelling of bombesin. The use of iodine as radionuclide has the additional advantages that [^{124}I] and [^{131}I] can be used as PET-tracer and radioimmunotherapy purposes, respectively.

We successfully synthesised the [^{123}I]-CABN under mild reaction conditions with good coupling yields and high radiochemical purities (>95%) achieved by HPLC purification. The GRPR targeting ability of [^{123}I]-CABN was evaluated *in vitro* by cellular uptake experiments with PC-3 prostate cancer cell line. The results of in vitro competitive binding assay indicate that the iodocubyl group effects the binding of the bombesin to GRPR. Compared to Aca-BN, the binding affinity of non-radiolabelled I-CABN was about 30 times lower. However, the *in vitro* cellular uptake of [^{123}I]-CABN was comparable to that of ^{99m}Tc labelled Aca-BN (data not shown). Compared to other bombesin tracers (*11-12*), a higher *logD* value of [^{123}I]-CABN was observed due to the hydrophobic character of the iodocubyl structure. Because of the lipophilicity of [^{123}I]-CABN, the non-specific

adhesion of the tracer to PC-3 cells was almost half of total cellular uptake. The internalization and efflux patterns of [^{123}I]-CABN were also evaluated in the PC-3 cell line. The internalization and efflux kinetics of [^{123}I]-CABN were similar to those of ^{99m}Tc-HABN (*12*). A rapid internalization was observed in 5 min after incubation..

Despite the excellent *in vivo* stability of the iodine-carbon bond has been proven (*24*), the *in vivo* stability of the entire tracer is still an issue. The *in vitro* stability results of [^{123}I]-CABN in human serum solution indicate that the radiotracer was sensitive towards degradation by serum enzymes. The results of *in vivo* stability experiments in blood showed comparable results to the *in vitro* stability data. The [^{123}I]-CABN was not able to maintain its initial structure in athymic mouse blood at 10 min after injection. Furthermore, the HPLC analysis of blood samples indicated that the major radioactive metabolites (Rt=17 and 19 min) were not in the form of [^{123}I]$^{-}$ (Rt=5 min). The metabolism will likely occur at the amide bond between the cubyl moiety and the ε-aminocaproic acid, since ^{99m}Tc-HABN and [^{123}I]-CABN share the same Aca-BN motif and ^{99m}Tc-HABN showed good *in vitro* stability in human serum solution. To prevent the hydrolysis of the amide bond by proteolytic enzymes in blood, introduction of the concept of click chemistry in tracer development would be a good choice to provide stable covalent links between the [^{123}I]-cubyl moiety and biomolecules. The triazole group formed in the click reaction resembles an amide bond regarding physiological behaviour.

Low radioactivity residence in blood and extremely high radioactivity accumulation in liver, small intestine and kidney at 1 hour after tracer injection indicate that the [^{123}I]-CABN and its metabolites were cleared rapidly from blood and predominately through the hepatobiliary route and partly via the renal route. [^{123}I]-CABN showed low accumulation in both tumor and pancreas, which are GRPR expressing tissues. In the blocking study, uptake of [^{123}I]-CABN in pancreas and tumor did not show significant difference compared to the control group which indicates the poor specificity of the tracer to GRPR. From the SPECT images of [^{123}I]-CABN acquired in 1 hour dynamic scans it was concluded that the human prostate cancer xenograft was not visible mainly due to the poor *in vivo* stability and low tumor accumulation mentioned above. No radioactivity accumulation was detected in thyroid from SPECT imaging proving the good stability of iodine-carbon bond *in vivo*. Although [^{123}I]-CABN is not suitable for prostate cancer imaging, the [^{123}I]-cubyl structure showed to be a stable radioiodine labeling synthon which can be widely applied in radiopharmaceutical development.

6.5 Conclusion

We synthesised a [^{123}I]-labelled bombesin tracer and evaluated *in vitro* and in prostate cancer bearing nude mice. Despite the fact that [^{123}I]-CABN showed its GRPR targeting ability in the prostate cancer cell line, it is not a suitable tracer for prostate cancer SPECT imaging due to the low *in vivo* stability.

Although [^{123}I]-CABN is unsuitable for prostate cancer imaging, the [^{123}I]-cubyl structure showed to be a stable radioiodine labeling synthon which can be widely applied in radiopharmaceutical development.

Acknowledgements

This work was made possible by a financial contribution from CTMM, project PCMM,

project number 03O-203 and STW project number 07048. We thank D.F. Samplonius for technical assistance on cell culturing, J. W. A. Sijbesma for assisting animal experiments. All animal experiments were approved by the local animal welfare committee in accordance with the Dutch legislation and carried out in accordance with their guidelines.

References:

(1) Erspamer, V., Erpamer, G. F., and Inselvini, M. (1970) Some pharmacological actions of alytesin and bombesin. *J Pharm Pharmacol 22*, 875-6.

(2) Battey, J., Wada, E., Corjay, M., Way, J., Fathi, Z., Shapira, H., Harkins, R., Wu, J., Slattery, T., Mann, E., and et al. (1992) Molecular genetic analysis of two distinct receptors for mammalian bombesin-like peptides. *J Natl Cancer Inst Monogr*, 141-4.

(3) Garcia, L. J., Pradhan, T. K., Weber, H. C., Moody, T. W., and Jensen, R. T. (1997) The gastrin-releasing peptide receptor is differentially coupled to adenylate cyclase and phospholipase C in different tissues. *Biochim Biophys Acta 1356*, 343-54.

(4) Hildebrandt, J. D. (1997) Role of subunit diversity in signaling by heterotrimeric G proteins. *Biochem Pharmacol 54*, 325-39.

(5) Ohki-Hamazaki, H., Iwabuchi, M., and Maekawa, F. (2005) Development and function of bombesin-like peptides and their receptors. *Int J Dev Biol 49*, 293-300.

(6) Bartholdi, M. F., Wu, J. M., Pu, H., Troncoso, P., Eden, P. A., and Feldman, R. I. (1998) In situ hybridization for gastrin-releasing peptide receptor (GRP receptor) expression in prostatic carcinoma. *Int J Cancer 79*, 82-90.

(7) Carroll, R. E., Matkowskyj, K. A., Chakrabarti, S., McDonald, T. J., and Benya, R. V. (1999) Aberrant expression of gastrin-releasing peptide and its receptor by well-differentiated colon cancers in humans. *Am J Physiol 276*, G655-65.

(8) Gugger, M., and Reubi, J. C. (1999) Gastrin-releasing peptide receptors in non-neoplastic and neoplastic human breast. *Am J Pathol 155*, 2067-76.

(9) Ananias, H. J., van den Heuvel, M. C., Helfrich, W., and de Jong, I. J. (2009) Expression of the gastrin-releasing peptide receptor, the prostate stem cell antigen and the prostate-specific membrane antigen in lymph node and bone metastases of prostate cancer. *Prostate 69*, 1101-8.

(10) Jemal, A., Siegel, R., Ward, E., Hao, Y., Xu, J., Murray, T., and Thun, M. J. (2008) Cancer statistics, 2008. *CA Cancer J Clin 58*, 71-96.

(11) Shi, J., Jia, B., Liu, Z., Yang, Z., Yu, Z., Chen, K., Chen, X., Liu, S., and Wang, F. (2008) ^{99m}Tc-labelled bombesin(7-14)NH_2 with favorable properties for SPECT imaging of colon cancer. *Bioconjug Chem 19*, 1170-8.

(12) Ananias, H. J. K., Yu, Z., Dierckx, R. A., van der Wiele, C., Helfrich, W., Wang, F., Yan, Y., Chen, X., de Jong, I. J., and Elsinga, P. H. (2011) ^{99m}Technetium-HYNIC(tricine/TPPTS)-Aca-Bombesin(7–14) as a Targeted Imaging Agent with MicroSPECT in a PC-3 Prostate Cancer Xenograft Model. *Molecular Pharmaceutics 8*, 1165-1173.

(13) Lantry, L. E., Cappelletti, E., Maddalena, M. E., Fox, J. S., Feng, W., Chen, J., Thomas, R., Eaton, S. M., Bogdan, N. J., Arunachalam, T., Reubi, J. C., Raju, N., Metcalfe, E. C., Lattuada, L., Linder, K. E., Swenson, R. E., Tweedle, M. F., and Nunn, A. D. (2006) ^{177}Lu-AMBA: Synthesis and characterization of a

selective ^{177}Lu-labelled GRP-R agonist for systemic radiotherapy of prostate cancer. *J Nucl Med 47*, 1144-52.

(14) Cagnolini, A., Chen, J., Ramos, K., Skedzielewski, T. M., Lantry, L. E., Nunn, A. D., Swenson, R. E., and Linder, K. E. (2010) Automated synthesis, characterization and biological evaluation of ^{68}Ga-AMBA, and the synthesis and characterization of ^{nat}Ga-AMBA and ^{67}Ga-AMBA. *Appl Radiat Isot 68*, 2285-92.

(15) Abd-Elgaliel, W. R., Gallazzi, F., Garrison, J. C., Rold, T. L., Sieckman, G. L., Figueroa, S. D., Hoffman, T. J., and Lever, S. Z. (2008) Design, synthesis, and biological evaluation of an antagonist-bombesin analogue as targeting vector. *Bioconjug Chem 19*, 2040-8.

(16) Hoffman, T. J., and Smith, C. J. (2009) True radiotracers: Cu-64 targeting vectors based upon bombesin peptide. *Nucl Med Biol 36*, 579-85.

(17) Liu, Z., Yan, Y., Liu, S., Wang, F., and Chen, X. (2009) ^{18}F, ^{64}Cu, and ^{68}Ga labelled RGD-bombesin heterodimeric peptides for PET imaging of breast cancer. *Bioconjug Chem 20*, 1016-25.

(18) Liu, Z., Li, Z. B., Cao, Q., Liu, S., Wang, F., and Chen, X. (2009) Small-animal PET of tumors with ^{64}Cu-labelled RGD-bombesin heterodimer. *J Nucl Med 50*, 1168-77.

(19) Liu, Z., Yan, Y., Chin, F. T., Wang, F., and Chen, X. (2009) Dual integrin and gastrin-releasing peptide receptor targeted tumor imaging using ^{18}F-labelled PEGylated RGD-bombesin heterodimer ^{18}F-FB-PEG$_3$-Glu-RGD-BBN. *J Med Chem 52*, 425-32.

(20) Zhang, X., Cai, W., Cao, F., Schreibmann, E., Wu, Y., Wu, J. C., Xing, L., and Chen, X. (2006) ^{18}F-labelled bombesin analogs for targeting GRP receptor-expressing prostate cancer. *J Nucl Med 47*, 492-501.

(21) Ananias, H. J., de Jong, I. J., Dierckx, R. A., van de Wiele, C., Helfrich, W., and Elsinga, P. H. (2008) Nuclear imaging of prostate cancer with gastrin-releasing-peptide-receptor targeted radiopharmaceuticals. *Curr Pharm Des 14*, 3033-47.

(22) Brake, A. H., Moet, F. P., van der Zwart, R. E., Eersels, J. L., and Herscheid, J. D. (2002) Adsorption of radioiodine on platinum: a fast and simple column method to obtain concentrated and pure radioiodide in either water or anhydrous solvents. *Appl Radiat Isot 57*, 475-82.

(23) Weiner, R. E., and Thakur, M. L. (2005) Radiolabelled peptides in oncology: role in diagnosis and treatment. *BioDrugs 19*, 145-63.

(24) Al Hussainy, R., Verbeek, J., van der Born, D., Braker, A. H., Leysen, J. e. E., Knol, R. J., Booij, J., and Herscheid, J. D. M. (2011) Design, Synthesis, Radiolabelling, and in Vitro and in Vivo Evaluation of Bridgehead Iodinated Analogues ofN-{2-[4-(2-Methoxyphenyl)piperazin-1-yl]ethyl}-N-(pyridin-2-yl) cyclohexanecarboxamide (WAY-100635) as Potential SPECT Ligands for the 5-HT1AReceptor. *Journal of Medicinal Chemistry 54*, 3480-3491.

Chapter 7

Synthesis and evaluation of ^{18}F labelled stabilized bombesin analogues for GRPR imaging

Zilin Yu, Anneke Kuipers, Hildo J. K. Ananias, Giuseppe Carlucci, Hilde D. Hoving, Rick Rink, Rudi A. J. O. Dierckx, Wijnand Helfrich, Fan Wang, Gert N. Moll, Igle J. de Jong, Philip H. Elsinga

Abstract

To enhance the resistance against proteolytic enzymes and to improve the gastrin releasing peptide receptor (GRPR) targeting ability of radiolabelled bombesin, we developed a series of lanthionine-stabilized full-length bombesin analogues. The best two candidates with the highest *in vitro* affinity were labelled with ^{18}F for positron emission tomography (PET) imaging of GRPR-expressing prostate cancer. The binding affinity, lipophilicity, stability and *in vivo* behaviour of two ^{18}F-labelled bombesins varied due to the position of intra-molecular cross-linkages and the N-terminal amino acid 1-6 sequence at the N terminal. Both tracers showed GRPR targeting potential in a PC-3 tumor bearing mouse model. The tumor uptake of ^{18}F-4-Fluorobenzoyl-Bombesin C5 (^{18}F-C5) and ^{18}F-4-Fluorobenzoyl-Bombesin C6 (^{18}F-C6) were 0.7 ± 0.1 and 3.5 ± 0.9 %ID/g at 1 h post injection. For ^{18}F-C5 and ^{18}F-C6, PC-3 tumors were clearly visualized on microPET images with best contrast at 3 h post injection.

Keywords: stabilized bombesin peptide, GRPR, prostate cancer, PC-3, N-succinimidyl 4-[^{18}F]asfluorobenzoate (^{18}F-SFB), PET

7.1 Introduction

Bombesin is a 14-amino acid peptide binding with high affinity to the receptor pockets of the GRPR with its [7-14] amino acids motif at the C-terminal (*1-2*). The GRPR is over-expressed in a variety of human malignancies including primary and metastasized prostate cancer while being absent or sparse present in normal or hyperplastic prostate (*3-7*). Hence, radiolabelled bombesin analogues combined with high resolution PET or single photon emission computed tomography (SPECT), exhibit potential as a diagnostic and immunotherapeutic tool in prostate cancer imaging.

Compared to truncated Bombesin(7-14), full-length bombesin has a larger size and shows relatively slower pharmacokinetics. However, full-length bombesin offers more modification and / or labeling possibilities within the first N-terminal 6 amino acids by substituting amino acids and / or attaching bifunctional groups. Lys^3-Bombesin is one of the best studied full-length bombesins (*8*). Its third amino acid at the N-terminus is replaced by a lysine. Bombesin has been labelled with ^{99m}Tc, ^{111}In, ^{64}Cu, and ^{18}F by coupling with bifunctional reagents to the amino acid side-chain of lysine (*9-14*). Although most of the radiolabelled Lys^3-Bombesin analogues show high binding affinity to GRPR *in vitro*, the stability of the peptide, the tumor uptake and *in vivo* the kinetics of radiolabelled Lys^3-Bombesin still needs to be improved.

To overcome the rapid degradation of full-length bombesin analogues, internal thioether cross-links were introduced within either the N-terminal 6 amino acids (C5, C6 and C7, table 1) or within the C-terminal amino acids [7-14] of the peptide (G and H, table 1). In this study, two of the five stabilized full-length bombesin analogues were selected according to the binding affinity to GRPR and labelled with ^{18}F. The properties of the two selected lanthionine-stabilized peptides were assessed *in vitro* and *in vivo*. The GRPR targeting ability and imaging potential of ^{18}F-labelled stabilized bombesin analogues were investigated in mice xenografted with human prostate cancer cells.

7.2 Experimental section

7.2.1 Materials

All chemicals were obtained from commercial suppliers Sigma-Aldrich, Fluka, and Merck and used without further purification. Solid phase extraction cartridges were obtained from Waters Chromatography Division, Millipore Corporation, USA.

Reversed phase high-performance liquid chromatography (RP-HPLC) was performed on a *HITACHI L-2130* HPLC system (Hitachi High Technologies America Inc., Pleasanton, CA, USA) equipped with a Bicron Frisk-Tech area monitor. Isolation and quality control of purified radiolabelled peptides were performed using a reversed phase Grace Smart RP-C18 column (Lokeren, Belgium) (4.6 mm × 250 mm, 5 μm). The flow was set at 1 mL/min using a gradient system starting from 90% solvent A (0.01 M phosphate buffer, pH = 6.0) and 10% solvent B (acetonitrile) (5 min), followed by a gradient mobile phase going from 40 % solvent A and 60 % solvent B at 15 min to 10 % solvent A and 90 % solvent B at 22.5 min.

7.2.2 Synthesis of stabilized Bombesin analogues

Peptides stabilized by a methyllanthionine in the C-terminal half were produced stereospecifically by *Lactococcus lactis* containing lanthionine introducing enzymes (*15-16*) followed by pGlu formation and amidation as performed previously (*17*). Since the N-terminal half of bombesin is too hydrophilic, no success was obtained with the stereospecific introduction of thioether bridges in this region. Therefore, lanthionines in the N-terminal half were introduced by base-assisted sulfur extrusion (*15*). In brief: the linear peptides bombesin-5 and bombesin-6 with respectively the sequences: pEQKdCGNCWAVGHLM-NH_2 and pEdCKLGCQWAVGHLM-NH_2 (pE stands for pyroglutamate and dC stands for D-cysteine) were obtained from JPT Peptide Technologies (Berlin, Germany). For introduction of the lanthionine bridge, both bombesin variants were dissolved in water to a concentration of 2 mg/mL. Ammonia was added till an final concentration of 0.3 % and mixtures were incubated at 37 ^{o}C overnight. The ammonia was removed and the peptide was dried by using a speedvac concentrator (Thermo Fisher Scientific Inc., Logan, UT, USA). Reaction mixtures were purified by HPLC. The final products, mixtures of lanthionine-stabilized bombesin analogues, were characterized by mass spectrometry (Table 1). Formation of a lanthionine by desulphurization of a disulfide-bridged peptide causes a loss in mass of 34 Dalton. Mass spectra were recorded with a Voyager DE Pro Maldi-TOF mass spectrometer.

7.2.3 Cell culture

The GRPR-positive human prostate cancer cell line PC-3 (ATCC, Manassas, VA, USA) was cultured in RPMI 1640 (Lonza, Verviers, France) supplemented with 10% fetal calf serum (Thermo Fisher Scientific Inc., Logan, UT, USA) at 37 ^{o}C in a humidified 5% CO_2 atmosphere.

7.2.4 *In vitro* competitive binding assay

In vitro competitive binding assay was performed by replacing the binding of GRPR specific targeting tracer ^{125}I-Tyr^{4}-Bombesin to the PC-3 tumor cells with C5, C6, ^{19}F-C5, ^{19}F-C6, C7, G and H as reported previously (*18*). The 50% inhibitory concentration (IC_{50}) value were calculated by fitting the data with nonlinear regression using GraphPad Prism 5.0 (GraphPad Software, San Diego, CA, USA) and expressed as an average plus the standard deviation. Experiments were performed with triplicate samples.

7.2.5 Synthesis of ^{19}F-C5 and ^{19}F-C6

The lanthionine-stabilized bombesin peptides C5 or C6 (1 mg) was dissolved with 0.1 mL 50% acetonitrile and added to a glass vial. Five equivalents of ^{19}F-Succimidyl-fluorobenzoic acid (SFB) (1 mg/mL, in acetonitrile) were slowly added to C5 or C6 and well mixed. The mixture was kept at room temperature for 2 hours and purified with HPLC. The acetonitrile in the final product was removed by

using Waters Sep-Pak Light C18 cartridge (55-105µm). The ^{19}F-C5 and ^{19}F-C6 were eluted with ethanol and dried. The molecular weights of ^{19}F-C5 and ^{19}F-C6 were measured by mass spectrometry. For ^{19}F-C5, $C_{75}H_{102}FN_{21}O_{18}S_2$ calculated molecular weight 1644.85, observed 1646.1 ($[M+H]^+$). For ^{19}F-C6, $C_{75}H_{107}FN_{20}O_{17}S_2$ calculated 1643.90, observed 1645.49 ($[M+H]^+$).

7.2.6 Synthesis of ^{18}F-SFB

^{18}F-SFB was prepared according the methods described previously by Wester *et al.*(*19*). Aqueous ^{18}F-fluoride was produced by irradiation of ^{18}O-water with a Scanditronix MC-17 cyclotron via the ^{18}O(p,n)^{18}F nuclear reaction. The ^{18}F-fluoride solution was passed through a SepPak Light Accell plus QMA anion exchange cartridge (Waters, USA) to recover the ^{18}O-enriched water.

^{18}F-fluoride was eluted from the QMA anion exchange cartridge with 1 mL of K_2CO_3 (1 mg/mL) and collected in a vial with 5 mg Kryptofix222. To this solution, 1 mL acetonitrile was added and the solvents were evaporated at 130 ^{o}C. The radioactive residue, (^{18}F-KF/Kryptofix complex) was carefully dried 3 times by addition and evaporation of anhydrous acetonitrile (0.5 mL at 130 °C). After addition of 10 mg of ethyl 4-[trimethylammonium]benzoate in DMF (0.250 mL), the mixture was heated at 90 °C for 12 min. Then, 1 M of HCl (0.5 mL) was added. The reaction mixture was heated at 100 °C for 5 min. After cooling the reaction mixture was passed through a Waters Sep-Pak Light C18 cartridge for solid phase extraction. After washing the cartridge with water, purified ^{18}F-fluorobenzoic acid was eluted from the cartridge with 2 mL of acetonitrile into a vial containing 10 mg of Kryptofix222 and 5 mg of K_2CO_3.

The eluate was dried under an argon stream at 130 °C. Complete drying was ensured by addition and evaporation of anhydrous acetonitrile (3-fold, 0.5 mL).

Then, the solution of O-(N-succinimidyl)-1,1,3,3-tetramethyluronium tetrafluoroborate (TSTU, 20 mg) in anhydrous acetonitrile (0.5 mL) was added, and the mixture was heated at 90 °C for 5 min. The mixture was cooled down and diluted with 0.03 M of HCl.

^{18}F-SFB was diluted with 15 mL of water before being passed through Oasis Cartridge HLB (30 mg, 1 mL) for solid phase extraction. The cartridge was washed with 5 mL of water and eluted with ethanol (0.5mL) to obtain the final pure ^{18}F-SFB solution. The purified ^{18}F-SFB was analyzed by HPLC.

To reduce the radiation burden to the operator, the labeling procedure has been fully automated using a Zymark robotic system.

7.2.7 Coupling ^{18}F-SFB with C5 or C6

^{18}F-C5 and ^{18}F-C6 were synthesized by coupling ^{18}F-SFB (300 MBq, in 0.1 mL acetonitrile) with stabilized peptide C5 and C6 (10 mg/mL, in 0.1 mL 50% acetonitrile) in 0.3 mL phosphate buffer (0.1 M, pH 8.3-8.6) at 50 ^{o}C for 30 minutes. The radiolabelled peptides were isolated and analyzed by using HPLC. Retention time of ^{18}F-SFB, ^{18}F-C5 and ^{18}F-C6 was 20.1, 18.4 and 19.6 min, respectively. To eliminate the acetonitrile, purified ^{18}F-C5 and ^{18}F-C6 were diluted with 10 mL of water and loaded on a Waters Sep-Pak Light C18 cartridge. Final products were eluted with 0.4 mL ethanol and diluted with saline solution for cell experiments and animal experiments.

7.2.8 Partition Coefficient

^{18}F-C5 or ^{18}F-C6 (37 kBq) was dissolved in a mixture of 0.5 mL *n*-octanol and 0.5 mL 25 mM PBS (pH 7.4) and well mixed for 5 min at room temperature. Afterwards, the mixture was centrifuged at 3000 rpm for 5 minutes. 100 μL samples were obtained from *n*-octanol and aqueous layers and counted in a *γ*-counter (Compugamma CS1282, LKB-Wallac, Turku, Finland). The *log D* value is reported as an average of three different measurements (mean ± SD).

7.2.9 *In Vitro* Stability

The *in vitro* stability of ^{18}F-C5 and ^{18}F-C6 in saline solution and human serum solution was evaluated following the protocol as reported previously (*18*). In brief, ^{18}F labelled C5 or C6 was incubated in saline solution (at room temperature) and human serum solution (at 37 ^{o}C), samples were collected after 1, 2, 3 or 4 h incubation. For solution stability in saline, samples were analyzed by HPLC. For stability in human serum solution, 250 μL of the sample was precipitated with 750 μL of ethanol/acetonitrile solution ($V_{ethanol}$: $V_{acetonitrile}$=1: 1), the supernatants of the mixture after centrifugation were filtered by 0.22 μm filter and analyzed by HPLC.

7.2.10 *In Vitro* Cell Uptake and Internalization Kinetics

One day prior to the assay, PC-3 cells at confluence were placed in 6-well plates (0.5 $\times 10^6$ cells/well). The cells were washed with PBS and incubated with ^{18}F-C5 or ^{18}F-C6 (0.04 MBq/well) at 37 °C for 0, 15, 30, 45, 60, 90, 120 and 240 minutes in triplicate to allow for cellular uptake. 20 μg of unlabelled bombesin was co-incubated with radiolabelled C5 or C6 in a blocking group. To remove unbound radioactivity, the cells were washed twice afterwards with ice-cold PBS. The cells were incubated with 1 mL of an acid glycine buffer (50 mM glycine−HCl/100 mM NaCl, pH 2.8) for 3 minutes twice and washed with ice-cold PBS. The glycine acid solutions and PBS solution were collected, and the radioactivity was measured in gamma counter as membrane receptor bound radioactivity. The cells were lysed by incubating with 1 M NaOH at 37 °C and the resulting lysate in each well was aspirated to determine the internalized radioactivity in a gamma counter. Total cellular uptake of ^{18}F-C5 or ^{18}F-C6 was calculated as the sum of the internalized and membrane receptor bound radioactivity and expressed as mean ± SD (n = 3).

7.2.11 Efflux Kinetics

About 24 h before the experiments, 1 million PC-3 cells were placed in 6 well plates and kept in a 37 °C incubator. The cells were washed with PBS and then incubated with ^{18}F-C5 or ^{18}F-C6 (0.04 MBq/well) for 1 h at 37 °C to allow for maximal internalization.

To remove unbound radioactivity, the cells were washed twice afterwards with ice-cold PBS and were then incubated in the prewarmed culture medium at 37 °C for 0, 15, 30, 45, 60, 90, 120, and 240 min in triplicate to allow for externalization. To remove cell-surface bound radiotracer, the cells were washed twice for 3 min with an acid glycine buffer (50 mM glycine−HCl/100 mM NaCl, pH 2.8). Then, the cells were lysed by incubation with 1 M NaOH at 37 °C, and the resulting lysate in each well was aspirated to determine the remaining radioactivity in a gamma counter. Results are expressed as the percentage of maximum intracellular radioactivity (remaining activity at specific time-point / activity at time-point 0) (mean±SD).

7.2.12 Animal Model

The xenograft tumor model for human prostate cancer in athymic mice was generated by subcutaneous injection of 1×10^6 PC-3 cells (suspended in 0.1 mL of sterile saline) in the flank of male athymic mice (Harlan, Zeist, The Netherlands). During the injection, animals were anesthetized with gas (3.5 % isoflurane in an air/oxygen mixture). The mice were used for biodistribution experiments and microPET/CT imaging when the tumor volume reached a mean diameter of 0.8 - 1.0 cm (3 - 4 weeks after inoculation). All animal experiments were performed in accordance with the regulations of Dutch law on animal welfare and the institutional ethics committee for animal procedures approved the protocol.

7.2.13 MicroPET/CT imaging and Biodistribution

The PC-3 prostate cancer bearing athymic mice were used for animal experiments when the tumor volume reached 250-300 mm^3 (4-5 weeks after inoculation).

MicroPET scans were performed by using a Focus 200 rodent scanner (CTI Siemens, Munich, Germany). PC-3 tumor bearing athymic nude mice were injected in the penis vein with ~ 8 MBq of ^{18}F-C5 or ^{18}F-C6 and imaged for 1h at 0, 2 and 3 h post injection. All mice were sacrificed before the acquisition of the 2 and 3 h images. MicroCT scans were performed after each microPET scans. For the receptor-blocking imaging studies, 300 μg of unlabelled ε-aminocaproic acid-bombesin(7-14)(Aca-BN(7-14)) was pre-injected 30 min before the tracer injection. Animals of the blocking group were scanned at 2 h after tracer injection as described above. PET/CT image confusion was accomplished with Inveon Research Workplace Software (Siemens Inveon Software, Erlangen, Germany).

Biodistribution studies of ^{18}F-C5 and ^{18}F-C6 were also performed in PC-3 tumor bearing athymic nude mice. Approximately 600 kBq of ^{18}F-C5 or 120 kBq of ^{18}F-C6 was administered by penis vein injection. The injection dose of ^{18}F-C5 was set 5-fold as high as that of ^{18}F-C5 according to the specific activity of both tracers. Animals were sacrificed at 1 h post injection. Blood, tumor, heart, liver, spleen, lung, kidney, stomach, bone, muscle and intestine samples were collected, weighed and measured by using a γ-counter. The percentage of injected dose per gram (%ID/g) was determined for each sample. For each mouse, radioactivity of the tissue samples was calibrated against a known aliquot of radiotracer. To investigate the specificity of ^{18}F-C5 and ^{18}F-C6, a receptor-blocking study was performed with 300 μg of unlabelled Aca-BN(7-14) pre-injected 30 min before tracer injection. Biodistribution of the blocking group was determined as well and reported as mean± SD (n=4).

7.2.14 Statistical Analysis

Quantitative data are expressed as mean ± SD. Means were compared using the Student t test. *P* values <0.05 were considered significant.

7.3 Results

7.3.1 Synthesis of Stabilized Bombesin Analogues, ^{19}F-SFB conjugated reference compound and *In Vitro* Competitive Receptor Binding Assay

The lanthionine-stabilized peptides C5, C6, C7, G and H (Table 1) were synthesized as described in the materials and methods and confirmed by HPLC and mass spectrometry (Table 1). The binding affinity of bombesin analogues to the GRPR was measured by replacing the binding of the well-known GRPR-specific ligand ^{125}I-Tyr^4-Bombesin to PC-3 prostate cancer cells. The IC_{50} values of stabilized bombesin analogues are presented in Table 2. The binding affinities of C5, C6 and C7 to GRPR were in the nanomolar range. For G and H, which contain the internal crosslink in the amino acid 7-14 region half of the peptide, the IC_{50} values of them were higher than 10000 nM. Based on the binding affinity of stabilized bombesin analogues, C5 and C6 were selected for developing their ^{18}F labelled PET derivatives. Reference compounds were synthesized by coupling bombesin C5, C6 and ^{19}F-SFB under basic conditions. The final products were confirmed by mass spectrometry, the conversions were higher than 95%. The binding affinity of ^{19}F-C5 and ^{19}F-C6 was determined by competitive receptor binding assay as well. When coupled to ^{19}F-SFB, the IC_{50} value of C5 and C6 increased from 248±6 and 26±1 nM to 1299±249 and 35±14 nM, respectively (table 3). Coupling of the fluorobenzoyl group had a minor effect on the binding affinity for both bombesin analogues.

Table 1. (Methyl) lanthionine–stabilized bombesin analogs.

Variant	Sequence	Mono-siotopic mass		Reference
		Observed ($M+H^+$)	*Calculated*	
G	*pEQKLGNQW[Abu$_c$VGA]$_c$LM-NH$_2$	1569.9	*1568.8*	(*110*)
H	pEQKLGNQWA[Abu$_c$GHA]$_c$M-NH$_2$	1565.7	*1564.7*	(*110*)
C5	pEQK[A$_c$GNA]$_c$WAVGHLM-NH$_2$	1522.7	*1521.7*	(*114*)
C6	pE[A$_c$KLGA]$_c$QWAVGHLM-NH$_2$	1521.7	*1520.7*	(*114*)
C7	pE[A$_c$KLGNA]$_c$WAVGHLM-NH$_2$	1507.7	*1506.7*	(*114*)

* pE is pyroglutamate; Abu is aminobutyric acid.

Table 2. IC_{50} values of stabilized Bombesin analogues, mean±SD (n=3).

	Crosslink within N-terminal amino acids 1-6			Crosslink in the C-terminal half	
Stabilized Bombesin analogues	C5	C6	C7	G	H
IC_{50} (nM)	248±6	26±1	719 ±12	>10000	>10000

Table 3. IC_{50} values of ^{19}F-C5 and ^{19}F-C6, mean±SD (n=3).

Bombesin analogues	^{19}F-C5	^{19}F-C6
IC_{50} (nM)	1299±249	35±14

7.3.2 Radiochemistry, Partition Coefficient and In Vitro Stability

Radiolabelled ^{18}F-SFB was synthesized in three steps based on the procedure described by Wester *et al.*(*19*). The synthesis of ^{18}F-SFB was optimized by our group. First, 4-^{18}F-fluorobenzoic acid was purified by using a C18 cartridge and eluted in a vial with 5 mg of potassium carbonate and 15 mg of Kryptofix 222 and secondly dried afterwards to avoid the deleterious effect of moisture during conversion of 4-^{18}F-fluorobenzoic acid into the corresponding activated ester. The automated system produced ^{18}F-SFB in 90-100 min with a good radiochemical yield (34–38%). The radiochemical purity after SPE ranged from 93% to 96%, as determined by HPLC.

^{18}F-C5 and ^{18}F-C6 were synthesized by coupling ^{18}F-SFB with C5 and C6 under slightly basic conditions (pH 8.3-8.6) at 50 ^{o}C for 30 min. The radiochemical yield of ^{18}F-C5 and ^{18}F-C6 was ~10 % and ~30% from ^{18}F-SFB. Radiochemical purity of both tracers was high (>95 %) after HPLC purification. Since the labelled ^{18}F-C5 and ^{18}F-C6 have similar retention times as their unlabelled peptide precursor, the HPLC separation of peptide precursor from the final product was not complete. The apparent specific activity of ^{18}F-C5 and ^{18}F-C6 was estimated to be 1437±329 and 218±135 MBq/μmol respectively, based on the HPLC analysis of purified product. The overall synthesis time for ^{18}F-C5 and ^{18}F-C6 was approximately 160 min.

The partition coefficient of ^{18}F-C5 and ^{18}F-C6 was determined in a 1: 1 mixture solution of *n*-octanol and PBS solution. Log D value of ^{18}F-C5 and ^{18}F-C6 was -0.5± 0.1 and 0.8± 0.1, respectively.

In vitro stability of ^{18}F-C5 and ^{18}F-C6 was evaluated in saline and human serum solution (Figure 1). Results were expressed as percentage of initial ^{18}F-labelled C5 and C6 at different time points. For both tracers, more than 90 % of the radioactivity remained in its initial form after 4 h incubation in saline. In human serum, 86% of ^{18}F dissociated from C6 at 1 h incubation, while after 3 h the dissociated ^{18}F from ^{18}F-C5 was less than 5 %.

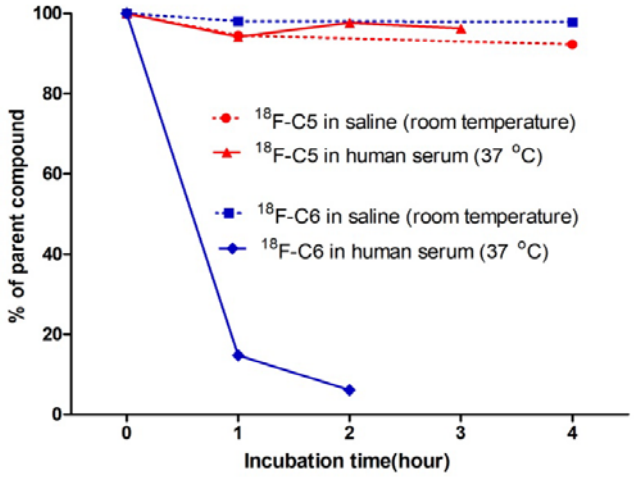

Figure 1. *In vitro* stability of ^{18}F-C5 and ^{18}F-C6 in saline and human serum solution. The radiochemical purity of ^{18}F-C5 and ^{18}F-C6 in the solutions was analyzed by HPLC.

7.3.3 Cell Uptake, Internalization and Efflux Kinetics.

The cellular uptake and internalization kinetics of ^{18}F-C5 and ^{18}F-C6 were evaluated in a PC-3 prostate cancer cell line at 37 ^{o}C up to 3 h. After removing the unbound tracer, radioactivity which accumulated on membrane was released by incubating with ice cold glycine-acid solution and collected. PC-3 cells were harvested and the radioactivity counted was a measure of the internalization of the tracer. Results are shown in Figure 2. For ^{18}F-C6, the internalization occurred within 15 min after start of incubation with a steady increase and reached the internalization plateau after 2 h incubation. The total cellular uptake of ^{18}F-C6 followed the same trend as the internalization with 6.7±0.3 % of initial applied radioactivity at 2 h.

Internalization of ^{18}F-C5 was observed within 15 min after incubation and reached the highest value at 15 min. The highest cellular uptake of ^{18}F-C5 was about 5 times lower than that of ^{18}F-C6. Co-incubated with an excess of unlabelled bombesin, the cellular uptake ratio of both tracers dropped to < 0.1 % at all experimental time points (not shown in figure 2), indicating high specificity of ^{18}F-C5 and ^{18}F-C6.

The efflux kinetics of ^{18}F-C5 and ^{18}F-C6 were also compared in the PC-3 prostate cancer cell line (Figure 3). Both tracers showed similar efflux characteristics. For ^{18}F-C5 and ^{18}F-C6, 36±5 % and 33±2 % of internalized radioactivity remained in PC-3 cells after 3 h incubation. The $t_{1/2}$ of ^{18}F-C5 and ^{18}F-C6 was 40 and 92 min, respectively.

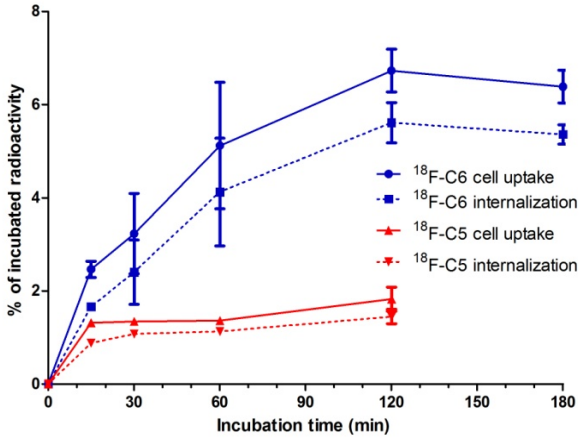

Figure 2. Cellular uptake of ^{18}F-C5 and ^{18}F-C6 in the PC-3 prostate cancer cell line.

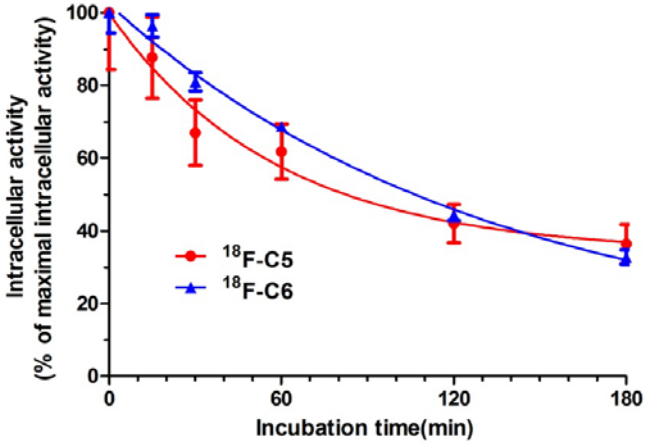

Figure 3. Efflux kinetics of ^{18}F-C5 and ^{18}F-C6 in the PC-3 prostate cancer cell line.

7.3.4 Biodistribution Experiments.

Biodistribution of ^{18}F-C5 and ^{18}F-C6 at 1 h post injection was determined in PC-3 prostate tumor-bearing athymic nude mice and specificity of both tracers was also evaluated by co-injecting excess of unlabelled bombesin peptide. Uptake of ^{18}F-C5 and ^{18}F-C6 in relevant organs is shown in Figure 4. The tumor uptake of ^{18}F-C5 and ^{18}F-C6 at 1 h was 0.7 ± 0.1 and 3.5±0.9 %ID/g, respectively. Low recovery of radiolabelled peptide from the blood might indicate rapid clearance of ^{18}F-C5 and ^{18}F-C6.

In a blocking study, where the radiolabelled analogs were co-injected with excess of unlabelled bombesin, tumor uptake of ^{18}F-C6 decreased from 3.5±0.9 %ID/g to 2.1 ±0.6 %ID/g. For ^{18}F-C5, the tumor uptake was slightly reduced from 0.7± 0.1 %ID/g to 0.6± 0.1 %ID/g by excess of blocking agent. No effect of blocking agent was found in

the presence of ^{18}F-C5 and ^{18}F-C6 in non-GRPR expressing organs, such as kidney, liver and heart.

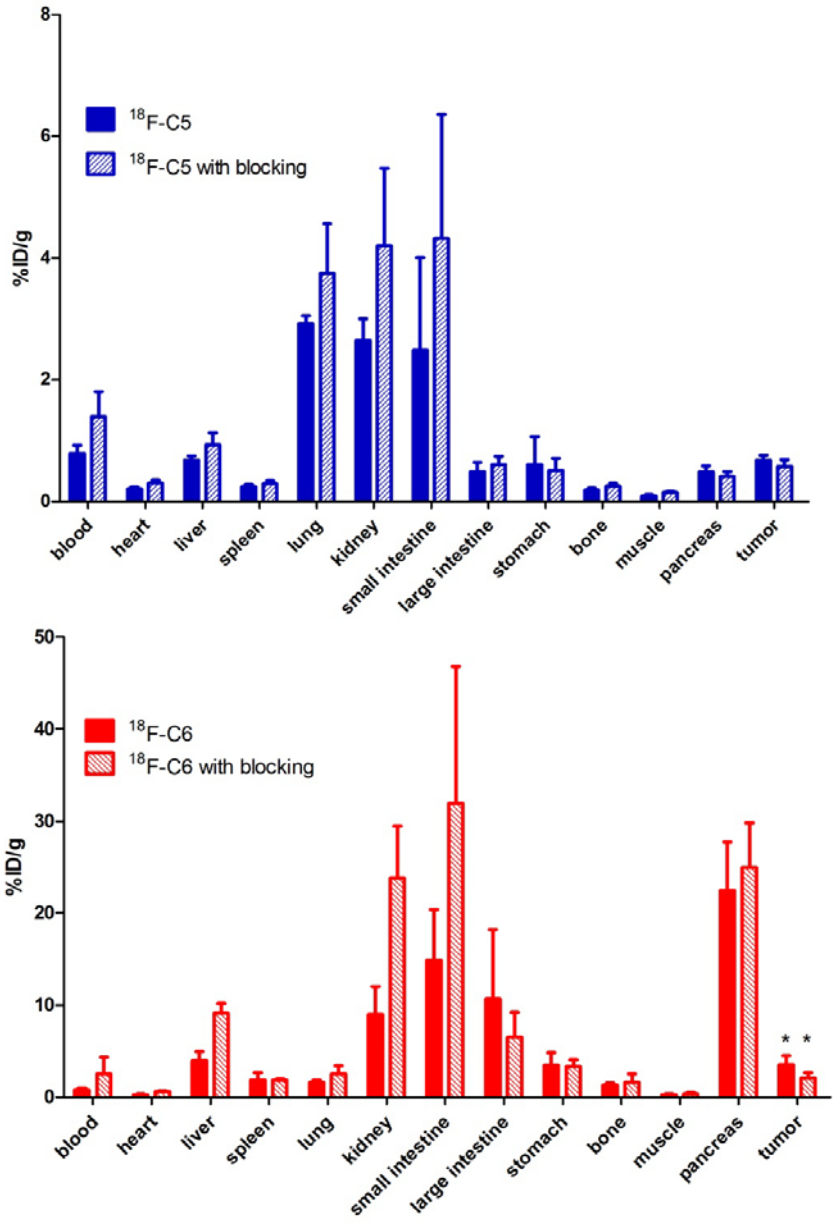

Figure 4. Biodistribution of ^{18}F-C5 and ^{18}F-C6 in PC-3 prostate tumor-bearing athymic nude mice at 1 h post injection. "*" = Significant difference.

7.3.5 MicroPET/CT imaging.

The microPET and CT coronal images of ^{18}F-C5 and ^{18}F-C6 in prostate tumor bearing athymic nude mice are shown in Figure 5 and Figure 6. High abdominal background was observed for both tracers in the 3 h experimental period. PC-3 tumor xenografts were visible from PET images of both tracers. With excess blocking agent, the radioactivity signal in PC-3 tumors was reduced compared to the images of the animals in the control group. The injection dose corrected region of interesting (ROI) values of PC-3 tumor from micro-PET images are shown in figure 7. For both tracers, the ROI values of PC-3 tumor rapidly decreased during 3 hours experimental period, and slightly reduction was observed when co-injected with excess of blocking agent, which is correlated to the results of blocking study.

7.4 Discussion

Despite rapid development of radiolabelled bombesin analogues for prostate cancer diagnosis and therapy in the last decade (*18*), the clinical transfer of bombesin radiopharmaceuticals is still limited due to unfavorable *in vivo* kinetics of bombesin tracers.

The lack of stability of radiolabelled bombesins is seriously hampering successful clinical application. A variety of bifunctional chelators and linkers has been reported to improve the *in vivo* stability (*20-24*). By applying the substitution of amino acids in positions 6 and 13 with the non-nature amino acids D-Phe and Leu-NHEt, a series of Bombesin like peptides were developed for SPECT imaging by Nock *et al.* (*25-26*). In this study, the stabilized bombesin analogues C5, C6 and C7 were generated by chemically introducing a thioether linkage by the desulphurization method described by Galande *et al.* (*27*). The stabilized bombesin analogues H and G were produced biologically by a modified *L. lactis* strain which procedure has been described by Kluskens *et al*. (*15*). For the bombesin analogues H and G, it was determined that the binding affinity was dramatically decreased by the modification of the binding motif. For analogues C5, C6 and C7, binding affinity to GRPR varied due to the different positions of the thioether cross-links and concomitant structural difference in the N-terminal [1-6] half of bombesin. With the acceptable remaining binding affinity for the GRPR receptor, C5 and C6 were selected for ^{18}F labeling through the side chain of lysine and we subsequently compared these analogs *in vitro* and *in vivo*. Compared to ^{18}F-C5, the cellular uptake of ^{18}F-C6 was 3 times higher which was caused by a higher binding affinity for GRPR. As agonists, both tracers ^{18}F-C5 and ^{18}F-C6 were mostly internalized into PC-3 cells via GRPR in the internalization experiments.

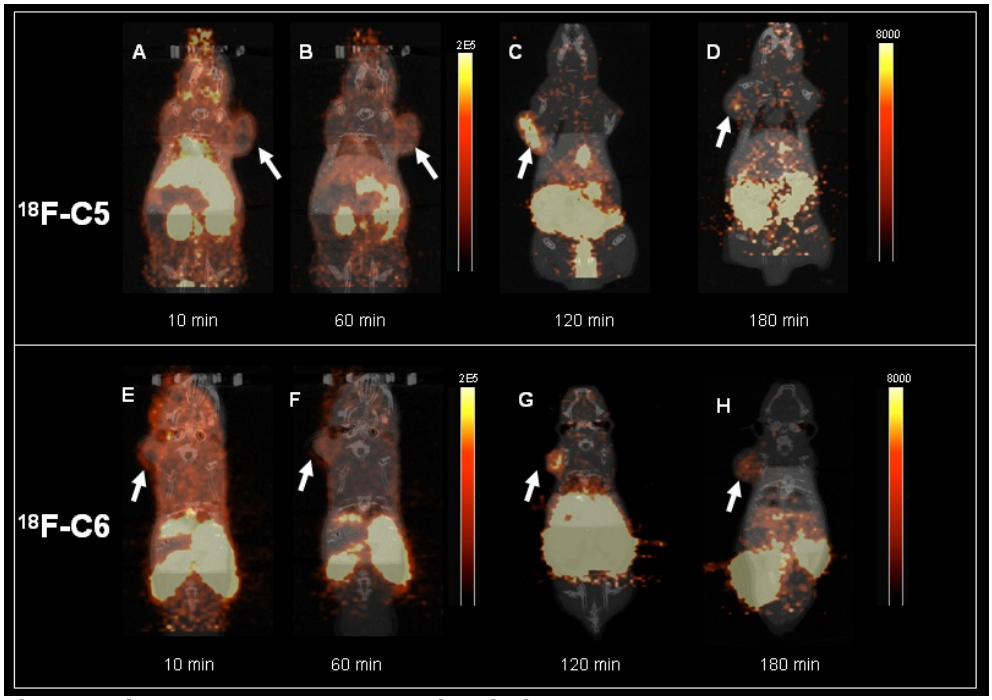

athymic nude mice at 10 min, 60 min , 2 h and 3 h post injection. Arrows point at PC-3 tumors.

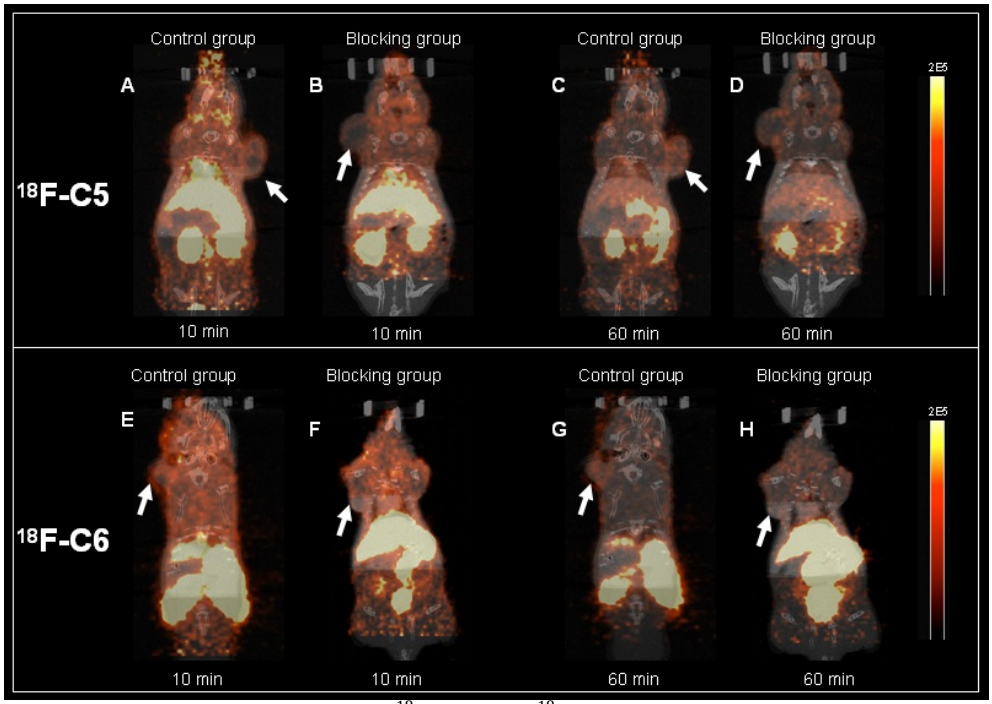

Figure6. MicroPET/CT scan of ^{18}F-C5 and ^{18}F-C6 in PC-3 prostate tumor-bearing

athymic nude mice at 10 min , 60 min post injection with or without blocking agent. A, C, E and G are same images correspond to Figure 5A, 5B, 5E and 5F, respectively. Arrows point at PC-3 tumors.

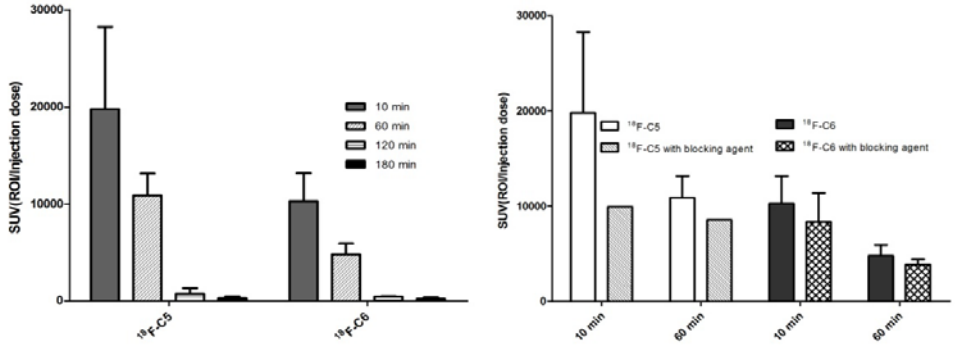

Figure 7. Injection dose corrected region of interesting values of PC-3 tumor from micro-PET images of ^{18}F-C5 and ^{18}F-C6 (mean± SD).

^{18}F labeling becomes increasingly attractive for tracer development. Furthermore, the application of PET is growing. Due to the optimal radionuclear characteristics of ^{18}F and the physical half-life of 110 min which fit the *in vivo* biological half-life of peptides, ^{18}F was selected for PET tracer development in this study. Lys^3-Bombesin, truncated bombesin and Arginine-Glycine-Aspartic acid-Bombesin(RGD-BN) heterodimers were coupled with ^{18}F-SFB, and proved to be potential probes for GRPR-expressing cancer targeting by Chen *et al*. (*14, 28-30*). The *in vitro* binding assay of ^{19}F-C5 and ^{19}F-C6, demonstrated that the conjugation of SFB motif has negative effect on the binding affinity of bombesin as reported (*14*). The reduction of binding affinity to GRPR was more serious for C5 than C6 which may be due to the distance between the lysine and bombesin(7-14) sequence which was smaller for C5 than that of C6.

A similar effect of the distance between SFB and the bombesin motif on the labeling yield has been reported by the group of Chen (*30*).

Although better stability may lead to longer blood circulation for ^{18}F-C5, 3-fold lower tumor uptake was observed compared to ^{18}F-C6. This likely is the result of the lower binding affinity to the GRPR which reduces the tumor uptake.

In blocking studies, no significant reduction was observed in biodistribution of both tracers in most organs at 1 h post injection. The absence of specificity of both tracers is presumably due to the relatively low specific radioactivity (1437±329 MBq/μmol for ^{18}F-C5 and 218±135 MBq/μmol for ^{18}F-C6), compared to other ^{18}F-bombesin analogues (which varied from 62 to 250 GBq/μmol)(*14, 28, 30*). The low specific radioactivity furthermore leads to reduced uptake of radioactivity in the tumor. The self-inhibition of receptor-specific uptake in PC-3 tumor in the control group was also observed in *in vivo* studies of ^{18}F-FB-Aca-BBN(7–14) (*14*).

Due to the low tumor-to-nontumor ratios of both tracers ^{18}F-C5 and ^{18}F-C6 at 1 h post injection, PC-3 tumor could not be detected with PET. A clear tumor-to-background contrast was observed for ^{18}F-C5 and ^{18}F-C6 in PC-3 tumor at 2 and 3 h post injection. This is mainly due to the faster wash out of the tracer from the normal organs than from the tumor. In the PET images of tumor-bearing mice with^{18}F-C6, a strong signal was shown in kidney and liver. This indicated that it was subject to both hepatobiliary and renal clearance

routes. For ^{18}F-C5, due to the hydrophilicity of the tracer, high kidney uptake was found in PET images during the 3 h experimental period.

7.5 Conclusion

To overcome stability issues of radiolabelled peptides for receptor-mediated cancer imaging, we synthesized a series of lanthionine-stabilized full-length bombesin-like peptides and two promising candidates were successfully labelled with ^{18}F. Both tracers showed GRPR targeting moderate potential in vitro and in a vivo mouse model.

Acknowledgements

This work was made possible by a financial contribution from CTMM, project PCMM, project number 03O-203 and IAG2, Province of Groningen. We thank V. Wiersma and L.D. Kluskens for initial studies on synthesis of lanthionine-stabilized bombesin analogues, D.F. Samplonius for technical assistance on cell culturing, J. W. A. Sijbesma for assisting animal experiments.

References

(1) Erspamer, V., Erpamer, G. F., and Inselvini, M. (1970) Some pharmacological actions of alytesin and bombesin. *J Pharm Pharmacol 22*, 875-6.

(2) McDonald, T. J., Jornvall, H., Nilsson, G., Vagne, M., Ghatei, M., Bloom, S. R., and Mutt, V. (1979) Characterization of a gastrin releasing peptide from porcine non-antral gastric tissue. *Biochem Biophys Res Commun 90*, 227-33.

(3) Ananias, H. J., van den Heuvel, M. C., Helfrich, W., and de Jong, I. J. (2009) Expression of the gastrin-releasing peptide receptor, the prostate stem cell antigen and the prostate-specific membrane antigen in lymph node and bone metastases of prostate cancer. *Prostate 69*, 1101-8.

(4) Xiao, D., Wang, J., Hampton, L. L., and Weber, H. C. (2001) The human gastrin-releasing peptide receptor gene structure, its tissue expression and promoter. *Gene 264*, 95-103.

(5) Schroeder, R. P., de Visser, M., van Weerden, W. M., de Ridder, C. M., Reneman, S., Melis, M., Breeman, W. A., Krenning, E. P., and de Jong, M. (2010) Androgen-regulated gastrin-releasing peptide receptor expression in androgen-dependent human prostate tumor xenografts. *Int J Cancer 126*, 2826-34.

(6) Cutz, E., Chan, W., and Track, N. S. (1981) Bombesin, calcitonin and leu-enkephalin immunoreactivity in endocrine cells of human lung. *Experientia 37*, 765-7.

(7) Price, J., Penman, E., Wass, J. A., and Rees, L. H. (1984) Bombesin-like immunoreactivity in human gastrointestinal tract. *Regul Pept 9*, 1-10.

(8) Ananias, H. J., de Jong, I. J., Dierckx, R. A., van de Wiele, C., Helfrich, W., and Elsinga, P. H. (2008) Nuclear imaging of prostate cancer with gastrin-releasing-peptide-receptor targeted radiopharmaceuticals. *Curr Pharm Des 14*, 3033-47.

(9) Mendoza-Sanchez, A. N., Ferro-Flores, G., Ocampo-Garcia, B. E., Morales-Avila,

E., de, M. R. F., De Leon-Rodriguez, L. M., Santos-Cuevas, C. L., Medina, L. A., Rojas-Calderon, E. L., and Camacho-Lopez, M. A. (2010) Lys3-bombesin conjugated to ^{99m}Tc-labelled gold nanoparticles for in vivo gastrin releasing peptide-receptor imaging. *J Biomed Nanotechnol 6*, 375-84.

(10) Cheng, K. T., Ferro-Flores, G., and Arteaga de Murphy, C. (2004) ^{99m}Tc-Ethylenenediamine-N,N'-diacetic acid/hydrazinonicotinamide[Lys^3]-bombesin.

(11) Santos-Cuevas, C. L., Ferro-Flores, G., Arteaga de Murphy, C., and Pichardo-Romero, P. A. (2008) Targeted imaging of gastrin-releasing peptide receptors with ^{99m}Tc-EDDA/HYNIC-[Lys^3]-bombesin: biokinetics and dosimetry in women. *Nucl Med Commun 29*, 741-7.

(12) Chen, X., Park, R., Hou, Y., Tohme, M., Shahinian, A. H., Bading, J. R., and Conti, P. S. (2004) microPET and autoradiographic imaging of GRP receptor expression with ^{64}Cu-DOTA-[Lys^3]bombesin in human prostate adenocarcinoma xenografts. *J Nucl Med 45*, 1390-7.

(13) Ho, C. L., Chen, L. C., Lee, W. C., Chiu, S. P., Hsu, W. C., Wu, Y. H., Yeh, C. H., Stabin, M. G., Jan, M. L., Lin, W. J., Lee, T. W., and Chang, C. H. (2009) Receptor-binding, biodistribution, dosimetry, and micro-SPECT/CT imaging of ^{111}In-[DTPA^1, Lys^3, Tyr^4]-bombesin analog in human prostate tumor-bearing mice. *Cancer Biother Radiopharm 24*, 435-43.

(14) Zhang, X., Cai, W., Cao, F., Schreibmann, E., Wu, Y., Wu, J. C., Xing, L., and Chen, X. (2006) ^{18}F-labelled bombesin analogs for targeting GRP receptor-expressing prostate cancer. *J Nucl Med 47*, 492-501.

(15) Kluskens, L. D., Kuipers, A., Rink, R., de Boef, E., Fekken, S., Driessen, A. J., Kuipers, O. P., and Moll, G. N. (2005) Post-translational modification of therapeutic peptides by NisB, the dehydratase of the lantibiotic nisin. *Biochemistry 44*, 12827-34.

(16) Rink, R., Kluskens, L. D., Kuipers, A., Driessen, A. J., Kuipers, O. P., and Moll, G. N. (2007) NisC, the cyclase of the lantibiotic nisin, can catalyze cyclization of designed nonlantibiotic peptides. *Biochemistry 46*, 13179-89.

(17) Rink, R., Arkema-Meter, A., Baudoin, I., Post, E., Kuipers, A., Nelemans, S. A., Akanbi, M. H., and Moll, G. N. (2010) To protect peptide pharmaceuticals against peptidases. *J Pharmacol Toxicol Methods 61*, 210-8.

(18) Ananias, H. J., Yu, Z., Dierckx, R. A., van der Wiele, C., Helfrich, W., Wang, F., Yan, Y., Chen, X., de Jong, I. J., and Elsinga, P. H. (2011) ^{99m}technetium-HYNIC(tricine/TPPTS)-Aca-bombesin(7-14) as a targeted imaging agent with microSPECT in a PC-3 prostate cancer xenograft model. *Mol Pharm 8*, 1165-73.

(19) Wester, H. J., Hamacher, K., and Stocklin, G. (1996) A comparative study of N.C.A. fluorine-18 labeling of proteins via acylation and photochemical conjugation. *Nucl Med Biol 23*, 365-72.

(20) Ait-Mohand, S., Fournier, P., Dumulon-Perreault, V., Kiefer, G. E., Jurek, P., Ferreira, C. L., Benard, F., and Guerin, B. (2011) Evaluation of ^{64}Cu-labelled bifunctional chelate-bombesin conjugates. *Bioconjug Chem 22*, 1729-35.

(21) Dapp, S., Garcia Garayoa, E., Maes, V., Brans, L., Tourwe, D. A., Muller, C., and Schibli, R. (2011) PEGylation of ^{99m}Tc-labelled bombesin analogues improves their pharmacokinetic properties. *Nucl Med Biol 38*, 997-1009.

(22) Pujatti, P. B., Santos, J. S., Couto, R. M., Melero, L. T., Suzuki, M. F., Soares, C. R., Grallert, S. R., Mengatti, J., and De Araujo, E. B. (2011) Novel series

of ^{177}Lu-labelled bombesin derivatives with amino acidic spacers for selective targeting of human PC-3 prostate tumor cells. *Q J Nucl Med Mol Imaging 55*, 310-23.

(23) Chen, J., Linder, K. E., Cagnolini, A., Metcalfe, E., Raju, N., Tweedle, M. F., and Swenson, R. E. (2008) Synthesis, stabilization and formulation of ^{177}Lu-AMBA, a systemic radiotherapeutic agent for Gastrin Releasing Peptide receptor positive tumors. *Appl Radiat Isot 66*, 497-505.

(24) Alves, S., Correia, J. D., Santos, I., Veerendra, B., Sieckman, G. L., Hoffman, T. J., Rold, T. L., Figueroa, S. D., Retzloff, L., McCrate, J., Prasanphanich, A., and Smith, C. J. (2006) Pyrazolyl conjugates of bombesin: a new tridentate ligand framework for the stabilization of fac-[M(CO)$_3$]+ moiety. *Nucl Med Biol 33*, 625-34.

(25) Nock, B. A., Nikolopoulou, A., Galanis, A., Cordopatis, P., Waser, B., Reubi, J. C., and Maina, T. (2005) Potent bombesin-like peptides for GRP-receptor targeting of tumors with ^{99m}Tc: a preclinical study. *J Med Chem 48*, 100-10.

(26) Nock, B., Nikolopoulou, A., Chiotellis, E., Loudos, G., Maintas, D., Reubi, J. C., and Maina, T. (2003) ^{99m}Tc-Demobesin 1, a novel potent bombesin analogue for GRP receptor-targeted tumour imaging. *Eur J Nucl Med Mol Imaging 30*, 247-58.

(27) Galande, A. K., Trent, J. O., and Spatola, A. F. (2003) Understanding base-assisted desulfurization using a variety of disulfide-bridged peptides. *Biopolymers 71*, 534-51.

(28) Li, Z. B., Wu, Z., Chen, K., Ryu, E. K., and Chen, X. (2008) ^{18}F-labelled BBN-RGD heterodimer for prostate cancer imaging. *J Nucl Med 49*, 453-61.

(29) Yan, Y., Chen, K., Yang, M., Sun, X., Liu, S., and Chen, X. (2011) A new ^{18}F-labelled BBN-RGD peptide heterodimer with a symmetric linker for prostate cancer imaging. *Amino Acids 41*, 439-47.

(30) Liu, Z., Yan, Y., Chin, F. T., Wang, F., and Chen, X. (2009) Dual integrin and gastrin-releasing peptide receptor targeted tumor imaging using ^{18}F-labelled PEGylated RGD-bombesin heterodimer ^{18}F-FB-PEG$_3$-Glu-RGD-BBN. *J Med Chem 52*, 425-32.

Chapter 8

Evaluation of a Technetium-99m Labelled Bombesin Homodimer for GRPR Imaging in Prostate Cancer

Zilin Yu, Giuseppe Carlucci, Hildo J. K. Ananias, Rudi A. J. O. Dierckx, Shuang Liu, Wijnand Helfrich, Fan Wang, Igle Jan. de Jong, Philip H. Elsinga

Amino Acids. 2013 Feb; 44(2):543-53.

Abstract:

Introduction: Multimerization of peptides can improve the binding characteristics of the tracer by increasing local ligand concentration and decreasing dissociation kinetics. In this study, a new bombesin homodimer was developed based on a ε-aminocaproic acid-bombesin(7-14) (Aca-bombesin(7-14)) fragment which has been studied for targeting the gastrin-releasing-peptide-receptor (GRPR) in prostate cancer.

Methods: The bombesin homodimer was conjugated to 6-Hydrazinopyridine-3-carboxylic acid (HYNIC) and labelled with ^{99m}Tc for SPECT imaging. The *in vitro* binding affinity to GRPR, cell uptake, internalization and efflux kinetics of the radiolabelled bombesin dimer were investigated in the GRPR-expressing human prostate cancer cell line PC-3. Biodistribution and the GRPR targeting potential were evaluated in PC-3 tumor-bearing athymic nude mice.

Results: When compared to the bombesin monomer, the binding affinity of the bombesin dimer is about 10 times lower. However the ^{99m}Tc labelled bombesin dimer showed a three times higher cellular uptake at 4 hours after incubation, but similar internalization and efflux characters *in vitro*. Tumor uptake and *in vivo* pharmacokinetics in PC-3 tumor bearing mice were comparable. The tumor was visible on the dynamic images in the first hour and could be clearly distinguished from non-targeted tissues on the static images after 4 hours.

Conclusion: The GRPR targeting ability of the ^{99m}Tc labelled bombesin dimer was proven *in vitro* and *in vivo*. This bombesin homodimer provides a good starting point for further studies on enhancing the tumor targeting activity of bombesin multimers.

Keywords: GRPR, bombesin homodimer, radiolabelled, imaging, prostate cancer, PC-3, ^{99m}Tc, HYNIC, SPECT.

8.1 Introduction

Prostate cancer is one of the most common cancers in men in the USA and in Europe (*1-2*). In the course of the disease bone metastases will develop in the majority of cases with advanced prostate cancer. This number will reach 90% in patients with castrate resistant prostate cancer treated with chemotherapy (*3*).

At present there is an unmet need to measure response to treatment of prostate cancer metastases in the skeleton. With a specific radiotracer and specific target in the tumor, positron emission tomography (PET) and single photon emission computed tomography (SPECT) would be powerful diagnostic tools in detection of prostate cancer.

The Gastrin-Releasing-Peptide Receptor (GRPR) is a subtype of the bombesin receptor family. Mammalian GRPR is preferentially expressed in non-neuroendocrine tissues of the breast and pancreas and in neuroendocrine cells of the brain, gastrointestinal tract, and lung (*4-8*). It has also been shown that GRPR is overexpressed in a large variety of human tumors, including prostate, breast, renal and (non) small cell lung cancer. Due to the enhanced expression of GRPR in prostate cancer, GRPR is considered as a potential target for the diagnosis, staging or treatment of prostate cancer.

Bombesin is a 14 amino acid peptide which was first isolated from the skin of frogs in the 1970 (*9*). Bombesin and its mammalian counterpart share 7 identical amino acid residues at the C-terminal, which was identified as the binding domain of the bombesin receptor (*10*).

Radiolabelled bombesin analogs have proven their GRPR binding ability in several cancer cell lines and in various tumor models (*11-14*). Previously, an ε-aminocaproic acid (Aca) modified bombesin analogue was labelled with ^{18}F and the compound was evaluated in a prostate cancer animal model (*11*). Although ^{18}F-FB-Aca-Bombesin(7–14) showed its ability to target GRPR in an animal model, due to the lipophilic character of the tracer detection of the orthotopic prostate cancer was hampered by high abdominal background levels.

Recently, we developed HYNIC conjugated Aca-BN(7–14) and labelled it with ^{99m}Tc for SPECT imaging of prostate cancer in an animal model (*15*). Compared to ^{18}F-FB-Aca-Bombesin(7–14), ^{99m}Tc-HYNIC(Tricine/TPPTS)-Aca-BN(7–14) (^{99m}Tc-HABN) showed reduced abdominal background and improved tumor-to-normal-tissue (T/NT) contrast (tumor-to-muscle ratio from lower than 5 increased to 13.9 ± 5.9 at 1 hour post injection) on SPECT images .

While most bombesin-like peptides are monomers, we applied the dimerization technology and synthesized a new dimeric bombesin with 2 identical Aca-Bombesin(7–14) units. Multivalent interactions are frequently found in nature where they increase the affinity of weak ligand–receptor interactions such as in the DNA-DNA duplex formation by multiple weak interactions between individual complementary nucleotides, or the typical Y-shaped antibody composed of two heavy chains and two light chains which are joined by disulfide linkages (*16-19*). Multivalent structures have become a strategy for the development of drugs and diagnostic agents. It has been shown by several research groups that multivalent compounds are able to enhance the interaction between the ligand and corresponding receptor (*20-25*). One of the most prominent examples are multivalent Arginine-Glycine-Aspartic acid (RGD) analogues. Several isotopes (^{99m}Tc, ^{111}In, ^{18}F, ^{68}Ga, etc) and chelators (HYNIC, DOTA, DTPA, etc) have been applied for the preparation of dimeric and tetrameric RGD tracers (*21-25*). The binding affinity is significantly increased at higher orders of binding valency, a principle usually referred to as avidity. The aim of this study is to investigate the GRPR targeting characteristics of the bombesin

homodimer as a potential imaging agent for prostate cancer.

8.2 Materials and Methods

8.2.1 Chemicals:

Tricine (N-(Tri(hydroxymethyl)methyl)glycine) was purchased from Sigma/Aldrich (St. Louis, Missouri, USA). Trisodium triphenylphosphine-3,3',3" -trisulfonate (TPPTS) was purchased from Alfa Aesar (Karlsruhe, Germany). Both were used without further purification. The peptide Glu[Aca-BN(7-14)]$_2$ was provided by Peptides International (Louisville, KY, USA). Na^{99m}TcO$_4$ was eluted from the ^{99}Mo/^{99m}Tc generator MTcG-4 (IAE Radioisotope Centre POLATOM, Świerk, Poland). ^{125}I-Tyr^4-BN was obtained from Perkin-Elmer Life and Analytical Sciences (Waltham, Massachusetts, USA).

8.2.2 Equipment:

Semi-preparative reversed-phase high-performance liquid chromatography (RP-HPLC) was performed on a HITACHI L-2130 HPLC system (Hitachi High Technologies America Inc., Pleasanton, California, USA) equipped with a Bicron Frisk-Tech area monitor. Isolation and quality control of ^{99m}Tc-HYNIC(Tricine/TPPTS)-Glu[Aca-BN(7-14)]$_2$ (^{99m}Tc-HABN$_2$) were performed using a Phenomenex reversed-phase Luna C18 column (10 mm × 250 mm, 5 μm) (Torrance, California, USA). The flow was set at 2.5 mL/min using a gradient system starting from 90% solvent A (0.01 M phosphate buffer, pH=6.0) and 10% solvent B (acetonitrile) (5 minutes) and ramped to 45% solvent A and 55% solvent B at 35 minutes (HPLC Method 1).

HPLC Method 2 used a LabAlliance semi-preparative HPLC system equipped with a UV-Vis detector (λ = 254 nm) and Zorbax C18 semi-prep column (9.4 mm x 250 mm, 100 Å pore size). The flow rate was 2.5 mL/min. The mobile phase was isocratic with 60% solvent A (0.1% acetic acid in water) and 40% solvent B (0.1% acetic acid in acetonitrile) at 0 – 5 min, followed by a gradient mobile phase going from 60% solvent A and 40% solvent B at 5 min to 20% solvent A and 80% solvent B at 30 min.

HPLC Method 3 used a LabAlliance semi-preparative HPLC system equipped with a UV-Vis detector (λ = 254 nm) and Zorbax C18 semi-preparative column (9.4 mm x 250 mm, 100 Å pore size). The flow rate was 2.5 mL/min. The gradient mobile phase goes from 90% solvent A (0.1% acetic acid in water) and 10% solvent B (0.1% acetic acid in acetonitrile) at 0 min to 75% solvent A at 5 min, followed by a gradient mobile phase going from 75% solvent A to 65% solvent A at 40 min.

8.2.3 Synthesis of HYNIC-Glu[Aca-BN(7-14)]$_2$

Sodium succinimidyl 6-(2-(2-sulfonatobenzaldehyde)hydrazono)nicotinate (HYNIC -NHS) was prepared according to literature method (*26*).

HYNIC-NHS (21.8 mg, 50 μmol) and Glu[Aca-BN(7-14)]$_2$ (5.8 mg, 2.6 μmol) were dissolved in 1.5 mL of DMF. The pH was adjusted to 8.5 – 9.0 with DIPEA. The

mixture was stirred for 7 days at room temperature to make sure that the reaction was complete as indicated by the disappearance of the peptide peak. The product was purified by HPLC (Method 1). The peak of interest at ~28 min was collected. The collected fractions were combined, and lyophilized to obtain 1.7 mg product, which was re-purified by HPLC (Method 2). Fraction at ~32.5 min was collected. Lyophilization of the collected fractions gave the final product 0.8 mg (13%) with the purity > 95% by HPLC. ESI-MS: $C_{114}H_{161}N_{33}O_{27}S_3$, calculated 2521.9, observed 2522 ($[M+H]^+$).

8.2.4 Radiochemistry

100 μL of the HYNIC-Glu[Aca-BN(7-14)]$_2$ solution (1 mg/mL in H_2O), 100 μL of tricine solution (50 mg/mL in 25 mM succinate buffer, pH 5.0), 100 μL of TPPTS solution (50 mg/mL in 25 mM succinate buffer, pH 5.0), 5 μL of $SnCl_2$ solution (3.0 mg/mL in 0.1 N HCl) and 100 μL of $Na^{99m}TcO_4$ (370 MBq) in saline were added to a 1.5 mL Eppendorf cup. The Eppendorf cup containing the reaction mixture was sealed and heated at 95 °C for 20 min. After cooling to room temperature, the mixture was purified by HPLC (Method 1). The product was then passed through a Waters Sep-Pak C18 light cartridge. ^{99m}Tc-HABN$_2$ was eluted with ethanol (0.4 mL) and diluted with saline solution for *in vitro* and *in vivo* experiments. A sample of the resulting solution was analyzed by the same HPLC system (method 1).

8.2.5 Partition Coefficient

The partition coefficient was determined using the method described previously(*15*). The tracer was dissolved in a mixture of 0.5 mL *n*-octanol and 0.5 mL 25 mM phosphate buffer (pH 7.4) and well mixed for 5 min at room temperature. Then the mixture was centrifuged at 3000 rpm for 5 minutes. 100 μL samples were obtained from *n*-octanol and aqueous layers. All samples were counted in a γ-counter (Compugamma CS1282, LKB-Wallac, Turku, Finland). The *log D* value is reported as an average of three different measurements.

8.2.6 *In Vitro* Stability

The tracer was dissolved in 1 mL saline or L-Cysteine solution (1 mg/mL), incubated at room temperature and analyzed by HPLC (Method 1) at 1, 2, 4, 6, and 24 hours post incubation.

Human serum from healthy donors was incubated at 37 °C with ^{99m}Tc-HABN$_2$ for different time periods (1, 2, 4, 6, 24 h). After incubation, a sample of 250 μL was precipitated with 750 μL acetonitrile/ethanol ($V_{acetonitrile}/V_{ethanol}$ =1:1) and then centrifuged (3 minutes at 3000 rpm), the supernatants were passed through a Millex-LG filter (Millipore, Co. Cork, Carrigtwohill, Ireland) and afterwards analyzed by HPLC (Method 1). Results were plotted as radiochemical purity (RCP) at different time-points.

8.2.7 Cell Culture

The GRPR-positive human prostate cancer cell line PC-3 (ATCC, Manassas, Virginia, USA) was cultured in RPMI 1640 (Lonza, Verviers, France) supplemented with 10% fetal calf serum (Thermo Fisher Scientific Inc., Logan, Utah, USA) at 37 °C in a humidified 5% CO_2 atmosphere.

8.2.8 *In Vitro* Competitive Receptor Binding Assay

The *in vitro* GRPR binding affinities of Glu[Aca-BN(7-14)]$_2$ and HYNIC-Glu[Aca -BN(7-14)]$_2$ were assessed via a competitive displacement assay with ^{125}I-Tyr^4-BN(1-14) as the GRPR specific radioligand. Experiments were performed with PC-3 human prostate cancer cells according to a method previously described (*15*). The 50% inhibitory concentration (IC_{50}) values were calculated by fitting the data with nonlinear regression using GraphPad Prism 5.0 (GraphPad Software, San Diego, California, USA). Experiments were performed with triplicate samples. IC_{50} values are reported as an average of these samples plus the standard deviation (SD).

8.2.9 Cellular uptake studies

One day prior to the assay, PC-3 cells at confluence were placed in 6-well plates (0.5 million cells/well). The cells were washed twice with PBS solution before using for the experiments. ^{99m}Tc-HABN or ^{99m}Tc-HABN$_2$ (0.0037 MBq/well) was incubated with cells at 37 °C for 0, 15, 30, 45, 60, 90, 120 or 240 minutes in triplicate to allow for cellular uptake. 20 µg of unlabelled Glu[Aca-BN(7-14)]$_2$ was co-incubated with ^{99m}Tc-HABN or ^{99m}Tc-HABN$_2$ in blocking groups. To remove unbound radioactivity, the cells were washed twice with ice-cold PBS and the cells were lysed by incubation with 1 M NaOH at 37 °C. The resulting lysate in each well was aspirated to determine the uptake of activity with a γ-counter. Results are expressed as percentage of incubated radioactivity (mean±SD).

8.2.10 Internalization and efflux Studies

For the internalization study, 1 million PC-3 cells were placed in 6-well plates before the experiments and kept at 37 °C overnight. The cells were washed with PBS and then incubated with ^{99m}Tc-HABN$_2$ (0.0037 MBq/well) for 2 hours at 4 °C. To remove unbound radioactivity, the cells were washed twice with ice-cold PBS and incubated with the pre-warmed culture medium at 37 °C for 0, 5, 15, 30, 45, 60, 90 and 120 minutes in triplicate to allow for internalization.

To remove cell-surface bound radiotracer, the cells were washed twice for 3 minutes with acid (50 mM glycine−HCl/100 mM NaCl, pH 2.8). The acid solution was collected and measured with a γ-counter. The results were collected as the surface-bound activity. Subsequently, the cells were lysed by incubation with 1 M NaOH at 37 °C and the resulting lysate in each well was measured to determine the internalized radioactivity with γ-counter.

Results are expressed as the percentage of total radioactivity (internalized activity / (surface-bound activity + internalized activity)), (mean±SD).

For the efflux study, 1 million PC-3 cells were placed in 6-well plates 1 day before the experiments and kept at 37 °C. The cells were washed with PBS and then incubated with ^{99m}Tc-HABN$_2$ (3.7 KBq/well) for 1 hour at 37 °C to allow for maximum internalization. To remove unbound radioactivity, the cells were washed twice afterwards with ice-cold PBS and were then incubated in the pre-warmed culture medium at 37 °C for 0, 15, 30, 45, 60, 90, 120, and 240 minutes in triplicate to allow for externalization. To remove cell-surface bound radiotracer, the cells were washed twice for 3 minutes with acid (50 mM glycine−HCl/100 mM NaCl, pH 2.8). Then, the cells were lysed by incubation with 1 N NaOH at 37 °C, and the resulting lysate in each well was aspirated to determine the remaining radioactivity in a γ-counter. Results are expressed as the percentage of maximum intracellular radioactivity (remaining activity at specific time-point / activity at time-point 0) (mean±SD).

8.2.11 Animal Model

In the PC-3 tumor model, 2×10^6 PC-3 cells (suspended in 0.1 mL sterile saline) were subcutaneous injected into the left front flank of male athymic mice (Harlan, Zeist, The Netherlands). During the injection, animals were anesthetized with a gas composed of ~3.5% isoflurane in an air/oxygen mixture. The mice were used for biodistribution experiments and microSPECT and CT imaging when the tumor volume reached a mean diameter of 0.8-1.0 cm (typically 3-4 weeks after tumor inoculation).

All animal experiments were performed in accordance with the regulations of Dutch law on animal welfare and the institutional ethics committee for animal procedures approved the protocol.

8.2.12 MicroSPECT imaging and Biodistribution

The subcutaneous tumor bearing mice were separated into 4 groups (4 animals per group) and used for imaging and biodistribution when the tumor volume reached 250-300 mm^3 (4-5 weeks after inoculation).

MicroSPECT scans were performed on a three-head γ-camera (MILabs, U-SPECT-II, Utrecht, The Netherlands) equipped with a multi-pinhole high-resolution collimator. For the microSPECT scans ~30MBq ^{99m}Tc-HABN$_2$ were administered by penis vein injection under isoflurane anesthesia. 60 min of dynamic microSPECT data was acquired immediately after injection. Mice (group 1) that were used for dynamic scanning were sacrificed directly after the scan with an overdose of isoflurane anesthesia. CT scan and biodistribution were performed afterwards. Blood, tumor, major organs and tissue samples were collected, weighted and counted by γ-counter. The percentage of injected dose per gram (%ID/g) was determined for each sample. For each mouse, radioactivity of the tissue samples was calibrated against a known aliquot of radiotracer.

For static imaging, mice were sacrificed at 4 (group 2) and 24 h (group 3) after injection. Afterwards, 60-min microSPECT and microCT images were acquired. Biodistribution was performed as described above.

For the receptor-blocking experiment 300 μg of unlabelled Aca-BN(7-14) was

pre-injected 30 min before the tracer injection. The animals of the blocking group (group 4) were sacrificed and 60-min static microSPECT & CT images were acquired at 4 hours after tracer injection. Biodistribution was performed after the CT scan.

Images were reconstructed by using U-SPECT-Rec v 1.34i3 (MILabs, Utrecht, the Netherlands) with a pixel-based ordered-subsets expectation maximum (POSEM) algorithm. Final images were 1 mm slices, made with Amide 0.9.1 (open source software).

8.2.13 Statistical Analysis

Quantitative data are expressed as mean ± SD. Means were compared using the Student t test. *P* values <0.05 were considered as significant.

8.3 Results

8.3.1 Synthesis, Radiolabelling, Partition Coefficient and In Vitro Stability

^{99m}Tc-HABN$_2$ (figure 1) was prepared at 95 °C with moderate labeling yield (>80%). After purification the radiochemical purity was higher than 95%. The specific activity was ~17.4 ± 9.7 GBq/μmol (n=7). ^{99m}Tc-HABN$_2$ was well separated from precursor using HPLC system. The retention time (HPLC Method 1) of ^{99m}Tc-HABN$_2$ and HYNIC-Glu[Aca-BN(7-14)]$_2$ was around 28 and 24 min, respectively.

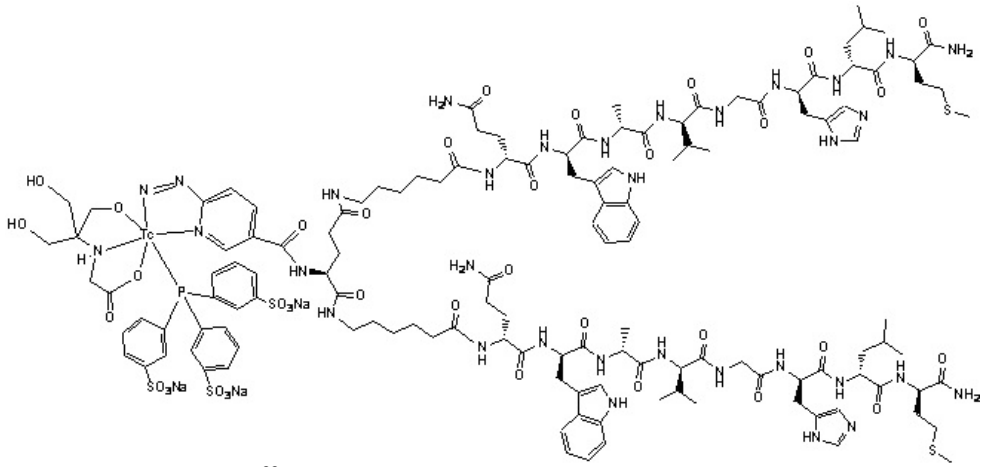

Figure 1 ^{99m}Tc-HYNIC(Tricine/TPPTS)-Glu[Aca-BN(7-14)]$_2$

The partition coefficient was determined in a mixture of *n*-octanol and phosphate buffer (pH=7.4). The *log D* value of ^{99m}Tc-HABN$_2$ was -1.54 ± 0.16. The *in vitro* stability of ^{99m}Tc-HABN$_2$ was evaluated in saline, human serum and in the presence of excess L-Cysteine (1.0 mg/mL, pH 7.4) (figure 2). ^{99m}Tc-HABN$_2$ was stable in the presence of excess L-Cysteine and human serum for at least 4 hours (RCP> 95 %). The RCP of ^{99m}Tc-HABN$_2$ in serum slowly decreased to ~84% after 24 hours.

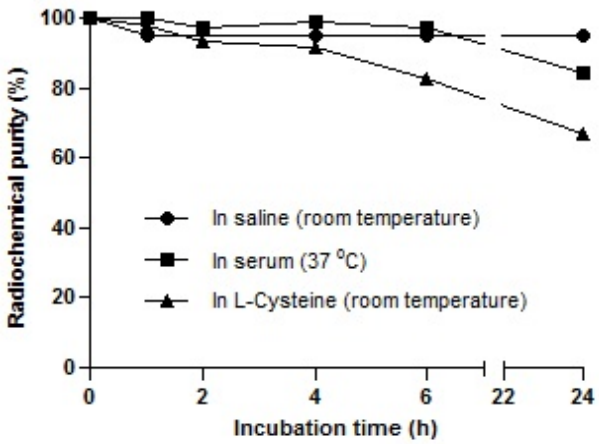

Figure 2 *In vitro* stability of ^{99m}Tc-HABN$_2$ in saline (at room temperature), human serum (at 37 ^{o}C) and L-Cysteine (at room temperature). Results are plotted as the radiochemical purity at different time points

8.3.2 *In vitro* Competitive Receptor Binding Assay

Using ^{125}I-Tyr^4-BN(1-14) as GRPR specific radioligand, the binding affinities of Glu[Aca-BN(7-14)]$_2$ and HYNIC-Glu[Aca-BN(7-14)]$_2$ for GRPR were compared via an in vitro competitive binding assay. Results are plotted as sigmoid curves for the displacement of ^{125}I-Tyr^4-BN(1-14) as a function of increasing concentrations of Glu[Aca-BN(7-14)]$_2$, and HYNIC-Glu[Aca-BN(7-14)]$_2$ (figure 3). The IC_{50} values were found to be 31.4 ± 0.4 nM and 63.4 ± 11.7 nM for Glu[Aca-BN(7-14)]$_2$ and HYNIC-Glu[Aca-BN(7-14)]$_2$, respectively.

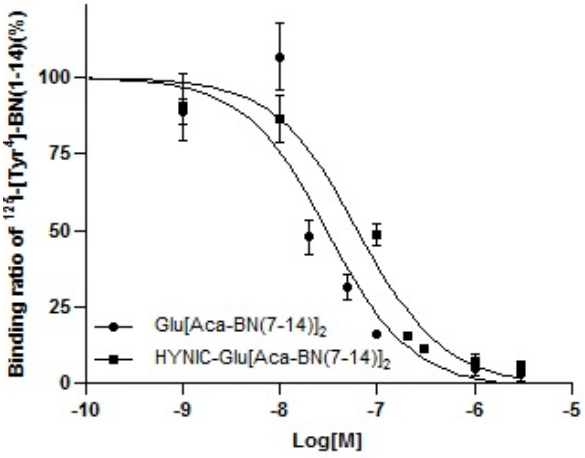

Figure 3 Inhibition of ^{125}I-[Tyr^4]-BN(1-14) binding to GRPR on PC-3 cells by Glu[Aca-BN(7-14)]$_2$ and HYNIC-Glu[Aca-BN(7-14)]$_2$. Log [M] = log of increasing

concentration (mol/L) of Glu[Aca-BN(7-14)]$_2$ and HYNIC-Glu[Aca-BN(7-14)]$_2$

8.3.3 Cellular uptake studies

The *in vitro* uptake of ^{99m}Tc labelled bombesin monomer and dimer in PC-3 cells are shown in Figure 4. Compared to ^{99m}Tc-HABN, ^{99m}Tc-HABN$_2$ has slower cellular uptake within 30 min of incubation, but keeps accumulating in PC-3 cells over the 4 hours experiment period. The highest cellular uptake for ^{99m}Tc-HABN and ^{99m}Tc-HABN$_2$ is 10.9 ± 0.7 % (1 hour post incubation) and 32.5 ± 1.8 % (4 hours post incubation) of added radioactivity, respectively. Co-incubation with excess unlabelled bombesin significantly reduced the cellular uptake of both tracers (<1% of added activity was belonging to non-specific uptake).

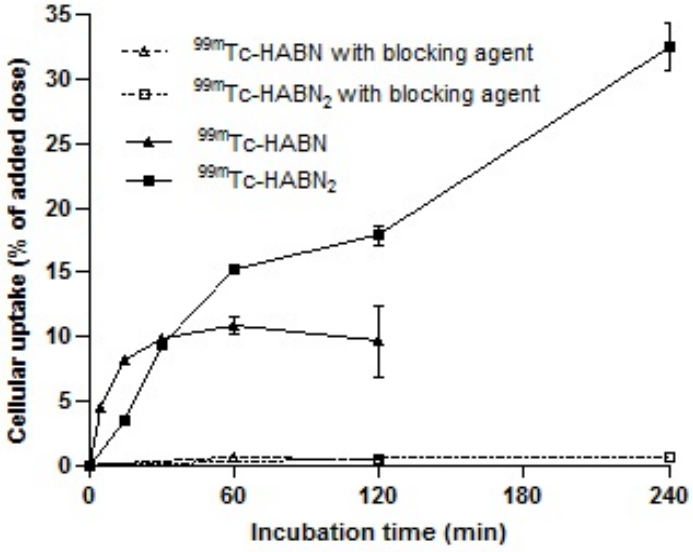

Figure 4 Cellular uptake assay of ^{99m}Tc-HABN and ^{99m}Tc-HABN$_2$ in PC-3 cells. The cellular uptake results were expressed as percentage added dose (n=3, mean ± SD)

8.3.4 Internalization and Efflux Studies

The internalization study depicted in figure 5 A showed rapid internalization of ^{99m}Tc-HABN$_2$ into PC-3 cells within 5 minutes incubation. The portion of intracellular activity reached a plateau at 15 min post incubation and 80% of cell bound activity internalized into the cells.

The results of the efflux study is shown in figure 5 B. For ^{99m}Tc-HABN$_2$, steady efflux was observed within 2 hours incubation. About 60% of the intracellular radioactivity was maintained in the cells at the end of the 4 hours experiment period. The efflux half life of ^{99m}Tc-HABN$_2$ was 84 min.

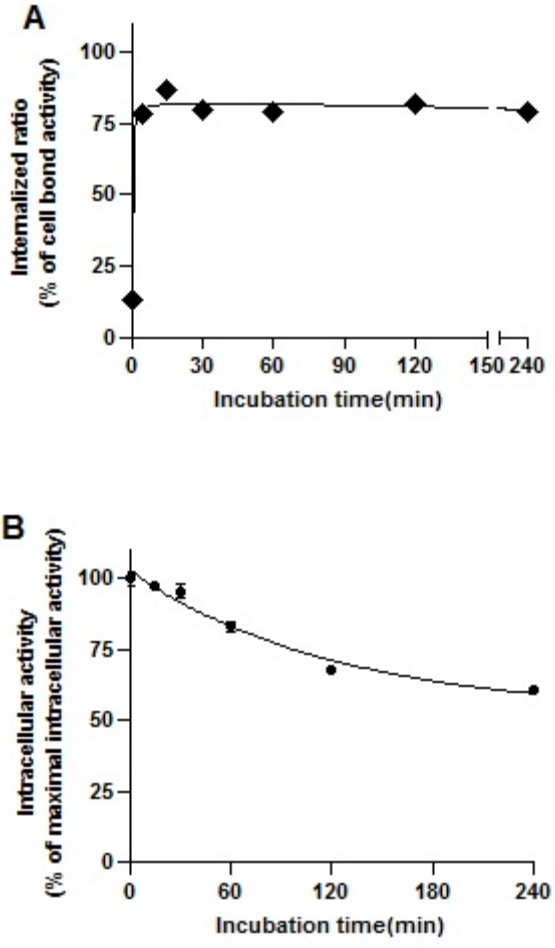

Figure 5. Internalization (A) and efflux (B) kinetics of ^{99m}Tc-HABN$_2$ in PC-3 cell line (n=3, mean ± SD)

8.3.5 Biodistribution Experiments

Biodistribution of ^{99m}Tc-HABN$_2$ was evaluated in athymic nude mice bearing subcutaneous PC-3 tumors after performing the microSPECT and CT scans. The results are shown in Figure 6. Tumor uptake of ^{99m}Tc-HABN$_2$ was 1.58 ± 0.18 %ID/g at 60 min after injection, with a steady decrease to 0.47 ± 0.13 %ID/g at 24 h after injection. The highest radioactivity uptake (15.1±6.4 %ID/g) in kidney was observed at 4 h post injection. The tracer has low blood uptake and was cleared from blood rapidly. The uptake of ^{99m}Tc-HABN$_2$ in non-targeting organs (except kidney and pancreas) such as liver, bone, intestines was lower than 3 %ID/g and washed out rapidly. Due to the slower washout from tumor compared to normal-tissue, the T/NT ratio increased during the 24 h experiment period.The tumor-to-muscle ratio increased from 3.7 ± 1.1 at 1h after injection to 24.1 ±

21.5 at 24 h after injection.

For determining the specificity of ^{99m}Tc-HABN$_2$ binding to GRPR, an excess of unlabelled Aca-BN(7-14) (300 µg/mouse) was injected before the tracer injection. At 4 hours post injection, the radioactivity accumulation was substantially reduced in tumour (from 0.8 ± 0.3 %ID/g to 0.4 ± 0.1 %ID/g) and pancreas (from 9.6 ± 7.6 %ID/g to 3.1 ± 0.2 %ID/g).

8.3.6 MicroSPECT Imaging

Typical microSPECT images of PC-3 tumor bearing mice at different time points after tracer injection are shown in figure 7. The tumors were clearly visible from static miroSPECT images acquired at 4 hours after injection of ^{99m}Tc-HABN$_2$ (B). Prominent uptake of ^{99m}Tc-HABN$_2$ was also observed in the kidneys and pancreas at all images during the 4 h experiment period (A, B). With excess blocking agent (Aca-BN(7-14), 300 µg/mouse), significant reduction of tumor uptake was observed from the images of the blocking group(C), but kidney and bladder (urine) uptake remained high.

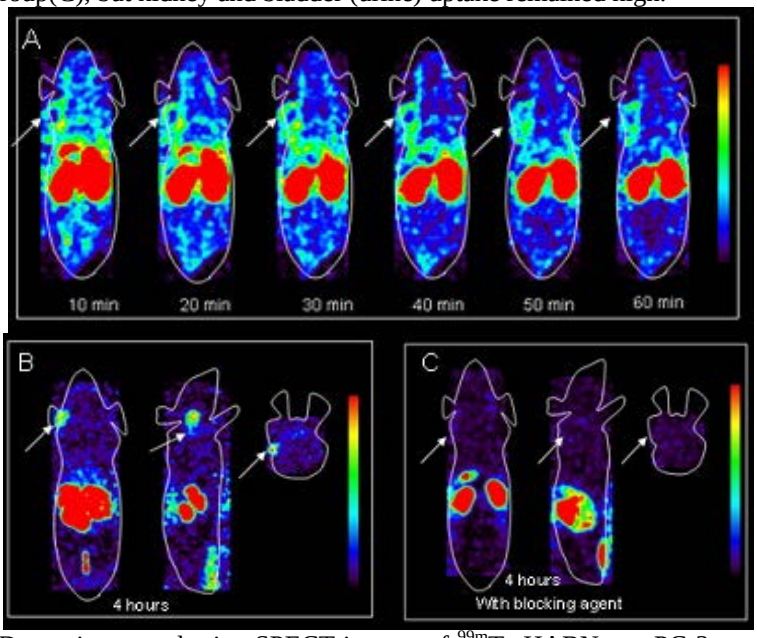

Figure 7. Dynamic coronal microSPECT images of ^{99m}Tc-HABN$_2$ on PC-3 tumor bearing athymic mice during first hour after injection without blocking agent (A) (10 min/frame). Static coronal, sagittal and axial images of ^{99m}Tc-HABN$_2$ on PC-3 tumor bearing mice without (B) and with blocking agent (C) at 4 h after injection. Arrows pointed at the tumor.

8.4 Discussion

Dimerization was applied to evaluate a new dimeric bombesin with 2 identical Aca-Bombesin(7–14) units for its GRPR targeting characteristics as a potential imaging agent for prostate cancer. A side by side comparison of the *in vitro* and *in vivo* behavior of monomer and dimer is listed in table 1.

In a comparative binding assay, bombesin dimer replaced 50% binding of ^{125}I-tyr^{4}-BN(1-14) from the GRP receptors in relatively higher nanomolar concentration (31.4 ± 0.4 nM) than the corresponding monomer (*15*). HYNIC conjugation showed similar slightly negative effect on binding affinity of HYNIC-Glu[Aca-BN(7-14)]$_2$. The additional Aca-BN(7-14) motif and the linker may not be sufficiently flexible to fit in the binding pocket of the GRP receptor as compared to the monomer. The linker may be too short thereby causing steric hindrance upon binding of the molecule to the receptor. However the IC_{50} of HYNIC-Glu[Aca-BN(7-14)]$_2$ is still in an acceptable range. Thus, we decided to label bombesin homodimer with ^{99m}Tc for in vitro and in vivo characterizations.

Although development of PET facilities and radiotracers for PET imaging is blooming nowadays, developing new tracers for SPECT imaging is still important because of the availability of SPECT in most areas all over the world. Due to the favorable radioisotope characters and widespread clinical use, we chose to use the γ-emitting isotope ^{99m}Tc. As we reported in previous study (*15*), the HYNIC/tricine/TPPTS complex was used to serve as chelator for our new tracer because of its high labeling efficiency (rapid and high yield radiolabelling), high solution stability and relatively easy use (*12, 15, 28*). It was also chosen because of its hydrophilic character leading to the preferred excretion route via the renal-urinary system. Although urinary activity can limit the clinical use in the pelvic and retroperitoneal areas, this limitation will not be relevant for evaluation of metastases in the skeleton.

Table 1 Comparison of the *in vitro* and *in vivo* behavior of bombesin monomer (*15*) and dimer.

	^{99m}Tc-HABN	**^{99m}Tc-HABN$_2$**
IC_{50} (nM) [a]	12.81±1.34	63.40 ± 11.70
In vitro stability (in human serum)	Stable in 6 h	Stable in 6 h
Log D value	_-1.60 ±0.06	-1.54 ± 0.16
Highest cellular uptake (% of incubation dose)	10.9 ± 0.7 [b]	32.5 ± 1.8 [c]
Half-life of efflux (Min)	37	84
Tumor uptake (%ID/g)	1.51±0.38	1.58 ± 0.18
Kidney uptake (%ID/g)	6.39±0.83	10.07±1.76
Pancreas uptake (%ID/g)	8.92±1.74	11.26±4.11
Tumor-to-muscle ratio	13.92	3.70

Uptake values (in %ID/g) and T/NT ratios are determined in several organs and PC-3 tumour at 1h p.i. unless stated otherwise; a=IC_{50} determined with HYNIC conjugations (HYNIC-Aca-BN(7-14) or HYNIC-Glu[Aca-BN(7-14)]$_2$); b= cellular uptake value determined at 1 h post incubation; c= cellular uptake value determined at 4 h post incubation.

^{99m}Tc-HABN$_2$ was prepared with high purity. Due to the same ^{99m}Tc labeling core, monomer and dimer shared similar character in labeling, hydrophilicity and solution stability in saline, cysteine and human serum. However, we noticed that several days of incubation is necessary to complete the conjugation of the HYNIC chelator to the bombesin homodimer due to the position of active glutamic acid. The slightly lower rate of ^{99m}Tc-HYNIC(Tricine/TPPTS)-Glu[Aca-BN(7-14)]$_2$ complex construction may be caused for the same reason.

The in vitro cellular uptake, internalization and efflux kinetics were evaluated using the GRPR-expressing human prostate cancer cell line PC-3. Although the binding affinity of bombesin homodimer was 10 times lower than monomer, the specific accumulation of ^{99m}Tc-HABN$_2$ showed almost a linear increasing during 4 h experiment period with highest cellular uptake of 32.5 ± 1.8 % added activity (3-fold as high as that of ^{99m}Tc-HABN), whereas that of ^{99m}Tc-HABN reached an uptake plateau in 30 min, which may due to the higher bombesin "local concentration" of the homodimer in the vicinity of the receptor. In the *in vitro* competitive receptor binding assay, PC-3 cells were incubated with the bombesin ligands for 1 h to allow for the replacement of the GRPR-bound of ^{125}I-tyr^4-BN(1-14). Cellular uptake of ^{99m}Tc-HABN$_2$ gradually increased over time and became higher than ^{99m}Tc-HABN only after 1 h post incubation. This finding indicated that ^{99m}Tc-HABN$_2$ may be more suitable for cancer imaging at later time points (for example 4 h, 24 h p.i.). Therefore, we decided to evaluate the biodistribition and SPECT imaging characters of radiolabelled homodimer in a human prostate cancer xenograft bearing mouse animal model till 24 h post injection.

For ^{99m}Tc-HABN and ^{99m}Tc-HABN$_2$, tumors are visualized in the first time frame of microSPECT image at 10 min post injection, it reflected the rapid receptor binding and internalization via GRPR. The slightly higher tumor uptake of ^{99m}Tc-HABN$_2$ (0.78±0.26 %ID/g) compared to ^{99m}Tc-HABN (0.67±0.26 %ID/g) at 4h post injection could be attributed to the combination of higher cellular uptake, slower efflux and molecular size effect. Instead of steady decreases over time, the uptake of ^{99m}Tc-HABN$_2$ remains constant high (11.2±4.9 %ID/g at 24 h post injection) in pancreas which may be because of same reasons.

Not only in the GRPR expressing tissues but also in the non-GRPR tissues, the ^{99m}Tc-HABN$_2$ showed a longer retention compared to ^{99m}Tc-HABN. The apparent increase in molecular size resulted in an increased circulation time and slower clearance of the bombesin dimer. The accumulation in blood for ^{99m}Tc-HABN$_2$ was 4 times higher as that for ^{99m}Tc-HABN at 1h post injection. Although T/NT ratios were constantly increasing due to the slower excretion of ^{99m}Tc-HABN$_2$ in tumor than in non-target tissues (Figure 6), it was well feasible to visualize the tumor with the SPECT images till 4 hours post injection. The contrast of tumor in SPECT images is expected to be better at 24 h post injection, but due to the short half life of ^{99m}Tc, it was not possible to perform the SPECT scan at 24h post injection.

Because of the doubled positive charge from 2 Aca-BN(7-14) motifs, the radioactivity accumulation of ^{99m}Tc-HABN$_2$ in kidney remains at high level within 24 hours, with highest accumulation of 15.1±6.4 %ID/g at 4 h post injection and decreased to 4.7±0.9%ID/g at 24 h. The high radioactivity accumulation in kidney and urine observed from SPECT imaging and/or biodistribution results indicate that the ^{99m}Tc-HABN$_2$ was excreted through renal-urine pathway which is consist with other ^{99m}Tc-HYNIC-peptides.

The agonist property of ^{99m}Tc-HABN$_2$ was confirmed by its rapid internalization. Although it's still unclear which of agonist and antagonist is more suitable for the imaging

of GRPR-expressing cancer, a few radiolabelled bombesin antagonists, such as Demobesin-1 (*29*), have already showed their superior to agonists in tumor accumulation, retention of radioactivity and in vivo pharmacokinetics. Compare to those antagonists, ^{99m}Tc-HABN$_2$ exhibited comparable tumor accumulation, but less favorable pharmacokinetics. Further studies which focus on improving the binding affinity and pharmacokinetics of bombesin homodimer are undergoing.

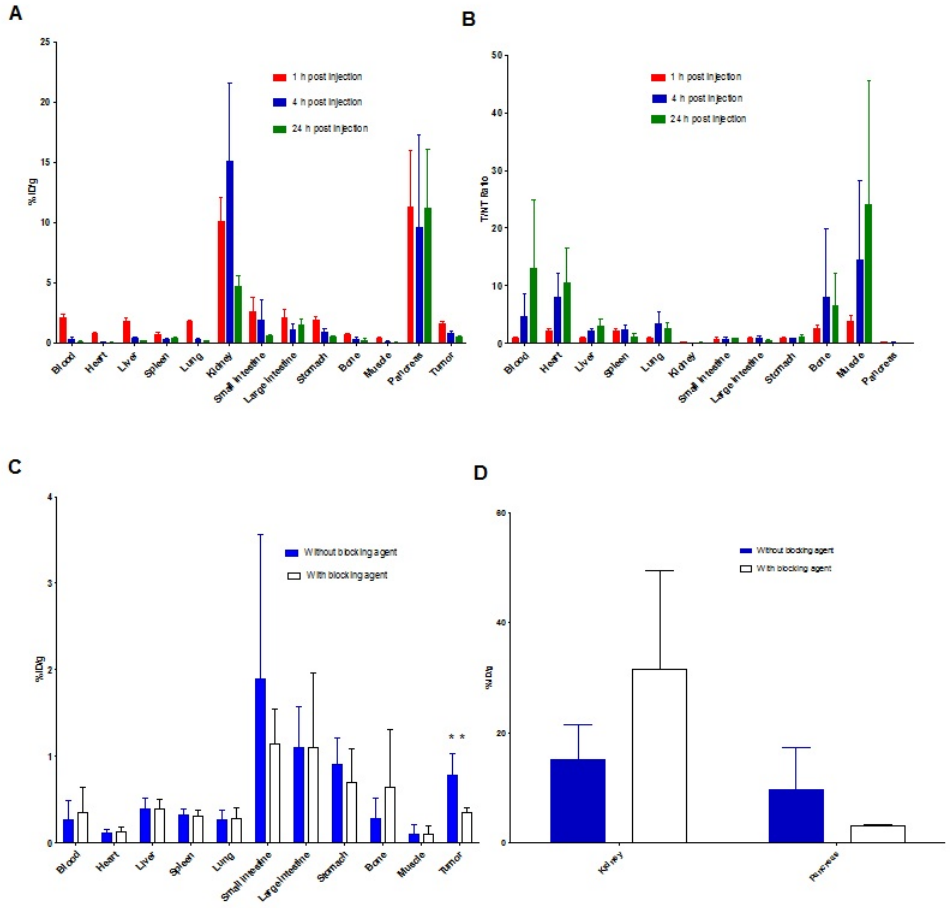

Figure 6. (A) Biodistribution of ^{99m}Tc-HABN$_2$ at 1, 4, 24 hours postinjection in athymic nude mice bearing subcutaneous PC-3 tumor (mean ± SD %ID/g), (B)T/NT ratio of ^{99m}Tc-HABN$_2$ at 1, 4, 24 hours postinjection (mean ± SD), (C) Biodistribution of ^{99m}Tc-HABN$_2$ at 4 hours postinjection with and without blocking agent (mean ± SD %ID/g), (D) Uptake of ^{99m}Tc-HABN$_2$ in kidney and pancreas at 4 hours postinjection with and without blocking agent (mean ± %ID/g); *= statistically significant difference (p<0.05).

Recently, series of radiolabelled Arginine-Glycine-Aspartic acid-bombesin (RGD-BBN) heterodimers for the GRPR targeting were reported (*14*, *30-33*). Those heterodimers aim for targeting two types of receptors simultaneously, to enhance tumor contrast when either or both receptor types are expressed. In the RGD-BBN heterodimer

molecular containing one bombesin motif and one RGD motif, the RGD motif is responsible for targeting integrin $\alpha_v\beta_3$-receptors which are upregulated on activated tumor endothelial cells and also highly expressed on some tumor cells such as glioblastoma, breast and prostate tumors, malignant melanomas, and ovarian carcinomas (*34*). Compared to the bombesin monomer or RGD monomer, the heterodimer shows a synergistic effect for in vivo PC-3 tumor targeting in an animal model (*33*). However using heterodimers the target specificity of the SPECT or PET image is lost, but general detection of tumor lesions may be improved. The RGD-BBN heterodimer labelled with radiometals (^{68}Ga and ^{64}Cu) showed higher background than ^{18}F-labelled tracer but slower washout and higher tumor uptake in nude mice bearing breast tumors (*14*). It's worth to explore the potency of different radioisotopes and chelators on the binding properties and pharmacokinetics of bombesin homodimers.

Within ^{99m}Tc-HABN$_2$, two identical bombesin ligands were conjugated with glutamic acid. Based on the results described in this paper it is not possible for the two bombesin moieties to bind to GRPR simultaneously. It would be interesting to investigate the effects of linkers with differences in length, lipophilicity and flexibility, on the *in vitro* and *in vivo* behavior of the tracer.

8.5 Conclusion

We successfully developed a ^{99m}Tc labelled homodimeric bombesin tracer which showed binding with acceptable affinity and specificity to the GRP receptor-positive PC-3 prostate cancer cells *in vitro* and *in vivo*. Moreover we have shown its ability of tumor imaging. Further studies on modification of homodimeric bombesin are required. The current dimer is a useful lead compound for this purpose.

Acknowledgements

This work was made possible by a financial contribution from CTMM, project PCMM, project number 03O-203. We thank Chao Wu for technical assistance on microSPECT images reconstruction and D.F. Samplonius for technical assistance on cell culturing, J. W. A. Sijbesma for assisting animal experiments. All animal experiments were approved by the local animal welfare committee in accordance with the Dutch legislation and carried out in accordance with their guidelines.

References

(1) Ferlay, J., Autier, P., Boniol, M., Heanue, M., Colombet, M., and Boyle, P. (2007) Estimates of the cancer incidence and mortality in Europe in 2006. *Ann Oncol 18*, 581-92.

(2) Jemal, A., Siegel, R., Ward, E., Hao, Y., Xu, J., Murray, T., and Thun, M. J. (2008) Cancer statistics, 2008. *CA Cancer J Clin 58*, 71-96.

(3) Eisenhauer, E. A., Therasse, P., Bogaerts, J., Schwartz, L. H., Sargent, D., Ford, R., Dancey, J., Arbuck, S., Gwyther, S., Mooney, M., Rubinstein, L., Shankar, L., Dodd, L., Kaplan, R., Lacombe, D., and Verweij, J. (2009) New response evaluation criteria in solid tumours: revised RECIST guideline (version 1.1). *Eur J Cancer 45*, 228-47.

(4) Aprikian, A. G., Cordon-Cardo, C., Fair, W. R., and Reuter, V. E. (1993) Characterization of neuroendocrine differentiation in human benign prostate and prostatic adenocarcinoma. *Cancer 71*, 3952-65.

(5) Price, J., Penman, E., Wass, J. A., and Rees, L. H. (1984) Bombesin-like immunoreactivity in human gastrointestinal tract. *Regul Pept 9*, 1-10.

(6) Spindel, E. R., Chin, W. W., Price, J., Rees, L. H., Besser, G. M., and Habener, J. F. (1984) Cloning and characterization of cDNAs encoding human gastrin-releasing peptide. *Proc Natl Acad Sci U S A 81*, 5699-703.

(7) Track, N. S., and Cutz, E. (1982) Bombesin-like immunoreactivity in developing human lung. *Life Sci 30*, 1553-6.

(8) Xiao, D., Wang, J., Hampton, L. L., and Weber, H. C. (2001) The human gastrin-releasing peptide receptor gene structure, its tissue expression and promoter. *Gene 264*, 95-103.

(9) Erspamer, V., Erpamer, G. F., and Inselvini, M. (1970) Some pharmacological actions of alytesin and bombesin. *J Pharm Pharmacol 22*, 875-6.

(10) McDonald, T. J., Jornvall, H., Nilsson, G., Vagne, M., Ghatei, M., Bloom, S. R., and Mutt, V. (1979) Characterization of a gastrin releasing peptide from porcine non-antral gastric tissue. *Biochem Biophys Res Commun 90*, 227-33.

(11) Zhang, X., Cai, W., Cao, F., Schreibmann, E., Wu, Y., Wu, J. C., Xing, L., and Chen, X. (2006) ^{18}F-labelled bombesin analogs for targeting GRP receptor-expressing prostate cancer. *J Nucl Med 47*, 492-501.

(12) Shi, J., Jia, B., Liu, Z., Yang, Z., Yu, Z., Chen, K., Chen, X., Liu, S., and Wang, F. (2008) ^{99m}Tc-labelled bombesin(7-14)NH_2 with favorable properties for SPECT imaging of colon cancer. *Bioconjug Chem 19*, 1170-8.

(13) Ait-Mohand, S., Fournier, P., Dumulon-Perreault, V., Kiefer, G. E., Jurek, P., Ferreira, C. L., Benard, F., and Guerin, B. (2011) Evaluation of ^{64}Cu-labelled bifunctional chelate-bombesin conjugates. *Bioconjug Chem 22*, 1729-35.

(14) Liu, Z., Yan, Y., Liu, S., Wang, F., and Chen, X. (2009) ^{18}F, ^{64}Cu, and ^{68}Ga labelled RGD-bombesin heterodimeric peptides for PET imaging of breast cancer. *Bioconjug Chem 20*, 1016-25.

(15) Ananias, H. J., Yu, Z., Dierckx, R. A., van der Wiele, C., Helfrich, W., Wang, F., Yan, Y., Chen, X., de Jong, I. J., and Elsinga, P. H. (2011) ^{99m}technetium-HYNIC(tricine/TPPTS)- Aca-bombesin(7-14) as a targeted imaging agent with microSPECT in a PC-3 prostate cancer xenograft model. *Mol Pharm 8*, 1165-73.

(16) Kramer, R. H., and Karpen, J. W. (1998) Spanning binding sites on allosteric proteins with polymer-linked ligand dimers. *Nature 395*, 710-3.

(17) Handl, H. L., Vagner, J., Yamamura, H. I., Hruby, V. J., and Gillies, R. J. (2004) Lanthanide-based time-resolved fluorescence of in cyto ligand-receptor interactions. *Anal Biochem 330*, 242-50.

(18) Mulder, A., Huskens, J., and Reinhoudt, D. N. (2004) Multivalency in supramolecular chemistry and nanofabrication. *Org Biomol Chem 2*, 3409-24.

(19) Vance, D., Shah, M., Joshi, A., and Kane, R. S. (2008) Polyvalency: a promising strategy for drug design. *Biotechnol Bioeng 101*, 429-34.

(20) Joosten, J. A., Loimaranta, V., Appeldoorn, C. C., Haataja, S., El Maate, F. A., Liskamp, R. M., Finne, J., and Pieters, R. J. (2004) Inhibition of Streptococcus suis adhesion by dendritic galabiose compounds at low nanomolar concentration. *J Med Chem 47*, 6499-508.

(21) Liu, Z., Shi, J., Jia, B., Yu, Z., Liu, Y., Zhao, H., Li, F., Tian, J., Chen, X., Liu, S.,

and Wang, F. (2011) Two Y-labelled multimeric RGD peptides RGD_4 and $3PRGD_2$ for integrin targeted radionuclide therapy. *Mol Pharm 8*, 591-9.

(22) Chang, E., Liu, S., Gowrishankar, G., Yaghoubi, S., Wedgeworth, J. P., Chin, F., Berndorff, D., Gekeler, V., Gambhir, S. S., and Cheng, Z. (2011) Reproducibility study of $[^{18}F]FPP(RGD)_2$ uptake in murine models of human tumor xenografts. *Eur J Nucl Med Mol Imaging 38*, 722-30.

(23) Dijkgraaf, I., Yim, C. B., Franssen, G. M., Schuit, R. C., Luurtsema, G., Liu, S., Oyen, W. J., and Boerman, O. C. (2011) PET imaging of alphavbeta integrin expression in tumours with Ga-labelled mono-, di- and tetrameric RGD peptides. *Eur J Nucl Med Mol Imaging 38*, 128-37.

(24) Shi, J., Kim, Y. S., Zhai, S., Liu, Z., Chen, X., and Liu, S. (2009) Improving tumor uptake and pharmacokinetics of ^{64}Cu-labelled cyclic RGD peptide dimers with Gly_3 and PEG_4 linkers. *Bioconjug Chem 20*, 750-9.

(25) Dijkgraaf, I., Kruijtzer, J. A., Liu, S., Soede, A. C., Oyen, W. J., Corstens, F. H., Liskamp, R. M., and Boerman, O. C. (2007) Improved targeting of the $alpha_vbeta_3$ integrin by multimerisation of RGD peptides. *Eur J Nucl Med Mol Imaging 34*, 267-73.

(26) Harris, T. D., Sworin, M., Williams, N., Rajopadhye, M., Damphousse, P. R., Glowacka, D., Poirier, M. J., and Yu, K. (1999) Synthesis of stable hydrazones of a hydrazinonicotinyl-modified peptide for the preparation of ^{99m}Tc-labelled radiopharmaceuticals. *Bioconjug Chem 10*, 808-14.

(27) Qiao, R., Yang, C., and Gao, M. (2009) Superparamagnetic iron oxide nanoparticles: from preparations to in vivo MRI applications. *Journal of Materials Chemistry 19*, 6274.

(28) Liu, S., Kim, Y. S., Hsieh, W. Y., and Gupta Sreerama, S. (2008) Coligand effects on the solution stability, biodistribution and metabolism of the ^{99m}Tc-labelled cyclic RGDfK tetramer. *Nucl Med Biol 35*, 111-21.

(29) Schroeder, R. P., Muller, C., Reneman, S., Melis, M. L., Breeman, W. A., de Blois, E., Bangma, C. H., Krenning, E. P., van Weerden, W. M., and de Jong, M. (2010) A standardised study to compare prostate cancer targeting efficacy of five radiolabelled bombesin analogues. *Eur J Nucl Med Mol Imaging 37*, 1386-96.

(30) Liu, Z., Li, Z. B., Cao, Q., Liu, S., Wang, F., and Chen, X. (2009) Small-animal PET of tumors with ^{64}Cu-labelled RGD-bombesin heterodimer. *J Nucl Med 50*, 1168-77.

(31) Liu, Z., Niu, G., Wang, F., and Chen, X. (2009) ^{68}Ga-labelled NOTA-RGD-BBN peptide for dual integrin and GRPR-targeted tumor imaging. *Eur J Nucl Med Mol Imaging 36*, 1483-94.

(32) Liu, Z., Yan, Y., Chin, F. T., Wang, F., and Chen, X. (2009) Dual integrin and gastrin-releasing peptide receptor targeted tumor imaging using ^{18}F-labelled PEGylated RGD-bombesin heterodimer ^{18}F-FB-PEG_3-Glu-RGD-BBN. *J Med Chem 52*, 425-32.

(33) Li, Z. B., Wu, Z., Chen, K., Ryu, E. K., and Chen, X. (2008) ^{18}F-labelled BBN-RGD heterodimer for prostate cancer imaging. *J Nucl Med 49*, 453-61.

(34) Hynes, R. O. (2002) Integrins: bidirectional, allosteric signaling machines. *Cell 110*, 673-87.

Chapter 9

Summary and Future Perspectives

9.1 Conclusion

Prostate cancer is one of the most common forms of cancer in western countries. A Transrectal ultrasound guided biopsy is the gold standard for histological prostate cancer diagnosis. Unfortunately this procedure can lead to over-estimation or under-estimation of disease due to sampling error. Therefore, a noninvasive specific imaging tool is urgently needed. Positron emission tomography (PET) and single photon computed tomography (SPECT) with high sensitivity, specificity and resolution may fit the requirements of prostate cancer diagnosis.

Gastrin releasing peptide receptor (GRPR) is a G-protein receptor. Due to the high expression in several human cancer cell lines (breast cancer, colon cancer, prostate cancer) and absence in most normal organs, GRPR could be used as a potential target for cancer detection. Radiolabelled bombesin analogues could be potential probes for nuclear imaging of cancer by targeting GRPR.

Although developments of PET facilities and radiotracers for PET imaging are blooming nowadays, developing new tracers for SPECT imaging is still important because of the availability of SPECT in most areas all over the world. ^{99m}Tc is the most commonly used radionuclide for nuclear imaging with SPECT due to its excellent nuclear properties ($t_{1/2}$ =6 h and single photon emission at 140 keV), rich and diverse coordination chemistry, easy availability at low cost, and high specific activity. In chapter 3, we reported the synthesis and preclinical evaluation of ^{99m}Tc(HYNIC-ABN)(tricine)(TPPTS),which is a combination of a truncated bombesin(7-16) peptide as biomolecules, a β-Alanine spacer, and ternary ligand system (HYNIC, tricine, and TPPTS). Rapid excretion of ^{99m}Tc(HYNIC-ABN)(tricine)(TPPTS) via the renal route with low radioactivity accumulation in the blood, liver, muscle and gastrointestinal was observed in HT-29 colon cancer bearing mice at 1 h post injection. The highest absolute tumor uptake of ^{99m}Tc(HYNIC-ABN)(tricine)(TPPTS) was 1.59 ± 0.23 %ID/g at 30 min p.i. Colon cancer xenografts were clearly visible with high contrast from static planar images of the tumor-bearing mice. ^{99m}Tc(HYNIC-ABN)(tricine)(TPPTS) is a promising tracer with favorable phamacokinetis for imaging colon cancer although the absolute tumor uptake was not the highest in reported bombesins.

We designed and developed our second bombesin tracer ^{99m}Tc-HABN (**Chapter 4**) based on experience from ^{99m}Tc(HYNIC-ABN)(tricine)(TPPTS). To further reduce the steric hindrance effect of ^{99m}Tc-HYNIC(tricine)(TPPTS) labeling core to the GRPR binding affinity of bombesin, a longer å-aminocaproic acid (Aca) linker was introduced instead of β-Alanine. ^{99m}Tc-HABN was evaluated in PC-3 prostate cancer bearing mice which is the most common animal model for the evaluation of GRPR targeting ability. Lower IC_{50} value (higher GRPR binding affinity), higher absolute tumor uptake, longer tumor retention, lower accumulation in liver and kidney, higher tumor-to-muscle, tumor-to-blood and tumor-to-liver ratios, but also a higher accumulation in gastrointestinal region was observed compared to ^{99m}Tc(HYNIC-ABN)(tricine)(TPPTS). Indeed, the Aca linker improved the *in vivo* kinetics of ^{99m}Tc-labelled bombesin. Therefore, ^{99m}Tc-HABN was selected for a clinical study of human primary prostate cancer imaging. The pharmaceutical translation work of ^{99m}Tc-HABN was summarized in **Chapter 5**. We successfully prepared the ^{99m}Tc-HABN with high specific activity and purity, in the absence of any signs of adverse or subjective side effect after administration to patients. Unfortunately the ^{99m}Tc-HABN SPECT/CT was not able to detect prostate cancer in patients with proven disease. We hypothesize that the low accumulation of ^{99m}Tc-HABN on prostate cancer was

mainly due to the rapid degradation and moderate binding to GRPR.

An attempt to increase the shelf time and retention of radioactivity signal in tumor was conducted by introducing a radioiodine labelled cubane moiety (**Chapter 6**). We successfully prepared the [^{123}I]-CABN under mild conditions with moderate yield and high purity after purification. The internalization and efflux profile of [^{123}I]-CABN were similar with ^{99m}Tc-HABN. The in vitro stability of [^{123}I]-CABN in saline solution was high, unfortunately, the metabolic stability of [^{123}I]-CABN *in vivo* was poor. No de-iodination was observed in SPECT imaging studies, the rapid degradation of [^{123}I]-CABN was possibly due to the breakdown of amide bond between cubyl moiety and the ε-aminocaproic acid. Therefore, it was not possible to visualize a prostate cancer xenograft with [^{123}I]-CABN SPECT imaging since not enough radioactivity could accumulate in the tumor.

Further studies were carried out to develop bombesin analogues which could have better stability against proteolytic enzymes (**Chapter 7**). A series of lanthionine-stablized bombesins were synthesized and two of them (C5 and C6) were selected according to the binding affinity to GRPR. Both ^{18}F-C5 and ^{18}F-C6 showed GRPR targeting potential, PC-3 tumors can be clearly observed from PET images at 2 h post injection. However, further improvement may be needed on radiochemical yield, specific activity, *in vivo* kinetics before it could be translated into a clinical trial.

In **Chapter 8**, we described the development of a novel bombesin homodimer. Although a higher IC_{50} value of bombesin homodimer than the monomer was observed, the ^{99m}Tc-$HABN_2$ exhibited comparable tumor uptake. The *in vitro* cellular uptake kinetics proved that the higher local concentration of bombesin moiety improved the GRPR targeting ability. However, the double positive charge and the molecular weight effect led to less optimal *in vivo* pharmacokinetic properties such as high radioactivity accumulation and long retention in kidney, and intestines. Further studies on optimizing the in vivo kinetics of bombesin homodimer by using other chelators, labeling methods, linkers based on ^{99m}Tc-$HABN_2$ are warranted.

9.2 Future Perspectives:

This thesis has solely focused on imaging of the GRPR, but several other receptors which are specifically expressed in prostate cancer, such as Prostate specific membrane antigen (PSMA) could also be considered as target for imaging prostate cancer. Already several lead structures both based on antibodies and small molecules have recently been published. The combination of information of the receptor status of GRPR with other molecular targets will be of great additional value.

Imaging of GRPR still needs further improvement. Improving absolute tumor uptake is still the key factor when developing new bombesin tracers for imaging prostate cancer. Multimerization is a promising strategy for improving binding affinity and kinetics of radiolabelled bombesin peptide. By incorporating multiple targeting moieties local receptor ligand concentrations can be enhanced resulting in higher overall binding affinities. The binding affinity of the bombesin dimer as investigated in this thesis was not increased as we expected but decreased possibly due to the lack of flexibility of the bombesin(7-14) moiety and the glutamine linker. Therefore studies on the linker (e.g. length and flexibility) and bifunctional chelator are necessary for improving the performance of the bombesin dimer.

Another way to improve binding characteristics of bombesin tracers is to improve their metabolic stability by introducing non-natural amino acids to replace certain amino acids

sequences of bombesin peptide without detrimental effect on the biological activity of the peptide. Several examples have already been published and showed their stabilizing effect.

Although most promising bombesin tracers are agonists, which may internalize and be captured in tumor cells, bombesin antagonists may offer better in vivo pharmacokinetic properties as cancer imaging probes. Bombesin antagonists could also be used for prostate cancer imaging due to fast clearance from normal organs and long retention in tumor cells.

All these issues could be combined to develop the bombesine tracer with optimal affinity, pharmacokinetics and metabolic stability. In combination with new versatile radiolabelling techniques such as click chemistry a tool can be provided to study GRPR in prostate cancer.

Chapter 10
Samenvatting en Toekomstige Ontwikkelingen

10.1 Conclusie

Prostaatkanker is een van de meest voorkomende vormen van kanker in de westerse wereld.

De diagnose prostaatkanker is definitief wanneer histologisch bewijs verkregen is. Meestal gebeurt dit door middel van transrectale echogeleide biopten. Deze procedure heeft echter 'sampling error' als nadeel. Hierdoor kan overschatting en onderschatting van prostaatkanker ontstaan. Dit is een van de belangrijkste redenen waarom een niet-invasieve beeldvormende techniek voor het diagnosticeren van prostaatkanker wenselijk is.

Positron emissie tomografie (PET) en single photon computed tomography (SPECT) hebben een hoge gevoeligheid, specificiteit en resolutie en kunnen bijdragen aan het verbeteren van de diagnostiek van prostaatkanker.

Gastrine-releasing peptide receptor (GRPR) is een G-eiwit gekoppelde receptor. GRPR kan worden gebruikt als een potentieel doelwit voor kankerdetectie, vanwege de hoge expressie in verschillende vormen van kanker (borstkanker, darmkanker en prostaatkanker) en de afwezigheid in gezond weefsel. Radioactief gelabelde bombesine analogen hebben potentie binnen de nucleaire beeldvorming van kanker doordat zij zich richten op GRPR.

De ontwikkeling van PET faciliteiten en radiotracers neemt een grote vlucht. Daarnaast is de ontwikkeling van nieuwe tracers voor SPECT nog steeds belangrijk, vanwege de grote beschikbaarheid van SPECT wereldwijd. ^{99m}Tc is de meest gebruikte radionuclide voor nucleaire beeldvorming met SPECT vanwege de uitstekende nucleaire eigenschappen (de halfwaardetijd bedraagt 6 uur en 'single photon emissie' vindt plaats bij 140 keV), rijke en gevarieerde coördinatie chemie, eenvoudige beschikbaarheid tegen lage kosten en de hoge specifieke activiteit. In hoofdstuk 3 wordt de synthese en preklinische evaluatie van ^{99m}Tc(HYNIC-ABN)(tricine)(TPPTS) beschreven. ^{99m}Tc(HYNIC-ABN)(tricine)(TPPTS) bestaat uit een verkorte vorm van bombesine (7-16), een β-alanine spacer en een tertiair ligand systeem (respectievelijk HYNIC, tricine en TPPTS) .

In vivo onderzoek met HT-29 coloncarcinoom geincubeerde muizen liet een snelle uitscheiding van ^{99m}Tc(HYNIC-ABN)(tricine)(TPPTS) via de nieren zien. Daarnaast werd er 1 uur na injectie een lage accumulatie van radioactiviteit waargenomen in het bloed, in de lever, in de spieren en in het gastro-intestinale systeem. De hoogste absolute opname van ^{99m}Tc(HYNIC-ABN)(tricine)(TPPTS) in tumorweefsel bedroeg 30 minuten na injectie 1,59 ± 0,23 %ID/g. Coloncarcinoom xenotransplaat was duidelijk zichtbaar met een hoog contrast in de tumordragende muizen. ^{99m}Tc(HYNIC-ABN)(tricine)(TPPTS) is een veelbelovende tracer met gunstige phamacokinetische eigenschappen voor de beeldvorming van coloncarcinoom. Echter, de absolute tumoropname in dit onderzoek was niet zo hoog als de tumoropname van andere reeds beschreven bombesine tracers.

Op basis van de ervaringen die opgedaan zijn door de productie en het gebruik van ^{99m}Tc(HYNIC-ABN)(tricine)(TPPTS) werd een tweede bombesine tracer, genaamd ^{99m}Tc–HABN, ontwikkeld (hoofdstuk 4). Om de sterische hindering van ^{99m}Tc-HYNIC (tricine)(TPPTS) te beperken werd een langere spacer dan β-alanine geïntroduceerd, namelijk aminocapronzuur (Aca). Hierdoor kan de bindingsaffiniteit van bombesine voor GRPR verhoogd worden. ^{99m}Tc-HABN werd geëvalueerd in muizen die geincubeerd waren met de humane PC-3 prostaatkankercellijn. PC-3 is het meest gebruikte diermodel voor de evaluatie van GRPR als aangrijpingspunt voor beeldvorming. In vergelijking met ^{99m}Tc(HYNIC-ABN)(tricine)(TPPTS), leidde ^{99m}Tc-HABN tot een lagere IC_{50} waarde (een hoger GRPR bindingsaffiniteit) , een hogere absolute tumoropname ,

toegenomen retentie van de tracer in tumorweefsel , een lagere accumulatie in de lever en nieren , een hogere tumor/spier- , tumor/bloed- en tumor/lever ratio , maar ook een hogere accumulatie in het gastro-intestinale systeem.De Aca spacer leidde zoals verwacht tot verbetering van de in vivo kinetiek van met ^{99m}Tc gelabeld bombesine. ^{99m}Tc-HABN werd vanwege bovengenoemde resultaten geselecteerd voor klinisch onderzoek naar de beeldvorming van prostaatkanker bij patiënten.

In hoofdstuk 5 wordt de overgang van de preklinische toepassing naar de klinische toepassing van ^{99m}Tc-HABN beschreven. ^{99m}Tc-HABN werd succesvol geproduceerd met hoge specifieke activiteit en zuiverheid. Er werden geen bijwerkingen gezien. Echter prostaatkanker kon niet aangetoond worden door middel van ^{99m}Tc-HABN SPECT/CT bij patiënten met histologisch bewezen ziekte. De hypothese is dat de lage accumulatie veroorzaakt wordt door de snelle degradatie van de tracer en de matige binding aan GRPR.

Een radioactief gelabeld synthetische koolstof werd in de de tracer gebracht met als doel om de bewaartijd en de retentie van het radioactieve signaal te vergroten (hoofdstuk 6). [^{123}I]-CABN werd succesvol geproduceerd met een goede opbrengst en een hoge zuiverheid. De mate van internalisatie en externalisatie van [^{123}I]-CABN was vergelijkbaar met ^{99m}Tc-HABN. De *in vivo* stabiliteit van [^{123}I]-CABN was hoog in een fysiologische zoutoplossing. Helaas was de metabole stabiliteit van [^{123}I]-CABN *in vivo* slecht. Er was geen sprake van deionidisatie tijdens SPECT scans. De slechte metabole stabiliteit van [^{123}I]-CABN wordt mogelijk veroorzaakt door de afbraak van de amide binding tussen de koolstof groep en het ε–aminocapronzuur. Als gevolg van de lage accumulatie van de tracer kon prostaatkanker niet afgebeeld worden door middel van [^{123}I]-CABN SPECT.

Aanvullende studies werden uitgevoerd om bombesine tracers te ontwikkelen die minder gevoelig zijn voor proteolytische enzymen en daardoor een hogere stabiliteit hebben (hoofdstuk 7). Een serie lanthionine-gestabiliseerde bombesine tracers werd ontwikkeld. Op basis van de hoge bindingsaffiniteit voor GRPR werden C5 en C6 geselecteerd. Zowel ^{18}F-C5 als ^{18}F-C6 was in staat om 2 uur na injectie de humane PC-3 prostaatkankercellijn *in vivo* af te beelden door middel van PET. Echter verdere verbetering van de radiochemische opbrengst, de specifieke activiteit en de *in vivo* kinetiek is nodig voordat deze tracers in een klinische studie geëvalueerd kunnen worden. In hoofdstuk 8 wordt de ontwikkeling van een nieuwe bombesine homodimeer beschreven. De bombesine homodimeer vertoonde een hogere IC_{50} waarde dan de bombesine monomeer. Desondanks was de tumoropname identiek. *In vitro* cellulaire opnamekinetiek toonde aan dat de hogere concentratie van bombesine de affiniteit voor GRPR verbeterde. Echter, de tweevoudige positieve lading en het moleculair gewicht, leidden tot minder gunstige *in vivo* farmacokinetische eigenschappen, zoals toegenomen radioactieve accumulatie en langdurige retentie in de nieren en de darmen. Nader onderzoek naar het optimaliseren van de *in vivo* kinetiek van de bombesine homodimeren, door het gebruik van andere chelators , radioactieve labbeling en linkers op basis van ^{99m}Tc - $HABN_2$, zijn nodig.

10.2 Toekomstperspectieven :

Dit proefschrift is uitsluitend gericht op beeldvorming van GRPR. Er zijn echter verschillende andere receptoren die specifiek bij prostaatkanker tot expressie komen , zoals prostate-pecific membrane antigen (PSMA), Deze receptoren kunnen ook beschouwd worden als een doelwit voor de beeldvorming van prostaatkanker. Er zijn reeds verschiedene tracers, zowel gebaseerd op antilichamen als ‘small molecules’, in de

literatuur beschreven. Informatie over de expressie van GRPR en andere moleculaire doelwitten is van grote toegevoegde waarde in de ontwikkeling van tracers.

De beeldvorming van GRPR moet verder verbeterd worden. Vergroting van de absolute tumoropname is noodzakelijk in de ontwikkeling van bombesine tracers voor de beeldvorming van prostaatkanker. Multimerisatie is een veelbelovende techniek voor het verbeteren van de bindingsaffiniteit en kinetiek van radioactief gelabelde bombesine tracers.

De bindingsaffiniteit van de in dit onderzoek onderzochte bombesine dimeer, was tegen de verwachting in niet toegenomen. Er was zelfs sprake van een afname van de bindingsaffiniteit, hetgeen mogelijk veroorzaakt werd door het gebrek aan flexibiliteit van bombesin(7-14) en van de glutamine spacer. Nader onderzoek naar de spacer (lengte en flexibiliteit) en de bifunctionele chelator zijn noodzakelijk om de prestaties van de bombesine dimeer te verbeteren.

Een andere manier om de bindingseigenschappen van bombesine tracers te verbeteren is om hun metabolische stabiliteit te verhogen. Dit kan gedaan worden door bepaalde aminozuurcomplexen in het bombesine eiwit te vervangen door niet-natuurlijke aminozuren zonder dat er nadelige effecten op de biologische activiteit van het eiwit ontstaat. Verschillende voorbeelden zijn reeds gepubliceerd en toonden hun stabiliserende werking. Ondanks dat de meest veelbelovende bombesine tracers agonisten zijn (waardoor influx en retentie van de tracer in de cel), vertonen bombesine antagonisten mogelijk betere farmacokinetische eigenschappen. Bombesine antagonisten kunnen ook gebruikt worden voor de beeldvorming van prostaatkanker vanwege de snelle klaring uit gezond weefsel en langdurige retentie in tumorcellen.

Bovengenoemde zaken kunnen worden gecombineerd om een bombesine tracer te ontwikkelen met een hoge affiniteit, gunstige farmacokinetiek en hoge metabolische stabiliteit. Nieuwe veelzijdige radiolabelling technieken zoals click chemie kunnen bijdragen aan de ontwikkeling van een tracer voor de beeldvorming van GRPR.

Acknowledgement

It is a challenge to finish a PhD project. It would have been impossible for me to reach this final chapter of my thesis without help from other people. Therefore, I would like to express my gratitude towards all of you who turned this thesis into reality.

First and foremost, I would like to thank Prof. Philip Elsinga for giving me the opportunity to conduct this PhD project. I am indebted to you for your guidance, insightful advice and encouragement. I would like to express my special thanks to Prof. Rudi Dierckx and Dr. Igle Jan de Jong who gave me the opportunity to work in research groups of NGMB and urology department. The thesis would not have existed without your priceless support, suggestions and comments. I am deary obliged to Prof. Fan Wang for supervising and supporting me during my master and PhD. I would like to thank Dr. Xiaoyuan Chen, Dr. Gert Moll and Dr. Wijnand Helfrich for your priceless supports and help in our collebration projects. I also greatly appreciate the help from Dr.Aren van Waarde.

I really greatful to the members of the Reading Committee, Prof. Jourik Gietema, Prof. Shuang Liu and Prof. Marion de Jong, for spending time in reading and approving my thesis. Shuang Liu, you also helped me a lot on my projects. I am deeply grateful for your invaluable help.

It has been great honor and privilege to work in NGMB, department of urology, surgical research laboratory and medical isotopes research center. I'm very much thankful to all my colledges in NGMB and department of urology. You are heros who make research so enjoyable and exciting! Hildo, Hilde and Rutger, my dutch supporting team. Thank you for turning me "north dutch" (open, freedam, never give up, enthusiastic, and grrroningen), especially Hildo, my dutch, English and urology teacher! Valentina and Giuseppe, my italian mates, you warmed me with the hotest italian friendship and the best tiramisu, thank you so much!!! I would like to express my appreciation to: Ines, Leila, Anna, Daniele and Mehrsima, from ladies' office; Anniek, Nisha and Nathalie, my office mates; Khayum, Siddesh, Shivashankar, Willem-Jan, Chao, Andrea and Vladimir, from gentlemen's office; ("Prof. Dr. Pillow")Bram, Janine, Joost, Sergiy, Roel, Jurgen, Hendrikus, Klaas Willem, Gert, Hans, Silke, Linda, Jan Pruim, Marjolijn and Michael, my dear colleagues fom UMCG; Douwe, colleatue from surgical research lab; Bin Jia, Zhaofei Liu, and Jiyun Shi, my colleagues from Peking university. I'm nothing without you!

My sincere thanks should be given to my paranymphs Hilde and Chao, I'm sure you "saved" my life and will "save" my life in my thesis defence!

"Last but not least", I would like to thank all my Chinese friends in groningen, especially, Ning Ding, 小铮铮，小赵，N 强，斌哥，嘉文，超哥及小刘畅，凯哥，边哥小白及安迪，谭洪涛，王洪伟，青松，刘博，魏哥，Miaoyan, 韩丽娜，老赵，小许哥及李阳姐一家，飞哥孝利一家，二妃一家，杜晓光一家，王仁轩及徐燕一家，UMCG 的同仁们（排名不分先后，不按阿拉伯字母或其他任何顺序），全荷学联及格罗宁根中国学生学者联合会所有同仁，格罗宁根羽毛球队所有朋友们。借此机会还要感谢陪伴我一生的好基友们：贱欣，精子，宝贝，小兰，超超，平平等等……

最真挚的感谢我亲爱的父母。没有你们就没有我的生命，以及我曾经和将要经历的一切。谢谢你们给予我的所有无私的亲情，无论是理解，支持，担心还是关爱。谢谢你们！

最最后，感谢我的妻子殷杰和小姑娘-佑宁，感谢你们对我的支持给我幸福的家庭。

Although there may be many who remain unacknowledged in this humble not of gratitude there are none who remain unappreciated.

Zilin Yu